VOL. 479 NO. 1 SEPTEMBER 22, 1989

OF HROMATOGRAPHY

TIONAL JOURNAL ON CHROMATOGRAPHY, ELECTROPHORESIS AND RELATED METHODS

ELSEVIER

JOURNAL OF CHROMATOGRAPHY

Scope. The *Journal of Chromatography* publishes papers on all aspects of chromatography, electrophoresis and related methods. Contributions consist mainly of research papers dealing with chromatographic theory, instrumental development and their applications. The section *Biomedical Applications*, which is under separate editorship, deals with the following aspects: developments in and applications of chromatographic and electrophoretic techniques related to clinical diagnosis or alterations during medical treatment; screening and profiling of body fluids or tissues with special reference to metabolic disorders; results from basic medical research with direct consequences in clinical practice; drug level monitoring and pharmacokinetic studies; clinical toxicology; analytical studies in occupational medicine.

Submission of Papers. Papers in English, French and German may be submitted, in three copies. Manuscripts should be submitted to: The Editor of *Journal of Chromatography*, P.O. Box 681, 1000 AR Amsterdam, The Netherlands, or to: The Editor of *Journal of Chromatography, Biomedical Applications*, P.O. Box 681, 1000 AR Amsterdam, The Netherlands. Review articles are invited or proposed by letter to the Editors. An outline of the proposed review should first be forwarded to the Editors for preliminary discussion prior to preparation. Submission of an article is understood to imply that the article is original and unpublished and is not being considered for publication elsewhere. For copyright regulations, see below.

Subscription Orders. Subscription orders should be sent to: Elsevier Science Publishers B.V., P.O. Box 211, 1000 AE Amsterdam, The Netherlands, Tel. 5803 911, Telex 18582 ESPA NL. The *Journal of Chromatography* and the *Biomedical Applications* section can be subscribed to separately.

Publication. The *Journal of Chromatography* (incl. *Biomedical Applications*) has 37 volumes in 1989. The subscription prices for 1989 are:

J. Chromatogr. + *Biomed. Appl.* (Vols. 461–497):
Dfl. 6475.00 plus Dfl. 999.00 (p.p.h.) (total *ca.* US$ 3428.50)

J. Chromatogr. only (Vols. 461–486):
Dfl. 5200.00 plus Dfl. 702.00 (p.p.h.) (total *ca.* US$ 2707.25)

Biomed. Appl. only (Vols. 487–497):
Dfl. 2200.00 plus Dfl. 297.00 (p.p.h.) (total *ca.* US$ 1145.50).

Our p.p.h. (postage, package and handling) charge includes surface delivery of all issues, except to subscribers in Argentina, Australia, Brasil, Canada, China, Hong Kong, India, Israel, Malaysia, Mexico, New Zealand, Pakistan, Singapore, South Africa, South Korea, Taiwan, Thailand and the U.S.A. who receive all issues by air delivery (S.A.L. — Surface Air Lifted) at no extra cost. For Japan, air delivery requires 50% additional charge; for all other countries airmail and S.A.L. charges are available upon request. Back volumes of the *Journal of Chromatography* (Vols. 1–460)are available at Dfl. 195.00 (plus postage). Claims for missing issues will be honoured, free of charge, within three months after publication of the issue. Customers in the U.S.A. and Canada wishing information on this and other Elsevier journals, please contact Journal Information Center, Elsevier Science Publishing Co. Inc., 655 Avenue of the Americas, New York, NY 10010. Tel. (212) 633-3750.

Abstracts/Contents Lists published in Analytical Abstracts, ASCA, Biochemical Abstracts, Biological Abstracts, Chemical Abstracts, Chemical Titles, Chromatography Abstracts, Clinical Chemistry Lookout, Current Contents/Physical, Chemical & Earth Sciences, Current Contents/Life Sciences, Deep-Sea Research/Part B: Oceanographic Literature Review, Excerpta Medica, Index Medicus, Mass Spectrometry Bulletin, PASCAL-CNRS, Pharmaceutical Abstracts, Referativnyi Zhurnal, Science Citation Index and Trends in Biotechnology.

See inside back cover for Publication Schedule, Information for Authors and information on Advertisements.

0021-9673/89/$03.50

This issue is printed on acid-free paper.

Printed in The Netherlands

CONTENTS

(Abstracts/Contents Lists published in Analytical Abstracts, ASCA, Biochemical Abstracts, Biological Abstracts, Chemical Abstracts, Chemical Titles, Chromatography Abstracts, Current Contents/Physical, Chemical & Earth Sciences, Current Contents/Life Sciences, Deep-Sea Research/Part B: Oceanographic Literature Review, Excerpta Medica, Index Medicus, Mass Spectrometry Bulletin, PASCAL-CNRS, Referativnyi Zhurnal and Science Citation Index)

Obituary: M. J. E. Golay (1902–1989)
by Cs. Horváth (New Haven, CT, U.S.A.) 1

Mobile phase effects on aromatic hydroxyl compounds with an aminopropyl column and interpretation by the Snyder model
by L. D. Olsen and R. J. Hurtubise (Laramie, WY, U.S.A.) (Received June 6th, 1989) . . 5

Gas chromatography of pure and surface-modified precipitated calcium carbonate
by T. Ahsan, B. A. Colenutt and K. S. W. Sing (Uxbridge, U.K.) (Received May 30th, 1989) 17

Kinetic analysis of the carboxypeptidase A hydrolysis of oligopeptides by reversed-phase high-performance liquid chromatography
by M. A. Serra, F. X. Avilés, E. Giralt and C. M. Cuchillo (Barcelona, Spain) (Received June 7th, 1989) 27

Reversed-phase high-performance liquid chromatographic separation of some indole and quinoline alkaloids from *Cinchona*
by A. Hermans-Lokkerbol, T. van der Leer and R. Verpoorte (Leiden, The Netherlands) (Received June 21st, 1989) 39

Multilayer coil planet centrifuge for analytical high-speed counter-current chromatography
by H. Oka, F. Oka and Y. Ito (Bethesda, MD, U.S.A.) (Received May 30th, 1989) . . . 53

Capillary gas chromatography–mass spectrometry and identification of substituted carboxylic acids in lipids extracted from a 4000-year-old Nubian burial
by F. O. Gülaçar, A. Buchs and A. Susini (Geneva, Switzerland) (Received June 19th, 1989) 61

Comparison of the use of mass spectrometry and methylene unit values in the determination of the stereochemistry of estranediol, the major urinary metabolite of 19-nortestosterone in the horse
by E. Houghton, A. Ginn, P. Teale, M. C. Dumasia and J. Copsey (Newmarket, U.K.) (Received May 23rd, 1989) 73

High-performance size-exclusion chromatography of poly- and oligoethylene terephthalate using a mixture of hexafluoroisopropanol and chloroform as the mobile phase
by N. Chikazumi, Y. Mukoyama and H. Sugitani (Ibaraki, Japan) (Received June 9th, 1989) 85

Application of high-performance liquid chromatography with spectrophotometric and electrochemical detection to the analysis of alkylenebis(dithiocarbamates) and their metabolites
by V. Bardarov, Chr. Zaikov and M. Mitewa (Sofia, Bulgaria) (Received April 24th, 1989) 97

Quantification and characterization of the trifluoroacetic anhydride derivatives of N,N′-ethylenebisstearamide and N,N′-ethylenebisoleamide
by P. A. Metz, F. L. Morse and T. W. Theyson (Williamsport, PA, U.S.A.) (Received May 26th, 1989) 107

Selective determination of benzo[*a*]pyrene in petroleum-based products using multi-column liquid chromatography
by P. R. Fielden and A. J. Packham (Manchester, U.K.) (Received June 5th, 1989) . . . 117

Chromatographic determination of amines in biological fluids with special reference to the biological monitoring of isocyanates and amines. I. Determination of 1,6-hexamethylenediamine using glass capillary gas chromatography and thermionic specific detection
by G. Skarping, M. Dalene, T. Brorson, J. F. Sandström, C. Sangö and A. Tiljander (Lund, Sweden) (Received June 2nd, 1989) 125

(Continued overleaf)

Chromatographic determination of amines in biological fluids with special reference to the biological monitoring of isocyanates and amines. II. Determination of 2,4- and 2,6-toluenediamine using glass capillary gas chromatography and selected ion monitoring
by J. F. Sandström, G. Skarping and M. Dalene (Lund, Sweden) (Received June 2nd, 1989) 135

Chromatographic determination of amines in biological fluids with special reference to the biological monitoring of isocyanates and amines. III. Determination of 4,4-'methylenedianiline in hydrolysed human urine using derivatization and capillary gas chromatography with selected ion monitoring
by A. Tiljander, G. Skarping and M. Dalene (Lund, Sweden) (Received June 9th, 1989) . 145

High-sensitivity high-performance liquid chromatographic analysis of diquat and paraquat with confirmation
by V. A. Simon and A. Taylor (Jacksonville, FL, U.S.A.) (Received May 5th, 1989) . . . 153

Notes

Optimization of size-exclusion separation of proteins on a Superose column
by P. L. Dubin and J. M. Principi (Indianapolis, IN, U.S.A.) (Received June 7th, 1989) . 159

Gas chromatographic retention indices of tear gases on capillary columns
by B. R. Gandhe, R. C. Malhotra and P. K. Gutch (Gwalior, India) (Received June 14th, 1989) 165

Use of a stop-flow technique to study on-column decomposition in supercritical fluid chromatography
by M. B. Evans and M. S. Smith (Hatfield, U.K.) and J. M. Oxford (Ware, U.K.) (Received June 13th, 1989) 170

Gas chromatographic separation of diastereomeric dicarbamate derivatives of γ- and δ-lactones
by K.-H. Engel (Berlin, F.R.G.), R. A. Flath (Albany, CA, U.S.A.) and W. Albrecht and R. Tressl (Berlin, F.R.G.) (Received June 7th, 1989) 176

Liquid chromatographic analysis of bromination reactions of metal trifluoroacetylacetonates
by T. J. Cardwell and T. H. Lorman (Bundoora, Australia) (Received July 4th, 1989) . . 181

High-performance liquid chromatographic analysis of *Solanum* steroidal alkaloids
by S. F. Osman (Philadelphia, PA, U.S.A.) and S. L. Sinden (Beltsville, MD, U.S.A.) (Received July 4th, 1989) 189

Determination of hydrogen sulphide by porous-layer open-tubular column gas chromatography–mass spectrometry
by S. Jacobsson and O. Falk (Solna, Sweden) (Received June 8th, 1989) 194

Supercritical fluid extraction of *s*-triazine herbicides from sediment
by V. Janda (Prague, Czechoslovakia) and G. Steenbeke and P. Sandra (Ghent, Belgium) (Received June 12th, 1989) 200

High-performance liquid chromatography of metribuzin and non-polar metabolites extracted from leaf tissues
by H. A. Norman, C. F. Mischke and J. B. St. John (Beltsville, MD, U.S.A.) (Received June 6th, 1989) 206

Separation of cationic technetium-99m amine complexes on porous graphitic carbon
by M. F. Emery and C. K. Lim (Harrow, U.K.) (Received June 12th, 1989) 212

Letter to the Editor

Reduced variation in retention times of biogenic amines by temperature control in liquid chromatography with electrochemical detection
by D. L. Palazzolo and S. K. Quadri (Manhattan, KS, U.S.A.) (Received July 3rd, 1989) . 216

In articles with more than one author, the name of the author to whom correspondence should be addressed is indicated in the article heading by a 6-pointed asterisk (*)

JOURNAL OF CHROMATOGRAPHY

VOL. 479 (1989)

JOURNAL *of* CHROMATOGRAPHY

INTERNATIONAL JOURNAL ON CHROMATOGRAPHY,
ELECTROPHORESIS AND RELATED METHODS

ELSEVIER
AMSTERDAM — OXFORD — NEW YORK — TOKYO

0021-9673/89/$03.50

Printed in The Netherlands

Journal of Chromatography, 479 (1989) 1–3
Elsevier Science Publishers B.V., Amsterdam — Printed in The Netherlands

CHROM. 21 818

Obituary

M. J. E. Golay (1902–1989)

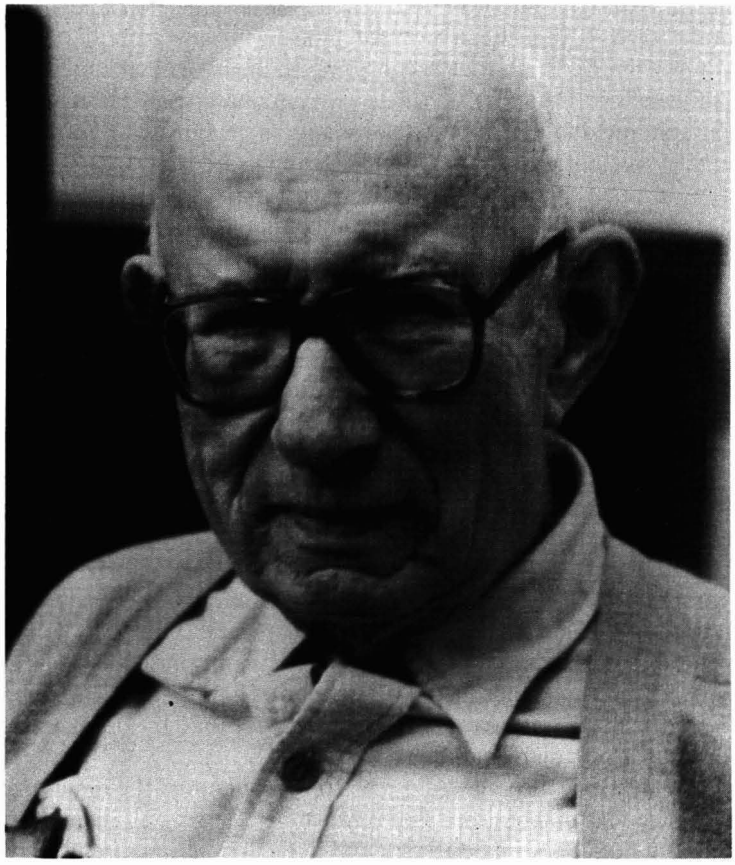

Marcel J. E. Golay, one of the leading scientists in chromatography, died at the age of 86 on April 27, 1989. As with some other prominent figures who laid down the foundation of modern chromatography, his training was not in chemistry but in other fields. Golay was an electrical engineer/physicist with excellent mathematical skills and an uncanny insight into the physical phenomena underlying the subject of his inquiry. Beyond that he was a distinguished inventor and innovator. To chromatographers he is best known as the father of capillary columns, which are often referred to as Golay columns. In the middle of the 1950s, as the meteoric growth of gas

0021-9673/89/$03.50

chromatography commenced, Golay concluded, after analyzing the disadvantages of packed columns, that open tubes with a retentive wall would require less pressure drop for a theoretical plate than comparable packed columns, and therefore would offer great advantages in gas chromatography. First, at fixed pressure drop the use of a comparatively long open tubular column would yield higher efficiency than that obtainable with a packed column. Alternatively, an open tubular column can be operated at a lower mean pressure of the carrier gas than a packed column chosen as the suitable reference, so that the concomitantly higher diffusivity results in increased efficiency. Indeed, Golay correctly perceived that the anfractuous flow field in a packed bed is associated with low mass to momentum transfer efficiency and open tubes offer a superior choice. It did not take much time for Golay to reduce this concept to practice in 1956, and to present a complete mathematical treatment of axial dispersion in laminar flow through open ducts with circular cross section and a retentive inner wall. It amounted to the Golay equation that first expressed rigorously the various plate height contributions in open tubular columns.

The introduction of open tubular columns, however, imposed a challenge on instrument design because, for practical reasons, the tube diameter has to be small: not greater than 0.5 mm. As a result the flow-rate of the carrier gas and the loading capacity of the column, which is adversely affected also by the typically low phase ratio, in such columns were much smaller than with the packed columns of those days. Thus open tubular columns required detectors with very small dead and sensing volumes, novel sampling techniques and a much more demanding construction than that of the usual gas chromatographs that were built for use with packed columns of rather large dimensions. Fortuitously, the flame ionization detector was invented at about the same time as the capillary column; the match was perfect and a new generation of gas chromatographs was born. Golay's columns were called capillary columns because of their small inner diameter. He always emphasized, however, that it is not the size but the openness of the column, *i.e.*, the absence of anastomosis, that is the distinguishing feature of capillary columns. Indeed, the Golay equation is just as applicable to a 3 ft. I.D. oil pipeline as to a 10 mm I.D. capillary column. For this reason the term "open tubular columns" appeared to be more appropriate, and now it is frequently used in the literature. Since then a variety of other columns of capillary dimensions, *e.g.*, packed capillaries, have been developed, so that the term open tubular column has gained a new significance.

Yet, Golay's work has to be also viewed as the starting point of the miniaturization of chromatographic instrumentation. Today we are witnessing an increasing use of capillary columns in liquid chromatography and in fact open tubes are widely employed in analytical instruments such as those for capillary electrophoresis or flow injection analysis.

Capillary columns have changed gas chromatography and with time capillary columns have also undergone changes. Golay recognized the major shortcoming of his columns, the low phase ratio that results in low loading capacity and low eluite concentrations in the effluent, and he proposed in 1960 to make columns with a porous layer at the inner wall. Shortly thereafter support-coated open tubular columns were introduced and thus columns with higher loading capacity became available. In the last decade glass and fused-silica capillaries have largely replaced the metal tubes used previously, and these columns, with sophisticated surface treatment

and novel stationary phases, manifest the final triumph of Golay's original concept.

M. J. E. Golay was born on May 3, 1902 in Neuchâtel, Switzerland. He studied electrical engineering at the Eidgenössische Technische Hochschule in Zürich and graduated in 1924. Subsequently he came to the U.S.A. and was employed by Bell Telephone Laboratories until 1928. Then he left for the University of Chicago where he received a Ph.D. in Physics in 1931. After graduation Dr. Golay joined the U.S. Signal Corps Engineering Laboratories in Fort Monmouth, NJ. At this large and prestigious center of research on electronics and communications he mainly worked with defense-oriented systems and made significant (unpublished) contributions to the war effort. At the end of his tenure with the U.S. Signal Corps he was Chief Scientist of the Components Division and then retired in 1955. After his retirement Dr. Golay devoted himself to consulting work with the Philco Corporation in the field of information theory and with The Perkin-Elmer Corporation in the field of scientific instrumentation. He was Professor at the Technische Hogeschool in Eindhoven, The Netherlands, in 1961–1962. From 1963 until his decease he had been Senior Research Scientist at Perkin-Elmer.

Dr. Golay authored close to 100 scientific papers and over 40 patents. He received numerous awards, among them the Harry Diamond Award of the Institute of Radio Engineers (1950), the American Chemical Society Award in Chemical Instrumentation (1961), the Distinguished Achievement Award of the Instrument Society of America (1962), the J. Hamilton Award of the American Society of Naval Engineers (1972), the Chromatography Anniversary Medal of the Academy of Sciences of the U.S.S.R. (1979), the American Chemical Society Award in Chromatography (1981), and the S. Dal Nogare Award in Chromatography of the Delaware Valley Chromatography Forum (1982). The École Polytechnique Fédérale of Lausanne, Switzerland, conferred an honorary doctorate on him in 1977.

He crossed many interdisciplinary lines and made numerous major scientific and technical contributions in addition to the invention of capillary columns for chromatography. In the field of radio communications he has been known for the so-called Golay delay line. In information theory and pattern recognition he introduced several powerful code systems and novel approaches to signal processing. He applied his experience in this field to analytical chemistry and developed elegant methods for processing analytical signals to reduce noise and improve resolution. In analytical instrumentation his work in infrared spectroscopy, which included the invention of the Golay detector, is well known.

Until his death Dr. Golay was active scientifically. His recent research interest was focussed on bandspreading under conditions of potential significance in high-speed liquid chromatography. Very recently his attention had turned again to open tubular columns and he became interested in the effect of turbulence. Indeed a logical further development of his original concept would lead to the use of open tubes with turbulent flow: a continuation that offers an even higher mass-to-momentum transfer efficiency, and if practicable, could provide higher speed of analysis and column efficiency. The community of chromatographers owes a great deal to Marcel Golay; through his accomplishments he will be remembered by generations to come.

New Haven, CT (U.S.A.) CSABA HORVÁTH

Journal of Chromatography, 479 (1989) 5–16
Elsevier Science Publishers B.V., Amsterdam — Printed in The Netherlands

CHROM. 21 671

MOBILE PHASE EFFECTS ON AROMATIC HYDROXYL COMPOUNDS WITH AN AMINOPROPYL COLUMN AND INTERPRETATION BY THE SNYDER MODEL

L. D. OLSEN and R. J. HURTUBISE*
Department of Chemistry, University of Wyoming, P.O. Box 3838, Laramie, WY 82071 (U.S.A.)
(First received April 17th, 1989, revised manuscript received June 6th, 1989)

SUMMARY

The Snyder chromatographic model was employed to correlate and interpret the retention data of hydroxyl aromatics on a high-performance aminopropyl bonded-phase column. Several *n*-heptane–2-propanol and *n*-heptane–ethyl acetate mobile phases were used to obtain the retention data. Plots of the logarithm of the capacity factor ($\log k'$) *vs.* solvent strength and $\log k'$ *vs.* log (mole fraction of the strong solvent) showed good linearity for all the hydroxyl aromatics studied. Because a value of the solvent strength for 2-propanol on the aminopropyl bonded-phase was not available, the solvent strength for 2-propanol on silica was used in an empirical fashion. The slopes from the plots of $\log k'$ *vs.* solvent strength for ethyl acetate from an aminopropyl bonded-phase column were used to obtain experimental areas of the solutes. The experimental molecular areas were compared with calculated values, and the results showed that the localization of the solutes and the polarity of the mobile phases were important considerations. The results also indicated that the *n*-heptane–ethyl acetate data correlated very well with the Snyder model.

INTRODUCTION

Reversed- and normal-phase high-performance liquid chromatography (HPLC) can provide information on highly complex mixtures. As retention and selectivity are dependent on specific functional group–stationary phase interactions, normal-phase HPLC offers some advantages in separating functional classes and isomers[1]. Normal-phase HPLC has been found to be very useful in separating coal-derived liquids because frequently coal liquids are not soluble in the water-based solvents often used in reversed-phase HPLC[2].

A number of models have been developed to explain the roles of the solvent, solute and stationary phase in normal-phase HPLC[3–16]. If a given model is capable of describing the retention of solutes, then the model can be used to predict retention for similar chromatographic systems. In addition, mobile phases that would provide the best resolution and selectivity could then be predicted from the model.

Scott and co-workers[10–13] have considered solute–mobile phase and solute–

0021-9673/89/$03.50

stationary phase interactions for silica gel. The Snyder adsorption model is based on displacement of solvent molecules by solute molecules from the stationary phase surface[8,9]. The model of Soczewiński and co-workers[3–7] is similar to that developed by Snyder. The Hennion *et al.*[14] approach for aminopropyl-bonded silica contains elements from the Snyder, Soczewiński and Scott models. Snyder and co-workers[8,17] have reviewed the first three models and all four models were summarized by Snyder and Schunk[18]. Hydrogen bonding and other interactions were used by Chang and co-workers[15,16] to explain the retention behavior on an aminopropyl bonded-phase column.

The models developed by Snyder and Soczewiński have been used to describe a number of interactions in several chromatographic systems. The approaches of Snyder and Soczewiński were used by Hurtubise *et al.*[19] to explain some of the retention characteristics of alkylphenols on an aminopropyl bonded-phase column and by Hussain *et al.*[20] to interpret retention results for alkylphenols on a cyanopropyl bonded-phase column and a silica column. Some of the interactions of polar solutes on a silica column and a nitrophenyl bonded-phase column were described by Ruckmick and Hurtubise[21,22] using the Snyder approach. Scolla and Hurtubise[23] concluded that elements of the Snyder model could describe the retention behavior of aromatic nitrogen compounds on an aminopropyl bonded-phase column. Olsen and Hurtubise[24] used the Snyder concepts to characterize the retention properties of several aromatic hydroxyl compounds on a silica stationary phase. Snyder[25] found that the behavior of diastereomers on a silica column could be evaluated by his model. In addition, Snyder and Schunk[18] employed the Snyder model to characterize an amino bonded-phase column. Hammers *et al.*[26] concluded that an amino bonded-phase column behaved like partially deactivated silica gel. Weiser *et al.*[27] reached similar conclusions for a cyanopropyl bonded-phase column. Smith and Cooper[28] applied Snyder's concepts to amino, cyano, and diol bonded-phase columns to describe solute retention with several different mobile phase systems.

In this study, aromatic hydroxyl compounds were investigated on an aminopropyl bonded-phase column using different solvent compositions of *n*-heptane–2-propanol and *n*-heptane–ethyl acetate. The data were interpreted with the Snyder displacement model. The compounds studied were selected on the basis of similar size and structure but differing acidities, polarities and hydrogen-bonding abilities.

EXPERIMENTAL

The equipment, experimental conditions and procedures have been reported previously[24]. However, there were a few differences, and these are indicated as follows. The detector was set at 254 nm. The columns used were 30 cm × 3.9 mm I.D. prepacked μBondapak NH_2 columns obtained from Waters Assoc. (Milford, MA, U.S.A.). The μBondapak NH_2 columns contained aminopropyl groups chemically bonded to irregular-shaped 10-μm porous silica. The compositions of the *n*-heptane–2-propanol mobile phases were 99:1, 98:2, 97:3, 96:4, 95:5, 94:6, 93:7, 92:8, 91:9, 90:10 and 89:11 (v/v), and those of the *n*-heptane–ethyl acetate mobile phases were 85:15, 82:18, 80:20, 77:23, 75:25, 73:27, 70:30, 65:35, 60:40, 55:45 and 50:50 (v/v). Table I gives the names, structures and pK_a values of the compounds investigated.

TABLE I

COMPOUNDS STUDIED ON AN AMINOPROPYL COLUMN AND THEIR pK_a VALUES

No.	*Compound*	*Structure*	*pK_a*
1	1-Naphthol	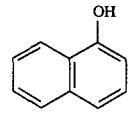	9.3[a]
2	2-Naphthol	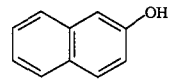	9.6[a]
3	1,2,3,4-Tetrahydro-1-naphthol	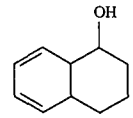	15.7[b]
4	5,6,7,8-Tetrahydro-1-naphthol	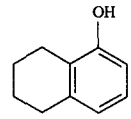	10.3[a]
5	1-Naphthalenemethanol	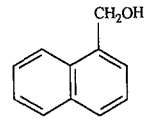	15.3[b]
6	1-Naphthaleneethanol	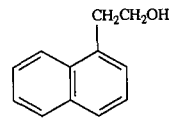	15.2[b]
7	2-Naphthalenemethanol	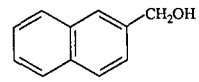	15.3[b]
8	2-Naphthaleneethanol	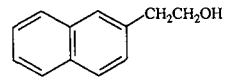	15.2[b]

[a] From ref. 29.

[b] Calculated from information in ref. 30.

RESULTS AND DISCUSSION

Theoretical considerations

The following equation is fundamental to the Snyder model:

$$X_m + nS_a \rightleftharpoons X_a + nS_m \quad (1)$$

where the subscripts m and a refer to the mobile phase and adsorbed phase, respectively. The adsorption of a solute molecule, X, causes the displacement of n solvent molecules, S. The solvent strength of a non-localizing binary mobile phase on a bonded-phase column can be calculated with eqn. 2 according to Snyder and Schunk[18] and Snyder[31] if the adsorbent activity, α', is known

$$\varepsilon_{AB} = \varepsilon_A + \log[N_B 10^{\alpha' n_b(\varepsilon_A - \varepsilon_B)} + 1 - N_B]/\alpha' n_b \quad (2)$$

where ε_{AB} is the solvent strength of the binary eluent, ε_A and ε_B are the solvent strengths of the pure weak and strong solvent, respectively, N_B is the mole fraction of solvent B and n_b is the relative molecular area of a molecule of solvent B. The ε_B term can vary with N_B owing to restricted-access delocalization of the strong solvent on silica and alumina according to Snyder and Schunk[18] and Snyder[32]. However, restricted-access delocalization should be minimal for aminopropyl bonded-phases because of the flexible nature of the bonded functional group in the stationary phase[18]. Therefore, ε_B in eqn. 2 should be a constant for an aminopropyl bonded-phase according to Snyder and Schunk[18] and Snyder[32].

Snyder[17] has shown that the retention of a solute will vary in a binary mobile phase of two different compositions according to the following equation:

$$\log (k'_2/k'_1) = \alpha' A_s(\varepsilon_1 - \varepsilon_2) \quad (3)$$

where k'_1 is the capacity factor of the solute in mobile phase 1 of solvent strength ε_1 and k'_2 is the capacity factor of the solute in the second mobile phase of solvent strength ε_2. If mobile phase 1 is n-heptane then ε_1 is zero. The α' term is defined arbitrarily as being equal to unity for the aminopropyl bonded-phase column[18]. The slope of $\log k'_2$ *vs.* ε_2 is equal to $\alpha' A_s$; hence experimental A_s values can be obtained from the slope. If the solutes are polar, they can localize and site-competition delocalization can occur on an aminopropyl bonded-phase column owing to the exposed nature of the functional group. Thus, the experimental A_s values will be larger than expected[18,33].

Another equation that can be derived from the Snyder approach is

$$\log k' = \log k'_0 - (A_s/n_b) \log X_s \quad (4)$$

where A_s is the molecular area of the solute, n_b is the strong solvent molecular area, k' is the capacity factor of the solute eluted in the binary mobile phase, k'_0 is the capacity factor of the solute eluted in the pure strong solvent, and X_s is the mole fraction of the strong solvent in the binary mobile phase[17]. In the derivation of eqn. 4, it is assumed that the $1 - N_B$ term in the logarithmic expression in eqn. 2 is small and ε_B does not vary with N_B. Eqn. 4 has been shown to be valid if very polar binary mobile phases are being used[17,25].

In this study, A_s values were calculated using the following equation developed by Snyder[34] for unsubstituted aromatic hydrocarbons:

$$A_s = 6 + 0.80(h - 6) + 0.25(c - h) \quad (5)$$

where h is the number of aromatic hydrogens in the solute and c is the number of aromatic carbons in the solute. The A_s values increase by 7.6 and 8.5 units for aromatic and aliphatic OH groups, respectively, for a silica stationary phase[34].

Plots of log k' vs. solvent strength

The solvent strength values used in this work were taken from data published by Snyder and Glajch[33] and Scolla and Hurtubise[23]. Snyder and Glajch[33] listed solvent strength values for *n*-hexane–2-propanol and *n*-hexane–ethyl acetate mobile phases on chromatographic silica. Scolla and Hurtubise[23] gave solvent strength values for *n*-heptane–ethyl acetate mobile phases on an aminopropyl bonded-phase column. To our knowledge, the solvent strength for 2-propanol has not been calculated for an aminopropyl bonded-phase column. The calculation of a solvent strength value for 2-propanol is complicated by the fact that 2-propanol can behave both as a hydrogen-bond donor and as a hydrogen-bond acceptor. In the past, the retention properties of polycyclic aromatic hydrocarbons have been used as a basis for the calculation of the solvent strengths for *n*-heptane–ethyl acetate[18,23]. However, with *n*-heptane–2-propanol the retention times of polycyclic aromatic hydrocarbons are so small that they cannot easily be used as a means of calculating solvent strengths. Therefore, in this work it was assumed that the solvent strengths for the *n*-hexane–2-propanol solvents from silica would be applicable to an aminopropyl bonded-phase column. In addition, a similar assumption was made for *n*-hexane–ethyl acetate when using solvent strengths from silica. The main reason for these assumptions was to determine if empirical correlations could be developed between the solvent strengths from silica and the capacity factors from the aminopropyl bonded-phase column.

The solvent strength of a given mole fraction of strong solvent should be almost the same whether *n*-hexane or *n*-heptane is used, as both solvents have essentially the same solvent strength (zero) and selectivity. The solvent strengths were determined for this work by plotting the solvent strength values against the mole fraction of the strong solvent listed by Snyder and Glajch[33] or Scolla and Hurtubise[23]. Then, by knowing the mole fraction of the strong solvent used in this work, the solvent strength values were obtained from the graphs. Tables II and III list the various mobile phase compositions, log k' values for the solutes, and the solvent strength values used in this work for *n*-heptane–2-propanol and *n*-heptane–ethyl acetate mobile phases, respectively.

Using eqn. 3, plots of log k' from the aminopropyl bonded-phase column *vs.* solvent strength values from silica for the solutes listed in Table I yielded linear correlation coefficients ranging from -0.994 to -0.996 for the 2-propanol binary mobile phases and from -0.987 to -0.990 for the ethyl acetate binary mobile phases (Table IV). The graphs for the standards were linear for a wide range of 2-propanol compositions, with one point well off each line for the weakest solvent compositions used. These points were from the capacity factor values for the solutes in the weakest mobile phase. These capacity factor values were near to or greater than 10, except for compound 3. The graphs for the ethyl acetate mobile phases were not as good since all

TABLE II

LOG k' VALUES FOR THE MODEL COMPOUNDS ON AN AMINOPROPYL BONDED-PHASE COLUMN WITH *n*-HEPTANE–2-PROPANOL MOBILE PHASES (25°C)

Compound No.	*Mole fraction 2-propanol*										
	0.019 (99:1)[a]	*0.038 (98:2)*	*0.056 (97:3)*	*0.074 (96:4)*	*0.094 (95:5)*	*0.109 (94:6)*	*0.126 (93:7)*	*0.143 (92:8)*	*0.159 (91:9)*	*0.175 (90:10)*	*0.191 (89:11)*
1	1.263	0.916	0.738	0.597	0.497	0.418	0.321	0.280	0.222	0.169	0.125
2	1.360	0.998	0.788	0.651	0.559	0.456	0.385	0.316	0.258	0.203	0.155
3	0.642	0.368	0.222	0.109	0.000	−0.07	−0.12	−0.19	−0.24	−0.28	−0.32
4	0.874	0.564	0.402	0.280	0.182	0.109	0.040	−0.02	−0.09	−0.12	−0.18
5	1.000	0.711	0.541	0.418	0.331	0.246	0.168	0.109	0.058	0.020	−0.02
6	0.940	0.637	0.463	0.340	0.258	0.155	0.093	0.040	0.010	−0.07	−0.12
7	1.045	0.738	0.564	0.441	0.350	0.246	0.183	0.125	0.076	0.020	−0.02
8	0.947	0.651	0.484	0.350	0.280	0.169	0.109	0.040	0.000	−0.07	−0.09
Log X_s	−1.721	−1.420	−1.252	−1.131	−1.036	−0.962	−0.900	−0.845	−0.799	−0.757	−0.719
ε_{AB}[b]	0.308	0.322	0.338	0.348	0.360	0.370	0.378	0.387	0.393	0.401	0.406

[a] *n*-Heptane–2-propanol composition (v/v) in parentheses.
[b] Solvent strength values on silica taken from information in ref. 33.

of the graphs had a slight curvature. However, the lowest correlation coefficient was −0.987, which indicated that they were approximately linear. The slopes, intercepts and correlation coefficients obtained for these log k' values from the aminopropyl bonded-phase column *vs.* solvent strength values from silica are given in Table IV. These results are strictly empirical and at present have no firm theoretical basis.

TABLE III

LOG k' VALUES FOR MODEL COMPOUNDS ON AN AMINOPROPYL BONDED-PHASE COLUMN WITH *n*-HEPTANE–ETHYL ACETATE MOBILE PHASES (25°C)

Compound No.	*Mole fraction ethyl acetate*										
	0.209 (85:15)[a]	*0.248 (82:18)*	*0.273 (80:20)*	*0.309 (77:23)*	*0.333 (75:25)*	*0.357 (73:27)*	*0.391 (70:30)*	*0.447 (65:35)*	*0.500 (60:40)*	*0.551 (55:45)*	*0.600 (50:50)*
1	0.787	0.679	0.612	0.522	0.468	0.422	0.369	0.258	0.179	0.111	0.045
2	0.888	0.780	0.701	0.615	0.561	0.506	0.449	0.340	0.260	0.179	0.124
3	0.655	0.554	0.481	0.401	0.344	0.294	0.248	0.140	0.064	0.000	−0.08
4	0.455	0.344	0.276	0.199	0.130	0.083	0.037	−0.08	−0.13	−0.21	−0.28
5	0.910	0.797	0.721	0.630	0.572	0.519	0.456	0.336	0.260	0.173	0.111
6	1.015	0.906	0.820	0.739	0.678	0.624	0.567	0.449	0.365	0.288	0.230
7	0.390	0.845	0.770	0.680	0.621	0.566	0.508	0.389	0.305	0.223	0.164
8	1.005	0.892	0.812	0.724	0.669	0.615	0.554	0.435	0.352	0.270	0.212
Log X_s	−0.680	−0.605	−0.564	−0.510	−0.478	−0.447	−0.408	−0.350	−0.301	−0.259	−0.222
ε_{AB}[b]	0.321	0.330	0.337	0.343	0.348	0.355	0.363	0.377	0.389	0.402	0.413
ε_{AB}[c]	0.054	0.060	0.063	0.068	0.070	0.073	0.076	0.080	0.083	0.086	0.090

[a] *n*-Heptane–ethyl acetate composition (v/v) in parentheses.
[b] Solvent strength values on silica taken from information in ref. 33.
[c] Solvent strength values on an aminopropyl bonded-phase column taken from information in ref. 23.

TABLE IV

SLOPES, INTERCEPTS AND CORRELATION COEFFICIENTS FOR LOG k' *VS.* SOLVENT STRENGTH DATA FOR 2-PROPANOL AND ETHYL ACETATE BINARY MOBILE PHASES

Log k' values are from an aminopropyl bonded-phase column with solvent strength values from silica.

Mobile phase component	*Compound No.*	*Slope*	*Intercept*	*Correlation coefficient*
2-Propanol	1	−9.19	3.83	−0.994
	2	−9.67	4.06	−0.995
	3	−8.06	2.94	−0.996
	4	−8.57	3.29	−0.996
	5	−8.56	3.43	−0.995
	6	−8.67	3.39	−0.996
	7	−8.84	3.54	−0.996
	8	−8.75	3.43	−0.996
Ethyl acetate	1	−7.84	3.45	−0.989
	2	−8.18	3.45	−0.988
	3	−7.68	3.06	−0.989
	4	−7.67	2.85	−0.987
	5	−8.51	3.58	−0.990
	6	−8.38	3.64	−0.989
	7	−8.50	3.63	−0.989
	8	−8.46	3.65	−0.989

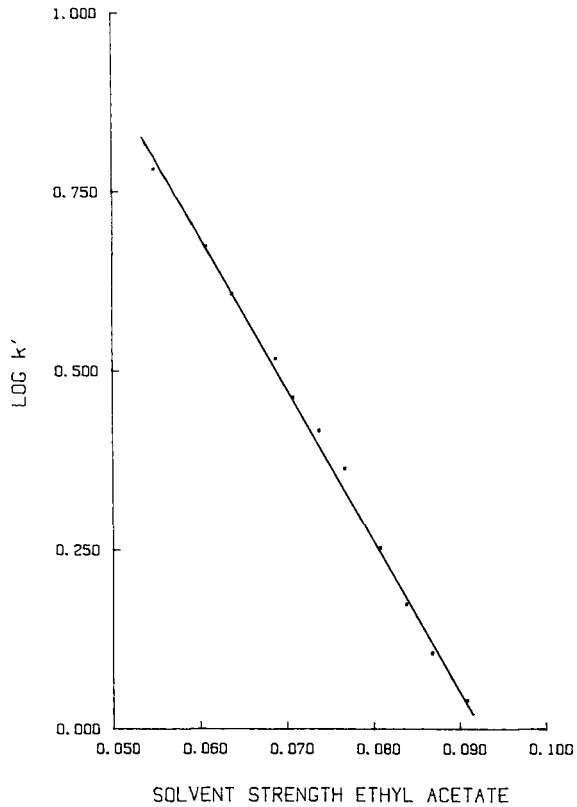

Fig. 1. Plot of log k' *vs.* solvent strength (ε) data from the aminopropyl bonded-phase column for 1-naphthol using *n*-heptane–ethyl acetate mobile phases.

TABLE V

SLOPES, INTERCEPTS AND CORRELATION COEFFICIENTS FOR LOG k' *VS.* SOLVENT STRENGTH FOR *n*-HEPTANE–ETHYL ACETATE MOBILE PHASES

Log k' and solvent strength values are from an aminopropyl bonded-phase column.

Compound No.	*Slope*	*Intercept*	*Correlation coefficient*
1	−20.66	1.92	−0.998
2	−21.45	2.06	−0.999
3	−20.21	1.76	−0.998
4	−20.24	1.56	−0.998
5	−22.40	2.14	−0.998
6	−22.07	2.22	−0.998
7	−22.40	2.19	−0.999
8	−22.27	2.22	−0.998

However, the results can be used in a practical fashion to predict the retention of hydroxyl aromatics.

If the solvent strength values for *n*-heptane–ethyl acetate mobile phases from an aminopropyl bonded-phase column from Scolla and Hurtubise[23] were used, plots of log k' *vs.* solvent strength yielded excellent correlation coefficients ranging from −0.998 to −0.999 (Fig. 1). The results for the slopes, intercepts and correlation coefficients are given in Table V. The main reason why the correlation coefficients are better in Table V than in Table IV is that the solvent strength data for an aminopropyl bonded-phase column were used rather than solvent strength values from silica. Use of

TABLE VI

SLOPES, INTERCEPTS AND CORRELATION COEFFICIENTS FOR LOG k' *VS.* LOG (MOLE FRACTION) PLOTS FOR 2-PROPANOL AND ETHYL ACETATE BINARY MOBILE PHASES

Mobile phase component	*Compound No.*	*Slope*	*Intercept*	*Correlation coefficient*
2-Propanol	1	−1.13	−0.68	−1.00
	2	−1.19	−0.70	−1.00
	3	−0.96	−1.00	−0.999
	4	−1.04	−0.90	−0.999
	5	−1.01	−0.73	−0.999
	6	−1.05	−0.85	−0.999
	7	−1.07	−0.78	−1.00
	8	−1.05	−0.84	−0.999
Ethyl acetate	1	−1.63	−0.31	−1.00
	2	−1.69	−0.25	−1.00
	3	−1.59	−0.42	−0.999
	4	−1.60	−0.62	−0.999
	5	−1.77	−0.28	−1.00
	6	−1.74	−0.16	−1.00
	7	−1.77	−0.23	−1.00
	8	−1.76	−0.18	−1.00

the solvent strength values from an aminopropyl bonded-phase column has a strong theoretical basis[9,18].

Plots of log k' vs. log (mole fraction of the strong solvent)

For polar mobile phases, eqn. 4 should give a linear relationship for log k' *vs.* log (mole fraction of the strong solvent)[17]. Results from the graphs of log k' *vs.* log (mole fraction of the strong solvent) are given in Table VI. The high correlation coefficients, ranging from -0.999 to -1.00, indicate that the plots are linear. Figs. 2 and 3 show log k' *vs.* log (mole fraction of the strong solvent) graphs for 1-naphthol in *n*-heptane–2-propanol and *n*-heptane–ethyl acetate mobile phases, respectively. This approach should be applicable to predicting retention for polar solutes with polar mobile phases on an aminopropyl bonded-phase column. The theoretical aspects of the graphs of log k' *vs.* log (mole fraction of the strong solvent) for aminopropyl bonded-phase columns have not been fully developed. In the remaining part of the paper, only the relationship between log k' and solvent strength values from an aminopropyl bonded-phase column will be discussed.

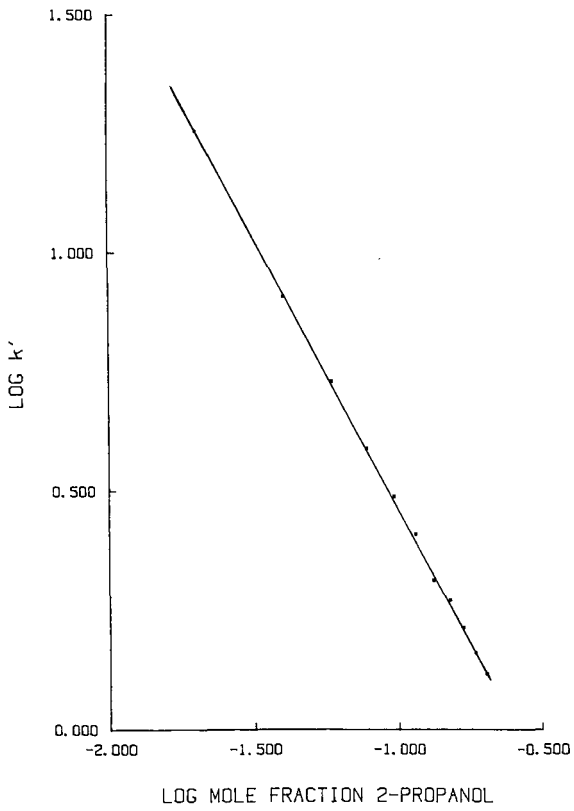

Fig. 2. Plot of log k' *vs.* log (mole fraction of 2-propanol) for 1-naphthol using *n*-heptane–2-propanol mobile phases.

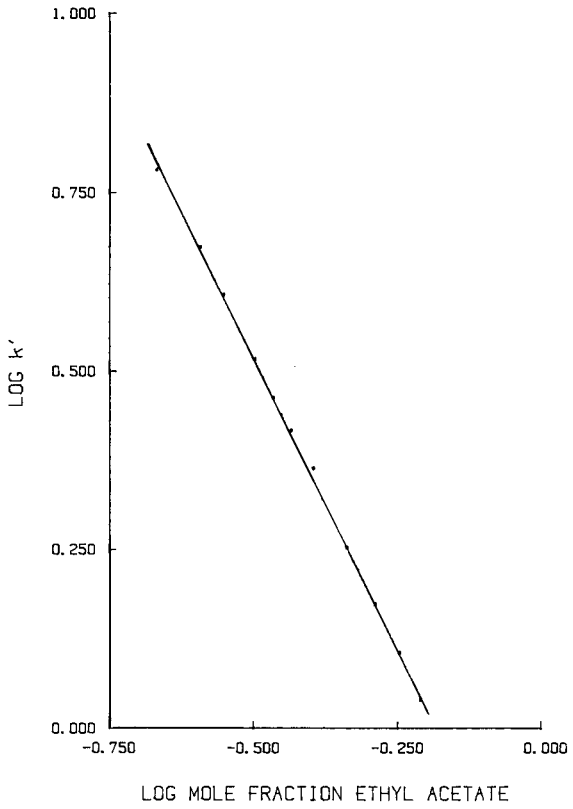

Fig. 3. Plot of log k' *vs.* log (mole fraction of ethyl acetate) for 1-naphthol using *n*-heptane–ethyl acetate mobile phases.

Theoretical interpretations

Snyder and Schunk[18] in comparing aminopropyl bonded-phase and silica columns, noted that retention on an aminopropyl bonded-phase column is generally lower. This means that the solutes and the solvents do not localize as strongly on an aminopropyl bonded-phase column. Also, the solvent strength values will differ on the two types of columns as restricted-access delocalization is minimal on an aminopropyl bonded-phase column[18] and therefore the solvent strength values will not be as large on the aminopropyl column. This is supported by the solvent strength data reported in Table III for the *n*-heptane–ethyl acetate mobile phases and other data reported in the literature[9,18].

Owing to the polar nature of the solutes (see Table I), localization and hydrogen bonding of these solutes to the stationary phase are expected. If localization or hydrogen bonding does occur, the experimental A_s values will be larger than the calculated A_s values[25,32,33]. Other factors to consider are interactions among solvent and solute molecules and their effects on solvent strength. Snyder[9] has shown that with an aminopropyl bonded-phase column the contribution of molecular interactions to solvent strength should be reduced by about half in comparison with silica.

The slopes in Table V are equal to $\alpha' A_s$, according to eqn. 3; α' will be arbitrarily

TABLE VII

CALCULATED AND EXPERIMENTAL A_s VALUES USING LOG k' *VS.* SOLVENT STRENGTH DATA FOR *n*-HEPTANE–ETHYL ACETATE MOBILE PHASES

Log k' and solvent strength values are from an aminopropyl bonded-phase column.

Compound No.	A_s *(calc.)*	A_s *(exptl.)*	ΔA_s
1	15.7	20.7	−5.0
2	15.7	21.4	−5.7
3	18.1	20.2	−2.1
4	17.2	20.2	−3.1
5	17.5	22.4	−4.9
6	18.4	22.1	−3.7
7	17.5	22.4	−4.9
8	18.4	22.3	−3.9

assumed to have a value of unity[18]. Using this information, the slopes in Table V and eqns. 3 and 5, the experimental and calculated A_s values can be determined. Table VII contains a list of the calculated A_s, experimental A_s and ΔA_s (calculated A_s − experimental A_s) values from plots of log k' from the aminopropyl bonded-phase column *vs.* solvent strength values from an aminopropyl bonded-phase column for the *n*-heptane–ethyl acetate mobile phases. In Table VII, all of the experimental A_s values are larger than the calculated A_s values, which indicates that site-competition delocalization is occurring[9,18]. It is expected that the compounds with the smaller pK_a values would donate a proton more readily and therefore more strongly localize or hydrogen bond with the stationary phase and have larger ΔA_s values. However, if the ΔA_s values are compared with the pK_a values in Table I, no pattern appears to stand out. This indicates that other factors are more important than pK_a values. This is not surprising, given the overall complexity of the chromatographic interactions.

CONCLUSIONS

The linearity for plots of log k' *vs.* solvent strength and log k' *vs.* log (mole fraction of the strong solvent) for both the aminopropyl bonded-phase column and earlier results with a silica column[24] would be useful for predicting the retention of hydroxyl aromatics. Because a solvent strength value for 2-propanol is not available for the aminopropyl bonded-phase column, it was not possible to correlate the *n*-heptane–2-propanol retention data directly with the Snyder model. However, the linear plots acquired for log k' *vs.* solvent strength for ethyl acetate from an aminopropyl bonded-phase column and the relatively large A_s (exptl.) values for the aminopropyl bonded-phase column showed that the Snyder model readily described the retention characteristics of the hydroxyl aromatics for this chromatographic system. Similar conclusions were reached for the *n*-heptane–ethyl acetate mobile phases on a silica column[24].

ACKNOWLEDGEMENTS

Financial support for this project was provided by the U.S. Department of Energy under contract No. DE-AC22-83PC60015. Partial support was provided to L.D.O. by the Patricia Roberts Harris Fellowship program through the University of Wyoming.

REFERENCES

1 L. R. Snyder and J. J. Kirkland, *Introduction to Modern Liquid Chromatography*, Wiley-Interscience, New York, 2nd ed., 1979.
2 R. S. Brown and L. T. Taylor, *Anal. Chem.*, 55 (1983) 723.
3 E. Soczewiński, *Anal. Chem.*, 41 (1969) 179.
4 E. Soczewiński and G. Matysik, *J. Chromatogr.*, 48 (1970) 57.
5 E. Soczewiński, *J. Chromatogr.*, 130 (1977) 23.
6 E. Soczewiński and T. Dzido, *Chromatographia*, 22 (1986) 25.
7 E. Soczewiński, *J. Chromatogr.*, 388 (1987) 91.
8 L. R. Snyder and H. Poppe, *J. Chromatogr.*, 184 (1980) 363.
9 L. R. Snyder, in Cs. Horváth (Editor), *High-Performance Liquid Chromatography—Advances and Perspectives*, Vol. 3, Academic Press, New York, 1983, pp. 157–223.
10 R. P. W. Scott and P. Kucera, *J. Chromatogr.*, 112 (1975) 425.
11 R. P. W. Scott, *J. Chromatogr.*, 122 (1976) 35.
12 R. P. W. Scott and P. Kucera, *J. Chromatogr.*, 149 (1978) 93.
13 R. P. W. Scott and P. Kucera, *J. Chromatogr.*, 171 (1979) 37.
14 M. C. Hennion, C. Picard, C. Combellas, M. Caude and R. Rosset, *J. Chromatogr.*, 210 (1981) 211.
15 C. A. Chang and C. S. Huang, *Anal. Chem.*, 57 (1985) 997.
16 C. A. Chang and L. T. Tan, *J. Liq. Chromatogr.*, 8 (1985) 995.
17 L. R. Snyder, *Anal. Chem.*, 46 (1974) 1384.
18 L. R. Snyder and T. C. Schunk, *Anal. Chem.*, 54 (1982) 1764.
19 R. J. Hurtubise, A. Hussain and H. F. Silver, *Anal. Chem.*, 53 (1981) 1993.
20 A. Hussain, R. J. Hurtubise and H. F. Silver, *J. Chromatogr.*, 252 (1982) 21.
21 S. C. Ruckmick and R. J. Hurtubise, *J. Chromatogr.*, 360 (1986) 343.
22 S. C. Ruckmick and R. J. Hurtubise, *J. Chromatogr.*, 361 (1986) 47.
23 P. L. Scolla and R. J. Hurtubise, *J. Chromatogr.*, 405 (1987) 107.
24 L. D. Olsen and R. J. Hurtubise, *J. Chromatogr.*, 474 (1989) 347.
25 L. R. Snyder, *J. Chromatogr.*, 245 (1982) 165.
26 W. E. Hammers, M. C. Spanjer and C. L. de Ligny, *J. Chromatogr.*, 174 (1979) 291.
27 E. L. Weiser, A. W. Salotto, S. M. Flach and L. R. Snyder, *J. Chromatogr.*, 303 (1984) 1.
28 P. L. Smith and W. T. Cooper, *J. Chromatogr.*, 410 (1987) 249.
29 G. Kortum, W. Vogeland and K. Andrussow, *Dissociation Constants of Organic Acids in Aqueous Solutions*, Butterworths, London, 1961.
30 D. D. Perrin, B. Dempsey and E. P. Serjeant, *pK_a Prediction for Organic Acids and Bases*, Chapman & Hall, New York, 1981.
31 L. R. Snyder, *Principles of Adsorption Chromatography*, Marcel Dekker, New York, 1968, p. 208.
32 L. R. Snyder, *J. Chromatogr.*, 255 (1983) 3.
33 L. R. Snyder and J. L. Glajch, *J. Chromatogr.*, 248 (1982) 165.
34 L. R. Snyder, *Principles of Adsorption Chromatography*, Marcel Dekker, New York, 1968, pp. 199–200.

Journal of Chromatography, 479 (1989) 17–25
Elsevier Science Publishers B.V., Amsterdam — Printed in The Netherlands

CHROM. 21 655

GAS CHROMATOGRAPHY OF PURE AND SURFACE-MODIFIED PRECIPITATED CALCIUM CARBONATE

T. AHSAN, B. A. COLENUTT* and K. S. W. SING
Department of Chemistry, Brunel University, Uxbridge, Middx UB8 3PH (U.K.)
(First received March 21st, 1989; revised manuscript received May 30th, 1989)

SUMMARY

Precipitated calcium carbonates, either pure or coated with stearic acid, are materials of major industrial importance. Gas chromatographic measurements of specific retention volumes have been used to derive isosteric heats of adsorption for various hydrocarbons on both pure and modified calcium carbonate samples. Significant differences in the heats of adsorption and peak skew ratios have been observed with the different samples. The results are explained by the presence of exposed polar cationic species at the surface of pure calcium carbonate. Modification by stearate coating masks these sites and so reduces specific interaction. Gas chromatography is shown to be a valuable tool for probing the nature of the calcium carbonate surface.

INTRODUCTION

Finely divided calcium carbonate is extensively used as a filler or extender in many industries, the rubber and plastics industry being particularly important[1]. Precipitated calcium carbonate is produced on the industrial scale by passing a stream of carbon dioxide through a suspension of calcium hydroxide. The solid product may be given a stearate coating as part of the production process. A stearate coating makes the material more easily wetted and so improves the incorporation and dispersion characteristics[2].

It is thought that strong filler–polymer interactions are required for good reinforcement[3], but although stearate coated calcium carbonate is readily dispersible it has a reduced degree of reinforcement. However, the lack of understanding of calcium carbonate reinforcement may be partially attributed to a lack of fundamental knowledge about the properties and surface characteristics exhibited by the pure and modified surfaces. It is in probing and elucidating the surface properties of calcium carbonates that gas chromatography (GC) may be a valuable tool. GC provides a unique means of studying the adsorption characteristics of surfaces at low coverage[4]. We have already reported that GC can be used as a convenient and effective technique to assess adsorbent–adsorbate interaction parameters such as heats of adsorption on calcium carbonate at low surface coverage provided that certain conditions such as stringent drying of the carrier gas and careful adsorbent conditioning are fulfilled[5].

0021-9673/89/$03.50

There are few accounts in the literature of previous GC studies of calcium carbonate. These have revealed the existence of polar sites at the surface[6–8]. In a recent study[8] a comparison was made of the entropy and heats of adsorption of some saturated hydrocarbons on pure and stearate coated calcium carbonate. To date little has been reported on the characterization of the surface and particularly its behaviour towards molecular probes of varying polarity.

Here we report the isosteric heats of adsorption of various hydrocarbon molecular probes on the surfaces of pure and modified calcium carbonates and compare the nature of the surfaces with those of other solid adsorbents such as graphitized thermal carbon black (GTCB) and silica gel using data from the literature.

EXPERIMENTAL

Gas chromatography

Comprehensive experimental detail and the necessary precautions have been described and discussed previously[5]. Thus to obtain reproducible and reliable data it is vital to remove all water from the carrier gas and to recondition the columns after injections have been made. This prevents build-up of adsorbed substances which might modify the surface during the study and is particularly vital in dealing with uncoated calcium carbonate.

Gas chromatography measurements were made on a Pye Model 104 gas chromatograph equipped with a flame ionization detector. Calcium carbonate particles were packed in 50 cm × 3 mm I.D. glass columns. Vapour samples of the hydrocarbon molecular probes were introduced into the nitrogen carrier gas stream by means of a Hamilton gas-tight 1-ml syringe. Each injection was equivalent to between 1 and 50 nmol of the compound. The hydrocarbons (Aldrich) were of high purity (better than 99%) and gave a single peak in the chromatogram. Sequences of injections were made until retention volumes were reproducible to within 2% for at least four consecutive injections. Injections were made over a range of oven temperatures between 70 and 190°C.

Preparation of calcium carbonate

The finely divided calcium carbonate was prepared by a precipitation process starting from granular calcium carbonate. The raw calcium carbonate (AnalaR grade, BDH) was heated to 1100°C and the resulting calcium oxide was added to water to produce a 0.9 *M* suspension. Calcium carbonate was precipitated by passing 40% carbon dioxide in air at a flow-rate of 200 l/h with continous stirring. This was continued until a pH of 7 was reached when the product was filtered and dried at 115°C for 16 h.

One sample (acetone washed) of the colloidal calcium carbonate collected at pH 7 was mixed with an equivalent volume of acetone, filtered and washed three times with more acetone. This product was also dried at 115°C for 16 h.

A further sample (Calgon treated) of the colloidal calcium carbonate was mixed with a 500 ppm (w/v) aqueous solution of Calgon S (sodium hexametaphosphate) and stirred for 10 min. The calcium carbonate was filtered and dried as described above.

A final sample (stearate coated) of the calcium carbonate was coated with 2.6% (w/w) of stearic acid by a proprietary method and once again dried at 115°C for 16 h.

TABLE I
SURFACE AREA OF CALCIUM CARBONATE SAMPLES

Type of sample	*BET surface area (m^2/g)*
Pure uncoated material	29.4
Acetone washed	34.1
500 ppm Calgon S impurity	44.2
2.5% (w/w) Ammonium stearate	30.0

The treatments with acetone and Calgon S were intended to reduce Ostwald ripening and so prevent aggregation. These products would be expected to have higher surface areas than the other two samples. The BET nitrogen surface areas of the samples were measured and are given in Table I.

RESULTS AND DISCUSSION

When the precautions described previously[5] are adopted it is possible to determine values of specific retention volume, V_g, from the expression

$$V_g = (t_R - t_o) F_c \cdot \frac{273}{T} \cdot \frac{1}{w}$$

where t_R and t_o are the retention times at the peak maxima of the hydrocarbon and methane, respectively, F_c is the corrected carrier gas flow-rate, T is the absolute column temperature and w is the mass of calcium carbonate.

The values of V_g are independent of any variables such as sample size. Under these conditions the isosteric heats of adsorption at low or essentially zero coverage, q^{st}, can be calculated using the equation

$$q^{st} = \frac{R \, \mathrm{d}(\ln V_g)}{\mathrm{d}(1/T)}$$

where R is the universal gas constant.

Fig. 1 shows examples of the linear plots which were obtained when log V_g was plotted against $1/T$. The heats of adsorption for the hydrocarbon probes on the four calcium carbonate samples calculated from the plots are given in Table II.

Comparisons can be made between the heats of adsorption in Table II and those reported for the same hydrocarbon molecular probes on GTCB[9] and macroporous silica[4].

Fig. 2 shows the plots of heat of adsorption against carbon number for the adsorption of a range of normal alkanes on various adsorbents. From this it is possible to compare the magnitude of the non-specific adsorbent–adsorbate interactions. It can be seen that the increase in the interaction energy is linear with the carbon number in all cases. The position of the plot for GTCB may be explained by its non-specific surface

TABLE II

ISOSTERIC HEATS OF ADSORPTION (kJ/mol) OF VARIOUS HYDROCARBONS ON CALCIUM CARBONATES

Adsorbate	*Adsorbent*			
	Unmodified	*Acetone washed*	*Calgon S treated*	*Stearate coated*
n-Hexane	36.4	35.5	37.3	35.3
n-Heptane	44.1	40.5	43.2	41.1
n-Octane	52.6	46.5	49.3	47.7
Cyclohexane		32.1	33.4	33.4
But-1-ene		46.9	41.1	34.7
Hex-1-ene	53.7	51.4	52.3	42.6
Hept-1-ene	60.3	56.9	58.5	47.0
Benzene			64.3	
Toluene			68.0	42.4

and the surface density of the carbon atoms[9]. The plots for calcium carbonate and macroporous silica start at a nearly common point at a carbon number of six but the individual slopes are very different. The greater slope for the calcium carbonate samples may be explained by the presence of cationic sites at the surface which undergo specific polarization interactions[10] with adsorbate molecules. Since the polarizability

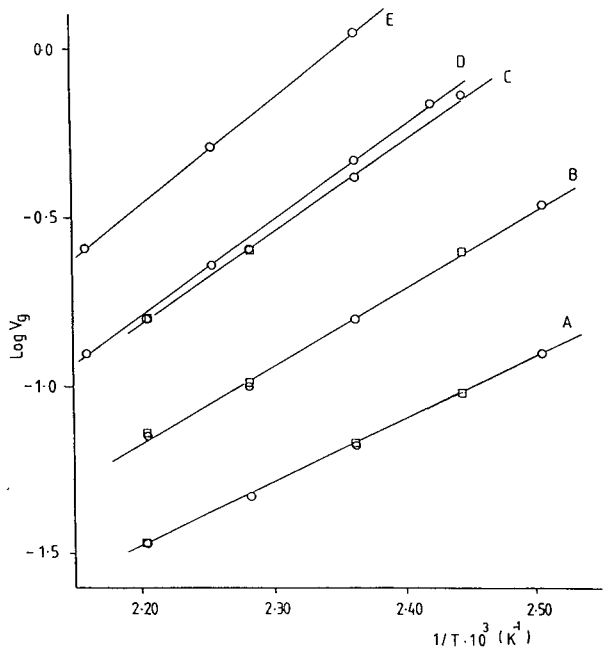

Fig. 1. Plots of log V_g against $1/T$ for hydrocarbons on pure calcium carbonate. (A) *n*-hexane; (B) *n*-heptane; (C) *n*-octane; (D) hex-1-ene; (E) hept-1-ene. Circles and squares indicate measurements made on different occasions on the same adsorbent after reconditioning.

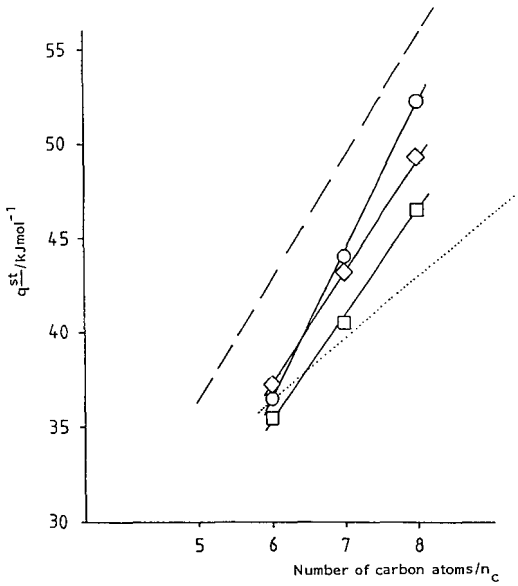

Fig. 2. Heats of adsorption of *n*-alkanes against carbon number for various adsorbents. ○ = Unmodified; ◇ = Calgon treated; □ = stearate coated; --------- = GTCB; ····· = macroporous silica[4].

of the hydrocarbons increases with increasing molecular weight, an enhancement of this interaction energy for the higher hydrocarbons in the homologous series would be expected and this is observed. Furthermore, the strongest interaction is apparent with the pure calcium carbonate surface as would be expected if the surface modification involves masking or reaction at the exposed cationic sites.

Fig. 3 shows the plots of heat of adsorption against carbon number for the normal alkanes and certain alkenes on various calcium carbonates. It can be seen that the corresponding plots for the alkanes and alkenes are nearly parallel for the unmodified and Calgon-treated calcium carbonates, but that this is not the case with the stearate coated sample. The greater rate of increase in heats of adsorption for the alkenes are due to the contribution made by the specific interactions between the π-bonds of the alkene molecules and the polar cationic sites on the surface of the pure calcium carbonate.

The skew ratios (the ratio of the horizontal distances at half peak height from the perpendicular at the peak maximum to the leading and trailing edges) were calculated from the chromatographic bands observed with unsaturated hydrocarbons on calcium carbonate samples at two different temperatures. The values are given in Table III. The skew ratios of the bands increase and approach unity, representing a completely symmetrical peak, as the high energy cationic sites are progressively masked as a result of the different treatments given to the calcium carbonate surfaces. The effect becomes most pronounced in the case of the stearate-coated sample where the coating has evidently played an important role in masking the polar catonic sites. This conclusion is supported by the calculated differences between the corresponding heats of adsorption of unsaturated and saturated C_6 and C_7 hydrocarbons on the calcium carbonate samples given in Table IV. The smallest difference, reflecting the least contribution by specific interactions, is given by the stearate coated sample.

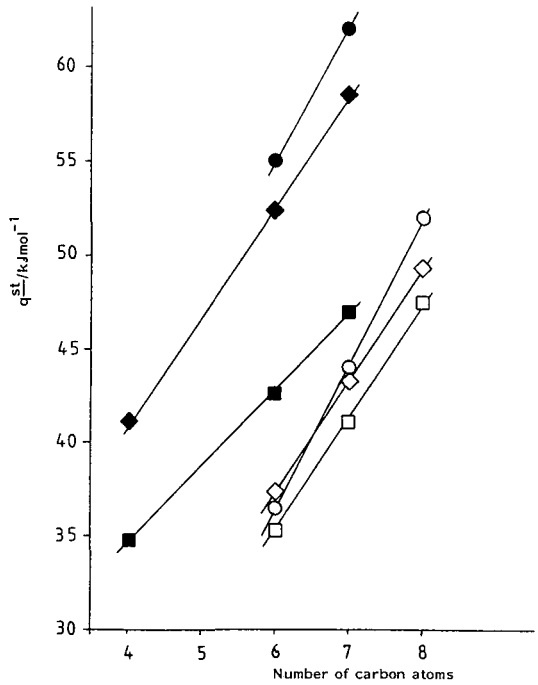

Fig. 3. Heats of adsorption against carbon number in hydrocarbons for various calcium carbonate samples. ○ = Unmodified; ◇ = Calgon treated; □ = stearate coated. Open symbols: *n*-alkanes. Filled symbols: alk-1-enes.

Table V shows the difference between the corresponding heats of adsorption for benzene and *n*-hexane on Calgon treated precipitated calcium carbonate, two barium sulphate samples, hydroxylated silica and GTCB. The data for the latter four adsorbents have been obtained from the literature[4,9,11]. The differences in heats of adsorption decrease in the order calcium carbonate, barium sulphate and hydroxylated silica, eventually becoming zero for GTCB. Thus the strongest specific

TABLE III

SKEW RATIOS OF THE CHROMATOGRAPHIC BANDS FOR POLAR HYDROCARBONS AT TWO DIFFERENT TEMPERATURES ON CALCIUM CARBONATES

Calcium carbonate	*Hex-1-ene*		*Hept-1-ene*	
	150°C	*170°C*	*150°C*	*170°C*
Unmodified	0.63	0.79	0.61	0.69
Acetone washed	0.77	0.77	0.65	0.73
Calgon S treated	0.83	0.86	0.68	0.69
Stearate coated	0.90[a]	0.99[b]	0.90[a]	0.91[b]

[a] At 100°C.
[b] At 120°C.

TABLE IV
DIFFERENCES BETWEEN THE ISOSTERIC HEATS OF ADSORPTION OF *n*-ALKANES AND ALKENES ON CALCIUM CARBONATE SAMPLES

Calcium carbonate	*Difference between hex-1-ene and hexane (kJ/mol)*	*Difference between hept-1-ene and heptane (kJ/mol)*
Unmodified	17.3	16.2
Acetone washed	15.9	16.4
Calgon treated	15.0	15.3
Stearate coated	7.3	5.9

interactions are observed on the calcium carbonate with phosphate covering about 10% of the surface. In fact the value of the heat of adsorption for benzene on pure calcium carbonate was probably larger but it could not be measured because of the greater asymmetry of the chromatographic band and problems of irreproducible retention data. The two sets of values for the barium sulphate samples are puzzling but could be explained by the effect of impurities, even at trace levels, at the surface.

The difference between the corresponding heat of adsorption values for calcium carbonate and barium sulphate may be explained by differences in cationic radii. The values for Ca^{2+} and Ba^{2+} ions are 0.099 and 0.139 nm respectively[12]. Since the positive charge for Ca^{2+} is concentrated over a smaller ionic radius it is likely that it interacts more strongly with the π electrons of the benzene ring than is the case with Ba^{2+}. It is evident that the specific contribution in the case of hydroxylated silica is considerably less than either of the other two adsorbents discussed above.

Recently heats of adsorption for *n*-alkanes from pentane to nonane on coated and uncoated calcium stearate have been reported[8]. The results for *n*-hexane, *n*-heptane and *n*-octane are directly comparable with the data reported here. Schmitt *et al.*[8] examined calcium carbonate coated with 8% stearate rather than the 2.6% used in this study. However, their results of 28, 37 and 46 kJ/mol for *n*-hexane, *n*-heptane and

TABLE V
HEATS OF ADSORPTION (kJ/mol) OF BENZENE AND HEXANE ON VARIOUS ADSORBENTS

Adsorbent	*Adsorbate*		
	Benzene	*n-Hexane*	*Difference between benzene and n-hexane*
Calgon treated calcium carbonate	64.3	37.3	27.0
Barium sulphate-1 (11)	70.3	46.8	23.5
Barium sulphate-2 (11)	50.6	30.5	20.1
Hydroxylated silica[4]	42.6	30.9	11.7
Graphitised thermal carbon black[9]	41.0	41.0	0

n-octane, respectively, are within a few kilojoules of the values we report here despite the difference in the degree of surface coating.

The effect of modifying surfaces with essentially non-volatile or chemically bound liquids has been demonstrated for the silica–polyethylene glycol system[13] and comparisons can be made with the coating of calcium carbonate. Papirer *et al.*[13] has shown that the heats of adsorption are related to the degree of surface coverage, effectively ranging from the heat of adsorption onto the solid to the heat of solution into the coating liquid. On that basis we would expect the heat of adsorption measured in the calcium carbonate–stearic acid system to vary with the degree of coating and the differences between the two sets of results might be explained in this way.

However, the calcium carbonate surface is clearly heterogeneous and treatment with stearic acid is unlikely to result in a uniform coating. Stearate will concentrate at the high energy sites and the effect of various degrees of coating cannot be predicted with confidence. Thus the apparent differences in the heats of adsorption for calcium carbonates with differing surface coatings is significant. The industrial scale production of calcium carbonate generally involves a stearate coating in the range 2.5–3.0%, a range which has developed for empirical reasons. The observation that an increase in loading produces relatively little change in the heat of adsorption indicates that although 2.6% may not be the optimum loading it has virtually eliminated the influence of the high energy cationic sites and increased loadings above that level would have relatively little effect.

So far as uncoated calcium carbonates are concerned there is poor agreement between the values of heats of adsorption we report here and those of Schmitt *et al.*[8]. Their values of 11, 15 and 17 kJ/mol for *n*-hexane, *n*-heptane and *n*-octane, respectively, are remarkably low, being less than half of the values of the corresponding heats of condensation. Such values are similar to those we obtained in experiments before taking all the precautions we eventually found to be necessary[5]. There may be problems with water adsorption from the carrier gas and, equally important, if columns are not repeatedly reconditioned between injections, trace amounts of hydrocarbon probe may adsorb at polar cationic sites modifying the surface during the analysis. This results in variable retention volumes and poor linearity of the plots of log V_g against $1/T$. Hence it is possible that Schmitt *et al.* were in fact studying a modified calcium carbonate surface rather than the uncoated one which was assumed. In such circumstances the nature of the surface would probably be changing during the determinations so that reliable results would be difficult to achieve. The relatively good agreement between our two sets of results for coated calcium carbonate suggests that there are no fundamental differences of chromatographic technique which could account for the differences in the uncoated calcium carbonate.

CONCLUSIONS

Gas chromatographic measurements of the specific retention volumes for various hydrocarbons have provided a means of characterizing the surfaces of different precipitated calcium carbonate samples. For each homologous series the derived values of isosteric heat of adsorption at very low surface coverage show a linear dependency on carbon number. For a given hydrocarbon the highest value of heat of

adsorption has been obtained with the pure calcium carbonate sample and the lowest with a stearate coated sample. The differences may be explained by the presence of exposed polar cationic sites on the surface of the pure material giving rise to specific interactions. These cations are masked by the stearate coating and there is thus less specific interaction in this case. There is some evidence that a coating of 2.6% stearate is sufficient to mask all of the cationic sites and that higher loadings have little effect.

The magnitude of the specific adsorbent–adsorbate interaction has been estimated as the difference between the corresponding values for unsaturated and saturated linear hydrocarbons. The pure sample again gives the highest value of heat of adsorption. The effect is further emphasized by the calculation of skew ratios for the various band since the value approaches unity, a symmetrical peak, on the stearate modified sample but is much lower on other samples.

ACKNOWLEDGEMENTS

We wish to thank the Science and Engineering Research Council (SERC) for the provision of a research studentship (to T.A.) and ICI Chemicals and Polymer Limited for financial assistance. In addition we thank Roger Rothon and David Harrison for their help and advice.

REFERENCES

1 H. S. Katz and J. V. Milewski (Editors), *Handbook of Fillers and Reinforcement for Plastics*, Van Nostrand-Reinhold, New York, 1978.
2 E. Suito, M. Arakawa and T. Arakawa, *Bull. Inst. Chem., Kyoto Univ.*, 33 (1975) 1.
3 E. M. Dannenburg, *Rubber Chem. Technol.*, 55 (1982) 872.
4 A. V. Kiselev and Y. I. Yashin, *Gas Adsorption Chromatography*, Plenum, New York, 1969, Ch. 4.
5 T. Ahsan, B. A. Colenutt and K. S. W. Sing, *J. Chromatogr.*, 464 (1989) 416.
6 H. P. Schreiber, M. R. Werlheimer and M. Lambla, *J. Appl. Polym. Sci.*, 27 (1982) 2269.
7 E. Papirer, J. Schultz and C. Turchi, *Eur. Polym. J.*, 20 (1984) 1155.
8 P. Schmitt, E. Koerper, J. Schultz and E. Papirer, *Chromatographia*, 25 (1988) 786.
9 O. G. Eisen, A. V. Kiselev, A. E. Pitt, S. A. Rang and K. D. Shcherbakova, *Chromatographia*, 4 (1971) 448.
10 R. M. Barrer, *J. Colloid Interface Sci.*, 21 (1966) 415.
11 L. D. Belyakova, A. V. Kiselev and G. A. Soloyan, *Chromatographia*, 3 (1970) 254.
12 P. W. Atkins, *Physical Chemistry*, Academic Press, New York, 1978.
13 E. Papirer, H. Balard, Y. Rahmani, A. P. Legrand, L. Facchini and H. Hommel, *Chromatographia*, 23 (1987) 639.

Journal of Chromatography, 479 (1989) 27–37
Elsevier Science Publishers B.V., Amsterdam — Printed in The Netherlands

CHROM. 21 673

KINETIC ANALYSIS OF THE CARBOXYPEPTIDASE A HYDROLYSIS OF OLIGOPEPTIDES BY REVERSED-PHASE HIGH-PERFORMANCE LIQUID CHROMATOGRAPHY

M. A. SERRA

Departament de Bioquímica i Biologia Molecular, Facultat de Ciències, Universitat Autonòma de Barcelona, 08193 Bellaterra (Barcelona) (Spain)

F. X. AVILÉS

Departament de Bioquímica i Biologia Molecular, Facultat de Ciències, and Institut de Biologia Fonamental "Vicent Villar Palasi", Universitat Autònoma de Barcelona, 08193 Bellaterra (Barcelona) (Spain)

E. GIRALT

Departament de Química Orgànica, Facultat de Química, Universitat de Barcelona, Martí i Franqués 1, 08028 Barcelona (Spain)

and

C. M. CUCHILLO*

Departament de Bioquímica i Biologia Molecular, Facultat de Ciències, and Institut de Biologia Fonamental "Vicent Villar Palasi", Universitat Autònoma de Barcelona, 08193 Bellaterra (Barcelona) (Spain)

(First received March 13th, 1989; revised manuscript received June 7th, 1989)

SUMMARY

A reversed-phase high-performance liquid chromatographic (HPLC)-based method was developed to follow the time course of the hydrolytic action of pancreatic carboxypeptidase A on oligopeptide substrates of the general formula benzoyl-(glycyl)$_n$-L-Phe, n being in the range 1–5. The proposed procedure is sensitive at the nanomolar level of substrate, but also allows the kinetics of substrate hydrolysis to be investigated over a wide range of concentrations. The prior quenching of the carboxypeptidase activity and the use of isocratic conditions for the rapid separation of the substrates and their products (in less than 8 min for the slowest one), allow the automation of the procedure, which could become an easy and versatile alternative to the commonly used spectrophotometric methods. A comparative evaluation of the use of a spectrophotometric method to measure carboxypeptidase A activity on the same substrates indicated that the latter is not valid for long oligopeptides ($n \geqslant 2$) at concentrations higher than 5 mM owing to an interference of a physico-chemical nature. For benzoylglycyl-L-Phe ($n = 1$), the apparent kinetic parameters were calculated by means of the HPLC method and by a well established spectrophotometric procedure, and both yielded similar values.

0021-9673/89/$03.50

INTRODUCTION

Pancreatic carboxypeptidase A (CPA, peptidyl-L-amino acid hydrolase, E.C. 3.4.17.1) catalyses the cleavage of the terminal bond of peptides and proteins with an aromatic or branched-aliphatic amino acid at the C-terminus[1]. The enzymic properties of CPA are usually studied by measuring the hydrolysis of synthetic dipeptide derivatives, either by continuous methods (spectrophotometric[2–4], fluorimetric[5] and conductimetric[6]) or by discontinuous spectrophotometric procedures[7–9]. A modified ninhydrin method for the determination of the C-terminal amino acid released during the hydrolysis[10] is the only one described for the analysis of the CPA-catalysed cleavage of longer oligopeptides such as those of the general formula benzoyl$(Gly)_n$-L-Phe, n being 1–5[11]. As this procedure requires large amounts of substrate and is also subject to interference from other ninhydrin positive substances[12], we became interested in finding an alternative procedure to quantify the CPA kinetics for the hydrolysis of the above-mentioned oligopeptides, which could be useful in a range of concentrations from 50 μM to 50 mM. Our aim is to use these substrates and analytical procedures to characterize further the enzymic properties of porcine CPA and its zymogens, which have been extensively studied in our laboratory[13–15].

In an initial attempt, an spectrophotometric assay was used to follow the decrease in absorbance in the peptide UV band. This had to be performed in the region of 220 nm for oligopeptides with $n \geqslant 2$, thus making necessary the use of very thin cells (0.1 mm optical path). Under these conditions we found an interference, of a physico-chemical nature, with the measurement of the enzymic activity that made its correct determination very difficult. Several tests were carried out in order to identify and to eliminate this interference, none of which was successful.

Because of these problems, we decided to develop a semi-automated method based on the instantaneous quenching of the action of CPA on peptide substrates by addition of trifluoroacetic acid (TFA), followed by separation and quantification of the components of the reaction mixture by reversed-phase high-performance liquid chromatography (HPLC). This method provides reliable kinetic measurements for a wide range of substrate sizes and concentrations in comparison with control spectrophotometric assays carried out at low substrate concentrations. The feasibility of this procedure is illustrated by the determination of the apparent kinetic parameters for the CPA hydrolysis of benzoylglycyl-L-Phe (BGP) by both spectrophotometric and HPLC methods. The results are also compared with those given in the literature.

EXPERIMENTAL

Apparatus

A Waters Assoc. (Milford, MA, U.S.A.) HPLC system, with a WISP 710B automatic injector, a Model M730 data module and an Altex Ultrasphere C_{18} ODS (particle size 5 μm) column (4.5 cm × 4.6 mm I.D.) was used. A double-beam Hitachi Model 220 thermostated spectrophotometer was used to calculate peptide and protein concentrations and to record CPA activity.

Chemicals

All chemicals were of analytical-reagent grade. Tris (Trizma-base) (Sigma),

sodium chloride (Merck) and zinc chloride (Panreac, Spain) were used for buffer preparation. Dithizone (Merck) and carbon tetrachloride (Merck) were used for metal extraction. Norganic-filtered Millipore water, HPLC-grade acetonitrile (Carlo Erba) and TFA (Aldrich) were used for all HPLC experiments.

Enzymes

Porcine pancreatic CPA_α was obtained from partial tryptic activation of pro-carboxypeptidase A (PCPA) by the method described previously[13]. The enzyme concentration was calculated spectrophotometrically using $A^{1\%}_{280} = 19.6\ \mathrm{l\,mol^{-1}\,cm^{-1}}$ (ref. 2).

Oligopeptide substrates and products

Hippuric acid (BG), BGP, N-(2-furanacryloyl)-L-phenyalanyl-L-Phe (FAPP) (Sigma), benzoylglycyl-Gly (BG2) and benzoyl$(glycyl)_2$-Gly (BG3) (Bachem) were used without further purification. Benzoyl$(glycyl)_4$-Gly (BG5) and benzoyl$(glycyl)_5$-L-Phe (BG5P) were synthesized by the procedure of Spilburg *et al.*[16] with minor modifications. The same method was adapted to the preparation of benzoyl$(glycyl)_2$-L-Phe (BG2P) and benzoyl$(glycyl)_3$-L-Phe (BG3P) via reaction of L-Phe with the N-hydroxysuccinimido esters of BG2 and BG3, respectively.

All the synthesized compounds were purified by recrystallization (ethanol–water) until chromatographic homogeneity [thin-layer chromatography on silica gel plates using chloroform–methanol–water (83:15:2) as solvent] and characterized by infrared and ^1H (200 MHz) and ^{13}C (50 MHz) NMR spectroscopy. The amino acid composition and concentration of the above oligopeptides in solution were checked by amino acid analysis following a dabsyl chloride–HPLC method[17].

Buffer preparation and metal extraction

A 50 m*M* Tris–HCl–0.5 *M* NaCl buffer (pH 7.5) was used for enzymic experiments. Zinc chloride up to 1 μM was always added before carrying out any CPA activity measurement in order to preserve the enzyme integrity[11]. When indicated, buffer and oligopeptide solutions were extracted with dithizone dissolved in carbon tetrachloride in order to remove metal ions[11].

Spectrophotometric-based kinetic analysis

BGP hydrolysis was measured by following the decrease in absorbance in the region of 280 nm, according to the method of Whitaker *et al.*[3]. For BGP, BG2P, BG3P and BG5P hydrolysis at low concentrations (less than 1 m*M*), the decrease in absorbance at 220 nm was recorded. Changes in the molar absorptivities ($\Delta\varepsilon$) were calculated from absorbance values when substrate hydrolysis was completed. For all four substrates, 2-mm optical-path cells (Hellma) with a reaction volume of 0.5 ml were employed and 50–100 n*M* enzyme concentrations were used. This allowed straight progress curves to be obtained for the first 3–5 min of the reaction (less than *ca.* 10% hydrolysis), from which initial velocities were calculated. Demountable micro-cells (Hellma) of 0.1-mm optical path with a volume of 50 μl were used to determine the kinetics of hydrolysis of BGP, BG2P, BG3P and BG5P at higher concentrations (greater than 1 m*M*) at 220 nm by the following procedure: the substrate solution was placed in an eppendorf tube and the reaction was initiated by the addition of 5–10 μl of

CPA to complete a reaction volume of 60 μl, which was immediately mixed in a vortex stirrer; 50 μl of the reaction mixture were transferred to the cell, which was closed and placed immediately in the spectrophotometer cell compartment. In this way recordings could begin less than 30 s from mixing. Initial velocities were calculated as described above. All experiments were performed at 25°C. Assay of FAPP hydrolysis by CPA was performed as described by Peterson *et al.*[4].

HPLC-based kinetic analysis

All HPLC analyses were carried out using isocratic elution at a flow-rate of 0.5 ml/min with different water–acetonitrile proportions in 0.1% TFA, according to the substrate being analysed, and monitored at 280 nm. Solvents were previously degassed. An automatic injector and a plotter with integrating built-in capabilities were always employed for the quantitative determination of the chromatographic peak areas of both peptide substrates and their products. The samples for the kinetic determinations were prepared as follows: 300 μl of each substrate (BGP, BG3P or BG5P) concentration were placed in an eppendorf tube and 10 μl of CPA (final concentration around 50 n*M*) were added to initiate the reaction; sample aliquots of 45 μl were withdrawn at fixed time intervals (0.5 min) for 3 min (less than *ca.* 10% hydrolysis) and the reaction was quenched by adding 5 μl of TFA (final concentration 0.1–1% TFA, depending on the substrate employed). Samples from the kinetic experiments were kept frozen (−20°C) if not analysed immediately. Standards of known concentrations of the different peptide substrates and products were analysed and used as references to calculate, by interpolation, the amount of each product as a function of the integration of the peak area corresponding to the sample.

Calculation of kinetic parameters

A linear regression program was used for the calculation of the apparent kinetic parameters, K_m and V, from v *versus* v/S plots, where K_m is the Michaelis–Menten constant, V the maximum velocity, v the initial velocity and S the substrate concentration. These parameters were refined by a non-linear regression procedure[18].

RESULTS AND DISCUSSION

Fig. 1 shows that the difference spectra for BGP, BG2P, BG3P and BG5P after their complete hydrolysis by CPA have a strong negative absortion band at 220 nm. BGP also exhibits two other cleavage-sensitive bands at 254 and 280 nm. Because the initial absorbances were higher than 1.8, even when using 2-mm optical-path cells, 0.1-mm optical-path cells had to be used in order to follow the reaction at 220 nm at substrate concentrations above 1 m*M* for BG2P, BG3P and BG5P.

In order to check the stability of the assayed oligopeptide substrates (BGP, BG2P, BG3P)[a] in the absence of enzyme, the UV absorbance at different wavelengths was recorded for some time. Surprisingly, a sigmoidal perturbation of the absorbances in the 220–270 nm range was apparent in the first 8 min after placing the sample in the cell (Fig. 2). This effect was noticeable for oligopeptide concentrations above 4–5 m*M*. Although the decrease in absorbance accounts for less than 5% of the absolute initial

[a] BG5P could not be tested because of its low solubility at concentrations higher than 5 m*M*.

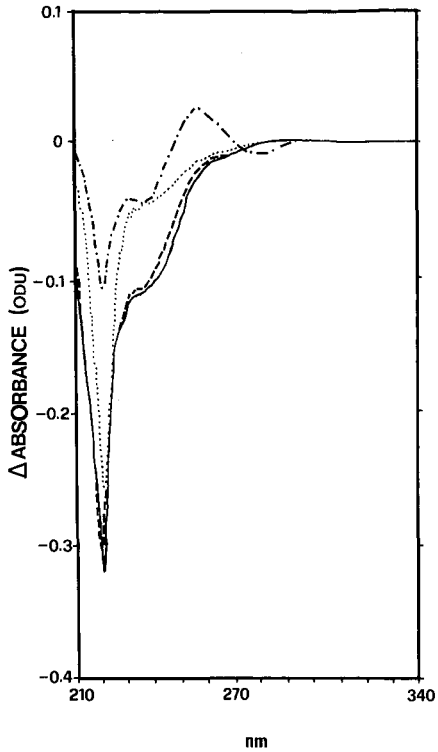

Fig. 1. Difference spectra for 0.5 m*M* solutions of benzoylglycyl-L-Phe (BGP) (· – · – ·), benzoyl(glycyl)$_2$-L-Phe (BG2P) (———), benzoyl(glycyl)$_3$-L-Phe (BG3P) (– – –) and benzoyl(glycyl)$_5$-L-Phe (BG5P) (·····) after complete hydrolysis by CPA in 50 m*M* Tris–HCl–0.5 *M* NaCl–1 μM $ZnCl_2$ (pH 7.5) at 25°C in 2-mm optical-path cells. ODU = Optical density units.

values, this perturbation makes the spectrophotometric assay difficult to apply. The rate and value of the perturbation increase both with increasing substrate concentration and increasing oligopeptide length, achieving stabilization in 4–8 min (being slower for the longer substrates). We also observed that this perturbation is independent of the exposure of the substrate solution to UV light, an indication that it is not a photochemical effect. When the assay is performed in the presence of enzyme, the above perturbation precludes a correct determination of the decrease in absorbance due to the enzymic activity. The possibility of allowing the substrate solution to stabilize before the addition of the enzyme is not feasible because of the closed design of the 0.1-mm optical-path cells.

Several unsuccessful attempts were made to eliminate the above interference. Prior degassing of all solutions and careful control of the temperature were carried out to avoid bubble formation and eliminate possible changes in the ε value of the substrates. Also, initial solubilization of the oligopeptide in acetonitrile–water solutions followed by ultracentrifugation was performed in order to avoid substrate aggregation. Finally, exhaustive metal extraction of all solutions was carried out to eliminate the possibility of formation of metal complexes, which could induce spectrophotometric perturbations. No improvements were observed after taking the

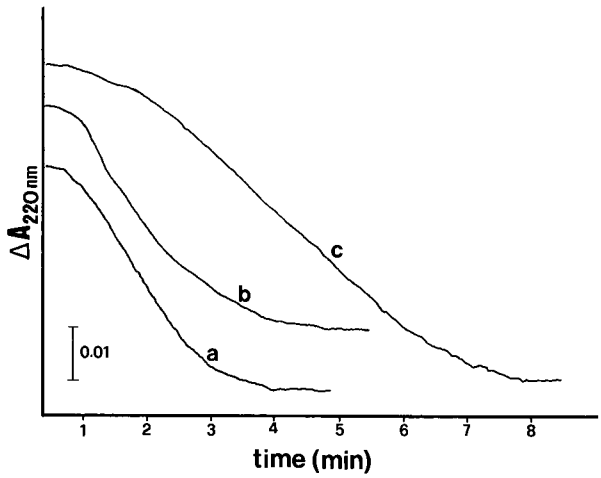

Fig. 2. Recordings of the absorbance perturbation at 220 nm of different peptide substrates when placed in a 0.1-mm optical-path microcell; (a) benzoylglycyl-L-Phe (BGP); (b) benzoyl(glycyl)$_2$-L-Phe (BG2P); (c) benzoyl(glycyl)$_3$-L-Phe (BG3P) in 50 m*M* Tris–HCl–0.5 *M* NaCl–1 μM $ZnCl_2$ (pH 7.5) at 25°C. All substrate concentrations were 15 m*M*. See Experimental for details.

above precautions. We also found a similar sigmoidal interference for unrelated proteins at high concentrations, such as chymotrypsin at 100 mg/ml or FAPP at 10 m*M*, when using the microcells. As a complementary test we recorded the sigmoidal interference for 5 m*M* FAPP in 0.1- and 0.2-mm optical-path cells at 330 nm, the absolute decrease in absorbance of the former being twice that of the latter. In addition, we recorded the sigmoidal interference for 10 m*M* BGP at 25 and 37°C, the value at the former temperature being 1.2 times higher than that at the latter.

We suggest that the UV spectrophotometric perturbation observed in ultra-thin cells with concentrated solutions of oligopeptides can originate from the co-operative interaction of molecules of a thin lamina of the solution with the walls of the cell, resulting in a particular alignment with respect to the walls, changing the isotropic nature of the solution into a partially anisotropic one. A comparative phenomenon has been described for polybenzoyl-L-glutamate, giving homeotropic liquid crystal preparations[19,20], which together with other features makes it partly similar to that described above[19–22].

To avoid the above problems, an HPLC-based method was developed for the analysis of the CPA hydrolysis of these oligopeptides. In Fig. 3, typical elution profiles for the reversed-phase HPLC analysis of the CPA-catalysed hydrolysis of BGP, BG3P and BG5P are shown. The two chromatographic peaks that appear in front of the corresponding product peak are due to optical interferences produced by sample injection. The concentration of acetonitrile had to be decreased with increasing peptide length in order to achieve a satisfactory and rapid (in less than 5, 6 and 8 min, respectively) separation between substrates (BGP, BG3P, BG5P), products (BG, BG3, BG5) and interference peaks. The other product, L-phenylalanine, common for all three oligopeptides, does not interfere in their determination at 280 nm. There was no detectable hydrolysis of BG3 or BG5 during the assay as they are very poor substrates of CPA[1].

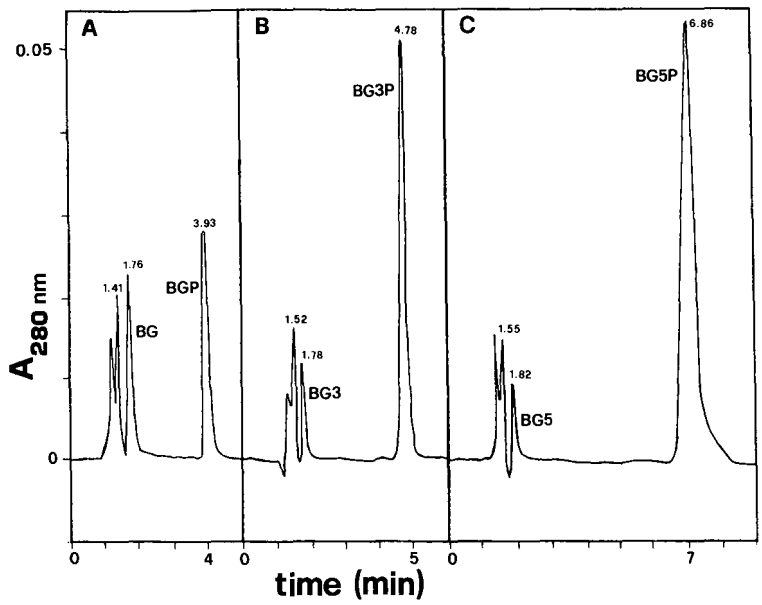

Fig. 3. Reversed-phase HPLC profiles of TFA-quenched samples of CPA-hydrolysed solutions of 0.5 m*M* of (A) benzoylglycyl-L-Phe (BGP), (B) benzoyl(glycyl)$_3$-L-Phe (BG3P) and (C) benzoyl(glycyl)$_5$-L-Phe (BG5P). Elution was carried out with 32%, 25% and 23% acetonitrile in water, respectively, in 0.1% TFA. CPA concentration, 57 n*M*; final TFA concentration in quenched samples, 1% for BGP and 0.1% for BG3P and BG5P.

The hydrolysis rate could be measured by following either the decrease in the peak of the substrate or the increase in the peak of the product. We adopted the latter approach because more accurate results were obtained and also the precision was lower when the peak of the substrate was used, especially at high concentrations. The calibration graphs for BG, BG3 and BG5 (with correlation coefficients from 0.997 to 0.999) that were used to calculate the corresponding amounts of products formed from the integration areas of the peaks are shown in Fig. 4. Chromatographic runs were always performed in duplicate over the range 0–0.1 absorbance and showed good reproducibility. Under the assay conditions described, unperturbed and well defined chromatographic elution profiles were obtained with 20-μl injection volumes; samples can be injected directly up to substrate concentrations of 15 m*M*. Above this concentration it is necessary to dilute the samples for kinetic determinations. In order to test concentrations of substrate below 0.1 m*M*, the injection volume and/or the sensitivity of the HPLC detector have to be increased. The CPA concentrations used in this work (*ca.*50 n*M*) can be reduced approximately 250-fold employing the same procedure.

The linearity of the peptide hydrolysis rate as a function of the enzyme concentration in the range used (20–200 n*M*), as determined by the HPLC method, was tested and yielded good results (correlation coefficients between 0.9903 and 0.9989). The proportionality between substrate concentration and integration areas before and after the addition of TFA was also verified for BGP, BG3P and BG5P,

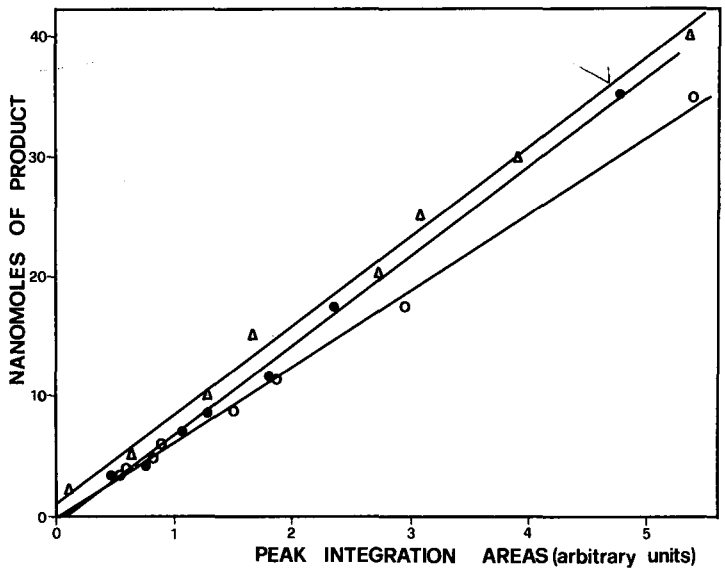

Fig. 4. Calibration graphs for hippuric acid (BG) (●), benzoyl(glycyl)$_2$-Gly (BG3) (○) and benzoyl-(glycyl)$_4$-Gly (BG5) (△) as a function of peak-integration areas of HPLC elution profiles, and nanomoles of each eluted product. Correlation coefficients, 0.9980, 0.9969 and 0.9985, respectively. HPLC conditions as in Fig. 3. Products were in 50 m*M* Tris–HCl–0.5 *M* NaCl–1 μM $ZnCl_2$ (pH 7.5) at 25°C. All measurements were made in duplicate.

together with the efficiency of TFA in quenching the enzymic activity (data not shown). It is very important to note that the concentration of TFA added for quenching had to be carefully selected in order to avoid substrate aggregation at very low pH values. A final value of 0.1% TFA can be generally used for all the oligopeptide substrates analysed over a wide range of concentrations (we tested up to 50 m*M* for BGP and BG3P and up to 5 m*M* for BG5P), although at low BGP concentrations higher TFA values can also be used (up to 1%).

The results for the quantification of the hydrolysis of the above-mentioned substrates by CPA employing both spectrophotometric and HPLC methods are summarized in Table I. It is seen that the initial velocities obtained with the two methods are in good agreement, although the spectrophotometric-derived values are slightly higher, probably owing to an underestimation of the substrates $\Delta\varepsilon$ values[23].

In Fig. 5, typical progress curves for the CPA-catalysed hydrolysis of BGP in the concentration range 0.5–6.5 m*M*, as obtained from HPLC data, are shown. The apparent kinetic parameters calculated by both the HPLC and the spectrophotometric methods are given in Table II, and agree well with those in the literature for bovine CPA[3,10]. This determination was restricted to the first part of the *v*–*S* curve for BGP and assuming Michaelis–Menten kinetics. A more complete kinetic analysis would be more complicated because anomalies at higher concentrations have been reported[3,10].

The method described in this work shows comparable sensitivity and speed to the HPLC method recently proposed by Galdes *et al.*[24] for the analysis of reaction mixtures of the CPA-catalysed hydrolysis of dansylated dipeptides and depsipeptides

TABLE I

COMPARISON OF THE CPA-CATALYSED HYDROLYSIS OF OLIGOPEPTIDES AS DETERMINED BY THE SPECTROPHOTOMETRIC AND HPLC METHODS

All assays were performed in duplicate at 0.5 m*M* of oligopeptide concentration in 50 m*M* Tris–HCl–0.5 *M* NaCl–1 μM $ZnCl_2$ (pH 7.5) at 25°C. CPA concentration, 57 n*M*. Specific activities are given in μmol min^{-1} $nmol^{-1}$. Values are not significantly different for $t_{0.95}$ (bounderies of the central interval of the Student *t* value).

Substrate	*Specific activity*	
	Spectrophotometric method[a]	*HPLC method*[b]
BGP	1.090	0.958[c]
BG3P	0.563	0.432[d]
BG5P	1.773	1.597[d]

[a] Specific activities calculated from spectrophotometric data using $\Delta\varepsilon_{280} = 0.072\,l\,mmol^{-1}\,cm^{-1}$ for benzoylglycyl-L-Phe (BGP), $\Delta\varepsilon_{220} = 1.28\,l\,mmol^{-1}\,cm^{-1}$ for benzoyl(glycyl)$_3$-L-Phe (BG3P) and $\Delta\varepsilon_{220} = 1.53\,l\,mmol^{-1}\,cm^{-1}$ for benzoyl(glycyl)$_5$-L-Phe (BG5P).

[b] Specific activities calculated from HPLC data at different proportions of solvent A (water–0.1% TFA) and solvent B (acetonitrile–0.1% TFA): 68:32 (BGP), 75:25 (BG3P) and 77:23 (BG5P).

[c] Withdrawn aliquots were quenched by adding TFA up to 1%.

[d] Withdrawn aliquots were quenched by adding TFA up to 0.1%.

in order to identify reaction intermediates in cryokinetic studies. It is also comparable to the method proposed by Grimwood *et al.*[25] for the quantification of carboxypeptidase N following the hydrolysis of furanacryloyl derivatives of Ala–Lys or Ala–Arg. In both instances the analysis is performed at fixed and low substrate concentrations. In this present work we use different peptide substrates for the

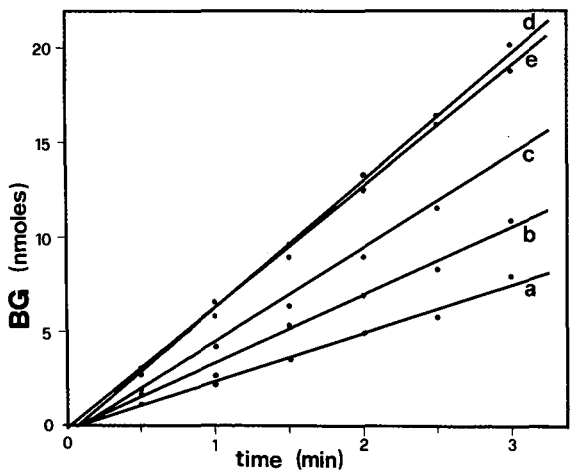

Fig. 5. HPLC-determined progress curves for the CPA-catalysed hydrolysis of benzoylglycyl-L-Phe (BGP) at (a) 0.65, (b) 1.62, (c) 3.23, (d) 4.85 and (e) 6.47 m*M*, in 50 m*M* Tris–HCl–0.5 *M* NaCl–1 μM $ZnCl_2$ (pH 7.5) at 25°C. CPA concentration, 56 n*M*; final TFA concentration in quenched aliquots, 1%. Correlation coefficients were 0.9925, 0.9949, 0.9948, 0.9978 and 0.9988, respectively. HPLC conditions as in Fig. 3. All measurements were made in duplicate.

TABLE II

APPARENT KINETIC PARAMETERS FOR THE CPA-CATALYSED HYDROLYSIS OF BGP DETERMINED BY THE SPECTROPHOTOMETRIC AND HPLC METHODS

Benzoylglycyl-L-Phe (BGP) range of concentrations analysed, 0.5–6.5 m*M*. All measurements were carried out in duplicate in 50 m*M* Tris–HCl–0.5 *M* NaCl–1 μM $ZnCl_2$ (pH 7.5) at 25°C. CPA concentration, 56 n*M*. Parameter values are not significantly different for $t_{0.95}$. Confidence limits for each parameter are also indicated.

Kinetic parameter	*Spectrophotometric method*[a]	*HPLC method*[b]
K_m (m*M*)	1.68 ± 0.02	1.39 ± 0.04
V (μmol min^{-1} nmol^{-1})	3.15 ± 0.01	2.95 ± 0.03

[a] According to the method described by Whitaker *et al.*[3].

[b] HPLC eluent, water–acetonitrile (68:32), both in 0.1% TFA. Withdrawn aliquots were quenched by adding TFA up to a final concentration of 1%.

determination of the CPA activity. Also, different conditions for its quenching (TFA instead of either hydrochloric or phosphoric acid) are applied in order to increase both the solubility of the peptide substrates and products (particularly when working with long oligopeptides) and the lifetime of the column. The more comprehensive design of our method, which is intended to be used in kinetic studies covering a wide range of substrate sizes (dipeptides to hexapeptides) and concentrations, required a careful selection of chromatographic conditions for their analysis. It is also interesting that the use of a very short HPLC column (and very cheap, as it is commercially available as a guard column) shortens the time that would be required to separate long oligopeptides and products in an HPLC column of standard length.

To summarize, we have developed a sensitive and flexible method for the analysis of the CPA kinetic properties with oligopeptides as substrates by means of an isocratic reversed-phase HPLC separation of quenched samples. The method can be automated and allows the sequential analysis of multiple samples by the use of an autosampler. This technique combines reproducibility together with accuracy and requires short times and small amounts to complete the analysis. Using oligopeptide substrates of the general formula benzoyl(glycyl)$_n$-L-Phe, n being 1–5, their hydrolysis products can be detected at the nanomole level. The practical CPA concentration range is from 0.2 n*M* to 0.2 μM. The range of peptide substrate concentrations that can be determined by the HPLC method described is very wide and the method is clearly much more convenient than currently used spectrophotometric procedures, particularly at high concentrations (no limit when combined with accurate dilutions prior to the HPLC analysis).

The application of this method can facilitate more detailed studies on the complex kinetic behaviour that was observed for CPA with N-benzoylated peptide derivatives either in solution or in crystals[11,16], and to provide further information about the configuration of the active site in several subsites[26–28], which could more easily accommodate longer substrates. It has already been described for bovine CPA in solution that non-Michaelis–Menten kinetics apparently disappear when longer substrates are employed[11,16], a fact that could be confirmed by the method described here. The proposed method can also be used in enzymological studies of carboxypeptidases in the presence of different salts and solvents, a field of growing interest[24,29].

ACKNOWLEDGEMENTS

This work was partially supported by grants PR84-0385, PB85-0097 and BT86-18 from the Comisión Interministerial de Ciencia y Tecnología (CICYT), Spain. M.A.S. is a recipient of a pre-doctoral fellowship from the Plan de Formación del Personal Investigador (PFPI), Ministerio de Educación y Ciencia (MEC), Spain.

REFERENCES

1 S. P. Blackburn, *Enzyme Structure and Function, Vol. 3, Enzymology*, Marcel Dekker, New York, 1976, Ch. 4, p. 183.
2 J. E. Folk and E. W. Schirmer, *J. Biol. Chem.*, 238 (1963) 3884.
3 J. R. Whitaker, F. Menger and M. L. Bender, *Biochemistry*, 5 (1966) 386.
4 L. M. Peterson, B. Holmquist and J. L. Bethune, *Anal. Biochem.*, 125 (1982) 420.
5 M. Roth and A. Rohner, *Clin. Chim. Acta*, 135 (1983) 65.
6 A. A. Baykov and E. B. Kostenko, *Anal. Biochem.*, 134 (1983) 330.
7 H. U. Bergmeyer (Editor), *Methods of Enzymatic Analysis*, Vol. 2, Academic Press, New York, 2nd ed., 1970.
8 K. S. Brown, W. D. Kingsbury, N. M. Hall, G. L. Dunn and C. Gilvarg, *Anal. Biochem.*, 161 (1987) 219.
9 J. E. Snoke and H. Neurath, *J. Biol. Chem.*, 181 (1949) 789.
10 R. C. Davies, J. F. Riordan, D. S. Auld and B. L. Vallee, *Biochemistry*, 7 (1968) 1090.
11 D. S. Auld and B. L. Vallee, *Biochemistry*, 9 (1970) 602.
12 S. Visser and H. S. Rollema, *Anal. Biochem.*, 153 (1986) 235.
13 M. Vilanova, J. Vendrell, M. T. López, C. M. Cuchillo and F. X. Avilés, *Biochem. J.*, 229 (1985) 605.
14 F. X. Avilés, J. Vendrell, F. J. Burgos, F. Soriano and E. Méndez, *Biochem. Biophys. Res. Commun.*, 130 (1985) 97.
15 J. M. Sánchez-Ruiz, J. L. López-Lacomba, P. L. Mateo, M. Vilanova, M. A. Serra and F. X. Avilés, *Eur. J. Biochem.*, 176 (1988) 225.
16 C. A. Spilburg, J. L. Bethune and B. L. Vallee, *Biochemistry*, 16 (1977) 1142.
17 J. Vendrell and F. X. Avilés, *J. Chromatogr.*, 358 (1986) 401.
18 *SAS User's Guide Statistics*, SAS Institute, Cary, NC, 5th ed., 1985, pp. 575–606.
19 W. G. Miller, *Annu. Rev. Phys. Chem.*, 29 (1978) 519.
20 D. B. DuPré, in A. Ciferri, W. R. Krigbaum and R. B. Meyer (Editors), *Polymer Liquid Crystals*, Academic Press, New York, 1982, Ch. 7, pp. 166–199.
21 P. J. Flory, *Proc. R. Soc., London, Ser. A*, 234 (1956) 60.
22 C. Robinson, *Trans. Faraday Soc.*, 52 (1956) 571.
23 A. Tsai, R. Kauten and G. Palmer, *Anal. Biochem.*, 151 (1985) 131.
24 A. Galdes, D. S. Auld and B. L. Vallee, *Biochemistry*, 25 (1986) 646.
25 B. G. Grimwood, A. L. Tarentino and T. H. Plummer, Jr., *Anal. Biochem.*, 170 (1988) 264.
26 N. Abramowitz, I. Schechter and A. Berger, *Biochem. Biophys. Res. Commun.*, 29 (1967) 862.
27 B. L. Vallee, J. F. Riordan, J. L. Bethune, T. L. Coombs, D. S. Auld and M. Sokolovsky, *Biochemistry*, 7 (1968) 3547.
28 D. C. Rees and W. N. Lipscomb, *J. Mol. Biol.*, 160 (1982) 475.
29 A. C. Williams and D. S. Auld, *Biochemistry*, 25 (1986) 94.

Journal of Chromatography, 479 (1989) 39–51
Elsevier Science Publishers B.V., Amsterdam — Printed in The Netherlands

CHROM. 21 729

REVERSED-PHASE HIGH-PERFORMANCE LIQUID CHROMATOGRAPHIC SEPARATION OF SOME INDOLE AND QUINOLINE ALKALOIDS FROM *CINCHONA*

A. HERMANS-LOKKERBOL*, T. VAN DER LEER and R. VERPOORTE
Centre for Bio-Pharmaceutical Sciences, Department of Pharmacognosy, University of Leiden, Gorlaeus Laboratories, P.O. Box 9502, 2300 RA Leiden (The Netherlands)
(First received March 6th, 1989; revised manuscript received June 21st, 1989)

SUMMARY

A high-performance liquid chromatographic method was developed for the separation of corynantheal, quinamine, cinchonamine, cinchonine, cinchonidine, quinidine and quinine. The eluent consists of 0.1 *M* potassium phosphate buffer (pH 3.0)–acetonitrile (85:15) to which is subsequently added 5 m*M* hexylamine, 85% phosphoric acid to give pH 3.0 and 2% (v/v) tetrahydrofuran. It proved necessary to develop another reversed-phase eluent, namely 1 *M* sodium acetate buffer–acetonitrile–tetrahydrofuran (80:20:5) (pH 5.5–6.0) for the separation of cinchoninone, quinidinone, cinchonine, cinchonidine, quinine and quinidine because of the epimerization of cinchoninone and quinidinone at one of the asymmetric carbon atoms during the chromatographic run. Both eluents were used in combination with a LiChrosorb RP-8 Select B column.

INTRODUCTION

The importance of and demand for the products of the *Cinchona* tree, *viz.* quinine (Q) and quinidine (Qd), as well as the non-methoxylated analogues cinchonidine (Cd) and cinchonine (C), is well known. The production of these quinoline alkaloids by means of plant cell cultures is under investigation in our laboratory. The fundamental knowledge of the biosynthesis of the *Cinchona* alkaloids in plant cell cultures still displays several gaps. Corynantheal (CorAL) is thought to be a key product in the biosynthetic pathway.

To investigate its conversion into the quinolines and to determine the activities of the enzymes involved, a high-performance liquid chromatographic (HPLC) system suitable for the separation of CorAL, cinchonamine (CAm), quinamine (QAm), Cd, C, Q and Qd had to be developed (see Fig. 1). As we also wanted to elucidate the enzymatic reaction of cinchoni(di)none (C-on) into C and Cd and of quini(di)none (Q-on) into Q and Qd, a system for the separation of these compounds was also required. It would be convenient to have one system for both assays. Therefore, the emphasis here was to analyse the end-products of the biosynthesis pathway in addition to the intermediates leading to these end-products.

0021-9673/89/$03.50

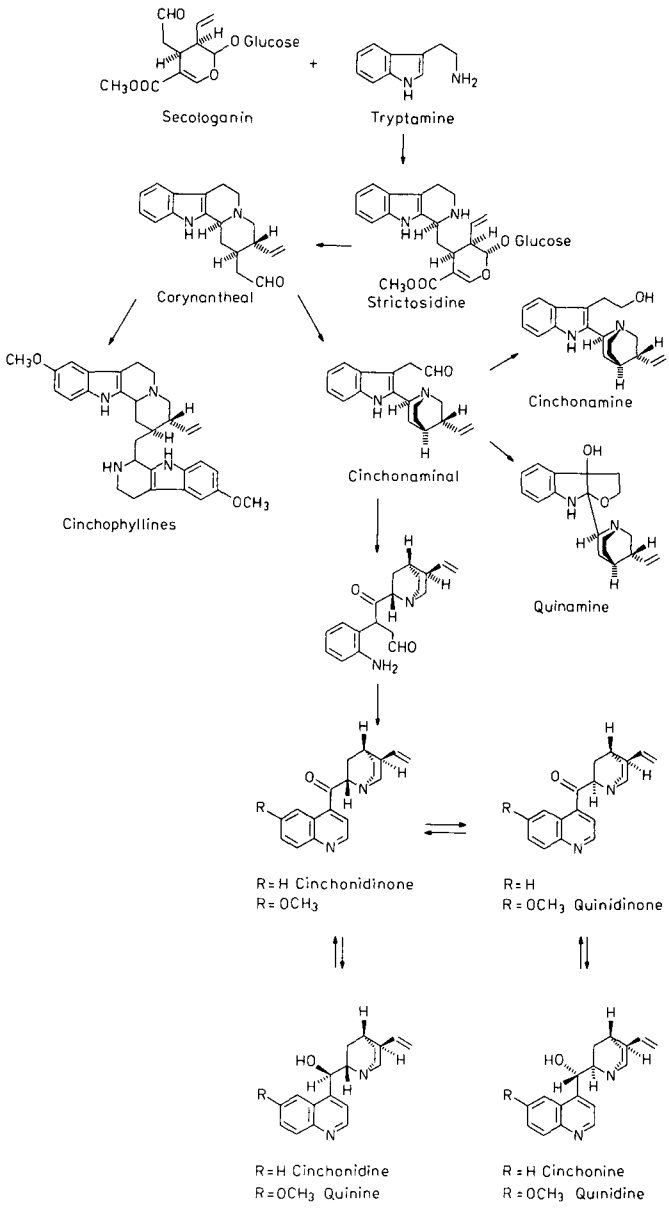

Fig. 1. Biosynthesis of *Cinchona* alkaloids.

So far some work has been done on the HPLC separation of *Cinchona* alkaloids[1]. However, in none of these systems was attention paid to the separation of the indole alkaloids CorAL, QAm and CAm in combination with the quinoline alkaloids.

In view of the procedures used to extract the compounds of interest of the

biomass, a reversed-phase (RP) HPLC system was to be preferred, with dihydroquinine (HQ) as the internal standard. HQ is preferred because its extraction properties are the same as those of the alkaloids to be separated. Strong bases, such as the quinoline alkaloids, usually show poor peak shapes in the reversed-phase HPLC mode. Hexylamine, as a long-chain molecule with an alkaline end-group, can be added to the eluent to improve the shape of the peaks of the eluted alkaloids, owing to its capacity to mask the free silanol groups of the column material[2].

EXPERIMENTAL

Apparatus

The HPLC system consisted of a high-pressure pump (Model 2150; LKB, Bromma, Sweden), a 100-μl loop injector (U6K; Waters Assoc., Milford, MA, U.S.A.), a 275-nm UV detector (2158 Uvicord SD; LKB) and a flat-bed recorder (BD41; Kipp, Delft, The Netherlands). A 25 cm × 4 mm I.D. RP-8 Select B column of LiChrosorb (5 μm) (Merck, Darmstadt, F.R.G.) was used. The flow-rate was adjusted to 1.5 ml/min for all analyses.

Alkaloids

Cinchonine, cinchonidine, quinine and quinidine were obtained from Fluka (Buchs, Switzerland) and cinchoninone and quinidinone from ACF Chemiefarma (Maarssen, The Netherlands). Quinamine and cinchonamine were obtained from plant material and corynantheal by semisynthesis by Dr. G. Massiot (Laboratoire de Pharmacognosie, Faculté de Pharmacie, Reims, France).

Chemicals

Analytical-reagent grade materials were used unless indicated otherwise and all water used was deionized and filtered.

Acetonitrile and methanol were freshly distilled before use. Tetrahydrofuran was of extra-pure quality (Merck), 1,4-dioxane and acetic acid were of Baker grade (Baker, Deventer, The Netherlands), phosphoric acid was 85% (Merck), hexylamine was of "for synthesis' quality (Merck) and KH_2PO_4 was obtained from Baker.

Eluents

The eluent described by McCalley[3] and used as a basis for developing a new system was prepared as follows: 0.1 *M* KH_2PO_4 solution was acidified with 0.1 *M* H_3PO_4 to pH 3.0 and 850 ml of this buffer were mixed with 150 ml of acetonitrile. Eluent A was prepared from this solution by the addition of 5 m*M* hexylamine, acidification to pH 3.0 with 85% H_3PO_4 and subsequent addition of 2% (v/v) tetrahydrofuran. The eluents were filtered and degassed before use.

RESULTS AND DISCUSSION

McCalley[3] compared the performances of six different RP columns related to the separation of the major *Cinchona* alkaloids; two of these (μBondapak C_{18} and LiChrosorb RP-8 Select B) gave good results without the use of a long-chain amine. We chose the LiChrosorb RP-8 Select B column and the eluent he described as a starting point for the development of a suitable system for our assays.

This system gave a poor separation of Qam, Q and CorAL and a very broad peak for CorAL. Moreover, C-on and Q-on both displayed two peaks, a small sharp one and a larger, very broad one (see Fig. 5 and Tables I–IV, where the first peak is indicated in parentheses). This phenomenon will be discussed below.

For optimization of the system, changes in the selectivity (pH, addition of hexylamine, addition of modifiers such as tetrahydrofuran and dioxane) of the eluent have been studied. An acceptable separation for most of the compounds was achieved; only the analysis of Q-on and C-on failed with this system. A separate RP eluent was developed for the separation of these ketones, C, Cd, Q, Qd and HQ, as described below.

Optimization for all components, except C-on and Q-on

Influence of pH. The pH was varied between 3.0 and 5.7. An increase in the pH caused increased retentions of C, Cd, Q, Qd and HQ. Differences in pH had less influence on the capacity factor, (k') of the weakly basic compounds CorAL, QAm and CAm. The shape of the corynantheal peak improved at lower pH (see Table I and Fig. 2). By varying the pH, the separation between the quinoline alkaloids and the indole alkaloids could be improved; however, within these groups little influence of the pH on the selectivity of the system was observed.

Influence of hexylamine. The addition of 5 m*M* hexylamine reduced the k' values of all compounds. For C, Cd, Q, Qd and HQ no improvement in the separation was achieved; the shape of the CorAL and CAm peaks improved. Apparently hexylamine does not change the selectivity of the system. The effect of the addition is shown in Table II and Fig. 3. The concentration of hexylamine in the eluent should be kept low, in order to prevent crystallization of the eluent at the HPLC connections and in the autosampler. Therefore, a 10 m*M* hexylamine concentration was not tested; the 5 m*M* solution gave satisfactory improvements.

Influence of tetrahydrofuran (THF). The percentage of THF added, was varied, 0, 2 or 4% (v/v) being added. All components of the test mixtures had shorter retention times and all peak shapes improved on addition of THF. On the other hand, C

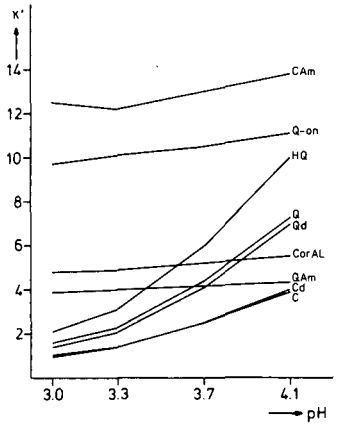

Fig. 2. Effect of pH on the capacity factors, k', of some quinoline alkaloids (C, Cd, Q, Qd, HQ and Q-on) and some indole alkaloids (CorAl, QAm, and CAm). For eluents, see Table I; eluents 3, 4, 5 and 6.

TABLE I

INFLUENCE OF pH

pH adjusted by means of H_3PO_4 or NaOH. Initial eluent: 0.1 *M* potassium phosphate buffer (pH 3.0)–acetonitrile (85:15).

No.	*Eluent*	*Plate number*		*k'*									
		HQ	*CorAl*	*HQ*	*CorAl*	*C*	*Cd*	*Q*	*Qd*	*QAm*	*CAm*	*C-on*	*Q-on*
1	Initial eluent + 5 m*M* hexylamine, pH = 4.06	3332	159	19.3	8.3	7.0	7.1	13.6	12.9	6.5	23.9	13.0	26.1
2	As 1, pH = 3.0	2800	323	4.1	7.3	1.5	1.7	2.9	2.6	5.7	21.6	11.1 (7.1)	21.6 (15.1)
3	Initial eluent + 5 m*M* hexylamine + 2% THF, pH = 3.0	4268	298	2.1	4.8	0.95	0.98	1.6	1.4	3.9	12.5	5.4 (3.4)	9.7 (6.4)
4	As 3, pH = 3.3	2652	371	3.1	4.9	1.4	1.4	2.3	2.1	4.0	12.2	5.7	10.1
5	As 3, pH = 3.7	2743	194	6.0	5.2	2.5	2.5	4.4	4.1	4.2	13.0	6.2	10.5
6	As 3, pH = 4.1	2100	174	10.0	5.5	3.9	4.0	7.3	7.0	4.3	13.8	6.3	11.1
7	Initial eluent + 4% THF, pH = 3.0	2064	233	1.5	4.9	0.74	0.70	1.2	1.1	3.8	11.5	4.3	7.4
8	As 7, pH = 3.5	1973	163	3.3	5.1	1.5	1.5	2.5	2.3	3.9	12.0	4.7	8.2
9	As 7, pH = 4.0	1940	–	6.4	5.5	2.7	2.7	4.8	4.6	4.2	12.9	5.2 (3.4)	9.1 (6.3)
10	Initial eluent + 5 m*M* hexylamine + 4% THF, pH = 4.0	1608	–	5.1	3.9	2.2	2.2	3.8	3.8	3.0	8.9	4.0 (fronting)	6.9
11	As 10, pH = 5.7	1382	–	10.9	–	4.6	4.3	8.2	8.5	3.6	10.9	8.1	13.3

TABLE II

INFLUENCE OF HEXYLAMINE

Initial eluent: 0.1 *M* potassium phosphate buffer (pH 3.0)–acetonitrile (85:15).

No.	*Eluent*	*Plate number*		*k'*									
		HQ	*CorAl*	*HQ*	*CorAl*	*C*	*Cd*	*Q*	*Qd*	*QAm*	*CAm*	*C-on*	*Q-on*
1	Initial eluent + 4% THF, pH = 4.0	1940	–	6.4	5.5	2.7	2.7	4.8	4.6	4.2	12.9	5.2 (3.4)	9.1 (6.3)
2	As 1, + 5 m*M* hexylamine, pH = 4.0	1608	–	5.1	3.9	2.2	2.2	3.8	3.8	3.0	8.9	4.0 (fronting)	6.9
3	Initial eluent, pH = 3.0	1357	245	4.3	10.3	1.6	1.7	3.1	2.8	–	30.2	14.0 (9.3)	27.4 (19.0)
4	As 3, + 5 m*M* hexylamine	2800	323	4.1	7.3	1.5	1.7	2.9	2.6	5.7	21.6	11.1 (7.4)	21.6 (15.1)

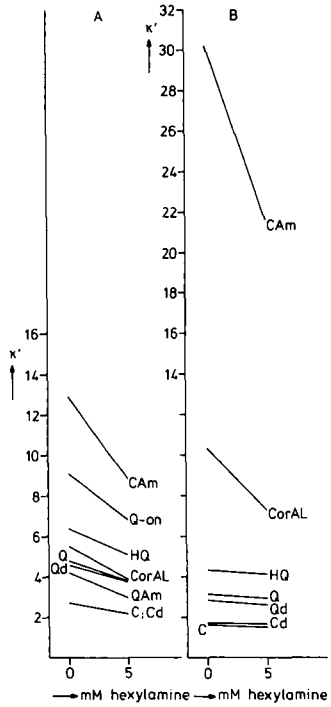

Fig. 3. Influence of hexylamine on the retention of quinoline alkaloids (C, Cd, Q, Qd, HQ, Q-on) and indole alkaloids (CorAL, QAm, CAm). For eluents, see Table II; for A eluents 1 and 2 and for B eluents 3 and 4.

and Cd now had almost identical k' values, and also for Q and Qd there was a tendency to co-elute, especially at the 4% THF level. The peak shapes of CorAL and CAm improved and the shorter analysis time, acquired by the lower k' of the last compound, CAm (17 *vs* 28.5 min), was an additional advantage. Results are given in Table III.

Influence of dioxane and pyridine. Modifiers other than THF were studied. Addition of 1,4-dioxane (2%, v/v) to the eluent resulted in only a slight improvement in peak shape. Retention times were shortened, but overall THF gave better results. Addition of pyridine to the eluent (1 m*M* pyridine; the pH was readjusted to 3.37 with H_3PO_4) did not improve the performance. Results are given in Table IV.

From these results, an eluent containing 5 m*M* hexylamine and 2% ~~(v/v)~~ THF at pH 3.0 was selected as the most suitable for the assay of CorAL, QAm, CAm, C, Cd, Q and Qd (eluent A; see Fig. 4). A disadvantage is that eluents containing hexylamine crystallize very easily at the HPLC connections, causing problems, especially in autosamplers. Nevertheless, the advantage of better peak shapes prevailed over this inconvenience.

Optimization for all quinoline alkaloids (C-on, Q-on, C, Cd, Q, Qd, HQ)

Eluent A was not suitable for the assay of the ketones (Q-on and C-on). Both Q-on and C-on gave two peaks in this solvent (see Fig. 5; in Tables I–IV the first of

TABLE III

INFLUENCE OF THF

Initial eluent: 0.1 *M* potassium phosphate buffer (pH 3.0)–acetonitrile (85:15).

No.	*Eluent*	*Plate number*		*k'*									
		HQ	*CorAl*	*HQ*	*CorAl*	*C*	*Cd*	*Q*	*Qd*	*QAm*	*CAm*	*C-on*	*Q-on*
1	Initial eluent + 5 m*M* hexylamine, pH = 3.0	2800	323	4.1	7.3	1.5	1.7	2.9	2.6	5.7	21.6	11.1 (7.4)	21.6 (15.1)
2	As 1, + 2% THF	4268	298	2.1	4.8	0.95	0.98	1.6	1.4	3.9	12.5	5.4 (3.4)	9.7 (6.4)
3	Initial eluent, pH = 3.0	1357	245	4.3	10.3	1.6	1.7	3.1	2.8	–	30.2	14.0 (9.3)	27.4 (19.0)
4	As 3, + 2% THF	1326	236	2.5	6.9	1.1	1.1	1.8	1.7	–	18.1	7.4 (4.8)	13.5 (9.1)
5	As 3, + 4% THF	2064	233	1.5	4.9	0.74	0.70	1.2	1.1	3.8	11.5	4.3 (2.8)	7.4 (5.0)

TABLE IV

INFLUENCE OF DIOXANE AND PYRIDINE

Initial eluent: 0.1 *M* potassium phosphate buffer (pH 3.0)–acetonitrile (85:15).

No.	*Eluent*	*Plate number*		*k'*								
		HQ	*CorAL*	*HQ*	*CorAL*	*C*	*Cd*	*Q*	*Qd*	*QAm*	*CAm*	*C-on*	*Q-on*
1	Initial eluent, pH = 3.3	1584	195	10.1	10.7	3.8	4.0	7.3	6.6	–	–	17.0 (fronting)	–
2	As 1, + 2% dioxane, pH = 3.38	1825	197	7.5	8.2	2.9	3.0	5.4	4.9	6.7	22.8	12.0 (much fronting)	22.6
3	As 2, + 1 m*M* pyridine pH = 3.37	1314	176	7.7	8.3	2.9	3.2	5.6	5.0	6.9	23.2	12.0 (much fronting)	23.0

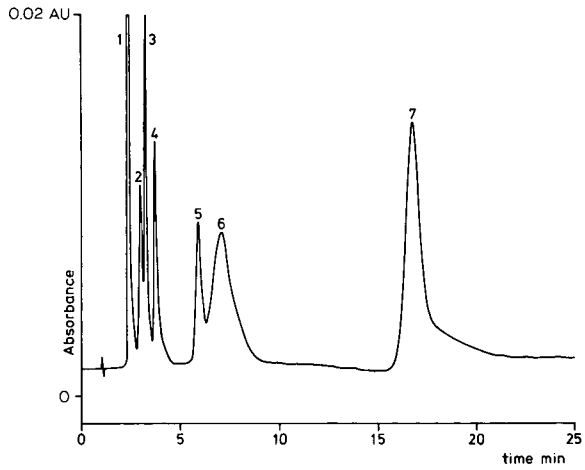

Fig. 4. Chromatogram of a test mixture. Peaks: 1 = cinchonine and cinchonidine (1.5 μg of each); 2 = quinidine (3 μg); 3 = quinine (3 μg); 4 = dihydroquinine (3 μg); 5 = quinamine (8 μg); 6 = corynantheal (2 μg); 7 = cinchonamine (4 μg). Eluent: 0.1 *M* potassium phosphate buffer (pH 3.0)–acetonitrile (85:15) plus 5 m*M* hexylamine; acidification to pH 3.0 with 85% H_3PO_4 and subsequent addition of 2% (v/v) tetrahydrofuran (eluent A). Column: LiChrosorb RP-8 Select B (25 cm); flow-rate, 1.5 ml/min.

the two peaks is indicated in parentheses). This can be explained by epimerization at C-8–C-9 (see Fig. 6), resulting in compounds with different stereochemistry, and consequently different chromatographic behaviour[4]. According to Robins and Rhodes[4], there is a slow mutarotation in polar solvents, resulting in a mixture of *R*- and *S*-epimers. The equilibrium of this epimerization proves to be pH dependent; at pH 4.5 or higher, of each of the ketones only one peak is visible in the chromatograms. Therefore, a rather high pH is needed for the analysis of the ketones. However, the other quinoline alkaloids (Q, Qd, C, Cd) showed poor peak shapes and very long retentions under such conditions, owing to the lower degree of protonation of the

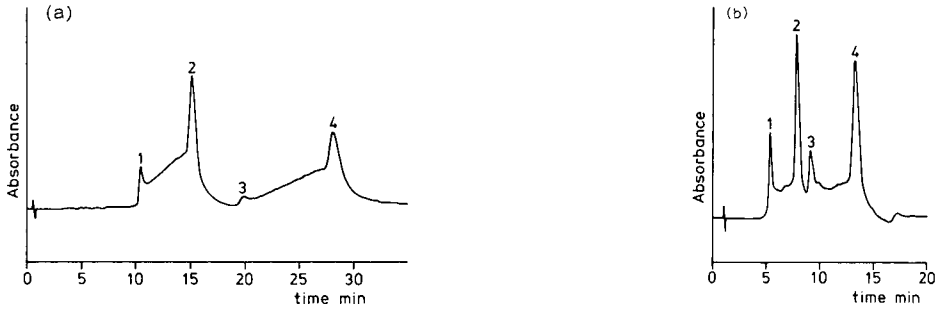

Fig. 5. Typical chromatograms of cinchoninone (1) and cinchonidinone (2), quininone (3) and quinidinone (4). (a) Eluent, 0.1 *M* KH_2PO_4 + 5 m*M* hexylamine in water–acetonitrite (85:15); H_3PO_4 added to pH 3.0 (eluent 1 in Table III). (b) Eluent as in (a) plus 2% (v/v) THF (eluent 2 in Table III). Flow-rate, amounts injected and detection are the same in both chromatograms.

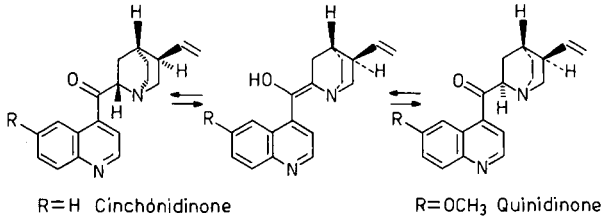

Fig. 6. Epimerization of C-on and Q-on.

alkaloids at higher pH. As is known from previous investigations[5], alkaloids will form ion pairs when acetate is the counter ion. In an HPLC eluent based on acetate buffer strong ion-pair formation is observed, even at higher pH; in phosphate buffer the alkaloids do not give rise to ion pairs extractable with non-polar solvents[5], *i.e.*, they will elute more rapidly than the alkaloid–acetate ion pairs. For acetate-based solvents a much higher concentration of acetonitrile is needed to ensure reasonable retention of the now less polar compounds.

At this time only the ketones were tested together with C, Cd, Q, Qd and HQ; as we already developed an HPLC system for the separation of CorAL, QAm and CAm in combination with these five alkaloids, their chromatographic behaviour in eluents based on an acetate buffer was not investigated.

Several acetate buffer eluents were tested (see Tables V and VI). The first was a 0.1 *M* acetate buffer (pH 5.5) mixed with an equal volume of methanol. The pH of this eluent after the addition of methanol was 6.4. The performance in this eluent was poor, with no separation between C and Cd or between Q and Qd, and severe tailing of all compounds. By varying the chromatographic parameters, attempts were made to find the optimum in separation quality. When methanol was replaced with acetonitrile as the organic part of the eluent in comparable volume ratios, the k' values decreased considerably owing to the higher eluotropic strength of acetonitrile (eluents with the same eluotropic strength were not compared). It is noteworthy that in acetate buffer–acetonitrile the sequence of elution is Cd–C–Q–Qd–HQ, whereas with methanol the sequence is C–Cd–Qd–Q–HQ (the same inversion in the retention of the stereoisomers was noted when phosphate buffer was used instead of acetate buffer).

Another variation was the acidity of the eluent: the pH was varied between 4.1 and 6.7, by adding 10 *M* sodium hydroxide solution or acetic acid; in the latter

TABLE V

ACETATE BUFFER–METHANOL ELUENTS

Eluent	k'						
	C	*Cd*	*Q*	*Qd*	*HQ*	*C-on*	*Q-on*
0.1 *M* sodium acetate (pH 5.5) + methanol (1:1), pH = 6.4	5.5	5.5	9.0	7.8	11.1	12.3	–
As above + acetic acid to pH 5.5	3.8	4.0	6.7	5.8	8.8	5.2	8.9

TABLE VI

ACETATE BUFFER–ACETONITRILE ELUENTS

Eluent		*k'*						
No.	*Composition*	*C*	*Cd*	*Q*	*Qd*	*HQ*	*C-on*	*Q-on*
1	0.1 *M* acetate (pH 5.5) + CH_3CN (1:1), pH = 6.7	2.1	1.9	2.2	2.4	2.7	3.9	4.9
2	1 + acetic acid to pH 5.5	1.1	1.1	1.3	1.4	1.6	1.7	2.2
3	2 + water to H_2O–CH_3CN (2:1), pH 5.05	2.5	2.3	3.2	3.5	4.0	3.2	4.5
4	3 + water to H_2O–CH_3CN (3:1), NaOH to pH 5.5	6.1	5.8	8.7	9.7	11.7	8.6	13.9
5	4 + acetic acid to pH 5.05	5.8	5.3	8.7	9.3	11.4	7.4	12.5
6	5 + 1% (v/v) THF	4.7	4.4	7.0	7.4	9.5	5.8	9.5
7	6 + water to H_2O–CH_3CN (4:1), pH 4.9	9.6	9.1	15.8	16.3	22.0	12.1	–
8	7 + acetic acid to pH 4.1	5.8	5.8	9.7	9.7	13.6	9.1	16.0
9	8 + THF to 5% (v/v), pH 4.15	2.5	2.5	3.7	3.7	4.8	3.2	5.1
10	9 + NaOH to pH 4.9	3.3	3.1	5.1	5.2	6.4	3.9	6.3
11	10 + NaOH to pH 5.5	4.1	3.7	6.0	6.5	7.8	5.4	8.4
12	11 + NaOH to pH 6.0	4.6	4.1	6.7	7.1	8.7	7.3	11.2

instance not only the [HA]:[Ac^-] ratio changed, but also the sum. In all instances a lower pH coincided with lower *k'* values.

The water to organic solvent ratio was varied between 1:1 and 4:1. The more water the eluent contained, the more all the compounds were retained. For example, in an eluent containing acetate buffer and acetonitrile, with 1% (v/v) THF added and a final pH of 5.0, the *k'* values of all compounds tested increased by a factor of 2 or more when the water to acetonitrile ratio was changed from 3:1 to 4:1.

The addition of THF to the eluent resulted in an improvement in the elution pattern; the peaks shapes were better and the retention times shorter. However, as in the phosphate buffer eluents, here also C and Cd had the same *k'* values and Q and Qd showed a tendency to co-elute when 5% THF was present. An increase in the THF content from 1 to 5% (v/v) in an eluent containing acetate buffer–acetonitrile (4:1) at pH 4.1 resulted in a 2–3-fold decrease in *k'* values. The same occurred with an eluent of pH 4.9.

Instead of THF, other organic modifiers from diverse classes in Snyder's classification[6] were tested. Both 1 and 5% (v/v) additions to the eluent of methoxyethanol, 1,4-dioxane and acetone were tried, but none gave satisfactory results; addition of chloroform, mixed with methanol to increase its solubility, gave no improvement.

When the column was situated in a water-jacket at 35°C, only a slight improvement in the separation was observed.

In spite of all these variations, no eluent could be found that fulfilled satisfactorily all the requirements stated above. The best eluent proved to be 1 *M* acetate buffer–acetonitrile (80:20) with pH between 5.5 and 6.0, to which 5% (v/v) THF was added. With this system C-on can be determined in the presence of C and Cd. However, C-on cannot be determined in combination with both Q *and* Qd; at pH 5.5 it elutes shortly before Q, without sufficient separation, and at pH 6.0 it elutes shortly after Qd.

For long-term satisfactory HPLC performance a lower molarity of the eluent is desired.

ACKNOWLEDGEMENTS

We thank Dr. G. Massiot for the kind gift of corynantheal and ACF Chemiefarma for supplying cinchinone and quinidinone.

REFERENCES

1 R. Verpoorte, J. Schripsema and T. van der Leer, in A. Brossi (Editor), *The Alkaloids*, Vol. 34, Academic Press, San Diego, 1988, Ch. 6, p. 371; and references cited therein.
2 D. V. McCalley, *Chromatographia*, 17 (1983) 264.
3 D. V. McCalley, *J. Chromatogr.*, 357 (1986) 221.
4 R. J. Robins and M. J. C. Rhodes, *Phytochemistry*, 26 (1987) 551.
5 A. Hermans-Lokkerbol and R. Verpoorte, *Planta Med.*, 4 (1986) 229.
6 L. R. Snyder, *J. Chromatogr. Sci.*, 16 (1978) 223.

Journal of Chromatography, 479 (1989) 53–60
Elsevier Science Publishers B.V., Amsterdam — Printed in The Netherlands

CHROM. 21 654

MULTILAYER COIL PLANET CENTRIFUGE FOR ANALYTICAL HIGH-SPEED COUNTER-CURRENT CHROMATOGRAPHY

HISAO OKA[a], FUMIE OKA and YOICHIRO ITO*

Laboratory of Technical Development, National Heart, Lung, and Blood Institute, National Institutes of Health, Building 10, Room 5D-12, Bethesda, MD 20892 (U.S.A.)

(First received March 20th, 1989, revised manuscript received May 30th, 1989)

SUMMARY

A compact portable model of a high-speed counter-current chromatograph enables efficient analytical separations of microgram sample quantities within 10 min. A series of preliminary experiments was conducted to study retention of the stationary phase of various two-phase solvent systems in short coils with different helical diameters. Under the optimal experimental conditions, analytical capability of the apparatus was successfully demonstrated in separation of flavonoids from a crude sea buckthorn ethanol extract in a multilayer coil with a total capacity of 8 ml.

INTRODUCTION

Counter-current chromatography (CCC) has many desirable features for performing analytical separations because it eliminates various complications such as sample loss, tailing of solute peaks, contamination, etc., all arising from the use of solid supports[1]. Nevertheless, the method has been used almost exclusively for preparative purposes mainly due to its long separation times required. Advent of high-speed CCC in early 1980s, however, remarkably improved the CCC technology to shorten the separation time from days to a few hours[1–3]. Recent development of an analytical coil planet centrifuge with a 5-cm revolution radius further reduced the separation time, thus providing a powerful tool for analyses of various natural products[4].

This paper introduces a new coil planet centrifuge with a 2.5-cm revolution radius which can be operated at the maximum speed of 4000 rpm. Performance of the apparatus was evaluated in terms of retention of the stationary phase of several two-phase solvent systems, and the analytical capability of the method was demonstrated in separation of microgram quantities of flavonoids from a crude ethanol extract of sea buckthorn (*Hippophae rhamnoides*) using a two-phase solvent system composed of chloroform–methanol–water (4:3:2, v/v/v).

[a] Visiting Scientist from Aichi Prefectural Institute of Public Health, Nagoya, Japan.

0021-9673/89/$03.50

APPARATUS

Fig. 1 shows a photograph of our prototype apparatus. The motor (Electro-Craft Corp., Hopkins, MN, U.S.A.) directly drives the rotary frame around the central stationary pipe of the centrifuge. The rotary frame consists of a pair of aluminum plates rigidly bridged together with multiple links and holds a column holder and a counterweight holder in the symmetrical positions at a distance of 2.5 cm from the central axis of the centrifuge. The column holder is equipped with a plastic planetary gear which interlocks to an identical stationary sun gear mounted around the central stationary pipe. This gear arrangement produces the desired planetary motion of the column holder, *i.e.*, rotation about its own axis and revolution around the central axis of the centrifuge at the same angular velocity in the same directions. This particular type of planetary motion not only permits high retention of the stationary phase in the rotating column but also prevents twisting the flow tubes, thus eliminating the need for the conventional rotary seal device which would produce leakage and contamination[2,3]. Both column and counterweight holders can be removed from the rotary frame by loosening a pair of screws on each bearing block.

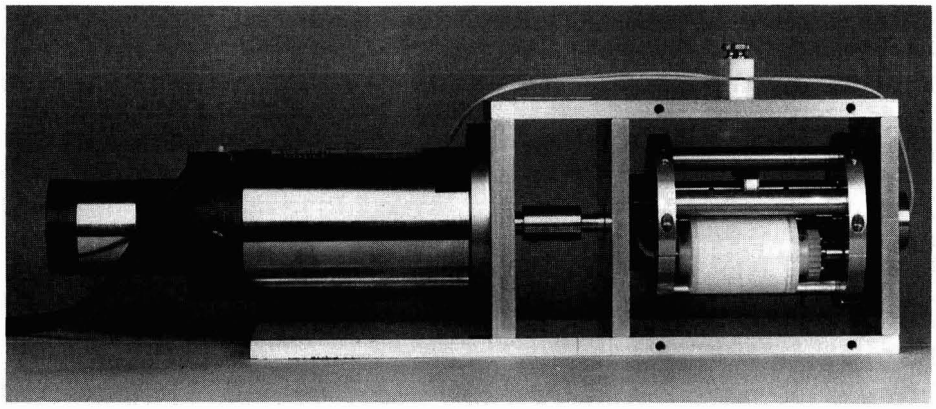

Fig. 1. Photograph of the apparatus.

Two types of coiled columns were prepared: short coils for preliminary studies on stationary phase retention and a multilayer coil for analytical separations, all from 0.85 mm I.D. polytetrafluoroethylene (PTFE) tubing (Zeus Industrial Products, Raritan, NJ, U.S.A.). The short coils were mounted on three interchangeable column holders measuring 1.4, 2.5 and 3.75 cm in hub diameters. Each coil was made by winding a 3.5–4 m length of the tubing directly onto the holder hub making tight helical turns between a pair of flanges spaced 5 cm apart. On the smallest holder hub of 1.4-cm diameter, the coil was made in double layers, while a single layer coil was formed on the other two holders. Each column had a total capacity of about 2 ml. The multilayer coil was prepared by winding approximately a 15-m length of the tubing onto the holder with 2.5-cm hub diameter making four coiled layers with a total capacity of about 8 ml.

Each terminal of these coils was connected to a PTFE flow tube of 0.45 mm I.D. and 0.5-mm wall thickness in the following manner: approximately a 1-cm length of the flow tube was inserted into the column terminal, and a piece of copper wire with 0.7-mm diameter was wound over the junction to limit heat expansion of the tubing. Then, heat was applied with a heat gun until the whole joint became transparent and fused together. The joint thus formed generally holds a pressure up to several hundred p.s.i. A pair of flow tubes from the coiled column first passes through the center hole of the column holder shaft, then forms an arch to reach the opening of the yoke mounted on the left end of the rotary frame and finally enters the opening of the central stationary pipe to exit the centrifuge. At the top of the centrifuge, these flow tubes are tightly supported with a silicone-rubber-padded clamp. These flow tubes were lubricated with silicone grease and protected with a sheath of Tygon tubing at each supported portion to prevent direct contact with metal parts. If these cautions are followed, the flow tubes can maintain their integrity for many months of operation.

EXPERIMENTAL

Reagents

Organic solvents used for preparation of the two-phase solvent systems include *n*-hexane, ethyl acetate, methanol, chloroform, acetic acid and *n*-butanol. Among those, *n*-hexane, acetic acid and *n*-butanol were of reagent grade and obtained from Polyscience (Warrington, PA, U.S.A.), Mallinckrodt (Paris, KY, U.S.A) and Tedia Company (Fairfield, OH, U.S.A.), respectively. All other solvents were glass-distilled chromatographic grade and purchased from Burdick and Jackson Labs. (Muskegon, MI, U.S.A.). Dried powder of sea buckthorn ethanol extract used as the test sample was obtained from China by the courtesy of Professor Tian You Zhang at Beijing Institute of New Technology Application, Beijing, China.

Preparation of two-phase solvent systems and sample solution

The following six volatile two-phase solvent systems were prepared for preliminary studies on stationary phase retention in short coils: *n*-hexane–water, *n*-hexane–ethyl acetate–methanol–water (1:1:1:1), chloroform–water, chloroform–acetic acid–water (2:2:1), *n*-butanol–water, *n*-butanol–acetic acid–water (4:1:5). The two-phase solvent system composed of chloroform–methanol–water (4:3:2) was prepared for the analytical separation of the sea buckthorn ethanol extract with the multilayer coil. Each solvent system was thoroughly equilibrated in a separatory funnel at room temperature by repeated shaking and degassing by opening the stopcock and two phases separated before use.

The sample solution for the analytical separation was prepared by dissolving 30 mg of the sea buckthorn extract dried powder in 1 ml of the lower non-aqueous phase of the above solvent system used for separation.

Procedures for preliminary studies on stationary phase retention in short coils

For each experiment, the short coil was first entirely filled with the stationary phase. Then, the apparatus was run at the desired revolutional speed while the mobile phase was continuously eluted through the coil at a flow-rate of 60 ml/h. In order to

provide a uniform flow, a 20-ml capacity glass syringe was driven by a multi-speed transmission syringe driver (Harvard Apparatus, Millis, MA, U.S.A.). The effluent from the outlet of the column was collected into a 5-ml capacity graduated cylinder. After 3 ml were eluted, the results were recorded by simply observing the amount of upper and lower phases comprising the total volume of the effluent. Then, the apparatus was stopped and the column flushed by allowing nitrogen gas to push out the contents. The experiments were performed by varying the experimental conditions such as revolutional speed (2000, 2500, 3000, 3500, 4000 rpm), elution modes (head to tail or tail to head) and the use of upper and lower phases as the mobile phase. The head-tail elution modes were changed by altering the direction of the planetary motion.

Construction of phase distribution diagram

From the volume of the stationary phase eluted from the column, V_s, the percentage retention of the stationary phase relative to the total column capacity was computed according to the expression $100(V_c + V_f - V_s)/V_c$, where V_c and V_f are the total column capacity and the dead space volume in the flow tubes, respectively. Using these retention data obtained from the suitable elution mode, a set of phase distribution diagrams was prepared by plotting the percentage retention of the stationary phase against the applied revolution speed in rpm.

Procedure for analytical separation of flavonoids from sea buckthorn ethanol extract with the multilayer coil

The column was first entirely filled with the upper aqueous stationary phase. Then, the coil planet centrifuge was rotated at the optimum speed of 3500 rpm, while the mobile phase was pumped into the head of the column at a flow-rate of 120 ml/h by a Shimadzu Model 6A HPLC pump (Shimadzu Corporation, Kyoto, Japan). After a steady state hydrodynamic equilibrium was reached, 4 μl of the sample solution containing 120 μg of the sample were injected into the head of the coil with a microsyringe via a Rheodyne Model 7152 syringe loading sample injector. Effluent from the outlet of the column was continuously monitored by the absorbance at 254 nm using a Shimadzu Model SPD-6A detector equipped with a preparative flow cell to record the elution curve with a Pharmacia 482 recorder (Pharmacia, Uppsala, Sweden).

The lower non-aqueous phase used as the mobile phase tends to produce microdroplets upon a slight fall of the ambient temperature. When this phenomenon occurs in the detector cell, the recording of the elution curve is disturbed by an intensive noise. In order to prevent this detrimental effect, the effluent from the column was first passed through a narrow PTFE tube (3 m × 0.45 mm I.D.) which was immersed into a water-bath heated at 40°C before entering the detector. A similar narrow tube was applied at the outlet of the detector to prevent sudden pressure drop which would generate gas bubbles from the mobile phase.

RESULTS AND DISCUSSION

The results of the preliminary studies on stationary phase retention in short coils are summarized in Fig. 2 where a set of phase distribution diagrams are arranged

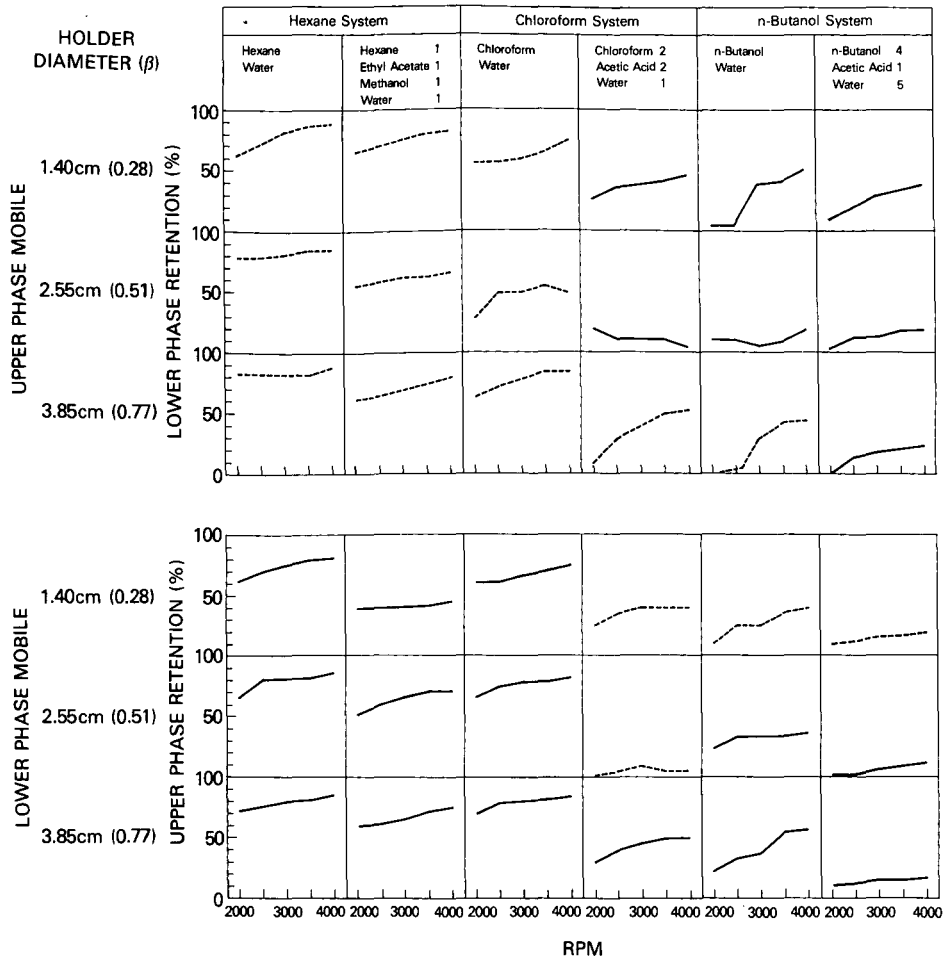

Fig. 2. Phase distribution diagrams of six volatile two-phase solvent systems obtained from short coils mounted on the present apparatus. ——, head to tail elution; – – –, tail to head elution. Flow-rate: 60 ml/h.

according to the applied two-phase solvent systems and the choice of the mobile phase.

Each column contains retention curves obtained from the same solvent system indicated at the top. These columns are placed from left to right in the order of hydrophobicity of the major organic solvent, *i.e.*, *n*-hexane, chloroform and *n*-butanol. In each solvent group, the left column shows the binary solvent system with a high interfacial tension, while the right column shows ternary or quaternary solvent system containing one or two additional solvents to moderate the interfacial tension.

These diagrams are also divided into upper and lower panels according to the choice of the mobile phase as indicated in the left margin: the upper panel was obtained by the upper phase mobile and the lower panel by the lower phase mobile. Each mobile phase group consists of three rows each obtained from a different helical

diameter or β value of the coil as indicated on the left. Here, parameter β indicates the ratio of the rotation radius (distance from the holder axis to the coil) to the revolution radius (distance from the holder axis to the central axis of the centrifuge). As stated elsewhere[5], the β value plays an important role in retention of the stationary phase in the rotating coil. Each diagram contains a single retention curve determined at five different rpms: the solid line indicates the head to tail elution mode and the broken line, the tail to head elution mode.

In all phase distribution diagrams obtained from the *n*-hexane systems, excellent retention of the lower phase is obtained by the tail to head elution of the upper phase (the upper panel) or by the head to tail elution of the lower phase (the lower panel). This phase distribution pattern indicates an ideal hydrodynamic trend that the upper phase distributes toward the head and the lower phase toward the tail, regardless of the applied β value. The above results clearly indicate that these hexane solvent systems can be retained in a multilayer coil with the full range of β values from 0.28 to 0.77.

In the chloroform solvent systems with moderate hydrophobicity, the binary system shows retention curves similar to those observed in the *n*-hexane solvent systems. However, the chloroform–acetic acid–water system displays a quite different phase distribution pattern which is largely affected by β values. In this ternary chloroform system, the largest β value of 0.77 produces satisfactory retention of around 50% at 4000 rpm as shown by the broken line with the upper phase mobile (the third row in the upper panel) or the solid line with the lower phase mobile (the third row in the lower panel) according to the typical hydrodynamic trend similar to that in the binary chloroform system. However, at the smaller β values of 0.51 to 0.28, the hydrodynamic trend of the ternary chloroform system is completely reversed as indicated by the solid lines in the upper phase mobile (first and second rows in the upper panel) and the broken lines in the lower phase mobile (first and second rows in the lower panel). At the transitional β value of 0.51, the retention level becomes lowest in both mobile phase groups. The large difference in retention between these two chloroform systems may be caused by an addition of a large proportion of acetic acid which lowered the interfacial tension between the two phases.

The hydrophilic *n*-butanol solvent systems show somewhat similar retention behavior to the ternary chloroform system. The ternary *n*-butanol system shows substantially lower retention level due to its reduced interfacial tension by the addition of acetic acid.

The above results provide useful information for the design of the multilayer coil with respect to the solvent systems to be used for the separation. A large capacity multilayer coil with full β values ranging from 0.28 to 0.77 can be used for various hexane systems and some chloroform systems containing a small amount of a modifier. On the other hand, the multilayer coil with the β value around 0.77 can yield satisfactory retention to all solvent systems except for the ternary *n*-butanol system, while the column capacity is limited to several milliliters. In the light of the above experimental results, a multilayer coil with the β value ranging from 0.51 to 0.77 was selected for performing analytical separations.

Using a multilayer coil consisting of four coiled layers with a total capacity of about 8 ml, analytical capability of the present apparatus was evaluated in separation of flavonoids in the crude ethanol extract of sea buckthorn with a two-phase solvent

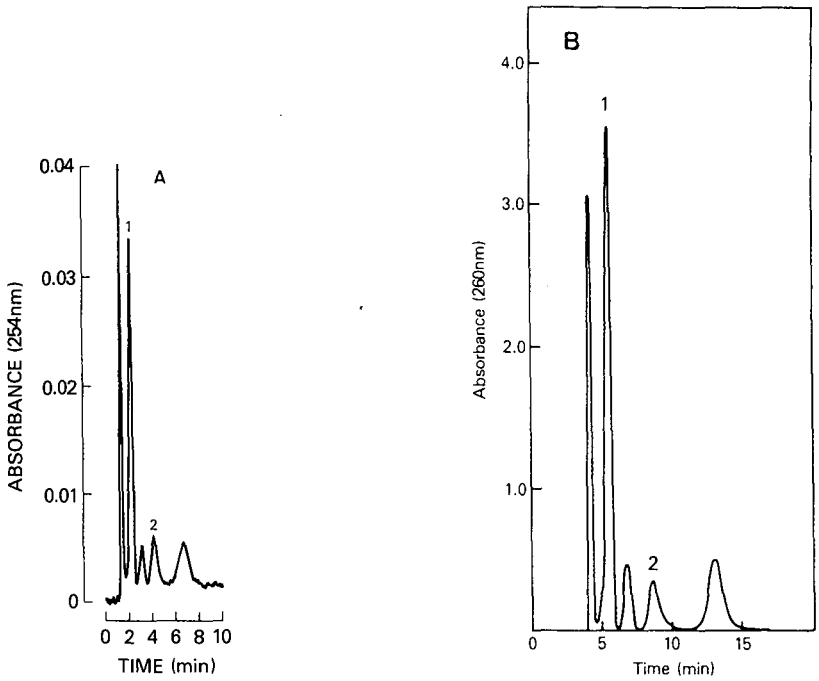

Fig. 3. Chromatograms of flavonoids in the crude sea buckthorn ethanol extract by the present apparatus (A) and by the existing analytical CCC centrifuge (B). The experimental conditions were as follows: (A) Coil planet centrifuge with 2.5-cm revolution radius; column, multilayer coil, 0.85 mm I.D. and 8-ml capacity with β = 0.51–0.77; solvent system, chloroform–methanol–water (4:3:2, v/v/v); mobile phase, lower phase; flow-rate, 2 ml/min; sample size, 120 μg; revolution, 3500 rpm. (B) Coil planet centrifuge with 6.35-cm revolution radius; column, multilayer coil, 0.85 mm I.D. and 43 ml capacity with β = 0.4–0.75; solvent system and mobile phase as in (A); flow-rate, 5 ml/min; sample size, 3 mg; revolution, 1800 rpm.

system composed of chloroform-methanol-water (4:3:2, v/v/v). Separation was performed with the lower non-aqueous mobile phase in the head to tail elution mode at a flow-rate of 2 ml/min under a coil rotation of 3500 rpm. Fig. 3A shows a chromatogram of flavonoids in a 120-μg quantity of the crude extract obtained by the present method by on-line UV monitoring of the effluent at 254 nm. Five peaks, including isorhamnetin (1) and quercetin (2) were well resolved and eluted within 8 min.

Fig. 3B shows a similar chromatogram obtained by Zhang *et al.*[6] which represents the most efficient analytical CCC separations ever achieved in the past. In an analytical column with a 40-ml total capacity, mounted on a high-speed CCC centrifuge with a 6.35-cm revolution radius, a 3-mg quantity of the same sample was separated at a flow-rate of 5 ml/min at 1800 rpm of coil rotation under otherwise identical conditions. In this experiment, on-line UV monitoring of the effluent produced an intensive noise in recording due to a thermolabile nature of the chloroform mobile phase and, therefore, the elution curve was manually drawn following the spectrophotometric analysis of each fraction.

The present apparatus further improved the analytical capability of CCC by reducing the sample size by less than 1/20 and shortening the separation time without

significantly affecting the peak resolution. In addition, the method permits on-line UV monitoring of the effluent by a minor modification of the conventional LC detection system as described elsewhere[7].

ACKNOWLEDGEMENTS

We are deeply indebted to Biomedical Engineering and Instrumentation Branch, National Institutes of Health, Bethesda, MD, U.S.A., for engineering and fabrication of the instrument.

REFERENCES

1 Y. Ito, in N. B. Mandava and Y. Ito (Editors), *Countercurrent Chromatography, Theory and Practice*, Marcel Dekker, New York, 1988, Ch. 3, pp. 79–442.
2 Y. Ito, *CRC Crit. Rev. Anal. Chem.*, 17 (1986) 65.
3 Y. Ito, J. Sandlin and W. G. Bowers, *J. Chromatogr.*, 244 (1982) 247.
4 Y. Ito and Y. W. Lee, *J. Chromatogr.*, 391 (1987) 290.
5 Y. Ito, *J. Chromatogr.*, 301 (1984) 387.
6 T. Y. Zhang, R. Xiao, Z. Y. Xiao, L. K. Pannell and Y. Ito, *J. Chromatogr.*, 445 (1988) 199.
7 H. Oka and Y. Ito, *J. Chromatogr.*, 475 (1989) 229.

Journal of Chromatography, 479 (1989) 61–72
Elsevier Science Publishers B.V., Amsterdam — Printed in The Netherlands

CHROM. 21 719

CAPILLARY GAS CHROMATOGRAPHY–MASS SPECTROMETRY AND IDENTIFICATION OF SUBSTITUTED CARBOXYLIC ACIDS IN LIPIDS EXTRACTED FROM A 4000-YEAR-OLD NUBIAN BURIAL

FAZIL O. GÜLAÇAR* and ARMAND BUCHS
Laboratory for Mass Spectrometry, University of Geneva, 16 Boulevard d'Yvoy, 1211 Geneva 4 (Switzerland)
and
ALBERTO SUSINI
Department of Anthropology, University of Geneva, 12 Rue Gustave Revillod, 1227 Carouge-Geneva (Switzerland)
(First received April 10th, 1989; revised manuscript received June 19th, 1989)

SUMMARY

Polar carboxylic acid fractions of lipids extracted from samples from a 4000-year-old Nubian mummy were investigated by capillary gas chromatography–mass spectrometry. They contain series of α,ω-dicarboxy, monohydroxy, dihydroxy and keto fatty acids, some of which were found for the first time outside the synthetic laboratory. Their chromatographic and mass spectrometric characteristic properties are reported.

INTRODUCTION

During an investigation of the extractable lipids from diverse parts of a 4000-year-old Nubian burial belonging to the Ancient Kerma[1] civilization, the substituted fatty acids in the polar acid fractions were examined by gas chromatography–mass spectrometry (GC–MS). In addition to a homologous series of C_7–C_{18} α,ω-dicarboxylic aliphatic acids and diverse C_{16}–C_{20} mid-chain vicinal dihydroxy fatty acids, we identified several homologous series of C_7–C_{18} monohydroxy fatty acids containing every positional isomer except the 4-hydroxy acids, and a series of all keto fatty acids excluding the α-, β-, $(\omega-2)$- and $(\omega-3)$-oxo positional isomers. Moreover, a homologous series of *n*-alkylsuccinic acids with alkyl substituents ranging from C_{11} to C_{16} were also found in the extract from inside of the skull. We report here the GC retention characteristics of these compounds on an OV-73 coated capillary column and their mass spectrometric fragmentation patterns.

0021-9673/89/$03.50

EXPERIMENTAL

Samples, extraction and preparation

The mummy, of a 40–50-year-old male, was found in a necropolis at Kerma in Upper Nubia (Sudan) excavated in 1983.

Samples of skin and concretions from the inside of the skull and of the thorax were extracted by homogenizing the tissue with chloroform–methanol (2:1) and the extracts were kept in a refrigerator until analysis. The extracted lipids were separated into various classes using chromatographic procedures that have already been described for geological[2,3] or biological[4] organic material. Briefly, the lipids were first separated into neutral and acidic fractions by chromatography on a silica gel column (200 x 12 mm I.D., 70–230 mesh, 10% potassium hydroxide). The acidic fraction was esterified with 14% boron trifluoride in methanol and the resulting methyl esters were separated by flash chromatography[5] on a second silica gel column (300 x 6 mm I.D., 70–230 mesh, nitrogen pressure 0.3–0.5 bar). After the elution of the monocarboxylic fatty acid methyl esters with 50 ml of hexane–methylene chloride (3:1), the polar carboxylic acid methyl esters were eluted with 50 ml of methylene chloride–ethyl acetate (9:1). Before the GC–MS analyses were performed, the polar acid fraction was trimethylsilylated at 70–90°C for 15 min with bis(trimethylsilyl)trifluoroacetamide containing 1% of trimethylchlorosilane (Fluka, Buchs, Switzerland).

GC–MS analyses

The equipment used was a Finnigan 4000 quadrupole mass spectrometer equipped with the SuperIncos data system and coupled to a Carlo Erba 5300 Mega Series gas chromatograph. Analyses were performed with laboratory made glass capillary columns (Duran, 25 m x 0.32 mm I.D.), coated with OV-73 (Alltech). After splitless injection at 60°C, the GC oven was heated to 130°C at 10°C/min and then to 280°C at 4°C/min. The detailed GC and MS conditions have been described elsewhere[2]. Equivalent chain lengths (ECL) of the unbranched α,ω-dicarboxylic acid dimethyl esters were first determined by coinjection of a sample with a standard mixture of *n*-alkanoic acid methyl esters and found to be equal to $(n + 3) + 0.33$ (± 0.04) where n is the number of carbon atoms in the free diacid. The ECL values of the other polar acids were calculated on the basis of their retention times relative to those of the α,ω-dicarboxylic acids which were present in all samples from the mummy.

RESULTS AND DISCUSSION

Fig. 1 shows the reconstructed total ion chromatogram (TIC) of the methylated and trimethylsilylated polar acid fraction separated from white concretions found inside the mummy's thorax. The early eluting part of the chromatogram is dominated by regularly spaced peaks arising from the saturated straight-chain α,ω-dicarboxylic acid dimethyl esters (C_7–C_{18}) identified on the basis of their mass spectra. The compounds of this series exhibit in their mass spectra[6] and intense m/z 98 peak which was used for their detection by mass fragmentography[7].

Between two successive homologues of the α,ω-dicarboxylic acids, the TIC shows a very complex pattern, especially in the late-eluting part, as exemplified by the

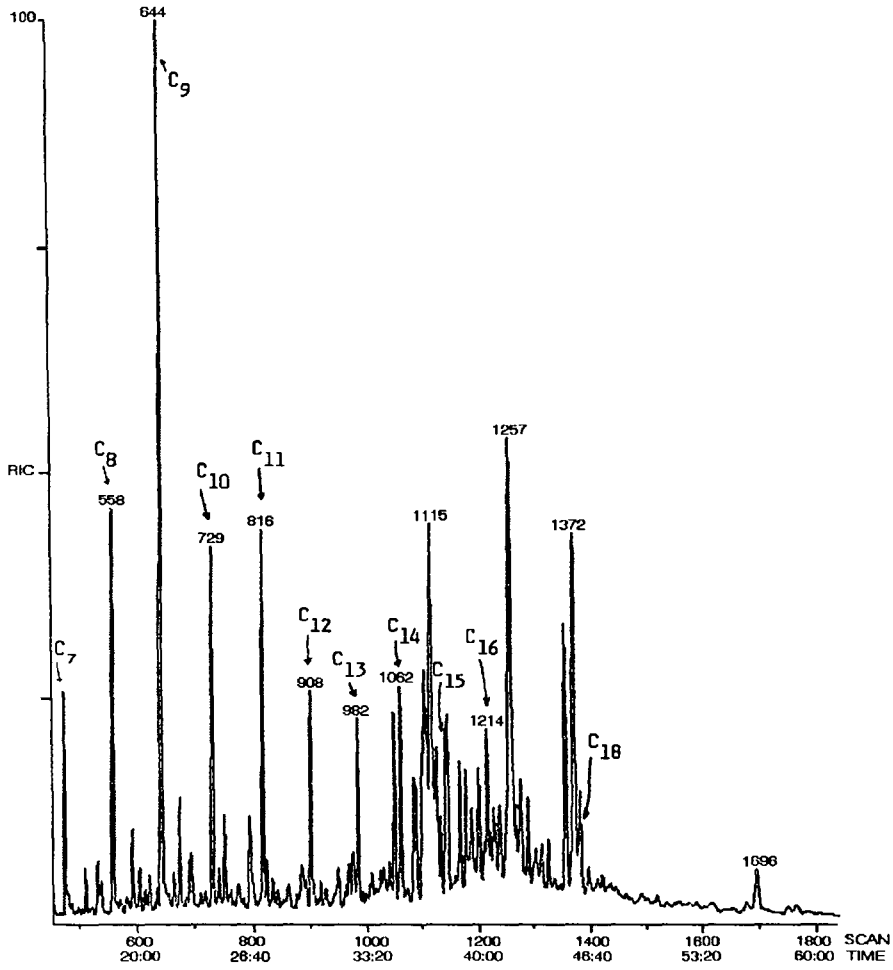

Fig. 1. Reconstructed total ion chromatogram of the esterified and trimethylsilylated polar acid fraction from the thorax extract (peaks marked C_n represent α,ω-dicarboxylic acids with n = number of carbon atoms in the free acid).

partial TIC in Fig. 2. A close examination of the mass spectra showed that most of the peaks appearing as single chromatographic peaks on this trace are in fact due to several coeluting components. Almost all components of this chromatogram were identified by comparison of their mass spectra and retention times with those of authentic analogues, with published spectra of lower homologues or by the interpretation of their mass spectra, as shown in Tables I and II.

Oxo fatty acids

The major oxo fatty acids included a homologous series of 4-oxo fatty acids in the C_{11}–C_{18} range with the C_{16} homologue being the most abundant. They are characterized by a major McLafferty rearrangement ion at m/z 130 and a secondary

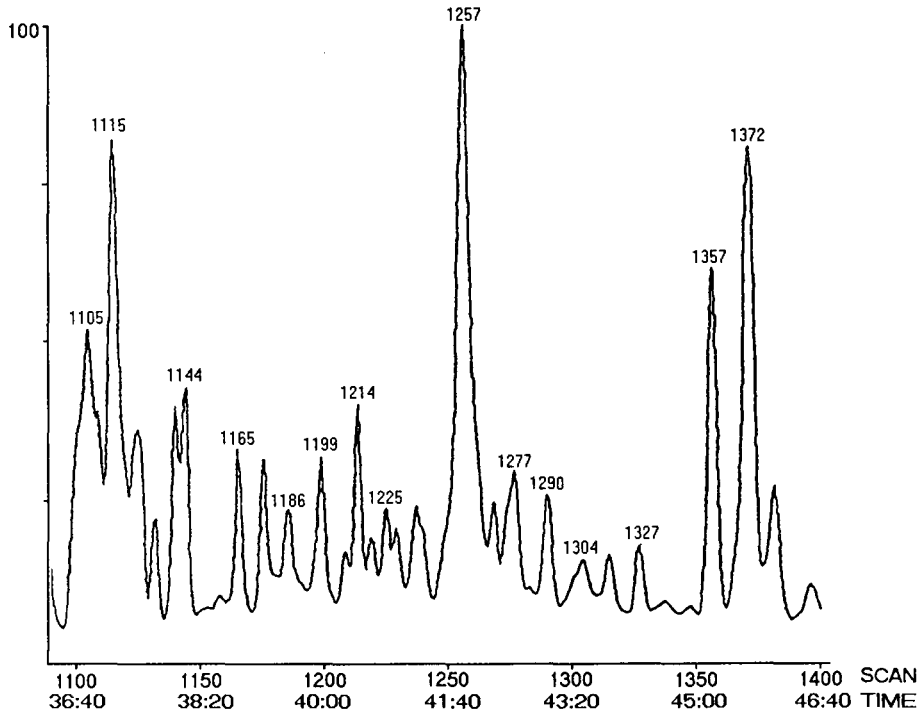

Fig. 2. Detail of part of the reconstructed total ion chromatogram of Fig. 1.

TABLE I

KETO ACIDS FOUND IN LIPIDS EXTRACTED FROM THE MUMMY

See Experimental for GC–MS conditions.

Compound	*Chain length (n)*	*ECL*	*Fragment*[a]	*Other peaks*[b]
4-Oxo	8–20	$(n+1)+0.61$	98, 130	115, (M − 31),(M − 87)
5-Oxo	9–20	$(n+1)+0.65$	144	112,129,(M − 31),(M − 101)
6-Oxo	12–18	$(n+1)+0.79$	158	126,143,(M − 31),(M − 115)
7-Oxo	12–18	$(n+1)+0.82$	172	(M − 114),(M − 31)
8-Oxo	13–18	$(n+1)+0.84$	186	(M − 128),(M − 31)
9-Oxo	16–18	$(n+1)+0.86$	200	(M − 142), (M − 31)
10-Oxo	16–18	$(n+1)+0.87$	214	(M − 156),(M − 31)
11-Oxo	16–18	$(n+1)+0.88$	228	(M − 170)
12-Oxo	16–18	$(n+1)+0.89$	242	(M − 184)
13-Oxo	18	$(n+1)+0.90$	256	(M − 198)
$(\omega-1)$-Oxo	8	$(n+2)+0.07$	58	71,(M − 89),(M − 57),(M − 31)
$(\omega-1)$-Oxo	to 18	$(n+2)+0.16$	58	71,(M − 89),(M − 57),(M − 31)

[a] *m/z* of ion(s) used for fragmentographic detection.
[b] *m/z* of other diagnostic ions, not necessarily major ones.

TABLE II

ECL VALUES OF MONOHYDROXY FATTY ACIDS (AS METHYL ESTER TMS ETHERS) FOUND IN THE EXTRACTS FROM THE MUMMY

See Experimental for GC–MS conditions. See text for ions a and b.

Chain length	*m/z of ion b and OH position*															
	103 ω	*117* (ω−1)	*131* (ω−2)	*145* (ω−3)	*159* (ω−4)	*173* (ω−5)	*187* (ω−6)	*201* (ω−7)	*215* (ω−8)	*229* (ω−9)	*243* (ω−10)	*257* (ω−11)	*271* (ω−12)	*285* (ω−13)	*299* (ω−14)	*301* (ω−15)	*315* (ω−16)
7	10.76	10.09															
8	11.72	11.03	10.91			10.39	10.39										
9	12.70	11.97	11.86	11.62			11.31	11.31									
10	13.64	12.95	12.83	12.58	12.45			12.21	12.21								
11	14.54	13.93	13.80	13.56	13.46	13.34			13.18	13.18							
12	15.52	14.91	14.77	14.51	14.41	14.30	14.24			14.12	14.12						
13	16.51	15.89	15.75	15.48	15.39	15.25	15.18	15.16			15.08	15.08					
14	17.50	16.87	16.73	16.46	16.29	16.22	16.15	16.12	16.12			16.05	16.05				
15	18.47	17.84	17.70	17.42	17.27	17.17	17.12	17.09	17.09	17.09			17.02	17.02			
16	19.51	18.80	18.66	18.37	18.21	18.14	18.05	18.02	17.98	18.01	18.02			17.97	17.97		
17		19.77	19.63	19.36		19.09	19.01			18.95					18.94	18.94	
18	21.46	20.73	20.60	20.33	20.15	20.03	19.97	19.91	19.89	19.88	19.87	19.89	19.90	19.93		19.89	19.89
m/z of ion a[a]	–	371	357	343	329	315	301	287	273	259	245	231	217	203	189	175	Absent[b]
OH position[a]	18	17	16	15	14	13	12	11	10	9	8	7	6	5	4	3	2

[a] Diagonal entries towards the top and left side of the table.

[b] α-Hydroxy acids are detected by fragmentograms of *m/z* 159 and (M − 59).

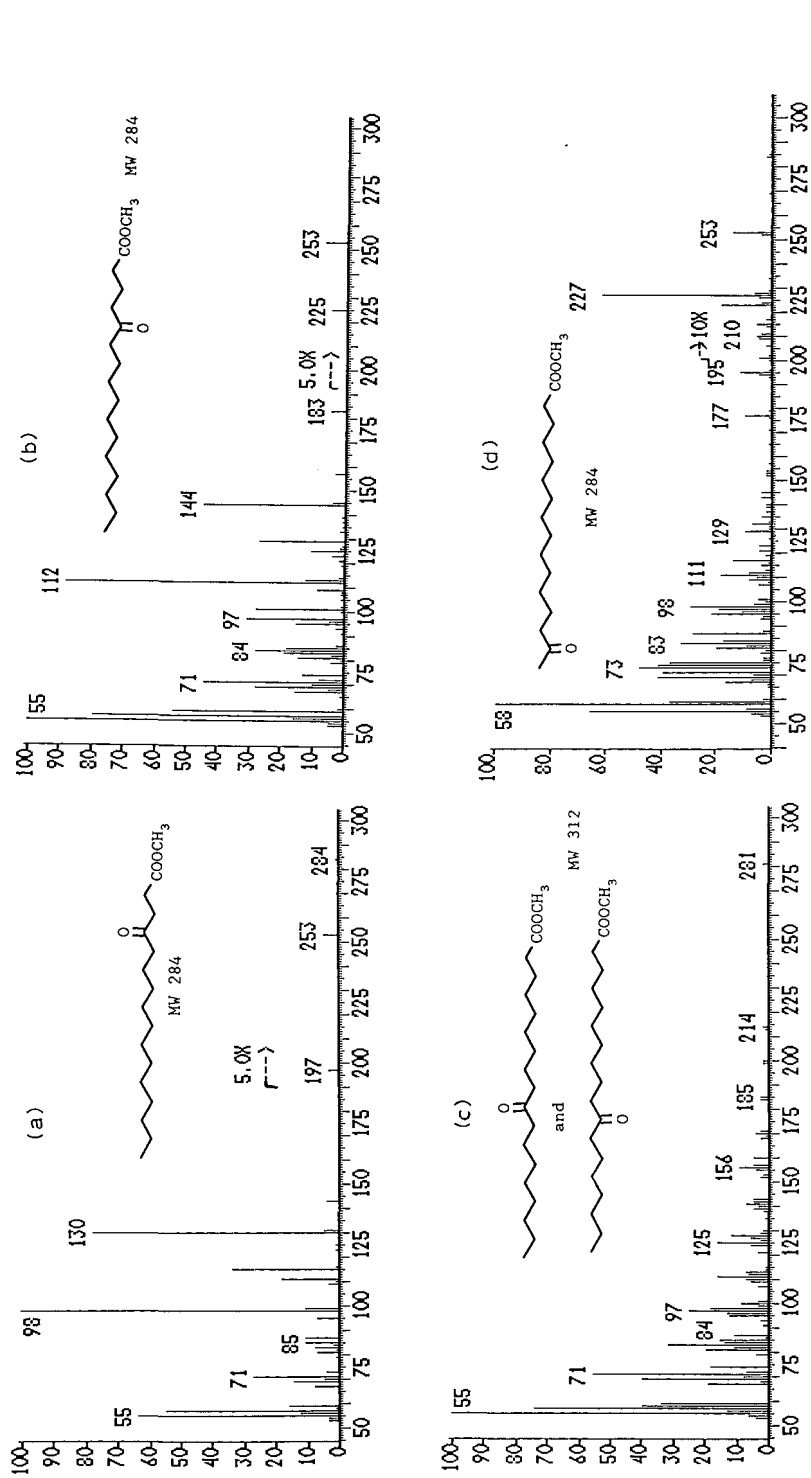

Fig. 3. Mass spectra of methyl esters for (a) 4-oxohexadecanoic acid, (b) 5-oxohexadecanoic acid, (c) mixture of 9- and 10-oxooctadecanoic acids and (d) 15-oxohexadecanoic acid found in the mummy extracts.

fragment at *m/z* 98 (130 − CH_3OH), and also by the α-cleavage ions at *m/z* 115 and *m/z* 197 (M − 87), as shown in the mass spectrum of the 4-oxohexadecanoic acid illustrated in Fig. 3a. Thus, 4-oxo fatty acids may also be detected by the *m/z* 98 mass fragmentogram as they are chromatographically well separated from the dicarboxylic acids. The 4-oxo acids are accompanied by smaller amounts of the corresponding 5-oxo isomers which are characterized by a similar fragmentation pattern [McLafferty ion at *m/z* 144, *m/z* 112 (144 − CH_3OH) and α-cleavage ions at *m/z* 129 and *m/z* (M − 101)] (Fig. 3b). They elute just after the 4-oxo isomers as only partially resolved peaks. The other prominent oxo-acids identified were coeluting mixtures of 9- and 10-oxo isomers of hexadecanoic and octadecanoic acids. The mass spectra of these isomers are also characterized by the same fragments as those produced from the 4- and 5-oxo isomers, but these fragments, although of diagnostic value, are not the major ones (Fig. 3c).

Another relatively important homologous series of keto acids is the one with the oxo function on C-(ω − 1). These acids have much higher ECL values than those of the mid-chain keto acids of the same chain length and their mass spectra are characterized by an intense *m/z* 58 ion from McLafferty rearrangement (Fig. 3d). Finally, minor or trace amounts of keto fatty acid positional isomers with the keto function located between C-6 and C-(ω − 4) were observed on the mass fragmentograms of the corresponding McLafferty rearrangement ions, as shown in Table I.

Oxo fatty acids with the keto function at a given position show a constant increase in their ECL value with increasing carbon number, except when the function is on the (ω − 1) carbon atom. Thus, a 4-oxo fatty acid methyl ester will elute (on the GC time scale) at a position corresponding to 61% of the distance between the elution positions of the *n*-fatty acid methyl esters with one and two more carbon atoms, respectively (Table I). If we call this a "constant increment", then the (ω − 1)-oxo fatty acids show a slightly "positive increment" of their ECL with increasing carbon number.

Monohydroxy fatty acids

The mass spectra of the two large peaks (*i.e.*, 1115 and 1257) in the chromatogram in Fig. 2 showed that they are produced by unresolved isomers of monohydroxypalmitic and monohydroxystearic acids, respectively. The mass spectra of monohydroxy fatty acid TMS ether methyl ester derivatives are characterized by intense fragments from α-cleavage to the OTMS group, specific to the position of the original hydroxy group[8,9], except for α- and ω-hydroxy acids which do not show ion *a*:

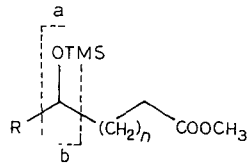

The other characteristic ions which are common to all spectra are *m/z* 73 (TMS group), the (*a* − 29) ion produced by the loss of CHO from ion *a* after migration of the TMS group to the carboxylic carbonyl group and the (*a* − 32) ion

($[a-CH_3OH]^+$). Table II gives the ECL values of all the monohydroxy acids found in the mummy samples and the m/z values of the ions a and b used for their detection. The ω-hydroxy acids which do not exhibit ion a were detected by the $(M-47)$ ions[8]. Every positional isomer of the monohydroxy acids in the range C_7–C_{18}, except the 4- and 5-hydroxy isomers, was present. The α- and β-hydroxy isomers having the same carbon number coelute in the entire carbon number range but the contribution of the α-hydroxy acids may be calculated through the abundance of the $(M-59)^+$ ion, present in their mass spectra[8]. The other positional isomers are all resolved for the acids with less than 13 carbon atoms. Acids with longer chains show either coelution or only partial resolution of the isomers bearing the hydroxyl group on carbon atoms α- to $(\omega-6)$ positions. ECLs of homologous acids in the series with the hydroxy substituent on a given carbon atom (from the carboxylic carbon side) clearly exhibit a "negative increment" with increasing chain length (Table II, diagonal entries). Two higher α-hydroxy acid homologues, C_{22} and C_{23} (not shown in Table II), were also found in significant amounts in all the extracts.

Dihydroxy fatty acids

Both the large peaks at 1357 and 1372 in the TIC in Fig. 2 show almost identical mass spectra (Fig. 4a); they were identified as the *threo* and *erythro* isomers

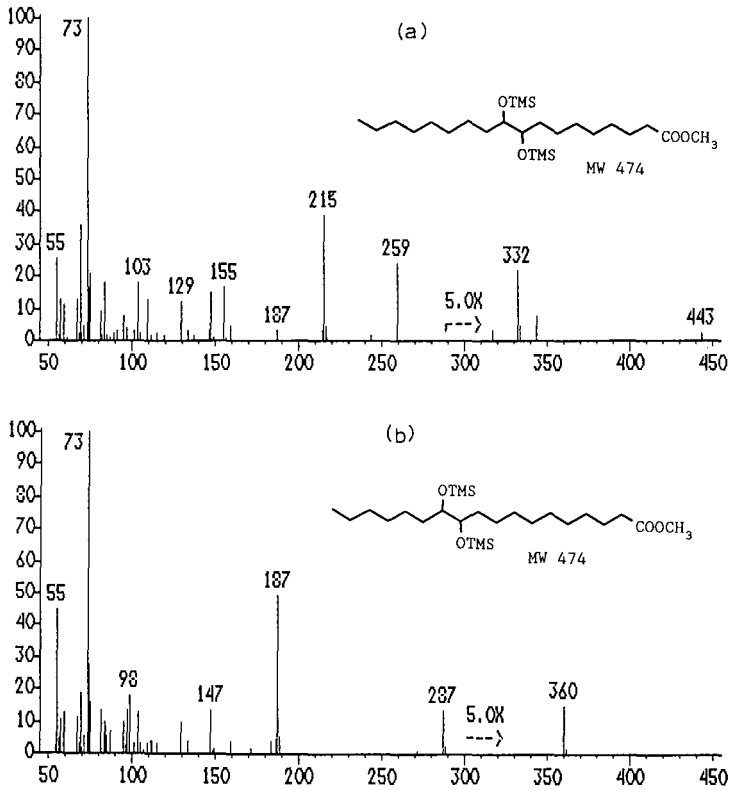

Fig. 4. Mass spectra of methyl ester TMS ethers for (a) 9,10-dihydroxyoctadecanoic acid and (b) 11,12-dihydroxyoctadecanoic acid found in the mummy extracts.

of methyl 9,10-(ditrimethylsilyloxy)octadecanoate[10], respectively. The mass spectra of these compounds are characterized by the two intense *o* and *p* ions, corresponding to the cleavage of the bond linking the carbon atoms which bear the OTMS groups, with retention of the charge on either side[8,10], as shown below.

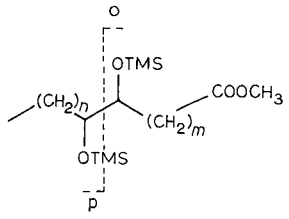

The other characteristic ions in the mass spectra of mid-chain vicinal dihydroxy acids are *m/z* 73 (base peak, TMS), *m/z* 147 and *m/z* 159, which are common to all spectra and the (M − 15), (M − 31) and [M − $CH_3(CH_2)_nCHO$] ions, which are of diagnostic value despite their low intensities ($\leqslant 3\%$ of the base peak). Other vicinal dihydroxy fatty acids, identified on the basis of their mass spectra, are listed in Table III, and the mass spectrum of 11,12-dihydroxyoctadecanoic acid is shown in Fig. 4b.

The abundance ratio of the *threo* and *erythro* isomers, as measured from the intensities of ions o, are very significantly dependent on the origin of the sample. In the thorax extract, for example, the *erythro* isomer of the 9,10-dihydroxy C_{18} acid is approximately twice as abundant as the *threo* isomer, whereas in the extract from the skull it is the *threo* isomer that is more prominent; in the skin the two enantiomers show similar abundances.

TABLE III

ECL VALUES OF DIHYDROXY FATTY ACIDS (AS METHYL ESTER TMS ETHERS) FOUND IN THE EXTRACTS FROM THE MUMMY

See Experimental for GC–MS conditions.

Chain length	*Position of OH groups*	*Diagnostic ions*		*ECL*
		o	*p*	
16	6,7 *threo*	217	229	19.24
16	6,7 *erythro*	217	229	19.40
16	7,8 *threo*	231	215	19.24
16	7,8 *erythro*	231	215	19.40
16	9,10 *threo*	259	187	19.29
16	9,10 *erythro*	259	187	19.44
17	8,9 *threo*	245	215	20.13
17	8,9 *erythro*	245	215	20.29
17	10,11 *threo*	273	187	20.23
17	10,11 *erythro*	273	187	20.41
18	9,10 *threo*	259	215	21.05
18	9,10 *erythro*	259	215	21.22
18	11,12 *threo*	287	187	21.17
18	11,12 *erythro*	287	187	21.33

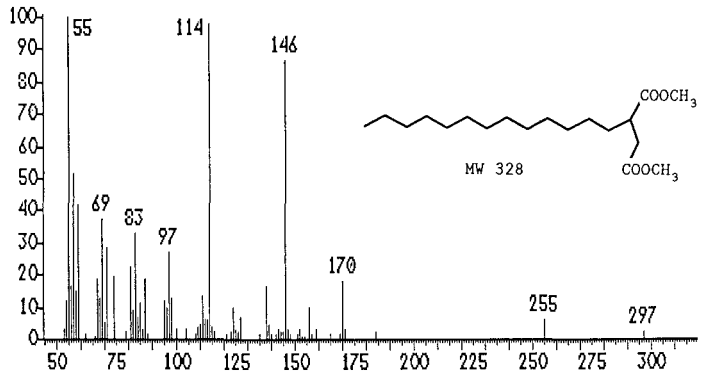

Fig. 5. Mass spectrum of the methyl ester of *n*-tridecylsuccinic acid found in the extract from the skull.

Alkylsuccinic acids

The mass spectrum of a relatively intense peak eluting at an ECL value of 18.84 in the TIC of the skull extract is shown in Fig. 5. The major ions at *m/z* 146 and 114 can be interpreted as originating from an alkyl-substituted succinic acid dimethyl ester by a McLafferty rearrangement and a subsequent loss of CH_3OH:

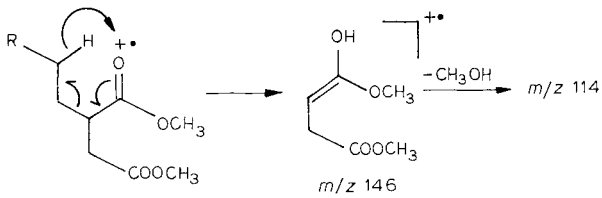

Indeed, a comparison of the spectrum in Fig. 5 with that of methyl *n*-dodecylsuccinate[11] confirms the unknown compound as being a C_{13}-alkyl-substituted succinic acid. A search for the occurrence of other homologues in the extract by means of *m/z* 146 and 114 fragmentograms indicated the presence of C_{11}- (ECL = 16.88), C_{12}- (17.86), C_{14}- (19.82), C_{15}- (20.79) and C_{16}- (21.79) alkylated analogues. The evolution of the ECL values suggests that the alkyl substituent is linear. These compounds could not be detected in the skin or thorax samples.

DISCUSSION

Most of the substituted fatty acids founds in the extracts from the mummy are normally not found in human or animal tissues. They are obviously produced by *post mortem* transformations of the original fatty acids. As will be reported elsewhere[12], other lipid compounds such as the sterols, the bile acids and, more particularly, the unsubstituted monocarboxylic acids also showed more or less intense modifications. The last group included only saturated fatty acids (indicating a complete disappearance of the unsaturated fatty acids normally found in human tissues), comprising *iso-*

and *anteiso*-methyl-branched homologues in the C_{13}–C_{19} range. This suggests a bacterial reworking of the original carboxylic acids. The relative abundances of the diverse substituted acids reported here suggest that most of them are produced by oxidation of the double bond of an unsaturated fatty acid originally present in the body. Thus, in the α,ω-dicarboxylic acid series, the most abundant compound is the C_9 homologue; in the mid-chain monohydroxy or keto acid series, those with 18 and 16 carbon atoms and the oxo function on C-9 and C-10 are the most abundant. In the dihydroxy fatty acid series, 9,10-dihydroxy acids, presumably produced by dihydroxylation of the double bonds of oleic and palmitoleic acids, are major compounds.

Among the acids reported here, the complete series of isomeric monohydroxy and keto acids have never been reported in natural samples, although recently they have been detected in aerosols in the C_6–C_{15} range, with maxima at C_9 or C_{11}[9,13]. The 10-oxo- and 10-hydroxy C_{18} and C_{16} acids have been reported in the adipocere from human bodies having been immersed in the sea for 3–6 months[14,15], but positional isomers and other homologues were not mentioned.

Mid-chain vicinal dihydroxy acids are well known compounds which are routinely prepared from unsaturated fatty acids in order to determine the position and the geometry of the double bonds[10,16] in the original compounds. However, to our knowledge, they have never been reported as occurring in samples from outside the laboratory. As we already pointed out, in the mummy samples they are obviously produced through dihydroxylation of the double bond in a suitable precursor. It is interesting that the enantiomeric composition of these acids is dependent on their origin. Two possibilities may explain this: (i) the original unsaturated precursor acids had the same double bond geometry but different mechanisms of dihydroxylation were operative, or (ii) the mechanism of formation was the same but the ratio of the *cis*- to *trans*-unsaturated acids in diverse parts of the body was different.

The mass spectrometric fragmentation patterns of the *n*-alkylsuccinic acids have been interpreted by using spectra obtained from methyl and ethyl esters of synthetic *n*-dodecylsuccinic acid[11]. The only report on the occurrence of this type of compound in a natural sample concerns Green River oil shale, a 60 million-year-old sediment, in which a homologous series with an alkyl substituent ranging from C_{13} to C_{29} (C_{18} and C_{28} members absent) was detected[17]. The fact that in the mummy they occur only in the skull extract and that only the C_{13} alkyl-substituted homologue is of significant abundance, must have either a biochemical or a diagenetic significance, but at present we have no explanation.

ACKNOWLEDGEMENTS

This work was supported in part by the Fonds National Suisse de la Recherche Scientifique (Grant No. 2000-5.222). We thank Mrs. O. Vaucher for valuable technical assistance.

REFERENCES

1 M. Klohn, A. Susini and C. A. Baud, *Am. J. Phys. Anthropol.*, 75 (1988) 232.
2 Y. A. Mendoza, F. O. Gülaçar and A. Buchs, *Chem. Geol.*, 62 (1987) 307.
3 Y. A. Mendoza, F. O. Gülaçar, Z.-L. Hu and A. Buchs, *Int. J. Environ. Anal. Chem.*, 31 (1987) 107.

4 Z.-L. Hu, Y. A. Mendoza, A. Buchs and F. O. Gülaçar, *Lipids*, 23 (1988) 679.
5 W. C. Still, M. Kahn and A. Mitra, *J. Org. Chem.*, 43 (1978) 2923.
6 G. Eglinton, D. H. Hunneman and K. Douraghi-Zadeh, *Tetrahedron*, 24 (1968) 5929.
7 K. Kawamura and R. Ishiwatari, *Geochim. Cosmochim. Acta*, 48 (1984) 251.
8 G. Eglinton, D. H. Hunneman and A. McCormick, *Org. Mass Spectrom.*, 1 (1968) 593.
9 K. Kawamura and R. B. Gagosian, *J. Chromatogr.*, 438 (1988) 309.
10 J. J. Boon, J. W. de Leeuw, G. J. v.d. Hoek and J. H. Vosjan, *J. Bacteriol.*, 129 (1977) 1183.
11 R. Ryhage and E. Stenhagen, *Ark. Kemi*, 23 (1964) 177.
12 F. O. Gülaçar, A. Susini and M. Klohn, *J. Lipid Res.*, in press.
13 K. Kawamura and R. B. Gagosian, *J. Chromatogr.*, 438 (1988) 299
14 T. Takatori and A. Yamaoka, *Forensic Sci.*, 9 (1977) 73.
15 T. Takatori and A. Yamaoka, *Forensic Sci.*, 10 (1977) 117.
16 N. J. Jensen and M. L. Gross, *Mass Spectrom. Rev.*, 7 (1987) 497.
17 A. G. Douglas, M. Blumer, G. Eglinton and K. Douraghi-Zadeh, *Tetrahedron*, 27 (1971) 1071.

Journal of Chromatography, 479 (1989) 73–83
Elsevier Science Publishers B.V., Amsterdam — Printed in The Netherlands

CHROM. 21 645

COMPARISON OF THE USE OF MASS SPECTROMETRY AND METHYLENE UNIT VALUES IN THE DETERMINATION OF THE STEREOCHEMISTRY OF ESTRANEDIOL, THE MAJOR URINARY METABOLITE OF 19-NORTESTOSTERONE IN THE HORSE

EDWARD HOUGHTON*, ANNETTE GINN, PHILIP TEALE, MINOO C. DUMASIA and JOHN COPSEY[a]

Horseracing Forensic Laboratory Ltd., P.O. Box 15, Snailwell Road, Newmarket, Suffolk CB8 7DT (U.K.)

(First received June 2nd, 1988; revised manuscript received May 23rd, 1989)

SUMMARY

The stereochemistry of an isomer of 5-estrane-3,17α-diol, the major metabolite of 19-nortestosterone in horse urine has been established by the use of methylene unit (MU) values. The empirical MU values of the bis-trimethylsilyl (TMS) derivatives of the eight available isomers of 5-androstane-3,17-diol and four isomers of 5-estrane-3,17β-diol were determined by capillary gas chromatography using three different columns. From this data the theoretical MU values for the bis-TMS derivatives of the four 5-estrane-3,17α-diol isomers were predicted. Comparison of the experimentally determined MU value of the urinary metabolite with those of the theoretical values established the correct stereochemistry of the steriod. This method has been compared with the use of gas chromatography–mass spectrometry in the determination of the stereochemistry of unknown metabolites.

INTRODUCTION

Studies related to the metabolism of 19-nortestosterone (estr-4-en-17β-ol-3-one), **1**, in the horse have demonstrated that an isomer of estrane-3,17-diol, **2**, is the major urinary metabolite excreted as a glucuronic acid conjugate[1]. Initial studies demonstrated that the hydroxyl function at the 17- position of this major metabolite had an α-configuration[1], a minor estrane-3,17-diol metabolite was also isolated with a 17β-OH configuration. Due to the unavailability of the isomers of estrane-3,17α-diol as reference steroids it was not possible to determine the stereochemistry at the 3- and 5- positions of the major metabolite by a direct comparison of gas chromatographic (GC) retention time data.

Gas chromatographic–mass spectrometric (GC–MS) studies[2] have shown differences in the relative intensities of some of the fragment ions in the mass spectra of

[a] Present address: Philips Scientific, York Street, Cambridge, CB1 2PX, U.K.

0021-9673/89/$03.50

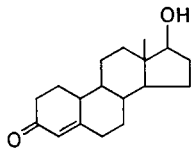

1
19–Nortestosterone

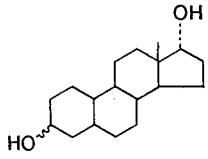

2
Estrane–3,17–diol

the trimethylsilyl (TMS) derivatives of the four isomeric 5α-androstanediols and considerable differences in the mass spectrum of 5β-androstane-3α,17β-diol bis-TMS when compared to the mass spectra of derivatives of the 5α-series. To investigate whether GC–MS could be used in determining the stereochemistry of the estrane-3,17α-diol metabolite a study of the mass spectra of the TMS derivatives of the eight isomers of androstane-3,17-diol and the four isomers of estrane-3,17β-diol has been undertaken and the results are reported in this paper.

It has been demonstrated that the retention behaviour of a steroid on GC analysis is a property of the steroid nucleus and additive contributions due to the substituent groups attached to the nucleus[3]. Thus changes brought about by a chemical reaction or a stereochemical change in structurally related compounds alters the retention time by a constant factor provided there is no interference from neighbouring groups[4].

Using the same series of twelve reference steroids, the additive contributions to the MU values[5] due to changes in the steroid nucleus and stereochemistry have been used to predict the MU values of the four isomers of estrane-3,17α-diol bis-TMS derivatives. The MU value of the TMS derivative of the estrane-3,17α-diol metabolite was compared with these predicted values and the stereochemistry at the 3- and 5-positions has been established.

EXPERIMENTAL

Solvents and chemicals

The even numbered hydrocarbons *n*-C_{16}–*n*-C_{32}, N,O-bis(trimethylsilyl) acetamide (BSA), trimethylchlorosilane (TMCS), 5α-androstane-3α,17β-diol, 5α-androstane-3β,17β-diol, 5β-androstane-3α,17β-diol, 5β-androstane-3β,17β-diol and undecane were obtained from Sigma (Poole, U.K.). 5α-Androstane-3α,17α-diol, 5α-androstane-3β,17α-diol, 5β-androstane-3α,17α-diol, 5β-androstane-3β,17α-diol and 5α-estrane-3β,17β-diol were obtained from the M.R.C. Steroid Reference collection. 5α-Estrane-3α,17β-diol, 5β-estrane-3α,17β-diol and 5β-estrane-3β,17β-diol were gifts from Organon (Oss, The Netherlands).

Isolation and purification of urinary metabolites

The administration of 19-nortestosterone to cross-bred gelded ponies, the collection of urine and the determination of urinary excretion have been reported previously[1].

For one animal, 70% of the administered dose was excreted in the first 24 h. The metabolites were isolated from this urine (900 ml) by lyophilisation, enzyme hydrolysis of the residue reconstituted in acetate buffer, pH 4.5 and solvent extraction. Purification by repeated chromatography on Kieselgel H^1 yielded a fraction which, following derivatisation and GC–MS analysis, was shown to contain two isomers of estrane-3,17-diol.

Derivatisation of steroids

The reference steroids (5–10 μg) were treated with BSA (50 μl) and TMCS (25 μl) and heated at 60°C for 2 h. The excess derivatisation reagents were removed in a stream of nitrogen at 40°C and the residue dissolved in undecane (100 μl) for analysis by GC and GC–MS. Aliquots of the purified fraction containing the estranediol metabolites were similarly derivatised.

Gas chromatography

GC was carried out using a Hewlett-Packard 5890A gas chromatograph with a HP3392A integrator. The steroid derivatives were analysed on three different columns, a 1701 (OV-1701), a BP5 (SE-S4) and a BP1 (SE-30) (25 m × 0.3 mm I.D.); the columns were purchased from S.G.E.

The analysis was carried out in the splitless injection mode with undecane as solvent. The initial temperature of 150°C was ramped to 300°C at 5°C/min; hydrogen was used as carrier gas (linear gas velocity approximately 40 cm/s).

The steroid derivatives were individually coinjected with the even numbered hydrocarbon mixture n-C_{16}–n-C_{32} in undecane. For each analysis a plot of retention time (min) *vs.* carbon number of the hydrocarbons was obtained and the methylene unit (MU) values for the steroids determined from linear regression analysis. To check the reproducibility of the injections replicate analysis ($n = 7$) of the bis-TMS derivative of 5β-androstane-3β,17β-diol with the hydrocarbon mixture were made.

Capillary column GC–MS

Mass spectra were obtained on the Hewlett-Packard 5970 mass selective detector interfaced to a HP 5890A gas chromatograph. A bonded polydimethylsiloxane fused-silica column (18 m × 0.25 mm I.D.) was used with helium as carrier gas. Splitless injections were made in undecane at 150°C, the oven temperature was ramped to 180°C at 10°C/min then to 280°C at 5°C/min; mass spectra were recorded over the range m/z 100–500.

RESULTS AND DISCUSSION

The relative intensities of the relevant ions in the mass spectra of the bis-TMS derivatives of the eight isomers of androstane-3,17-diol are shown in Table I. The mass spectra were similar in that they showed molecular ions ($M^{+\cdot}$, m/z 436) with fragment ions a m/z 421 $[M - 15]^+$; m/z 346 $[M - 90]^{+\cdot}$; m/z 331 $[M - (90 + 15)]^+$; m/z 256 $[M - (90 + 90)]^{+\cdot}$; m/z 241 $[M - (90 + 90 + 15]^+$ and m/z 129 (D-ring fragment).

TABLE I

MASS SPECTRAL DATA FOR THE TMS DERIVATIVES OF THE EIGHT ANDROSTANE-3,17-DIOL ISOMERS

Androstanediol isomer	*Relative intensities (%)*							
	Molecular ion $M^{+\cdot}$ (m/z 436)	*Fragment ions*						
		$[M-15]^+$ (m/z 421)	*$[M-90]^{\ddagger}$ (m/z 346)*	*$[M-(90+15)]^+$ (m/z 331)*	*$[M-(90+90)]^{\ddagger}$ (m/z 256)*	*$[M-(90+90+15)]^+$ (m/z 241)*	*m/z 215*	*m/z 129*
5α-A-3β,17β-diol	29	70	54	37	35	70	37	100
5β-A-3β,17β-diol	14	18	52	27	100	67	40	97
5α-A-3α,17β-diol	24	18	35	45	65	100	47	65
5β-A-3α,17β-diol	9	15	45	10	100	65	38	52
5α-A-3β,17α-diol	34	80	60	40	40	77	26	100
5β-A-3β,17α-diol		8	50	30	100	54	26	62
5α-A-3α,17α-diol	29	20	46	56	70	100	43	67
5β-A-3α,17α-diol	6	2	39	12	100	62	34	40

The inability of MS to unequivocally identify all stereoisomers of androstane-3,17-diol bis-TMS derivatives is illustrated in Table I. However some structural information could be obtained from the mass spectral data. In both the 17β-series and the 17α-series it is possible to differentiate between the 5β- and 5α-isomers on the basis of the ions at m/z 256 and m/z 241. In the 5β-isomers the ion at 256 is of greater intensity than the ion at 241 as previously reported by Vihko[2]; for the 5α-isomers the reverse is true. For the 5α-isomers it is possible to establish the stereochemistry at C_3 on the basis of the intensity of the molecular ion ($M^{+\cdot}$, m/z 436) and that of the fragment ion at m/z 421. The 5α,3β-isomers show a prominent fragment ion at m/z 421 of greater intensity than the molecular ion; for the 5α,3α-isomers this pattern is reversed.

For the 5α,3α/5α,3β-isomers differences, although less prominent, are also observed in the ratios of the ions at m/z 346 and m/z 331. It was not possible to distinguish between 5β,3α/5β,3β-isomers nor between the 17α/17β-isomers.

The structures of the reference steroids are shown in Fig. 1. The ability of MS to distinguish between steroid isomers at the 5-position has been reported previously[6]. The stereochemical change 5α- to 5β-results in the loss of planarity in the steroid nucleus producing a marked change in its shape (Fig. 2). Following loss of two moles of trimethylsilanol in the androstanediol series $[M-(90+90)]^{+\cdot}$ and a methyl radical it would appear that the planar ring system of the 5α isomers is better able to stablize the ion at m/z 241. A study of the fragmentation pathways of stereoisomeric androstane-3,17-diol bis-*tert.*-butyldimethylsilyl ethers by linked field scanning has demonstrated the value of a combination of conventional electron impact (EI) data and parent and daughter ion spectra in distinguishing between stereoisomers[7].

The mass spectra of the bis-TMS derivatives of the four isomers of estrane-3,17β-diol are shown in Fig. 3. The spectra show weak molecular ions ($M^{+\cdot}$, m/z 422)

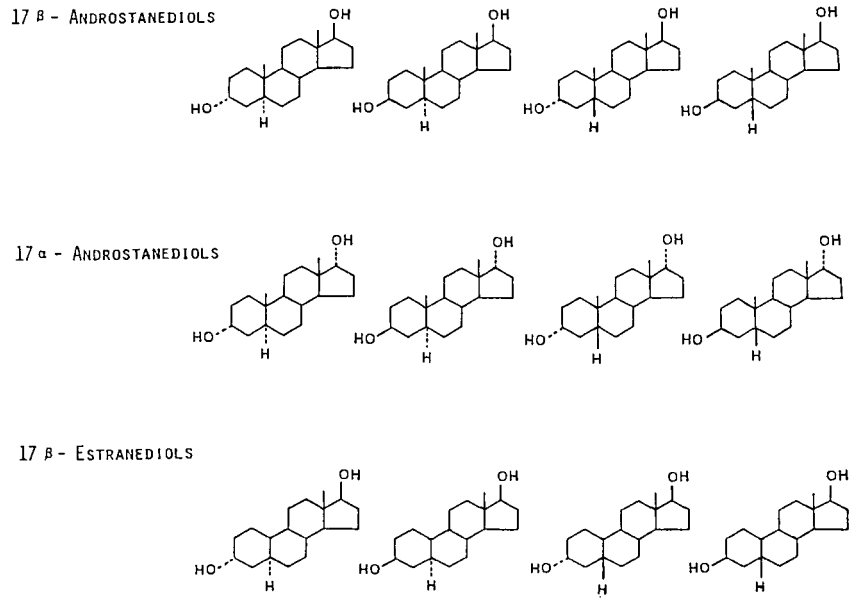

Fig. 1. Structures of reference steroids.

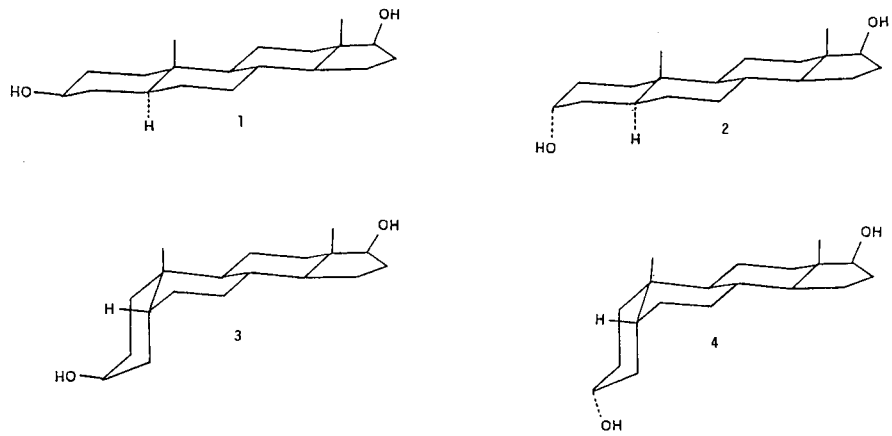

Fig. 2. Perspective views of 5α- and 5β-androstane-3,17β-diols. (1) 5α-Androstane-3β,17β-diol, (2) 5α-androstane-3α,17β-diol, (3) 5β-androstane-3β,17β-diol and (4) 5β-androstane-3α,17β-diol.

with fragment ions at m/z 407 $[M-15]^+$; m/z 332 $[M-90]^{\ddagger}$; m/z 242 $[M-(90+90)]^{\ddagger}$ and m/z 129. As the loss of a methyl radical from the fragment ions m/z 332 and 242 was of little significance, the characteristic differences observed between the mass spectra of the 5α/5β androstane-3,17-diol bis-TMS derivatives were not apparent in the spectra of the derivatised estrane-3,17β-diols and no conclusion could be drawn with regard to stereochemistry. A similar conclusion has been drawn for a series of

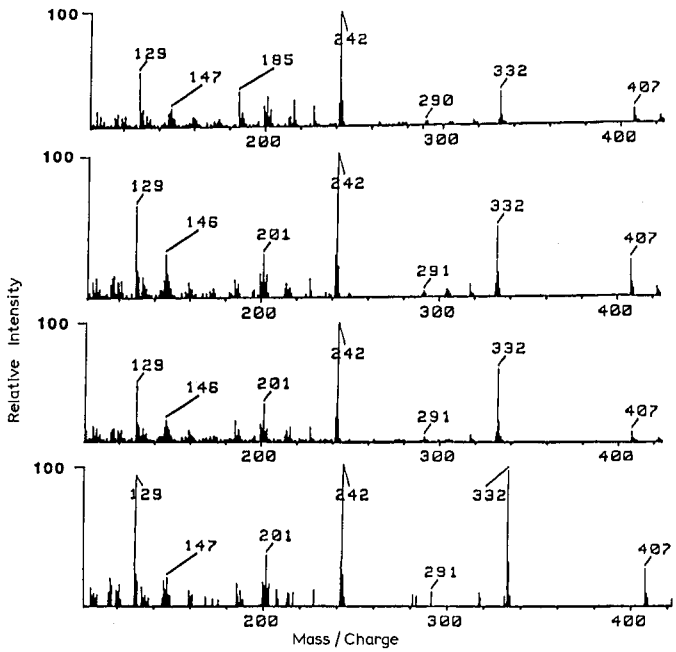

Fig. 3. Mass spectra of the bis-TMS derivatives of the four isomers of estrane-3,17β-diol. From top to bottom: 5β,3α,17β; 5α,3α,17β; 5β,3β,17β; 5α,3β,17β.

5α/5β androstanetriols where mass spectra of the TMS derivatives were dominated by rearrangement ions[8]. The mass spectrum (Fig. 4) of the bis-TMS derivative of the major estrane-3,17-diol metabolite was similar to those of the estrane-3,17β-diol isomers (Fig. 3) and stereochemical distinction on the basis of MS was impossible. On the basis of relative intensities of the ions, the spectrum was different to that reported previously[1], presumably due to the use of a different instrument. MS analysis of the TMS derivatives of androstane-3,17-diol and estrane-3,17β-diol isomers therefore failed to provide sufficient characteristic information to unequivocally determine the stereochemistry of the metabolite.

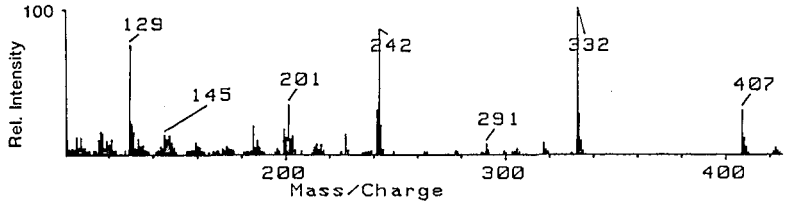

Fig. 4. Mass spectrum of the bis-TMS derivative of the most abundant isomer of estrane-3,17-diol isolated from horse urine following administration of 19-nortestosterone.

Although it is known that GC can separate stereoisomers, the determination of the stereochemistry of the metabolite on the basis of a direct comparison of retention time data was not possible due to the unavailability of the estrane-3,17α-diol isomers as reference steroids. An indirect approach was therefore adopted which depended upon the prediction of the MU values of the estrane-3,17α-diol bis-TMS derivatives and a comparison of these predicted values with the experimentally determined values for the metabolites. The TMS derivatives of the reference steroids were analysed on three different columns. As reported previously the 17β-isomers had longer retention times than the 17α-isomers[9].

To determine MU values a typical GC chromatogram, obtained for coinjection of the bis-TMS derivative of 5β-androstane-3β,17β-diol and the hydrocarbon mixture, is shown in Fig. 5. A plot of the retention time (min) *vs.* carbon number gave a linear relationship over the range *n*-C_{16}–*n*-C_{28} (correlation coefficient, 0.9997) (Fig. 6). The MU value 25.71 for 5β-androstane-3β,17β-diol bis-TMS was determined from linear regression analysis. Reanalysis of this mixture ($n = 6$) gave the following MU values for this steroid derivative, 25.70, 25.71, 25.71, 25.71, 25.71 and 25.71. The MU values, determined for the TMS derivatives of the eight isomers of androstane-3,17-diol and four isomers of estrane-3,17β-diol on the three different columns are shown in Table II. The MU values of the derivatised estrane-3,17-diol metabolites are shown in Table III.

MU values allow retention indices to be determined under temperature programmed conditions and can be regarded, for practical purposes, to be equivalent to the Kovats retention indices. Based upon the concept that the paper chromatographic mobility of a compound results from the additive contributions of its components[10], it has been shown that the logarithm of the retention time of a steroid is made up of the additive contributions of the substituents together with that of the nucleus[3,11,12]. For the TMS derivatives of the eight isomers of androstanediol and

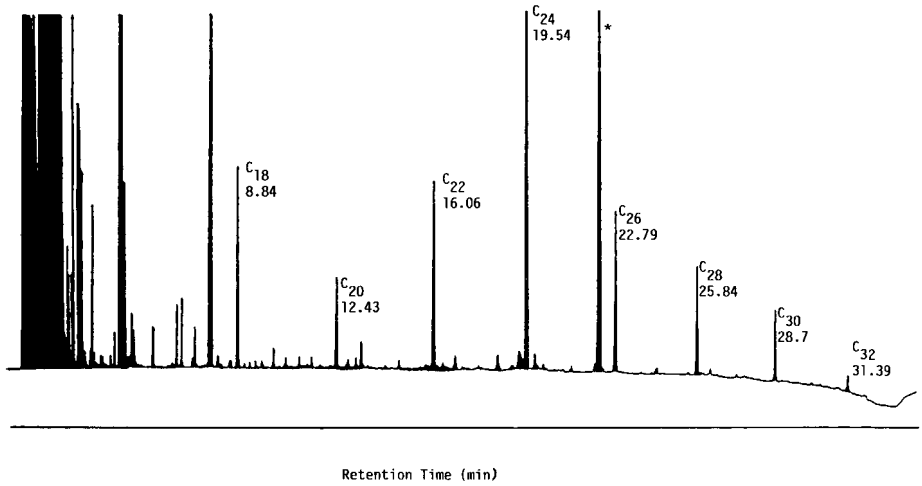

Fig. 5. Capillary column gas chromatogram for coinjection of the hydrocarbons n-C_{16}–n-C_{32} with the bis-TMS derivative of 5β-androstane-3β,17β-diol* (column BP5).

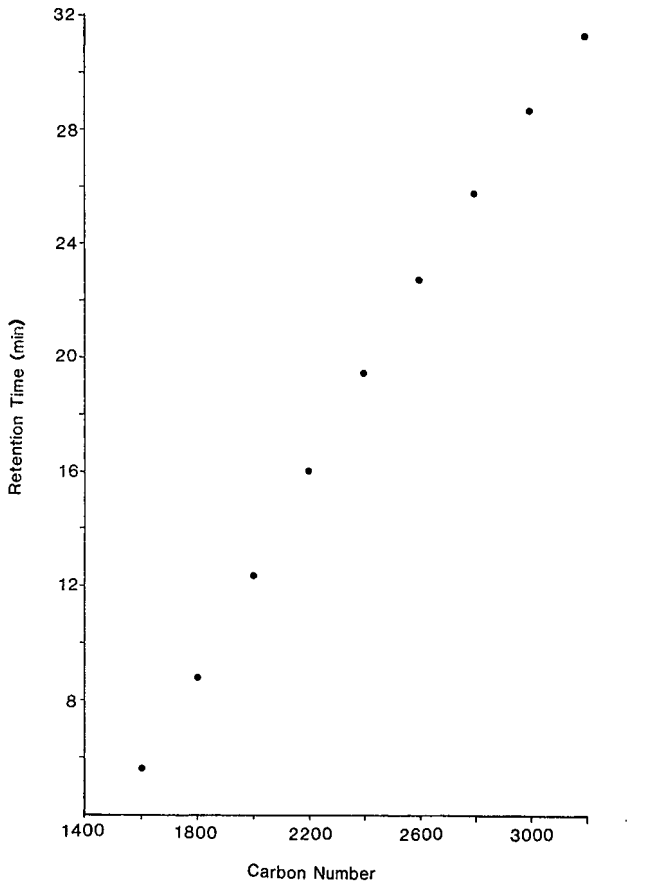

Fig. 6. Plot of retention time *vs.* carbon number for hydrocarbons n-C_{16}–n-C_{32} (column BP5; correlation coefficient, 0.9996 n-C_{16}–n-C_{28}; regression equation $y = 58.6x + 1269$).

TABLE II
MU VALUES FOR THE REFERENCE STEROIDS ON THREE COLUMNS
A = Androstanediol; E = estranediol.

Steroid	*MU values*		
	1701	*BP5*	*BP1*
5α-A-3α,17α	24.98	24.89	24.74
5α-A-3β,17α	26.29	26.12	25.97
5β-A-3α,17α	24.84	24.63	24.45
5β-A-3β,17α	24.92	24.86	24.69
5α-A-3α,17β	26.12	25.80	25.70
5α-A-3β,17β	26.80	26.64	26.49
5β-A-3α,17β	26.04	25.81	25.70
5β-A-3β,17β	25.74	25.71	25.60
5α-E-3α,17β	25.03	25.02	24.91
5α-E-3β,17β	25.87	25.73	25.58
5β-E-3α,17β	25.66	25.50	25.37
5β-E-3β,17β	25.47	25.44	25.32

TABLE III
MU VALUES FOR THE URINARY ESTRANE-3,17 DIOL METABOLITES OF 19-NORTESTOSTERONE IN THE HORSE

	1701	*BP5*	*BP1*
Major metabolite	25.38	25.11	25.13
Minor metabolite	25.86	25.84	25.56

four isomers of estrane-3,17β-diol this principle has been used to calculate the contributions to the MU values of the stereochemical change (17β-OH to 17α-OH) and also a change in the steroid nucleus (androstane to estrane).

For isomers of androstane-3,17β-diol and androstane-3,17α-diol having the same stereochemistry at the 3- and 5- positions, subtraction of the MU values gives the contribution to the retention behaviour of the stereochemical change from 17β-OH to 17α-OH (Table IV). Subtraction of these contributions from the MU values of the

TABLE IV
CONTRIBUTION TO THE MU VALUES FOR THE CONVERSION 17β-OH TO 17α-OH
A = Androstanediol.

	Column		
	1701	*BP5*	*BP1*
(5α-A-3α,17β) → (5α-A-3α,17α)	1.14	0.91	0.96
(5α-A-3β,17β) → (5α-A-3β,17α)	0.51	0.52	0.52
(5β-A-3α,17β) → (5β-A-3α,17α)	1.20	1.18	1.25
(5β-A-3β,17β) → (5β-A-3β,17α)	0.82	0.85	0.91

TABLE V
CALCULATED MU VALUES FOR THE FOUR ESTRANE-3,17α-DIOL ISOMERS

	Column		
	1701	*BP5*	*BP1*
5α-Estrane-3α,17α-diol	23.89	24.11	23.95
5α-Estrane-3β,17α-diol	25.36	25.21	25.06
5β-Estrane-3α,17α-diol	24.26	24.32	24.12
5β-Estrane-3β,17α-diol	24.65	24.59	24.41

TMS derivatives of the isomers of estrane-3,17β-diol having the corresponding stereochemistries at the 3- and 5- positions gives the predicted MU values for the isomers of estrane-3,17α-diol-bis-TMS derivatives (Table V).

The contribution of the C-10 methyl group can be obtained by subtracting the MU values of the TMS derivatives of the estrane-3,17β-diol isomers from those of the androstane-3,17β-diol isomers having the same stereochemistries at the 3- and 5-positions (Table VI). Subtraction of this contribution from the MU values of the TMS derivatives of isomers of androstane-3,17α-diol having the corresponding stereochemistries at the 3- and 5-positions again gave the predicted MU values shown in Table V. In predicting the MU values of the TMS derivatives of the estrane-3,17α-diol isomers the assumption is made that the contribution due to the change in stereochemistry at the 17-position is independent of the presence/absence of the methyl group at C-10 or, this is equivalent to stating the contribution due to the presence/absence of the methyl group at C-10 is independent of the stereochemistry at C-17. This assumption is thus dependent upon the non-interaction of the methyl group at C-10 with the hydroxy function at C-17; due to the remoteness of the two groups any such interaction is improbable. The non-interaction of the methyl group at C-10 with substituents at C-17 has been demonstrated for a series of 4-en-3-one steroids for which, irrespective of the substituent at C-17 the contribution to retention time data of this methyl group was constant[3].

The above assumption can only be applied when the steroid 3,17-diols have the same stereochemistry at the 3- and 5-positions. The fact that the contributions to MU

VALUES VI
CONTRIBUTION TO THE MU VALUES FOR THE C_{10} METHYL GROUP
A = Androstanediol; E = estranediol.

	Column		
	1701	*BP5*	*BP1*
(5α-A-3α,17β) → (5α-E-3α,17β)	1.09	0.78	0.79
(5α-A-3β,17β) → (5α-E-3β,17β)	0.93	0.91	0.91
(5β-A-3α,17β) → (5β-E-3α,17β)	0.38	0.31	0.33
(5β-A-3β,17β) → (5β-E-3β,17β)	0.27	0.27	0.28

values of the 17β-OH to 17α-OH conversion (Table IV) and the methyl group at C-10 (Table VI) are not constant for different isomers demonstrates their dependence upon the stereochemistry at these positions. The predicted MU values for the TMS derivatives of the four estrane-3,17α-diol isomers are shown in Table V. Comparison of the experimentally determined MU values on the three columns for the major estrane-3,17α-diol metabolite (Table III) with the predicted MU values (Table V) established the configurations at the 3- and 5-positions to be β and α, respectively. This configuration was later confirmed by custom synthesis of 5α-estrane-3β,17α-diol and comparison of retention time data with that of the metabolite. Comparison of the MU values of the TMS derivative of the minor metabolite with those of the reference steroids confirmed the configuration to be 5α,3β,17β.

CONCLUSIONS

The value of GC–MS in the identification of a variety of steroids, isolated from biological samples, and their derivatives has been well documented over the past two decades. On the basis of MS alone it is not normally possible to differentiate between steroid stereoisomers. However, stereoisomers of most steroids can be resolved by capillary GC and thus the combination of GC–MS can yield full structure elucidation provided the appropriate reference steroids are available for direct comparison of mass spectral and retention time data. In determining the stereochemistry of estrane-3,17α-diol alternative approaches had to be considered as it was not possible to obtain the four isomers of estrane-3,17α-diol as reference steroids.

The results demonstrate that MU values can be used for the elucidation of the stereochemistry of steroid isomers when the appropriate reference compounds are unavailable.

REFERENCES

1 E. Houghton, *Xenobiotica*, 7 (1977) 683.
2 R. Vihko, *Acta Endocrinol.*, Suppl., 109 (1966) 1.
3 B. A. Knights and G. H. Thomas, *Anal. Chem.*, 34 (1962) 1046.
4 R. B. Clayton, *Biochemistry*, 1 (1962) 357.
5 E. C. Horning, K. B. Eik-Nes and E. C. Horning, *Monographs on Endocrinology, Vol. 2, Gas Phase Chromatography of Steroids*, Springer-Verlag, Berlin, Heidelberg, New York, 1968.
6 M. Friedmann-Spiteller and G. Spiteller, *Fortschr. Chem. Forsch.*, 12 (1969) 440.
7 S. J. Gaskell, A. W. Pike and D. S. Millington, *Biomed. Mass Spectrom.*, 6 (1979) 78.
8 H. Grote and G. Spiteller, *Biomed. Mass Spectrom.*, 4 (1977) 216.
9 R. J. Heitzmann and G. H. Thomas, *Biochem. J.*, 96 (1965) 22 p.
10 E. C. Bate-Smith and R. G. Westall, *Biochim. Biophys. Acta*, 4 (1950) 427.
11 B. A. Knights and G. H. Thomas, *Chem. Ind.*, (1963) 43.
12 J. Chamberlain, B. A. Knights and G. H. Thomas, *J. Endocrinol.*, 26 (1963) 367.

Journal of Chromatography, 479 (1989) 85–95
Elsevier Science Publishers B.V., Amsterdam — Printed in The Netherlands

CHROM. 21 675

HIGH-PERFORMANCE SIZE-EXCLUSION CHROMATOGRAPHY OF POLY- AND OLIGOETHYLENE TEREPHTHALATE USING A MIXTURE OF HEXAFLUOROISOPROPANOL AND CHLOROFORM AS THE MOBILE PHASE

NOBUTOSHI CHIKAZUMI*[a], YOSHIYUKI MUKOYAMA and HATUO SUGITANI
Ibaraki Research Laboratory, Hitachi Chemical Co., Ltd., 4-13-1 Higashichou Hitachi, Ibaraki 317 (Japan)
(First received February 27th, 1989; revised manuscript received June 9th, 1989)

SUMMARY

Solvent systems using a mixture of hexafluoroisopropanol (HFIP) and chloroform ($CHCl_3$) were developed for the analysis of polyethylene terephthalate (PET) and its oligomers by high-performance size-exclusion chromatography (SEC) at room temperature (25°C). The molecular weight distribution of PET and PET film were determined using HFIP–$CHCl_3$ (1:9) and the SEC calibration graph of polystyrenes, which are insoluble in HFIP. These mixed solvents also had considerable advantages with regard to cost reduction and safety in comparison with HFIP alone.

INTRODUCTION

Size-exclusion chromatography (SEC), also known as gel permeation chromatography (GPC), can be used to separate polymers with respect of their molecular size in solution using appropriate calibration graphs based on their elution volumes. SEC columns packed with spherical particles of styrene–divinylbenzene copolymer[1] have been indispensable for the analysis of organic polymeric materials using high-performance liquid chromatography (HPLC) with organic solvents.

The selection of solvents is one of the most important problems in the use of SEC analysis for measuring molecular weight distributions (MWD) of organic materials. With a column packed with styrene–divinylbenzene copolymer, SEC eluents such as tetrahydrofuran (THF), chloroform and toluene have generally been used at room temperature. However, for the analysis of polymers that are insoluble in these common solvents, SEC eluents such as N,N-dimethylformamide, *m*-cresol and *o*-dichlorobenzene have been used at high temperatures.

In SEC measurements of polyethylene terephthalate (PET)[2–4] and polyamides (*e.g.*, nylon)[5–7], various difficulties have been encountered in dissolving these polymers in polar solvents such as *m*-cresol, *o*-chlorophenol and phenol–tetrachloroethane. In addition, the exposure of PET to high temperatures in these solvents during the course of the SEC measurement causes undesirable degradation of the polymer.

[a] Present address: Research and Development Division, Hitachi Chemical Co., Ltd., P.O. Box 233, Shinjuku-Mitsui Bldg. No. 1-1, 2-Chome, Nishishinjuku, Shinjuku-ku, Tokyo 163, Japan.

0021-9673/89/$03.50

The solvent hexafluoroisopropanol (HFIP)[8,9] is known to dissolve PET and polyamides at room temperature. However, polystyrenes, usually used for preparing SEC calibration graphs to determine the MWD of polymers, are insoluble in HFIP alone. Further, as HFIP is expensive and irritating to the skin and eyes, it is preferable to reduce the amount of HFIP used in any industrial analytical method.

Several attempts have been made to apply SEC to PET and polyamides using solvents mixed with HFIP, such as HFIP–toluene[10], HFIP–pentafluorophenol[11] and HFIP–methylene chloride[12–14]. This paper describes an effective mixed solvent system consisting of a mixture of HFIP and chloroform which permits the successful SEC measurement of various kinds of PET samples at room temperature.

EXPERIMENTAL

Samples and solvents

PET samples with different degrees of polymerization [$\overline{P_n}$ = 150, 110, 52, 35 and 5 (data given by the manufacturer)], two kinds of PET oligomers and PET film were obtained from the Industrial Plant Engineering Office of Hitachi. Epoxy resins, polyester resins and narrow-MWD polystyrene standards were obtained from Shell, NBS, Tosoh and Pressure Chemical, respectively.

THF and chloroform for SEC solvents were obtained from Wako and HFIP from Hidoras Chemical and DuPont. All the SEC solvents were degassed by ultrasonic treatment.

Test of solubility of PET and polystyrene

HFIP–chloroform mixed solvents in the ratios 0.5:9.5, 1:9, 2:8, 3:7, 4:6 and 1:1 (v/v) were prepared to determine the solubility of three kinds of PET samples with different degrees of polymerization ($\overline{P_n}$ = 150, 52 and 5) and two kinds of polystyrene standards (molecular weights $4.98 \cdot 10^5$ and $2.8 \cdot 10^3$). The HFIP–chloroform mixed solvents were added to PET samples and polystyrenes to give a concentration of 0.2% (w/v). The vials containing the solutions were tightly sealed and kept at room temperature (25°C) for one night. The solubility of the samples was also measured in the same manner by using HFIP–THF (1:9 and 1:1).

Preparation of SEC columns

All the packing materials and SEC columns used in this study (Gelpack) were made by Hitachi Chemical.

GL-S300HC-1 series columns with HFIP–$CHCl_3$ (1:9) mixed solvent. Porous spherical particles of styrene–divinylbenzene copolymer with an exclusion limit (M_{lim}) of $1 \cdot 10^3$ were packed in a 500 × 8 mm I.D. stainless-steel column with a slurry prepared by using HFIP–$CHCl_3$ (1:9) (designation: GL-S310HC-1).

GL-S320HC-1 (M_{lim} $5 \cdot 10^3$), GL-S330HC-1 (M_{lim} $2 \cdot 10^4$) and GL-S340HC-1 (M_{lim} $7 \cdot 10^4$) columns were prepared using HFIP–$CHCl_3$ (1:9) in the same manner as described above. A GL-S300MHC-1 column (mixed gel of M_{lim} $7 \cdot 10^4$, $5 \cdot 10^5$, $4 \cdot 10^6$ and $5 \cdot 10^7$) was prepared for measuring the MWD of PET and PET film, because its calibration graph was linear.

GL-S300HC-5 series columns with HFIP–$CHCl_3$ (1:1) mixed solvent. GL-S350HC-5 (M_{lim} $5 \cdot 10^5$) and GL-S360HC-5 (M_{lim} $4 \cdot 10^6$) columns were prepared as described above except that HFIP–$CHCl_3$ (1:1) was used.

GL-A100 series columns with THF solvent. GL-A110 (M_{lim} $1 \cdot 10^3$), GL-A120 (M_{lim} $5 \cdot 10^3$), GL-A130 (M_{lim} $2 \cdot 10^4$), GL-A140 (M_{lim} $7 \cdot 10^4$), GL-A150 (M_{lim} $5 \cdot 10^5$), GL-A160 (M_{lim} $4 \cdot 10^6$) and GL-A100M (mixed gel of M_{lim} $7 \cdot 10^4$, $5 \cdot 10^5$, $4 \cdot 10^6$ and $5 \cdot 10^7$) columns were prepared by packing the particles in 500 × 8 mm I.D. stainless-steel columns as described above except that THF was used as the solvent.

SEC and mass spectrometry

A Hitachi 635 high-performance liquid chromatograph with a UV detector set at 254 nm and a Hitachi 635A high-performance liquid chromatograph with a UV detector set at 250 nm, both instruments also with a refractive index detector, were used. All SEC experiments were carried out at room temperature (25°C).

For column protection, a column packed with HFIP–$CHCl_3$ (1:9) should be used with the same solvent as the SEC eluent, and the same rule should be followed with the HFIP–$CHCl_3$ (1:1) and THF columns. SEC experiments using THF as solvent were carried out under the same analytical condition as for the HFIP–$CHCl_3$ systems.

The number of theoretical plates (N) was determined by using 0.1% or 0.2% (w/v) benzene with UV detection at 254 or 250 nm at a flow-rate of 1.0 ml/min and calculated using the equation $N = 5.54\,(V_R/W)^2$, where V_R is the retention volume and W is the peak width at half-height. The height equivalent to a theoretical plate (HETP) is expressed by L/N, where L is the column length and N is the number of theoretical plates. The column pressure drop (P) was measured at a flow-rate of 1.0 ml/min. M_{lim} was determined from a calibration graph for polystyrene, obtained using the THF solvent column.

The number-average molecular weight (M_n), the weight-average molecular weight (M_w), the Z-average molecular weight (M_z) and the polydispersion index (D) of PET samples were calculated from the following equations: $M_n = \Sigma H_i/\Sigma(H_i/M_i)$, $M_w = \Sigma(H_iM_i)/\Sigma H_i$, $M_z = \Sigma(H_iM_i^2)/\Sigma(H_iM_i)$ and $D = M_w/M_n$, where H_i is peak height and M_i is molecular weight obtained from the calibration graph for polystyrene standards using HFIP–$CHCl_3$ (1:9).

The peaks collected from the SEC fractions of PET samples and oligomers present in PET films were identified using a Hitachi M-60 mass spectrometer.

RESULTS

Test of solubility of PET and polystyrene

The results of the solubility tests on the samples are given in Table I. With HFIP–$CHCl_3$ mixed solvents, PET samples ($\overline{P_n} = 5$ and $\overline{P_n} = 52$) were soluble in the solvents with ratios of 1:9 or higher, while the PET sample ($\overline{P_n} = 150$) was soluble in solvents with ratios of 4:6 or higher. On the other hand, the polystyrene standard of lower molecular weight ($2.8 \cdot 10^3$) was soluble in the solvents at all ratios, while the standard of higher molecular weight ($4.98 \cdot 10^5$) did not dissolve in HFIP–$CHCl_3$ with ratios of 4:6 and 1:1. Unfortunately, we could not find an HFIP–$CHCl_3$ mixture with a ratio in which all the PET samples and polystyrenes were soluble.

None of the PET samples, even that with $\overline{P_n} = 5$, were soluble in the HFIP–THF solvents at the ratios tested. It was evident that HFIP–THF solvents are unsuitable for SEC measurements of PET samples.

TABLE I
TEST OF SOLUBILITY OF PET AND POLYSTYRENE AT A CONCENTRATION OF 0.2% (w/v)

Solvent	*Mixture ratio (v/v)*	*PET*			*PS*	
		$\overline{P_n} = 5$	$\overline{P_n} = 52$	$\overline{P_n} = 150$	$2.8 \cdot 10^3$	$4.98 \cdot 10^5$
$HFIP–CHCl_3$	0.5:9.5	I[a]	I	I	S[a]	S
	1:9	S	S	I	S	S
	2:8	S	S	I	S	S
	3:7	S	S	I	S	S
	4:6	S	S	S	S	I
	1:1	S	S	S	S	I
HFIP–THF	1:9	I	I	I	S	S
	1:1	I	I	I	I	I

[a] I = Insoluble; S = soluble.

In accordance with these results, $HFIP–CHCl_3$ (1:9) and (1:1) were selected for SEC measurements of PET samples.

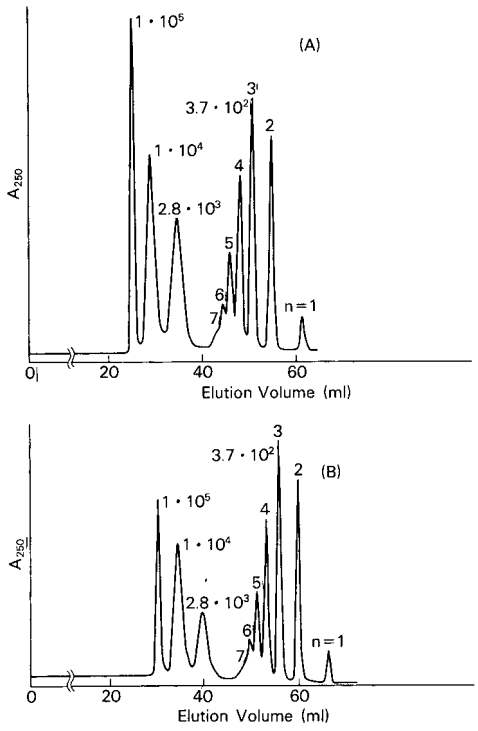

Fig. 1. Chromatograms of polystyrene standards of molecular weights $1.0 \cdot 10^5$, $1.0 \cdot 10^4$, $2.8 \cdot 10^3$ and $3.7 \cdot 10^2$ using (A) $HFIP–CHCl_3$ (1:9) or (B) THF as the mobile phase. HPLC instrument, Hitachi 635A; columns, (A) Gelpack GL-S310HC-1 + GL-S320HC-1 + GL-S330HC-1, (B) Gelpack GL-A110 + GL-A120 + GL-A130; all three columns, 500 × 8 mm I.D.; flow-rate, 1.0 ml/min; detector, UV (250 nm); column temperature, 25°C.

SEC experiments on PET oligomers using the HFIP–$CHCl_3$ (1:9) mixed solvent system

Fig. 1 shows the chromatograms of several kinds of polystyrene standards for the same column combination, using (A) HFIP–$CHCl_3$ (1:9) and (B) THF as the mobile phase. The number of theoretical plates (N) and HETP of system A were 46 000 and 0.003261 cm, respectively. As THF is an excellent solvent for SEC analysis, the column performance of system B was N = 61 200 plates and HETP = 0.002451 cm. The column pressure drops of systems A and B at a flow-rate of 1.0 ml/min were 62 and 36 kgf/cm^2, respectively. The higher pressure drop of system A was due to the high viscosity of HFIP.

However, these differences between the two systems did not affect the efficiency of the SEC separation of polystyrenes, as shown in Fig. 1. Excellent separation, as good as with THF, was obtained with HFIP–$CHCl_3$ (1:9).

Fig. 2 shows the chromatograms of two kinds of PET oligomers of different molecular weights, obtained using HFIP–$CHCl_3$ (1:9). The SEC patterns of the higher molecular weight PET oligomer A and the lower molecular weight PET oligomer B were obtained by UV monitoring at 254 nm at room temperature (25°C). Each peak of PET oligomer B was collected from SEC fractions and identified by mass spectrometry. The formula of PET samples used in this study was determined and found to be that shown in Fig. 2, where n represents the degree of polymerization.

Fig. 3 shows the SEC calibration graphs for polystyrene (PS), isophthalic acid–propylene glycol-type polyester resin [ER(IP/PG)] and bis-phenol-type epoxy resin (Ep) using (A) HFIP–$CHCl_3$ (1:9) and (B) THF with the same column combination. In addition, the SEC calibration graph for PET, obtained from the chromatogram of PET oligomer B shown in Fig. 2, was plotted as shown in Fig. 3. SEC calibration graphs for PS, ER(IP/PG) and Ep were obtained from the chromatograms with both solvent systems. The SEC calibration graph for PET was located between those of PS and Ep.

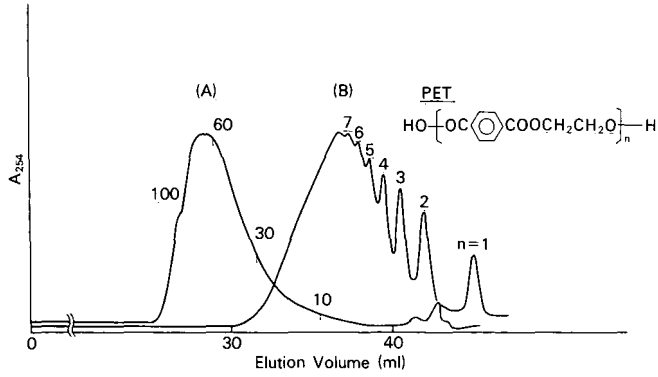

Fig. 2. Chromatograms of PET oligomer A and PET oligomer B using HFIP–$CHCl_3$ (1:9) as the mobile phase. HPLC instrument, Hitachi 635; columns, Gelpack GL-S320HC-1 + GL-S340HC-1 + GL-S340HC-1; all three columns, 500 × 8 mm I.D.; flow-rate, 1.0 ml/min; detector, UV (254 nm); column temperature, 25°C.

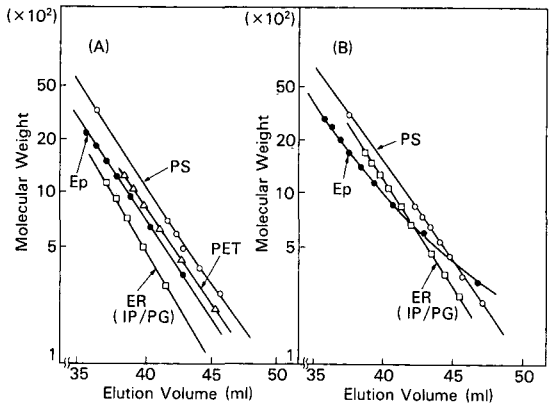

Fig. 3. SEC calibration graphs for (○) PS, (●) Ep, (□) ER(IP/PG) and (△) PET using (A) HFIP–$CHCl_3$ (1:9) and (B) THF as mobile phases. HPLC instrument, Hitachi 635; columns, (A) Gelpack GL-S320HC-1 + GL-S340HC-1 + GL-S340HC-1, (B) Gelpack GL-A120 + GL-A140 + GL-A140; all three columns, 500 × 8 mm I.D.; flow-rate, 1.0 ml/min; detector, UV (254 nm); column temperature, 25°C.

As shown in Fig. 3, all the calibration graphs exhibit good linearity in the HFIP–$CHCl_3$ (1:9) system. In particular, the Ep calibration graph with HFIP–$CHCl_3$ (1:9) shows good linearity in comparison with that obtained with THF. The strong adsorption effect between the sample (Ep) and solvent (THF), which makes the Ep calibration graph non-linear when THF is used, was eliminated by using HFIP–$CHCl_3$ (1:9).

The performances of the column combinations shown in Fig. 3 were $N = 53\,000$ plates, HETP = 0.002830 cm and $P = 56$ kgf/cm^2 in system A and $N = 55\,700$ plates, HETP = 0.002693 cm and $P = 41$ kgf/cm^2 in system B. It is remarkable that the HETP values were almost identical in both systems.

These results indicate that the HFIP–$CHCl_3$ (1:9) has a column efficiency comparable to that of THF and is suitable for SEC measurements of PET oligomers.

SEC experiments on PET polymers and PET films

Fig. 4 shows the chromatograms of three kinds of PET samples, (A) $\overline{P_n} = 150$, (B) $\overline{P_n} = 52$ and (C) $\overline{P_n} = 5$, using HFIP–$CHCl_3$ (1:1) as the mobile phase. SEC patterns of PET samples were obtained by UV monitoring at 254 nm at room temperature. The performances of the column combinations were $N = 25\,200$ plates, HETP = 0.003968 cm and $P = 30$ kgf/cm^2 in HFIP–$CHCl_3$ (1:1) and $N = 36\,300$ plates, HETP = 0.002755 cm and $P = 16$ kgf/cm^2 in THF (Gelpack GL-A150 and GL-A160 columns were used). We also obtained chromatograms of PET films under the same conditions as in Fig. 4.

However, as shown in Table I, the higher-molecular-weight PS was not soluble in HFIP–$CHCl_3$ (1:1). As a result, the MWD of PET samples and PET films could not be determined because the complete SEC calibration graph for PS could not be obtained with this solvent system.

This problem was successfully solved by modifying the method of sample preparation. We found that solutions of PET samples and PET films in HFIP–$CHCl_3$

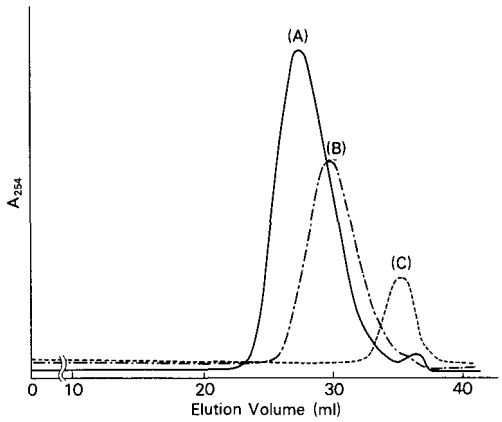

Fig. 4. Chromatograms of PET samples (A) $\overline{P_n}$ = 150, (B) $\overline{P_n}$ = 52 and (C) $\overline{P_n}$ = 5 using HFIP–$CHCl_3$ (1:1) as the mobile phase. HPLC instrument, Hitachi 635; columns, Gelpack GL-S350HC-5 + GL-S360HC-5; column dimensions, 500 × 8 mm I.D. × 2; flow-rate, 1.0 ml/min; detector, UV (254 nm); column temperature, 25°C.

(1:1) could be diluted with $CHCl_3$ to produce HFIP–$CHCl_3$ (1:9) with no polymer precipitation. Injection of these sample solutions into the HPLC instrument caused no problems in operation with HFIP–$CHCl_3$ (1:9).

Table II shows the SEC measurements of five PET samples ($\overline{P_n}$ = 150, 110, 52, 35 and 5) using HFIP–$CHCl_3$ (1:9). The column used for measuring the MWD of PET was Gelpack GL-S300MHC-1, which gave an almost linear calibration graph for polystyrene. The performances of this column were N = 16300 plates, HETP = 0.003067 cm and P = 11 kgf/cm^2 with HFIP–$CHCl_3$ (1:9) and N = 18200 plates, HETP = 0.002747 cm and P = 7 kgf/cm^2 with THF (Gelpack GL-A100M column was used).

From the degree of polymerization ($\overline{P_n}$), the number-average molecular weights of PET samples ($\overline{P_n}$ = 150, 110, 52, 35 and 5) were calculated to be 28948, 21248, 10054, 6773 and 983, respectively, from the formula shown in Fig. 2. These M_n data calculated from the degree of polymerization ($\overline{P_n}$) were in good agreement with the SEC results for M_n shown in Table II.

TABLE II

SEC MEASUREMENT OF PET SAMPLES USNG HFIP–$CHCl_3$ (1:9)

SEC conditions: column, Gelpack GL-S300MHC-1 (500 × 8 mm I.D.); eluent, HFIP–$CHCl_3$ (1:9); flow-rate, 1.0 ml/min; detector, UV (250 nm); column temperature, 25°C; HPLC instrument, Hitachi 635A.

PET sample	M_n	M_w	M_z	D
$\overline{P_n}$ = 150	$2.70 \cdot 10^4$	$6.88 \cdot 10^4$	$1.19 \cdot 10^5$	2.55
$\overline{P_n}$ = 110	$2.31 \cdot 10^4$	$5.43 \cdot 10^4$	$9.78 \cdot 10^4$	2.35
$\overline{P_n}$ = 52	$1.11 \cdot 10^4$	$2.76 \cdot 10^4$	$4.76 \cdot 10^4$	2.48
$\overline{P_n}$ = 35	$6.83 \cdot 10^3$	$1.41 \cdot 10^4$	$2.33 \cdot 10^4$	2.06
$\overline{P_n}$ = 5	$5.82 \cdot 10^2$	$8.90 \cdot 10^2$	$1.55 \cdot 10^3$	1.53

These results show that the SEC analysis of all kinds of PET samples and PET films is possible if HFIP–$CHCl_3$ (1:9) is used and that the MWD of these polymers can be determined from the SEC calibration graphs for PS.

SEC experiments on oligomers present in PET films

Oligomers present in the PET samples or PET films can be analysed by SEC measurement of their $CHCl_3$ extracts, using THF as the solvent. The $CHCl_3$ extracts of the PET sample ($\overline{P_n} = 5$) and the PET film were dissolved in THF after removing $CHCl_3$.

Fig. 5 shows the chromatograms of oligomers present in the $CHCl_3$ extract of the PET sample ($\overline{P_n} = 5$) and oligomers present in the $CHCl_3$ extract of the PET film using THF. The peak of each SEC fraction was collected and identified by mass spectrometry. The formula of each oligomer was determined and is shown in Fig. 5.

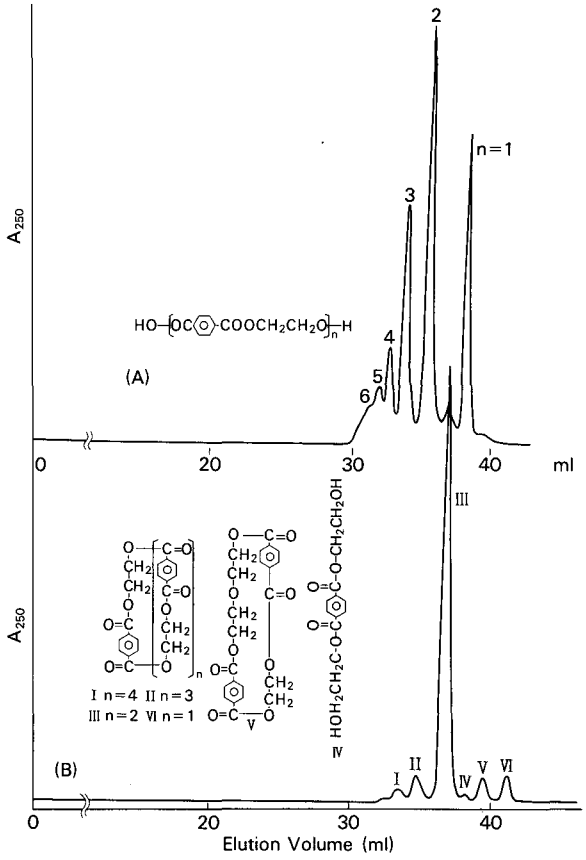

Fig. 5. Chromatograms of oligomers present in PET and PET film using THF as mobile phase. Samples: (A) $CHCl_3$ extract of PET sample ($\overline{P_n} = 5$); (B) $CHCl_3$ extract of PET film. HPLC instrument, Hitachi 635A; columns, Gelpack GL-A110 + GL-A120 + GL-A130; all three columns, 500 × 8 mm I.D.; flow-rate, 1.0 ml/min; detector, UV (250 nm); column temperature, 25°C.

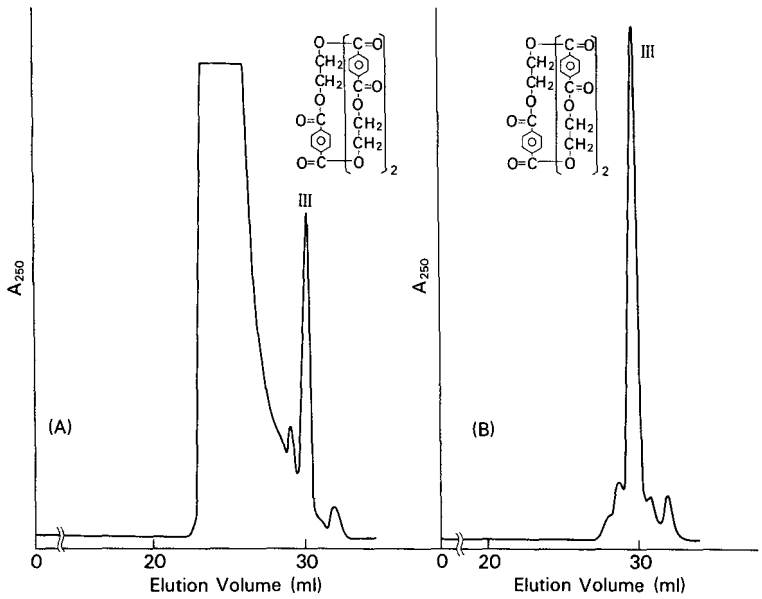

Fig. 6. Chromatograms of PET film using HFIP–$CHCl_3$ (1:9) as the mobile phase. Samples: (A) PET film; (B) $CHCl_3$ extract of PET film. HPLC instrument, Hitachi 635A; columns, Gelpack GL-S310HC-1 + GL-S320HC-1 + GL-S330HC-1; all three columns, 500 × 8 mm I.D.; flow-rate, 1.0 ml/min; detector, UV (250 nm); column temperature, 25°C.

Although this method is effective for identifying the oligomers, it is doubtful that these chromatograms accurately reflect the amount of such oligomers because it was difficult to extract all of the oligomers by the extraction process used. SEC analysis of the PET film oligomer using HFIP–$CHCl_3$ (1:9) was tried in order to overcome this disadvantage.

Fig. 6 shows the chromatograms of PET film and the $CHCl_3$ extract of PET film using HFIP–$CHCl_3$ (1:9). The fractions of the main peaks were collected and identified by mass spectrometry by the same method as with THF. The main oligomer peak of the PET film and the $CHCl_3$ extract of the PET film shown in Fig. 6 was identified as the same cyclic oligomer as peak III in Fig. 5.

DISCUSSION

Even at high temperatures, PET samples and PET films cannot be dissolved in most of the common SEC solvents such as THF, chloroform, toluene, dimethylformamide, dimethyl sulfoxide, anisole, 2-nitropropane, ethyl acetate, 1,1,2-trichloroethane, 1,1,2,2-tetrachloroethane, 1,2,4-trichlorobenzene and acetonitrile. Only a few polar solvents can dissolve PET, *viz.*, trifluoroacetic acid, *m*-cresol, phenol–tetrachloroethane, *o*-chlorophenol, nitrobenzene, HFIP and hexafluoroacetone. Of these solvents, *m*-cresol has been the most commonly used for the SEC analysis of PET at temperatures of 110–135°C. However, there is ample evidence that PET is degraded in *m*-cresol by acid-catalyzed hydrolysis. Further, SEC analysis must be carried out at

high temperature to reduce the high viscosity of *m*-cresol. The operation of HPLC under this condition is not easy and it lacks safety, reproducibility and reliability.

Paschke *et al.*[16] reported that SEC of PET using nitrobenzene–tetrachloroethane (0.5:99.5) at room temperature minimizes polymer degradation and distribution equilibration. However, in this instance, PET was first dissolved in pure nitrobenzene at 180–200°C and then diluted with tetrachloroethane, whereas the samples in our study, in which we used the HFIP–$CHCl_3$ to dissolve PET, were prepared under mild conditions at room temperature.

SEC experiments using HFIP alone have been carried out with PET[11], polytetramethyleneterephthalate[15], polyamide 6[5] and polyamide 12[10]. However, the SEC measurement of these polymers in HFIP had the serious disadvantage that polystyrenes, usually used for preparing a calibration graph to determine the MWD of polymers, are insoluble in HFIP.

In our study, we found that the solutions of PET samples in HFIP–$CHCl_3$ (1:1) could be diluted with $CHCl_3$ to give HFIP–$CHCl_3$ (1:9) with no polymer precipitation. We confirmed that this new method of sample preparation could be applied to PET films. The MWD of PET film calculated from the calibration graph for PS under the same analytical conditions as for Table II gave $M_n = 2.33 \cdot 10^4$, $M_w = 5.64 \cdot 10^4$, $M_z = 1.02 \cdot 10^5$ and $D = 2.42$.

We also found that the MWD of PET samples prepared in HFIP–$CHCl_3$ (1:9) by the dilution method described above showed little difference from the MWD of those dissolved in undiluted HFIP–$CHCl_3$ (1:1). For example, the MWDs of the PET sample with $\overline{P_n} = 150$ using HFIP–$CHCl_3$ (1:9) were $M_n = 2.70 \cdot 10^4$, $M_w = 6.88 \cdot 10^4$, $M_z = 1.19 \cdot 10^5$ and $D = 2.55$ when the sample was dissolved and diluted so as to give HFIP–$CHCl_3$ (1:9), and $M_n = 2.55 \cdot 10^4$, $M_w = 6.62 \cdot 10^4$, $M_z = 1.16 \cdot 10^5$ and $D = 2.60$ when the sample was dissolved in HFIP–$CHCl_3$ (1:1). This problem is being studied further and will be the subject of a subsequent paper.

Several SEC experiments using mixed solvents of HFIP with other compounds have been attempted, *e.g.*, HFIP–methylene chloride (30:70)[12–14] and HFIP–pentafluoropropanol (1:1)[11] for PET and HFIP–toluene (20:80)[10] for polyamide 12. In these studies, a refractive index detector, a UV detector and a laser low-angle light scattering photometer[5,11] were used as SEC detectors. For the detector with the HFIP–$CHCl_3$ systems, it has been our experience that a UV detector is to be peferred because of its high sensitivity, high resolution and stability of the baseline.

As HFIP is expensive and irritating to the skin and eyes, the HFIP–$CHCl_3$ system has a considerable advantage in diluting the HFIP with $CHCl_3$, which is much cheaper and safer than HFIP. Moreover, as the HFIP–$CHCl_3$ system can be separated into two phases at low temperature (below 10°C), HFIP–$CHCl_3$ waste solvent can be easily recovered by cooling and redistillation. We were able to re-use the HFIP–$CHCl_3$ solvent as the SEC eluent several times by applying this method.

CONCLUSIONS

HFIP–$CHCl_3$ mixed solvent columns packed with styrene–divinylbenzene copolymer have been developed for SEC measurements of PET, PET film and their oligomers at room temperature. In comparison with THF, HFIP–$CHCl_3$ (1:9) and (1:1) showed sufficient column efficiency. Especially in HFIP–$CHCl_3$ (1:9), the

polystyrenes usually used for preparing calibration graphs were soluble and the MWD of PET samples and PET films could be determined. The direct SEC analysis of oligomers present in PET film was also possible with this solvent system.

ACKNOWLEDGEMENTS

The authors gratefully acknowledge helpful discussions with and valuable advice from Professor Takahisa Ohta, University of Tokyo, and also thank the members of the Industrial Plant Engineering Office of Hitachi, who kindly supplied the PET samples and offered valuable advice on the analytical conditions for this study.

REFERENCES

1 J. C. Moore, *J. Polym. Sci., Part A2*, (1964) 835.
2 E. L. Lawton and D. M. Cates, *Polym. Prepr. Am. Chem. Soc. Div. Polym. Chem.*, 9 (1968) 851.
3 R. S. Montserrat, J. P. Selga and V. P. Colomer, *Afinidad*, 38 (1982) 379.
4 N. A. Borshch and N. G. Mal-tseva, *Zh. Anal. Khim.*, 41 (1986) 916.
5 H. Schorn, R. Kosfeld and M. Hess, *J. Chromatogr.*, 282 (1983) 579.
6 R. Panaris and G. Pallas, *Polym. Lett.*, 8 (1970) 441.
7 D. J. Goedhart, J. B. Hussem and B. P. M. Smeets, *J. Chromatogr. Sci.*, 13 (1980) 203.
8 M. Ladika and Z. Mihalic, *Kem. Ind.*, 32 (1983) 433.
9 K. F. Purcell, J. A. Stikeleather and S. D. Brunk, *J. Mol. Spectrosc.*, 32 (1969) 202.
10 M. Sakai and T. Ogawa, *Bunseki Kagaku*, 32 (1983) 258.
11 S. Berkowitz, *J. Appl. Polym. Sci.*, 29 (1984) 4353.
12 B. L. Neff and J. R. Overton, *J. Liq. Chromatogr.*, 7 (1984) 1537.
13 J. R. Overton and H. L. Browning, Jr., *ACS Symp. Ser.*, No. 245 (1984) 219.
14 J. R. Overton and H. L. Browning, Jr., *Org. Coat. Appl. Polym. Sci. Prepr.*, 48 (1983) 940.
15 E. L. Slagowski, R. C. Gebauer and G. J. Gaesser, *J. Appl. Polym. Sci.*, 21 (1977) 2293.
16 E. E. Paschke, B. A. Bidlingmeyer and J. G. Berkmann, *J. Polym. Sci.*, 15 (1977) 983.

Journal of Chromatography, 479 (1989) 97–105
Elsevier Science Publishers B.V., Amsterdam — Printed in The Netherlands

CHROM. 21 658

APPLICATION OF HIGH-PERFORMANCE LIQUID CHROMATOGRAPHY WITH SPECTROPHOTOMETRIC AND ELECTROCHEMICAL DETECTION TO THE ANALYSIS OF ALKYLENEBIS(DITHIOCARBAMATES) AND THEIR METABOLITES

V. BARDAROV and Chr. ZAIKOV
Institute of Hygiene and Occupational Health, 1431 Sofia (Bulgaria)
and
M. MITEWA*
Department of Chemistry, University of Sofia, 1126 Sofia (Bulgaria)
(First received June 8th, 1988; revised manuscript received April 24th, 1989)

SUMMARY

The application of high-performance liquid chromatography with spectrophotometric or electrochemical detection was demonstrated for the determination of some alkylenebis(dithiocarbamates) (ABDTCs) and some of their degradation products and metabolites, especially alkylenethiourea, for toxicological investigation. First the ABDTCs were dissolved in the presence of EDTA and antioxidant, followed by ion-exchange chromatography with electrochemical detection (0.1–20 ng injected) or UV detection (20–5000 ng injected). Then normal-phase chromatography with UV detection was performed to determine ethylene- and propylenethioureas (0.1–1000 ng injected). The above-mentioned compounds were determined in technical products, air, blood, tissues, etc.

INTRODUCTION

Alkylenebis(dithiocarbamates) (ABDTCs), being metal (M^+ or M^{2+}) or ammonium salts of propylene- or ethylenebis(dithiocarbamic) acids (**1–7**) exhibit fungicidal activity. The M^+ salts are water-soluble, having a high toxicity and short-lived fungicidal action and are not widely used. In contrast, the ABDTCs of some bivalent metal ions, being polymeric products, are practically insoluble, have a low toxicity (LD_{50} = 4000–9000 mg/kg) and durable fungicidal action and are widely used in agricultural practice. However, they are unstable compounds, undergoing degradation to alkylenethioureas[1], the latter being some of the metabolites as well[2]. It has been shown that compounds of this type exhibit a high degree of carcinogenicity, mutagenicity and teratogenicity[2–4]. For that reason, the application of this type of fungicides in practice requires convenient methods for their determination as well as that of their degradation (metabolite) products. However, their analysis is hampered by their low solubility, low stability and polymeric structure. Compounds

0021-9673/89/$03.50

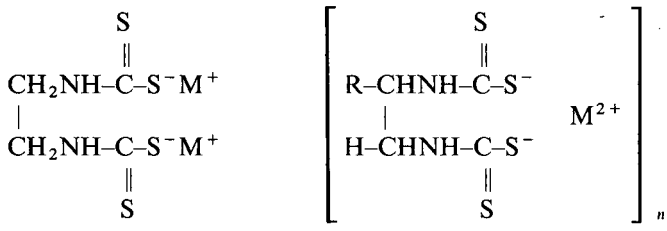

1 $M^+ = Na^+$ (Nabam)
2 $M^+ = NH_4^+$ (Amobam)

3 R = H; M = Zn (Zineb)
4 R = H; M = Mn and Zn (Mankozeb)
5 R = H; M = Mn (Maneb)
6 R = H; M = mixture of Zn, Cu, Mn, Fe (Cufram)
7 R = CH_3; M = Zn (Propineb)

1–7 are typical representatives of ABDTCs, **3–7** being the most frequently used fungicides in agricultural practice.

The methods developed for their determination, mainly volumetric, have low selectivity[5]. A number of them are indirect, based either on spectrophotometric, gas chromatographic (GC) or thin-layer chromatographic (TLC) determinations of the reaction products, liberated after reduction (in an acidic medium) by carbon disulphide[6–10], ethylenediamine or propylenediamine[11,12]. These determinations are not specific (they are not direct), and some are rather time-consuming. Some high-performance liquid chromatographic (HPLC) methods have also been described for the analysis of ABDTCs after extractive alkylation[13,14] and for alkylenethiourea after derivatization[15–17], as well as direct HPLC methods with spectrophotometric[18,19] or electrochemical[18,20] detection and a TLC method[21].

The aim of the present work was to apply HPLC for direct determination of the anionic part of these compounds (bis-dithiocarbamates) and their degradation products and metabolites (mainly alkylenethiourea) for toxicological investigations.

EXPERIMENTAL

Apparatus and chemicals

The HPLC equipment consisted of a Series 4 solvent delivery system (Perkin-Elmer, Norwalk, CT, U.S.A.), equipped with a Model 550 SE UV–VIS spectrometer (Perkin-Elmer) used as an UV detector with an 8-μl flow cell, an LC-95 UV detector

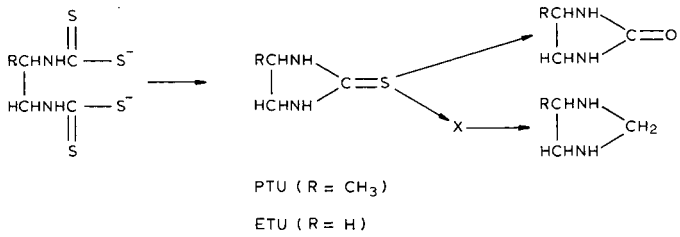

Metabolic degradation of ABDTCs according to Vogeler *et al.*[2]; X = unidentified product.

with a 4,5-μl flow cell or an electrochemical detector Model LC-4B with a glassy carbon working electrode (Bioanalytical Systems, West Lafayette, IN, U.S.A.), an injector Model 7125 with a 20-μl loop (Rheodyne, Cotati, CA, U.S.A.) and a Model R-100 recorder (Perkin-Elmer). The UV spectra were recorded on a Lambda-5 UV–VIS spectrometer (Perkin-Elmer). A precise pH meter "Radelkis", Type OP-207 (Metrimpex, Budapest, Hungary) and an ultrasonic bath Model RK-100 Sonorex (Bandelin, Berlin, F.R.G.) were used in the course of the sample and mobile phase preparation.

All solvents used, anhydrous methanol and ethanol, pentane, heptane and water, were of HPLC grade and all other chemicals, $NaClO_4$, EDTA disodium salt, dipotassium phosphate, sodium dihydrogenphosphate and ascorbic acid, were of analytical-reagent grade.

Water- and methanol-extracted zinc propylenebis(dithiocarbamate) $(Zn–PBDTC)_n$, supplied by Agria (Plovdiv, Bulgaria), Zineb (Zn–EBDTC), supplied by Bayer (F.R.G.), propylenethiourea (PTU), synthesized according to McKay and Hatton[22] and twice recrystallized from heptane–ethanol and ethylenethiourea (ETU) (2-imidazolidinethione), supplied by Aldrich (Milwaukee, WI, U.S.A.), were used as standard substances.

All solutions were degassed by helium purging, and thermostatted at ambient temperature in capped flasks.

HPLC procedures

Ion-exchange HPLC (HPIEC) was performed using a 250 mm × 4.6 mm Partisil SAX 10-μm (Whatman) column. The mobile phase was 1 g EDTA, 0.150 mol ClO_4 and 0.05 mol phosphate per litre water, pH 6.8, at a flow-rate of 2 ml/min. UV detection was used for concentrations higher than 1 μg/ml (285 nm), and electrochemical detection (ED) for the concentration range 1 ng/ml–1 μg/ml at a glassy carbon working electrode potential of 0.80 V; the reference electrode was 1 M Cl^-/Ag/AgCl.

Normal-phase HPLC was performed using a PE 250 mm × 4.6 mm Si-60 10-μm, a 125 mm × 4 mm LiChrosorb Si 100 5-μm, a 250 mm × 4 mm LiChrosorb CN 5-μm or a 125 mm × 4 mm LiChrosorb 5-μm RP-8 column. The mobile phase: comprised 6–8% (v/v) of methanol and ethanol in pentane at a flow-rate of 3 ml/min (overpressure 50 kPa helium in the mobile phase container to prevent flow fluctuations). UV detection was performed at 235 nm.

The hydrodynamic voltammogram of $PBDTC^{2-}$ was obtained by injection of aliquots equivalent to 500 ng $(Zn–PBDTC)_n$ in the mobile phase (see above) at a flow-rate of 2 ml/min.

All solutions of $(Zn–PBDTC)_n$ and $(Zn–EBDTC)_n$ were obtained by dissolution in the mobile phase (presence of EDTA) and adding ascorbic acid as an antioxidant in degassed water.

The determination of $(Zn–PBDTC)_n$ in air in the course of measurement of the inhalatory toxicity of $(Zn–PBDTC)_n$ (technical product) to experimental animals was carried out by aspiration of 20 l of the assay air through a 13-mm-diameter polymeric 1.5-μm polyvinyl acetate (PVA) fibre FPP-15 filter (U.S.S.R.), held in a filter holder. The latter was connected to a syringe and washed with 2.0 ml of methanol. After that the filter was removed and sonicated for 15 min in a capped sample tube with 5.0 ml of 0.1% EDTA and 0.1% ascorbic acid in degassed water. Aliquote of both solutions,

methanolic and water, were analysed by normal-phase HPLC–UV detection and HPIEC–ED respectively.

The sample preparation for determination of PTU and ETU in Zineb, $(Zn–PBDTC)_n$ and Maneb technical products involved a single extraction of an aliquot (10.0 mg) of the sample in a 25.0-ml flask with methanol (sonication is recommended). A part of the solution obtained was filtered through an 0.45-μm filter and an aliquot was analyzed by normal-phase HPLC–UV detection at 235 nm.

The blood samples (1 ml whole blood) were diluted in 1 ml water and 1 ml acetonitrile and then extracted with 2 ml ethyl acetate. The extract obtained was dried over magnesium sulphate and the solvent was evaporated by purging with nitrogen. The solution of the dry residue in ethyl acetate was analysed by normal-phase HPLC–UV detection at 235 nm.

The samples of rat suprarenal glands were homogenized in water–acetonitrile media. The supernatant obtained after centrifugation was extracted with ethyl acetate and the extract was dried, concentrated and analyzed as described for blood samples.

RESULTS AND DISCUSSION

Method development

The procedure for determination of ABDTCs is based on HPLC quantitation of the anionic part of the compounds (determining the biological activity of the ABDTCs) *i.e.*, on quantitation of ethylene- and propylenebis(dithiocarbamates) (see compounds **1–7**). Due to the insolubility of compounds **3–7**, a procedure for their dissolution in water based on a substitution complexation reaction[23] was used:

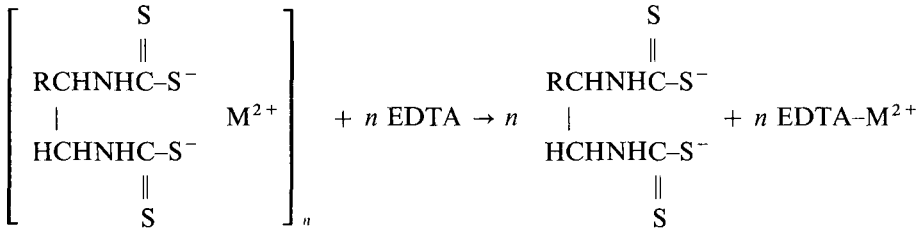

The presence of EDTA in the mobile phase is also necessary to prevent the accumulation of M^{2+} in the column and sedimentation of $ABDTC^{2-}$. The optimum concentration of EDTA was found to be *ca.* 1 mg/ml as at lower concentrations the dissolution of ABDTC proceeded very slowly. The same concentration was kept in the mobile phase in order to prevent the appearance of "injection peaks".

The UV spectrum of the $PBDTC^{2-}$ (that of $EBDTC^{2-}$ is similar and its change with time is presented in Fig. 1. It is evident that UV detection at 285 nm is possible for concentrations higher than 1 μg/ml (molar absorptivity, $a = 2.2 \cdot 10^4$ a.u.). The spectral changes observed indicate oxidation reactions. For that reason the use of oxygen-free water (degassed) and addition of an antioxidant (ascorbic acid) is obligatory (as confirmed by the chromatographic results presented in Fig. 2b and c).

A typical chromatogram in Fig. 2a shows the possibility of separating $EBDTC^{2-}$ and $PBDTC^{2-}$ using an ion-exchange column. The application of HPIEC–UV detection is demonstrated for quantitation of (Zn–PBDTC) in a technical product dissolved in the absence (b) and presence (c) of ascorbic acid.

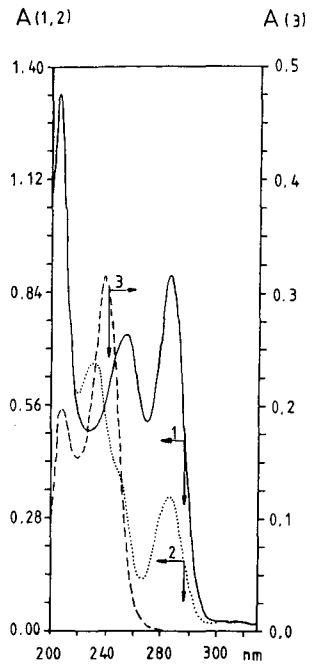

Fig. 1. UV spectra of $PBDTC^{2-}$ and PTU (optical cell length, l = 10 mm): (1) 1.2 mg $(Zn–PBDTC)_n$, dissolved in 50.0 ml degassed water in the presence of 1 mg/ml EDTA, *vs.* 1 mg/ml EDTA in water, recorded 40 min after preparation. (2) solution 1, recorded after 16 h (sealed vessel); (3) 1 μg/ml PTU solution in methanol, *vs.* methanol.

For ED to be used, the hydrodynamic voltammogram of $EBDTC^{2-}$ and $PBDTC^{2-}$ were obtained in the mobile phase as described above. The data obtained show that glassy carbon working electrode potentials above 0.6 V should be applied. The presence of EDTA in the mobile phase, however, limits the upper value of the potential, the optimum being 0.8 V.

The data presented in Fig. 3 show the optimum conditions for HPIEC determination of $PBDTC^{2-}$ using ED: pH 6.5–7 (at lower values peak broadening and tailing are observed, while values above pH 7 are harmful to the silica-based stationary phase); the retention times might be optimized by changing the perchlorate concentration; a decrease in the EDTA concentration in the mobile phase as well as the use of another complexation agent for M^{2+} with lower electrochemical activity are ways of increasing the sensitivity in HPLC–ED of $ABDTC^{2-}$. For our purposes however, the sensitivity achieved [limit of determination 100 pg injected $(Zn–PBDTC)_n$ after ionisation in EDTA solution] was satisfactory and no attempts were made to increase it.

We have demonstrated that normal-phase HPLC–UV detection is the most convenient method for determination of PTU and ETU among the well known chromatographic variants[18–20], showing a wide range of linearity (up to 2 μg injected), high efficiency and sensitivity. Both methanol and ethanol were used as polar modifiers of the mobile phase because of the impossibility of dissolving more than 6% methanol in pentane, while the use of ethanol only results in a loss of efficiency. The

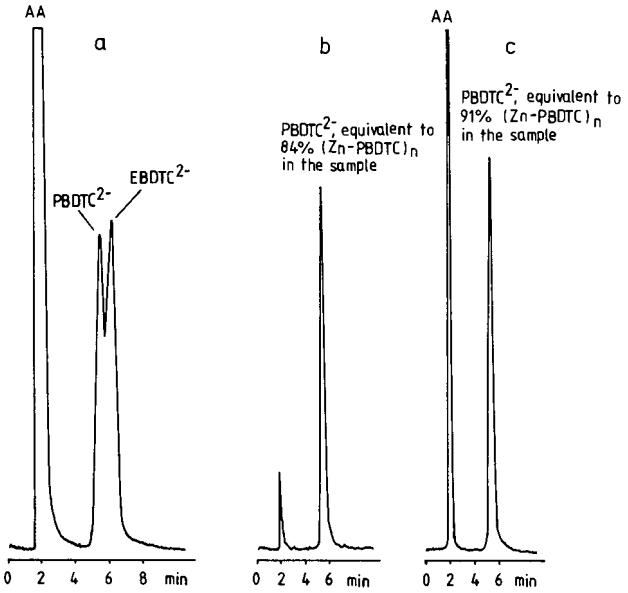

Fig. 2. Chromatograms of solutions of Zineb and $(Zn–PBDTC)_n$. Column: 250 mm × 4.6 mm SAX, 10 μm. Mobile phase: 1 g EDTA, 0.150 mol ClO_4^- and 0.05 mol phosphate per litre water, pH 6.8, flow-rate 2 ml/min. UV detection at 235 nm. (a) Equal amounts of Zineb and $(Zn–PBDTC)_n$, dissolved in the mobile phase in presence of AA; (b) 2.0 mg of $(Zn–PBDTC)_n$, dissolved in 100.0 ml of mobile phase, 10 μl injected 10 min after preparation; (c) 2.0 mg of the same $(Zn–PBDTC)_n$ as used for (a), dissolved in 100.0 ml of mobile phase containing 100 mg ascorbic acid (AA).

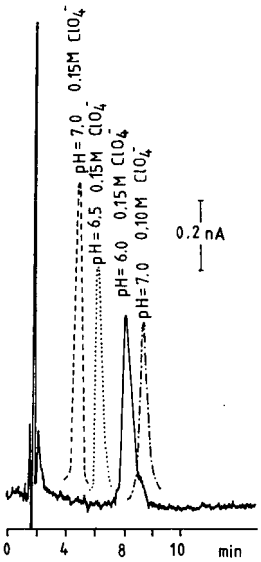

Fig. 3. HPIEC–ED of $PBDTC^{2-}$ and changes in its retention with acidity and perchlorate concentration in the mobile phase. Column: 250 mm × 4.6 mm SAX, 10 μm. The mobile phase contains 1 g/l EDTA; pH and perchlorate concentrations as shown. ECD at 0.8 V on glassy carbon working electrode (1 M Cl^-/Ag/AgCl reference electrode).

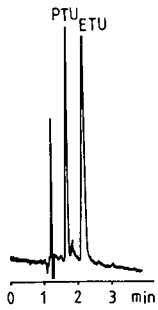

Fig. 4. Normal-phase HPLC separation of ETU and PTU. Column: 125 mm × 4 mm LiChrosorb RP-8, 5 μm. Mobile phase: 6% methanol and 6% ethanol in *n*-pentane, flow-rate 3 ml/min. Detection: UV, LC-95 (4.5-μl flow cell), 235 nm. Sample: 10 μl standard solution containing 1 ng PTU and 1 ng ETU.

typical normal-phase chromatogram obtained on a LiChrosorb RP-8 5-μm column, presented in Fig. 4, shows the possibility of separating ETU and PTU. Similar results can be obtained using Si or CN columns in the normal-phase mode. The high absorbance at 235 nm ($a = 1.0 \cdot 10^4$ a.u. for ETU and PTU) and high efficiency of

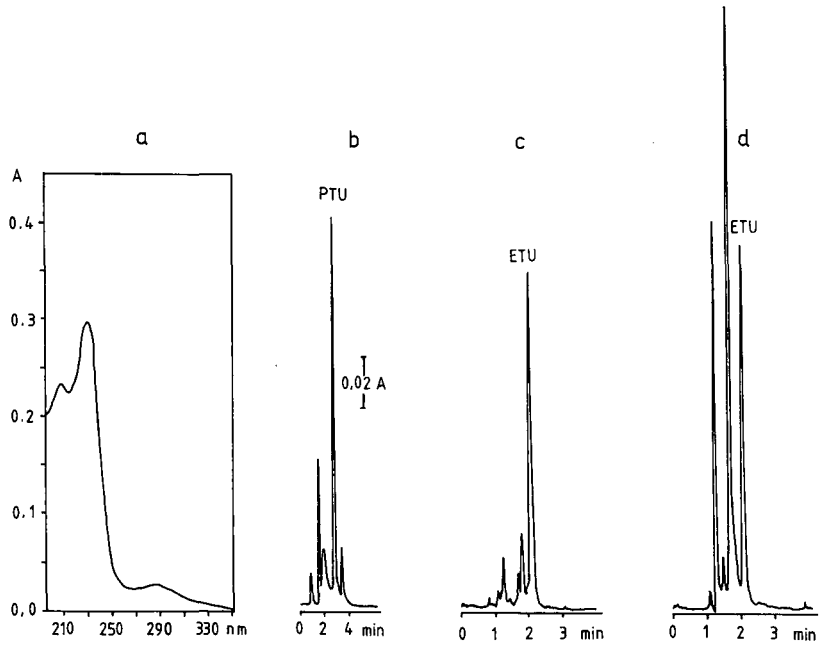

Fig. 5. Spectrophotometric and normal-phase HPLC determination of PTU and ETU in $(Zn–PBDTC)_n$, Zineb and Maneb technical products: (a) UV spectrum of a methanolic extract (25.0 ml) of 10.0 mg $(Zn–PBDTC)_n$ *vs.* methanol ($l = 10$ mm). (b) Normal-phase chromatogram of the same extract as in (a). Column: PE 250 mm × 4.6 mm Si-60, 10 μm. Mobile phase: 8% methanol and 8% ethanol in pentane, flow-rate 3 ml/min. Detection: UV, 235 nm. (c) Normal-phase chromatogram of a methanolic extract (50 ml) of 10 mg Zineb. Column: 125 mm × 4 mm LiChrosorb RP-8, 5 μm. Mobile phase 6% methanol and 6% ethanol in *n*-pentane, flow-rate 3 ml/min. Detection: UV, 235 nm. (d) Normal-phase chromatogram of a methanolic extract (50 ml) of 10 mg Maneb. Conditions as in (c).

normal-phase HPLC of the compounds allow a highly sensitive determination to be achieved (100 pg injected for PTU and ETU when an LC-95 UV detector is used).

Applications

The applications of the procedure developed for determination of PTU in a methanolic extract from a technical product $(Zn–PBDTC)_n$ is shown in Fig. 5b (the UV spectrum of the extract is shown on Fig. 5a). The appearance of several peaks in the chromatogram obtained with UV detection at 235 nm shows unequivocally that the absorbance at this wavelength is due to different compounds and selective determination of PTU is possible only by means of HPLC. In Fig. 5c and d chromatograms of methanolic extracts of Zineb and Maneb, obtained in the same way, are represented. The other peaks observed are due to impurities, formed in the course of prolonged storage of the samples (more than 4 years).

The determinations of $(Zn\text{-}PBDTC)_n$ and PTU by means of HPIEC–ED and normal-phase HPLC–UV detection, respectively, in air in the course of measurement of the inhalatory toxicity of the $(Zn–PBDTC)_n$ technical product to experimental animals are demonstrated in Fig. 6. The high reproducibility of the HPLC

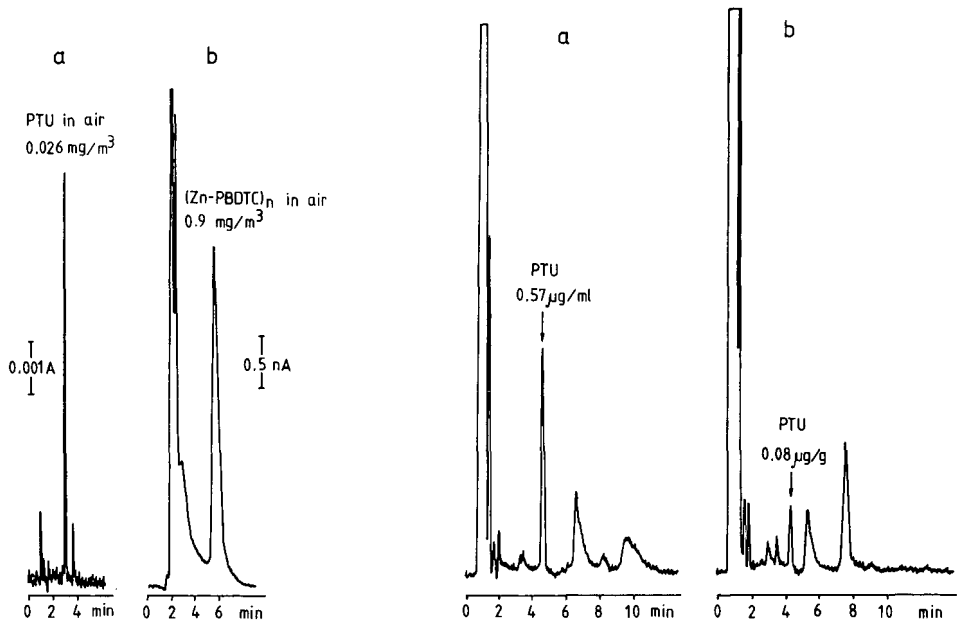

Fig. 6. Determination of $(Zn–PBDTC)_n$ and PTU in air from a camera for inhalatory experiments with experimental animals. (a) Normal-phase chromatogram of the methanolic extract from the sampling filter after aspiration of 20 l air. Conditions as in Fig. 5b. (b) Ion-exchange chromatogram of the extract of the same filter as in (a) in mobile phase in the presence of antioxidant (ascorbic acid). Conditions as in Fig. 2.

Fig. 7. Determination of PTU in biological samples. (a) Normal-phase chromatogram of a blood sample from a rat, given a dose of 60 mg/kg PTU daily for 1 month. Column: 125 mm × 4 mm LiChrosorb Si 100, 5 µm. Mobile phase: 5% methanol and 5% ethanol in pentane, flow-rate 2 ml/min. Detection: UV, 235 nm. Sample preparation as described in the text. (b) Normal-phase chromatogram of a suprarenal gland sample from a rat, dosed as in (a). Conditions as in (a). Sample preparation as described in the text.

determination was confirmed when the sample solution from a separate air sample was injected five times in 3 h [coefficient of variation C.V. = 4.6% for PTU and 8.3% for $(Zn–PBDTC)_n$]. A considerably lower reproducibility was obtained in the course of measurement of the air concentrations of PTU and $(Zn–PBDTC)_n$ [four determinations daily, C.V. 20–40% for PTU and $(Zn–PBDTC)_n$], which is connected mainly with inconsistent dosage of $(Zn–PBDTC)_n$ in the air.

Chromatograms of rat blood and rat suprarenal gland samples for determination of PTU are presented in Fig. 7. The recoveries from the procedures described are 93–97% (six determinations) for blood samples, where a known amount (5.00 μg/ml) of PTU was added, and 61–75% (three determinations) for suprarenal gland samples, where 1.0 μg PTU per gram sample was added before homogenization.

REFERENCES

1 J. F. Seiler, *Mutat. Res.*, 26 (1974) 189.
2 K. Vogeler, Ph. Dreze, A. Rapp, St. H. Steffan and H. Ullemeyer, *Pflanzenschutz-Nachr.*, 30 (1977) 72.
3 J. R. M. Innes, M. Valerio, B. Ulland, A. J. Pallotta, L. Petrucelli, R. R. Bates, H. L. Falk, J. J. Gart, M. Klein, I. Mitchel and J. Peters, *J. Natl. Cancer Inst.*, 42 (1969) 1101.
4 K. S. Khera, *Teratology*, 7 (1973) 243.
5 D. G. Clarke, H. Baum, E. L. Stanley and W. F. Haster, *Anal. Chem.*, 23 (1951) 1842.
6 *British Standard*, BS 5202 Part II, 1983; *Anal. Abstr.*, 46 (1984) 6–30.
7 G. E. Keppel, *J. Assoc. Off. Anal. Chem.*, 54 (1971) 528.
8 T. E. Cullen, *Anal. Chem.*, 23 (1951) 1842.
9 H. A. McLeod and K. A. McCulley, *J. Assoc. Off. Anal. Chem.*, 52 (1969) 1226.
10 Report of the Panel on the Determination Dithiocarbamate Residues, *Analyst (London)*, 106 (1981) 782.
11 M. Uno, Y. Onji, M. Nozawa, H. Nakahira and K. Tangawa, *Shokuhin Eiseigaku Zasshi*, 24 (1983) 201.
12 K. K. Mazumbar, N. Samajpati and I. Chakrabarti, *Indian J. Exp. Biol.*, 20 (1982) 865.
13 K. H. Gustafsson and Ch. H. Fahlgren, *J. Agric. Food Chem.*, 31 (1983) 461.
14 K. H. Gustafsson and R. A. Thompson, *J. Agric. Food Chem.*, 29 (1981) 729.
15 R. M. Smith, C. Madaher, W. G. Salt and N. A. Smart, *Chromatographia*, 19 (1984) 411.
16 R. R. King, *J. Agric. Food Chem.*, 25 (1977) 73.
17 S. Lembo, G. Marzillo and C. Sgambati, *J. Chromatogr.*, 267 (1983) 427.
18 F. J. Lawrence, F. Iverson, H. B. Hanekamp, P. Bos and R. W. Frei, *J. Chromatogr.*, 212 (1981) 245.
19 J. C. Van Damme, M. Galoux and J. Verdier, *J. Chromatogr.*, 206 (1981) 125.
20 H. B. Hanekamp, P. Bos and R. W. Frei, *J. Chromatogr.*, 186 (1979) 489.
21 G. Czegledi-Janko and A. Hollo, *J. Chromatogr.*, 31 (1967) 89.
22 A. F. McKay and W. G. Hatton, *J. Am. Chem. Soc.*, 78 (1956) 1618.
23 J. Pflugmacher and W. Ebing, *Z. Lebensm.-Unters.-Forsch.*, 179 (1980) 349.

Journal of Chromatography, 479 (1989) 107–116
Elsevier Science Publishers B.V., Amsterdam — Printed in The Netherlands

CHROM. 21 650

QUANTIFICATION AND CHARACTERIZATION OF THE TRIFLUOROACETIC ANHYDRIDE DERIVATIVES OF N,N′-ETHYLENEBISSTEARAMIDE AND N,N′-ETHYLENEBISOLEAMIDE

P. A. METZ*, F. L. MORSE and T. W. THEYSON
LONZA Inc., Research and Development Laboratories, 3500 Trenton Avenue, Williamsport, PA 17701 (U.S.A.)
(First received March 1st, 1989; revised manuscript received May 26th, 1989)

SUMMARY

An analytical technique for the measurement of low levels (0.1–3.0%) of N,N′-ethylenebisstearamide (EBS) and N,N′-ethylenebisoleamide (EBO) in polymeric matrices has been developed. The method involves reaction of the secondary bis-amides with trifluoroacetic anhydride (TFAA) followed by high-performance liquid chromatographic (gel permeation chromatographic) separation and quantification of the N-trifluoroacyl derivatives. The method is linear in ranges typical of polymer compounding applications and offers a direct measurement of EBS and EBO without the need for prior extraction. The TFAA derivatives were isolated and characterized by infrared and direct-probe mass spectrometry.

INTRODUCTION

Trifluoroacetic anhydride (TFAA) is a powerful electrophilic acylating reagent that has been shown to react with primary and secondary amines[1–3], amino acids[4], amides[5] and polyamides[6], as well as a number of other nucleophiles[7]. Historically, TFAA derivatizations have been employed in gas–liquid chromatography (GC) to improve the volatility and chromatographic behavior of otherwise non-volatile or difficult to separate compounds[8]. Recently, TFAA has been employed as a derivatization reagent for gel permeation chromatography (GPC) of polymers such as polyamides[9–11] and polyurethanes[12]. N-Trifluoroacylation of these polymers improves their solubility in common GPC solvents allowing characterization of the polymer based upon the chromatographic distribution of the TFAA analogue.

N,N′-Ethylenebisstearamide (EBS) and N,N′-ethylenebisoleamide (EBO) are high-melting aliphatic amides that are used as additives in a variety of polymers, functioning as lubricants, mold release agents and slip agents. EBS is widely used in acrylonitrile–butadiene–styrene (ABS) and other styrene co-polymers[13]. EBO has shown utility as a slip agent and a dispersant for other additives including flame retardants, pigment and colorants in polyolefins[14]. In addition, numerous patents have been issued for the application of EBS and EBO in a varity of thermoplastics, including polyurethane elastomers, polyacetals, nylons and acrylates. For these

0021-9673/89/$03.50

applications, compounders require accurate quantitation of additive loadings, particularly where low levels of additives are used. Large variations in polymer performance are known to occur with relatively small differences in additive loadings.

This paper describes an analytical derivatization–GPC procedure for the measurement of low levels (0.1–3.0%) of EBS and EBO in polymer compounds. The derivatization procedure involves reaction of EBS and EBO with TFAA followed by GPC analysis of the N-trifluoroacyl derivatives. In addition, qualitative data are presented on the isolated TFAA derivatives, confirming the N-trifluoroacylation reaction.

EXPERIMENTAL

Reagents

EBS and EBO were prepared in-house and are commercially available. ABS, styrene–acrylonitrile (SAN) and low-density polyethylene (LDPE) were obtained from commercial sources. Reagent-grade TFAA, trichloroacetic anhydride and acetic anhydride were purchased from Aldrich (Milwaukee, WI, U.S.A.). High-performance liquid chromatography (HPLC) grade chloroform, dichloromethane, carbon tetrachloride and tetrahydrofuran (THF) were obtained from J. T. Baker (Philipsburg, NJ, U.S.A.). ACS reagent-grade heptane was purchased from EM Science (Cherry Hill, NJ, U.S.A.). All other incidental chemicals were ACS reagent grade.

Apparatus

The HPLC system used for the GPC separation of EBS-TFAA and EBO-TFAA derivatives consisted of a Model 510 pump (Waters Assoc., Milford, MA, U.S.A.), a Model 7125 injector equipped with a 100-μl loop (Rheodyne, Cotati, CA, U.S.A.) and a Model LC-100 column oven, maintained at 60 $\pm$ 1°C (Perkin-Elmer Corporation, Norwalk, CT, U.S.A.). Separations were performed at a flow-rate of 1.0 ml/min, with THF as the mobile phase. The gel permeation column set consisted of two μStyragel® 100 A and two μStyragel 500 A columns (Waters). Detection was performed with a Model 410 differential refractive index detector (Waters), with the internal temperature maintained at 50 $\pm$ 1°C. Chromatographic recording, integration and data handling were performed with a Model 4270/Chromatation AT system (Spectra-Physics, Santa Clara, CA, U.S.A.).

GC separations of the TFAA derivatives of EBS and EBO were performed on a Model 5890 GC system (Hewlett-Packard, Palo Alto, CA, U.S.A.). The gas chromatograph was equipped with a 3.5 m $\times$ 0.53 mm I.D. SPB-5 (d_f 1.0 μm) fused-silica column (Supelco, Bellefonte, PA, U.S.A.). Split injections (5:1) of 1.0 μl were performed with helium as the carrier gas at 65 cm/s. The column inlet temperature was 300°C. The flame ionization detector was set at 325°C. The column temperature program was from 280 to 320°C at 5°C/min with a final hold time of 5 min.

For identification of the N-trifluoroacyl derivatives a Model 4021 gas chromatograph–mass spectrometer was used (Finnigan, Sunnyvale, CA, U.S.A.). The gas chromatograph was equipped with a 12 m $\times$ 0.20 mm I.D. cross-linked methyl silicone (d_f 0.33 μm) fused-silica column (Hewlett-Packard). Split injections (20:1) of 1.0 μl were performed with helium as the carrier gas at 40 cm/s. The column inlet was set at 300°C and the column temperature program was from 280 to 320°C at 5°C/min with

a hold time of 15 min. Direct-probe mass spectral (MS) sampling was performed with ballistic heating from 50 to 300°C. In all experiments the mass spectrometer was used in the electron-impact (EI) mode with the ionization energy set at 70 eV. The scan rate was one scan per 3 s over a mass range of 35–950 a.m.u.

Infrared (IR) spectra were recorded on a Model 281 IR spectrophotometer (Perkin-Elmer) using a thin film preparation on a thallium bromide window (Model KRS-5; Foxboro Company, North Haven, CT, U.S.A.).

SAN and LDPE were compounded in a Model EPL-V3302 Brabender Plasticorder (C.W. Brabender, Hackensack, NJ, U.S.A.) equipped with a No. 6 roller head and roller blades. LFPE was pelletized in a 3/4-in. single screw extruder. ABS was powder blended with EBS and melt blended in an Instron Model 1123 universal testing instrument (Instron Corp., Canton, MA, U.S.A.) equipped with a Model 3210 capillary rheometer.

Procedure

TFAA derivatization of EBS in SAN was performed by transferring 5.000 g (± 5 mg) of SAN containing between 0.3 and 3.0% EBS into a 100-ml pressure-tight reaction vessel (Model 3-3110, Supelco). To the reaction vessel were added 50.00 ml of chloroform and 2.00 ml of TFAA. The vessel was sealed and heated on a hot plate (115°C) for 1.5 h. After reaction, the sample was cooled to ambient temperature, diluted ten-fold in THF and chromatographed by GPC with THF as the mobile phase at 1.0 ml/min. Multi-level calibrations were performed by following the same procedure with the addition of 15.0 (± 0.5), 75.0 (± 0.5) and 150.0 mg (± 0.5 mg) of EBS to each of three reaction vessels containing 5.000 g SAN with no additives.

TFAA derivatization of EBS in ABS was performed as described above for SAN samples. Multilevel calibrations were carried out in the same manner, with the same EBS standard levels.

TFAA derivatization of EBO in LDPE was performed by transferring 1.000 g (± 5 mg) of LDPE containing between 0.2 and 0.5% EBO to a 100-ml pressure tight reaction vessel. To the vessel were added 30.00 ml of chloroform plus 2.00 ml of TFAA. The vessel was sealed and heated for 1.5 h on a hot plate (115°C). After reaction, the sample was cooled to ambient temperature, during which time the LDPE precipitated. The resulting mixture was centrifuged at 3070 *g* for 10 min (Model HN-SII; International Equipment Company, Needram Heights, MA, U.S.A.). The lighter polyethylene gel separated from the reaction mixture and migrated to the top of the vessel. A 10-ml luer lock syringe, with a 3-in. No. 17 gauge needle, was used to penetrate the LDPE layer and collect the chloroform layer for HPLC analysis. The collected portion was chromatographed directly by GPC without further dilution. Multilevel calibrations of EBO in LDPE were performed by following the same procedure as above with the addition of 2.00 (± 0.05), 3.50 (± 0.05) and 5.00 mg (± 0.05 mg) of EBO to each of the reaction vessels containing 1.000 g LDPE containing no additives.

TFAA derivatives of EBS and EBO were prepared for the purpose of isolation and identification by reacting 0.150 g (± 5 mg) of the bis-amide with 2 ml TFAA in 50 ml of chloroform in a 100-ml reaction vessel. The mixture was heated for 1.5 h at 115°C, and then dried under a stream of high-purity nitrogen. The EBS-TFAA derivative was recrystallized twice from scrupulously dried diethyl ether. The

EBO-TFAA formed a yellow oil that would not recrystallize. The latter was analyzed without further purification. The derivatives were stored over desiccant prior to GC, IR and GC–MS analysis.

RESULTS AND DISCUSSION

HPLC analysis of EBS and EBO in polymer compounds is made difficult by the fact that neither the polymers nor the aforementioned additives is readily soluble in routine HPLC solvents. GC analysis is limited by both the solubility and volatility of the fatty secondary amides and the polymer matrix. Edwards[15] has reported an HPLC method for the analysis of amide slip agents in polyethylene and polyethylene–vinyl acetate copolymers. However, the slip agents reported were the more soluble primary amides. The latter were readily extracted from resin granules and thin film strips with methanol. Additives in polyolefins have also been analyzed by capillary GC with on-column injection of dichloromethane–methanol (1:1) extracts[16]. In-house procedures for separation and analysis of the less soluble secondary bis-amides, EBS and EBO, in various polymer compounds historically involved high temperature Soxhlet extractions (6–24 h), followed by total nitrogen (Kjeldahl) analysis. These methods are time consuming, require significant amounts of sample handling and lack specificity and sensitivity. This lab has also investigated dispersive IR and Fourier transform (FT)-IR analysis of polymer thin film for EBS and EBO using reflectance and attenuated total reflectance accessories. While IR spectroscopy shows promise for higher levels of these additives (1–5%)in a limited number of polymer compounds, it does not represent a universal analytical approach. Furthermore, IR techniques have been hampered by the ability to prepare and/or reproduce thin films. Differential scanning calorimetry (DSC) has also been investigated. Preliminary results indicate that subtle changes in the polymer glass transition state may be correlated to additive loading levels.

TFAA derivatization of EBS and EBO in polymer compounds followed by HPLC (GPC) analysis of the N-trifluoroacyl derivatives allows direct measurement of low levels of these additives without the need for extraction.

Eqn. 1 shows the reaction of TFAA with EBS/EBO:

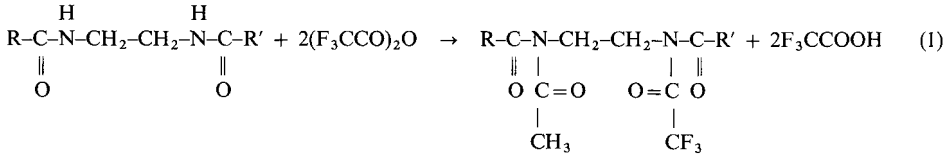

(1)

Although both N- and O-trifluoroacetylation reactions have been reported[7] and EBS/EBO derivatization may proceed through the enolic intermediate, no evidence of O-trifluoroacetylation has been found. Other anhydrides were also tested for their ability to derivatize EBS and EBO. Trichloroacetic anhydride, chloroacetic anhydride and acetic anhydride, respectively, were less reactive towards the secondary bis-amides. The latter two anhydrides did not react with EBS or EBO in polymer matrices. TFAA not only reacts with the secondary bis-amides, but significantly enhances polymer solubility in the reaction media.

TABLE I
TYPICAL ALKYL DISTRIBUTION OF COMMERCIAL STEARIC AND OLEIC ACIDS

Commercial acid	*Component (%)*								
	C_{14}	$C_{14:1}$	C_{16}	$C_{16:1}$	C_{17}	C_{18}	$C_{18:1}$	$C_{18:2}$	$C_{18:3}$
Stearic	5	–	45	–	1.5	48	0.5	–	–
Oleic	2	2	6	6	–	3	72	8	1

Table I lists the typical fatty acid distributions of the aliphatic portion of EBS and EBO. Although the aliphatic portion of these compounds shows no apparent effect upon the reaction with TFAA, the chain length distribution does effect chromatographic behavior of the resulting derivatives, and was a determining factor in choosing the GPC column set and GC capillary column.

Fig. 1A is a chromatogram showing the GPC separation of the N-trifluoracyl derivative of EBS from SAN copolymer. Fig. 1B is a chromatogram showing the GPC separation of the N-trifluoroacyl derivative of EBO from LDPE. In both separations the derivative peak is well resolved from the polymer distribution (or residual polymer in the case of LFPE) and the reaction solvent and by-products. The latter elute near the total permeation volume of the GPC column set. The negative deflection in both chromatograms at 32–34 min is due to residual TFAA. In some cases, low levels of other additives such as stabilizers and antioxidants may be compounded along with

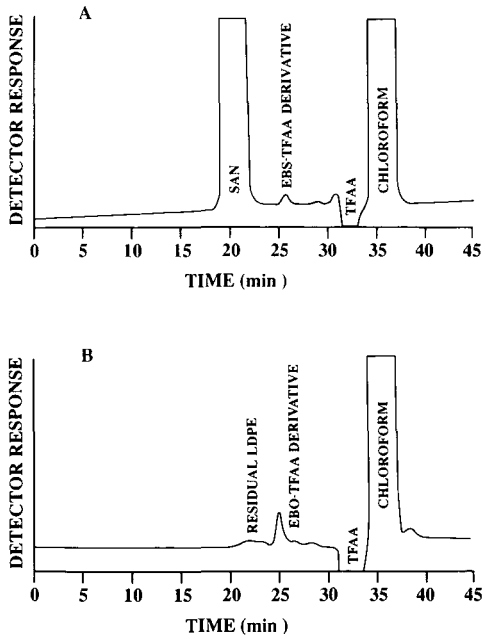

Fig. 1. Gel permeation chromatogram of (A) TFAA derivatized EBS (3%) in SAN copolymer and (B) TFAA derivatized EBO (1%) in LDPE. Instrument operating conditions given in the Experimental section.

TABLE II
LINEAR RANGES AND MINIMUM DETECTION LIMITS FOR EBS AND EBO DERIVATIVES

Sample	*Working range (%,w/w)*	*Linearity, R^2*	*MDL*[a]
EBS in SAN	0.3–3.0	0.9999	0.01
EBS in ABS	0.3–3.0	0.9996	0.02
EBO in LDPE	0.2–0.5	0.9989	0.05

[a] MDL = Minimum detection limit, based on a signal-to-noise ratio of 2:1.

EBS or EBO. Such components may present a problem in quantitation of EBS or EBO if they fall in the same molecular-weight range as the respective TFAA derivatives. In this study, the EBS and EBO derivatives were sufficiently resolved from any other interferences to allow for good quantitation. Preliminary results obtained in this laboratory for complex polymer blends indicate that quantitation by the method of standard addition may be used where additives of similar molecular weight interfere with EBS or EBO measurement. Also, changing data handling from peak area to peak height improves quantitation when EBS and EBO derivatives are not completely resolved from interfering peaks.

Table II lists the linear ranges and minimum detection limits for EBS and EBO compounded in three polymers, ABS, SAN and LDPE. The secondary bis-amide/polymer combinations and the corresponding working ranges are consistent with specific plastic applications. EBS and EBO response linearity are based on a three point standardization. The minimum detection limits have been obtained experimentally and represent that quantity of analyte that produces a signal equal to twice the baseline noise.

Table III lists the precision and accuracy of the method for EBS and EBO measurement in the respective polymer matrices. The standard deviation is less than 2% relative for both standards and samples ($n=5$ determinations). Good agreement was found between the measured level and the actual compounded amounts of EBS and EBO. The accuracy of the determination is largely dependent upon the method of standardization. A multipoint external standard calibration of the secondary bis-amide in the polymer matrix was found to give the best results.

Fig. 2 shows the effect of the polymer matrix upon the standardization of EBS in SAN. It is evident that the polymer matrix affects the standardization, decreasing the

TABLE III
PRECISION AND ACCURACY FOR EBS AND EBO USING TFAA DERIVATIZATION METHOD

Sample	*R.S.D.*[a] *(%)*		*Accuracy*	
	Standards	*Samples*	*% Compounded*	*% Found*
EBS in SAN	1.42	1.88	2.00	2.08
EBS in ABS	1.69	1.98	1.00	0.96
EBO in LDPE	1.35	2.00	0.40	0.41

[a] R.S.D. = Relative standard deviation ($n=5$).

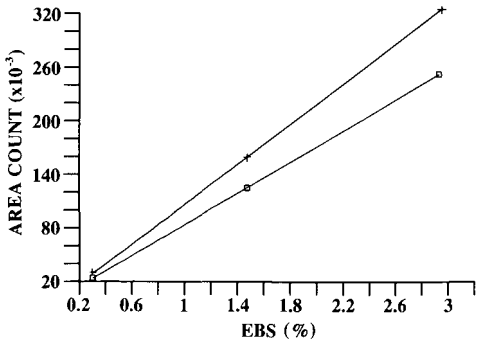

Fig. 2. Comparison of SAN copolymer matrix (□) and non-matrix (+) three-point calibration of TFAA-derivatized EBS (range 0.3–3.0%).

slope of the standard curve. This trend was consistent, regardless of the secondary bis-amide or polymer matrix studied. Table IV lists calibration data for polymer matrix and non-matrix standardization of EBS and EBO in the three polymers studied. The response is always greater for the analyte in the matrix-free environment. However, the polymer matrix does not appear to affect the linearity of response as evidenced by the correlation coefficients shown. These results indicate that improved accuracy may be expected when standards are prepared in the polymer matrix in which they intend to be measured. However, it may be possible to apply a calculated correction factor to non-matrix standardization results based on the differences between the two calibration curves.

As noted previously, TFAA addition to chloroform greatly improved the solubility of otherwise insoluble or very slow to dissolve polymers. Hence, some controversy arose as to whether EBS and EBO were in fact derivatized, or perhaps more readily dissolved with the aid of TFAA. Four pieces of evidence indicate the formation of bis-amide -N-trifluoroacyl derivatives: IR spectral data, melting point data, MS analysis and GC analysis.

Fig. 3 shows IR spectra of EBO and the isolate from the reaction of EBO with TFAA, respectively. Strong bands at 3350 cm^{-1} (N–H stretching vibrations) and 1565 cm^{-1} (N–H bending vibrations) characteristic of secondary amides were not present in the TFAA derivative isolate spectrum. Furthermore, the shift of the amide band in the derivative spectrum from 1640 to 1720 cm^{-1} is consistent with the formation of

TABLE IV
EFFECT OF POLYMER MATRIX ON EXTERNAL STANDARDIZATION

Sample	*Slope*[a]		*y Intercept*		R^2	
	Matrix	*Non-matrix*	*Matrix*	*Non-matrix*	*Matrix*	*Non-matrix*
EBS in SAN	$4.97 \cdot 10^{-6}$	$3.63 \cdot 10^{-7}$	0.010	0.002	0.9999	1.0000
EBS in ABS	$1.23 \cdot 10^{-5}$	$9.48 \cdot 10^{-6}$	0.190	0.001	0.9996	0.9999
EBO in LDPE	$2.3 \cdot 10^{-7}$	$1.37 \cdot 10^{-8}$	0.001	0.001	0.9989	0.9997

[a] Slope based on a three-point external standardization.

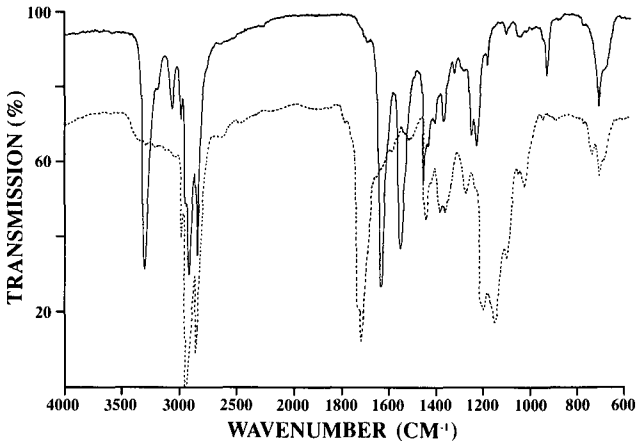

Fig. 3. Infrared spectrum of (———) EBO and (--------) the isolate from the reaction of EBO with TFAA.

a tertiary amide and with the addition of an electron withdrawing group to the nitrogen. Analogous IR spectral differences between EBS and the EBS/TFAA isolate were observed. These results are consistent with those published previously for the N-trifluoroacyl derivatives of polyamides[12].

The EBS and EBO derivative isolates also displayed different melting ranges than their respective starting materials. The EBS derivative isolate displayed a melting range of 61–69°C. The EBS starting material melts between 140 and 145°C. Recrystallization of the EBS-TFAA isolate was performed in scrupulously dried solvents since the N-trifluoroacyl derivatives favor hydrolysis back to the secondary amide. The EBO starting material had a melting range of 110–117°C, the EBO-TFAA derivative isolate was a liquid at room temperature. Repeated attempts to recrystallize this isolate, even under cryogenic conditions (−72°C), were unsuccessful. Decreased melting ranges are consistent with the formation of tertiary amide derivatives, due to loss of available protons for inter-molecular bonding.

Fig. 4 and 5 are direct-probe EI mass spectra (DP-EI-MS) of EBS and the EBS-TFAA derivative isolate, respectively. The molecular ion (M^+) at m/z = 784 (Fig. 5) represents the derivatized bis-amide with two stearate groups making up the aliphatic portion of the molecule. As shown in Table I, the aliphatic portion of EBS is derived form a complex distribution of fatty acids. Although the molecular ions throughout the probe profile were weak (<0.1% total ion current), M^+ ions of m/z = 770, 756, 742 and 728 representing other possible combinations of fatty amide derivatized species were found in other MS runs. Molecular ions and high-molecular-weight fragments were als quite weak in the DP-EI-MS of the EBS starting material. However, some common low-molecular-weight fragments (m/z = 43, 57, 71, 84 and 98) were found in both this spectra and the EBS/TFAA derivative isolate spectra. These data indicate that the isolate is likely a derivative of the EBS starting material. No clear assignment could be made for fragments associated with the trifluoracyl fragment. Similar DP-EIMS results were obtained for the EBO-TFAA derivative, with weak M^+ ions of m/z = 780, 778, 766, 754, 752 and 750 being observed.

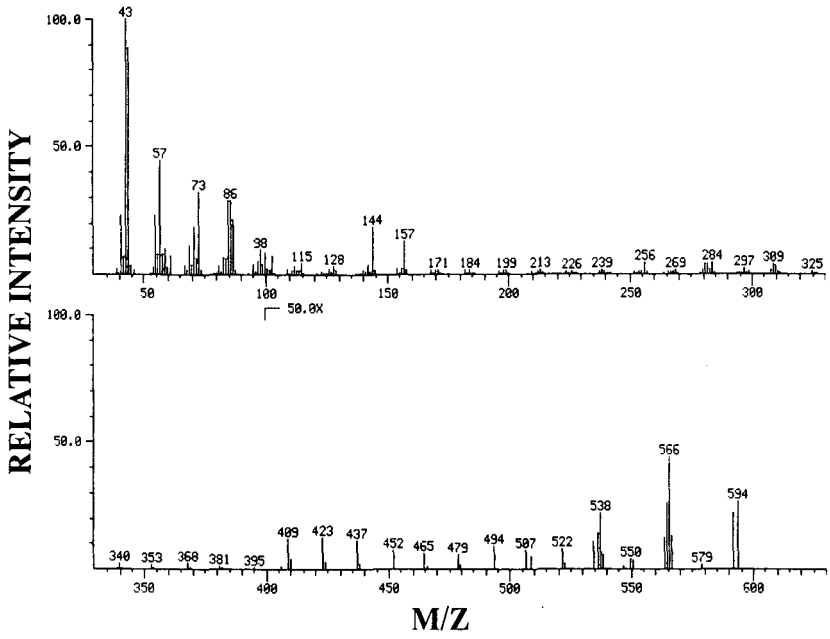

Fig. 4. Direct-probe EI (70 eV) mass spectrum obtained by analysis of underivatized EBS. Instrument operating conditions given in the Experimental section.

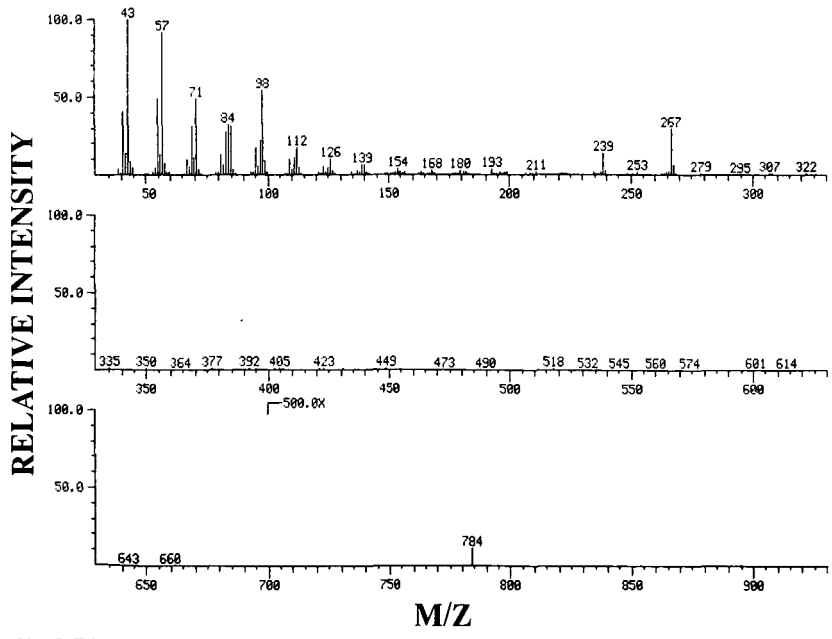

Fig. 5. Direct-probe EI (70 eV) mass spectrum obtained by the analysis of TFAA derivatized EBS, showing the weak molecular ion (*m/z* 784) for the distearate bis-amide derivative. Instrument operating conditions given in the Experimental section.

GC–EI-MS analysis of both the EBO-TFAA and EBS-TFAA derivatives was unsuccessful, presumably because not enough material was ionized to produce a strong mass spectrum. In either case, no molecular ions were observed for the N-trifluoroacyl derivatives. A softer ionization mechanism, such as chemical ionization (CI) or fast atom bombardment (FAB) may have given improved results, especially with respect to generating stronger molecular ions. However, these techniques were not available during this study. The use of ammonia reagent gas in desorption CI-MS has been reported to be a useful technique for obtaining strong pseudo molecular ions ($M + NH_4$) in high-molecular-weight compounds containing long chain aliphatic functions[17]. This technique may be successful for MS analysis of the TFAA derivatives.

The TFAA derivatives of EBS and EBO have also been analyzed by GC on a short non-polar stationary phase column (3.5 m, SPB-5) with high carrier gas flow-rate (65 cm/s). This fact alone supports the formation of the N-trifluoroacyl derivative, since EBS and EBO are themselves not sufficiently volatile to undergo GC. While TFAA derivatization of EBS or EBO followed by GC would not be applicable to polymer analysis, it may be an attractive approach for product characterization. The TFAA derivatives are readily formed at room temperature and the GC separation may be fine-tuned to give a distinct "finger print" of the final product distribution. An important consideration in the GC technique is the removal of excess TFAA and trifluoroacetic acid by evaporation or neutralization prior to GC analysis. Residual acid and anhydride are highly corrosive and may damage stainless steel surfaces on the GC injector and detector, and may also depolymerize the stationary phase.

ACKNOWLEDGEMENTS

The authors wish to thank Bucknell University for the use of their MS facilities and Peter Findise for his expert assistance with MS studies.

REFERENCES

1 W. J. A. VandenHeuvel, W. L. Gardner and E. C. Horning, *Anal. Chem.*, 36 (1964) 1550.
2 W. J. Irvine and M. J. Saxby, *J. Chromatogr.*, 70 (1972) 141.
3 R. A. Morrisette and W. E. Link, *J. Gas Chromatogr.*, 3 (1965) 67.
4 M. Hasegawa and I. Matsubara, *Anal. Chem.*, 63 (1975) 308.
5 G. P. Slater, *J. Chromatogr.*, 64 (1972) 166.
6 H. S. Schuttenberg and R. C. R. C. Schultz, *Angew. Chem., Int. Ed. Engl.*, 15 (1976) 777.
7 D. R. Knapp, *Analytical Derivatization Reactions*, Wiley-Interscience, New York, 1979, p. 687.
8 W. J. A. VandenHeuvel, J. Sjövall and E. C. Horning, *Biochim. Biophys. Acta*, 48 (1961) 596.
9 E. Jacobi, H. Schutlenberg and Schultz, *Makromol. Chem.*, 1 (1980) 397.
10 K. Weisskopf, *Polymer*, 24 (1983) 72.
11 K. Weisskopf, *Polymer*, 26 (1985) 1187.
12 E. Bragini, E. Gattiglia, E. Pedemonte and S. Russo, *Makromol. Chem.*, 184 (1983) 1213.
13 L. L. Blyler, Jr., *Soc. Plast. Eng. (Tech. Pap.)*, 20 (1974) 33.
14 T. E. Breuer, N. B. Martin and H. Tomilson, *ANTEC Conference Proceedings, Washington, DC, April 29–May 2, 1985.*
15 D. H. Edwards, *J. High Resolut. Chromatogr. Chromatogr. Commun.*, 5 (1982) 161.
16 G. diPasquale, L. Giambelli, A. Suffientini and R. Paiella, *J. High Resolut. Chromatogr. Chromatogr. Commun.*, 8 (1985) 618.
17 P. A. Metz, D. R. Omstead, L. Kaplan, J. A. Liesch, R. A. Stearns and W. J. A. VandenHeuvel, *J. Chromatogr.*, 441 (1988) 31.

Journal of Chromatography, 479 (1989) 117–124
Elsevier Science Publishers B.V., Amsterdam — Printed in The Netherlands

CHROM. 21 659

SELECTIVE DETERMINATION OF BENZO[*a*]PYRENE IN PETROLEUM-BASED PRODUCTS USING MULTI-COLUMN LIQUID CHROMATOGRAPHY

P. R. FIELDEN* and A. J. PACKHAM
Department of Instrumentation and Analytical Science, U.M.I.S.T., P.O. Box 88, Manchester M60 1QD (U.K.)

(First received April 24th, 1989; revised manuscript received June 5th, 1989)

SUMMARY

A method is presented to enable the rapid on-line determination of benzo[*a*]-pyrene in petroleum-based products such as diesel oil and aviation fuel. A column-switching technique is employed to achieve the necessary resolution due to the complex sample matrix. Fluorescence detection is employed to further increase the selectivity towards the polynuclear aromatic hydrocarbons. A cyclodextrin bonded phase column was used to give the initial fractionation. The fraction of interest was then heart cut onto a reversed-phase C_{18} analytical column and separated using gradient elution. This technique removes, with the exception of dilution and filtration, any necessary pre-analytical step.

INTRODUCTION

Polynuclear aromatic hydrocarbons (PAHs) are common environmental pollutants derived from both natural and man-made combustion of a variety of carbon based materials. The carcinogenic nature of some of the group members, notably benzo[*a*]pyrene, has been well documented[1,2] as have both selective and general analytical techniques[2,3]. The determination of these compounds in petroleum products, and especially diesel oils, causes significant analytical problems due to the complex nature of the matrix. Diesel oil is a complex mixture of hydrocarbons with a boiling range of between 180 and 360°C. Between 15 and 30% has an aromatic nature, while the remainder is essentially aliphatic[4].

Multi-column techniques have been used to overcome the non-availability of highly efficient columns capable of resolving petroleum products. However, to achieve a final fraction of suitable complexity, incompatible techniques such as normal- and reversed-phase or size-exclusion and reversed-phase chromatography need to be used. The solvent-exchange procedures that are therefore necessary are complex and result in long analysis times and analyte loss or degradation. Sonnefeld *et al.*[5] have reported an on-line normal-/reversed-phase technique using a gas-dried intermediary diamine exchange column. May and Wise[6] have proposed a similar technique.

0021-9673/89/$03.50

although the solvent exchange was achieved using off-line solvent evaporation. The unique selectivity of the cyclodextrin bonded phases has been used to resolve the solvent incompatibility problem. The chromatographic technique involves fractionating an oil sample on a γ-cyclodextrin column. The fraction obtained from this column that contains benzo[*a*]pyrene is then passed directly to the head of a C_{18} column rather than to the detector. The fraction can then be eluted from this column and the analyte determined at a later time.

The cyclodextrins are torus-shaped polymers consisting of α-1,4 D-glucoside oligosaccharides. The external surface is ringed by hydroxyl groups giving a hydrophilic environment. The internal environment is hydrophobic and responsible for the selective nature of the column by the formation of inclusion complexes with molecules of the correct size and charge distribution[7]. Three cyclodextrins have been successfully bound to a 5-μm spherical silica base. These have been named α-, β- and γ-cyclodextrins and consist of six, seven and eight glucose monomers, respectively. The internal diameters are 0.57, 0.78 and 0.95 nm, respectively, and in all three cases the torus is about 0.78 nm deep[8]. The size of benzo[*a*]pyrene, across the wide axis, is approximately 0.88 nm suggesting that only the β- and γ-cyclodextrins will be able to form inclusion complexes. This has been confirmed[8] and benzo[*a*]pyrene has been shown to form a 2:1 analyte–cavity complex. In a recent study by Olsson *et al.*[9] the retention of a range of PAHs by monomeric and polymeric C_{18} bonded phases and by the β-cyclodextrin bonded phase were compared. While the resolving power of the cyclodextrin phase was not found to be as high as that of conventional reversed-phases, the authors did suggest that the cyclodextrin-bonded phases may offer significant advantages where the separation of PAHs of different molecular weights is required. In this study only the γ-cyclodextrin bonded phase was used.

The cyclodextrins are a relatively new group of bonded phases and have been used successfully for the separation of a number of chiral compounds such as benzo[*a*]- and benzo[*e*]pyrene, dansyl D- and L-leucine[7], and *ortho; para-* and *meta*-nitroanilines[7]. β- and γ-bonded phases have been used by Armstrong *et al.*[11] to resolve mixtures of PAHs. These separations have been achieved due to the ability of the phase to form an inclusion complex. The stability of the complex depends on the charge distribution, and the shape and size of the molecule forming the complex. There must be a hydrophobic region within the molecule that is the correct size to enter the cavity; the complex stability may be enhanced by the presence of external polar groups that are able to interact with the secondary hydroxyls. If the analyte is too large it will be unable to enter the cavity and no inclusion-derived retention will occur, although retention may still be observed due to an ionic interaction mechanism. In this mode the column acts as a high-density diol column. If the analyte is too small it will enter the cavity, but the stability of the complex is poor and the retention will be low. It is also possible to use non-polar solvents such as hexane with these phases; in this case no inclusion occurs and retention is due purely to external adsorption.

EXPERIMENTAL

Materials

Benzo[*a*]pyrene was obtained from BDH (Poole, U.K.). Chromatographic solvents were also obtained from BDH and were of HiPerSolv grade. The water used in

this study was distilled and stored in glass without further purification. The γ-cyclodextrin column (250 × 4.6 mm I.D.) was packed by Astec (U.S.A.) and supplied through Technicol (Stockport, U.K.). The Vydac C_{18} 201TP54 (250 × 4.6 mm I.D.) column was also obtained from Technicol. Standard benzo[*a*]pyrene solutions were made up in acetonitrile and stored in the dark to avoid photo-induced degradation. The oil samples were obtained from commercial sources.

Equipment

Chromatography was carried out using the following equipment. A Waters Series 6000 high-performance liquid chromatography (HPLC) pump was used, the mobile phase being generated by a modified Micrometeritic gradient former. All solvents were filtered through a 2-μm Millipore filter under negative pressure and continuously degassed with helium. A Rheodyne Model 7125 syringe loading injection valve with a 20-μl sample loop was used to introduce the sample. A Perkin-Elmer series 3000 fluorescence detector was used to monitor the eluent.

The excitation and emission wavelengths were 254 nm and 420 nm, respectively. Excitation and emission slits were set at 5 nm. A Hewlett-Packard 3390A integrator was used to determine the retention times and a Goerz BBC SE 120 chart recorder was used to record the chromatograms. A schematic diagram of the column arrangement is given in Fig. 1. Column selection was achieved using two Rheodyne Model 7000 column-selection valves. These valves were actuated manually.

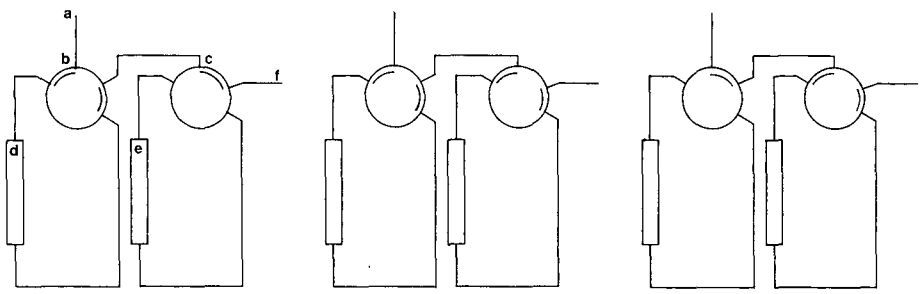

Fig. 1. Schematic of the column arrangement used in this study. Valve positions correspond to the following operations: (left): fractionation; (middle): heart cut; (right): analysis. a = Inlet from pump and sample introduction valve; b = switching valve 1, column 1 bypass; c = switching valve 2, heart cut and column 2 bypass; d = column 1, γ-cyclodextrin fractionation column; e = column 2, Vydac C_{18} analytical column; f = outlet to detector and to waste.

Chromatographic technique

Cyclodextrin fractionation column. The oil sample was fractionated, after filtration, using a cyclodextrin pre-column with an acetonitrile – water (40:60) isocratic mobile phase. The timing for the heart cut was determined by the use of a benzo[*a*]pyrene standard. The retention time was determined to be just over 4 min and did not alter significantly during this study. After the heart cut had been taken the column was cleaned using 100% acetonitrile until the baseline was re-established, as viewed on the fluorescence detector. When not in use the column was cleaned with 100% methanol and stored with this solvent.

Heart cut analysis. The heart cut was analysed on the 25-cm Vydac C_{18} column using a 40-min linear gradient from 30 to 100% aqueous acetonitrile at 1 ml min^{-1}. The valve timings, for a sample of low to medium complexity (*e.g.*, aviation fuel) are outlined in Table I.

The analytical column was equilibrated at an acetonitrile concentration 10% below that of the fractionation column, to ensure that the heart cut remained as a small plug on the head of the analytical column in order to minimize peak dispersion.

TABLE I

OUTLINE OF THE SWITCHING VALVE ACTUATION TIMINGS USED FOR AN AVIATION FUEL SAMPLE

Time (min:s)	*Action*
0:00	Column 1 in line Inject sample, start data collection
3:45	Valve 2 to position B Column 1 and 2 in line
4:30	Valve 2 to position A Column 1 in line Clean and re-equilibrate column
30:00	Valve 1 to position B Valve 2 to position B Column 2 in line Start gradient
80:00	Reset gradient
90:00	Valve 2 position A Valve 1 position A

RESULTS AND DISCUSSION

The γ-cyclodextrin column produced a suitable fraction to allow the rapid on-line determination of benzo[*a*]pyrene in petroleum samples covering a wide range of complexities. The detection limit for this technique, determined as three times the detector noise, was 0.1 ng benzo[*a*]pyrene per injection; this is equivalent to 5 ng ml^{-1}. The recovery for a 40-ng ml^{-1} benzo[*a*]pyrene standard was 98.9% using a 45-s heart cut centered on the analyte retention time. The analysis time for a light oil such as aviation fuel, including re-equilibration times was under 90 min; for a more complex sample the analysis time increases to a maximum of 120 min. If a dual pump system were used the analysis time can be reduced to under 60 min for all types of sample. This reduction may be achieved by using parallel re-equilibration and analysis. If multiple heart cuts are made, and a small, high-carbon-loaded column is used as an intermediary exchange column, a number of different PAHs may be analysed.

Fig. 2 shows a chromatogram obtained from the cyclodextrin fractionation column. The heart cut (labelled ✳) can clearly be seen in this chromatogram as a

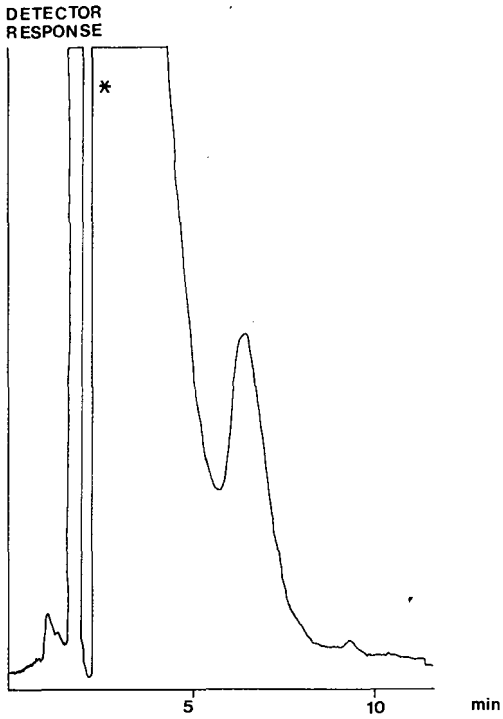

Fig. 2. Chromatogram showing a 45-s heart cut (marked *) taken from a sample of aviation fuel fractioned on a γ-cyclodextrin column. The mobile phase was acetonitrile – water (40:60), flow-rate 1 ml min^{-1}.

vacancy in the detector signal output, the rapid drop in fluorescence is due to solvent eluting from the bottom of the C_{18} column. The length of the heart cut influences the sensitivity of the analysis. A reduced heart-cut time will decrease the amount of benzo[*a*]pyrene that can be transferred to the second column but also decreases the amount of interfering substances present in the fraction. The timing and length of the heart cut was not optimized in this study, however, it would be expected that optimization of this parameter would result in a reduced minimum level of detection. This reduction could also be achieved using further fractionation columns especially when highly complex samples are to be analysed. The time of the heart cut is limited by the necessity to introduce the sample as a small plug on the head of the second column. Failure to do this leads to poor sample resolution when the final analysis is carried out. The mobile phase used to elute the benzo[*a*]pyrene fraction from the cyclodextrin column was acetonitrile–water (40:60). At this acetonitrile concentration, the organic modifier enters the cyclodextrin cavity in preference to the analyte. This has the effect of reducing inclusion formation for benzo[*a*]pyrene to a minimum and allowing it to elute in less than 4.5 min. The vast majority of interfering components are more strongly retained on the column by a mechanism, that is as yet, not fully understood. The use of lower acetonitrile concentrations would cause strong retention of benzo[*a*]pyrene and probably produce a fraction of similar complexity. However, this

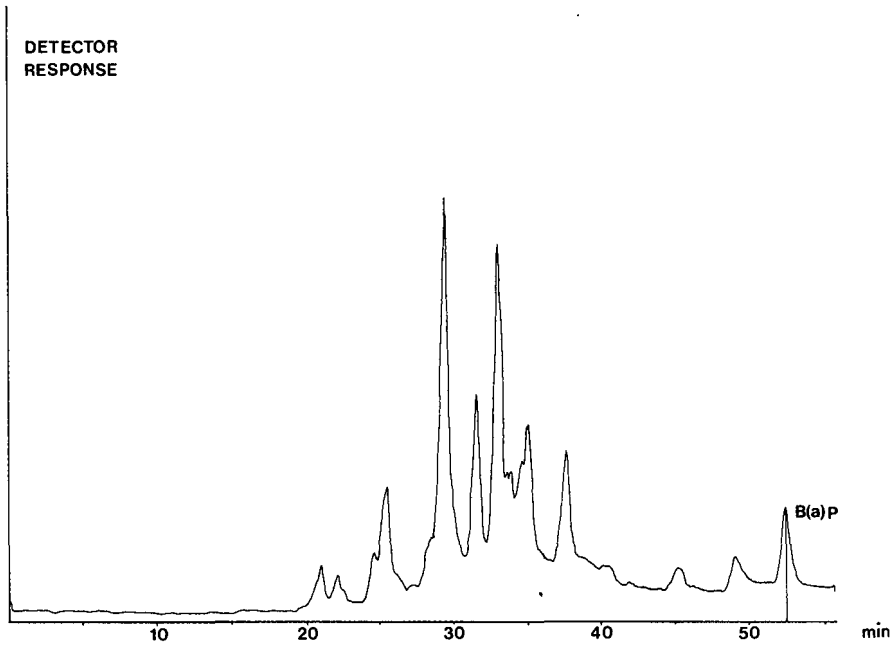

Fig. 3. Chromatogram of the benzo[*a*]pyrene [B(a)P] containing heart cut obtained from a sample of aviation fuel. The sample was spiked with 8 ng of benzo[*a*]pyrene, the analyte is labelled. The chromatographic conditions are outlined in the Experimental section.

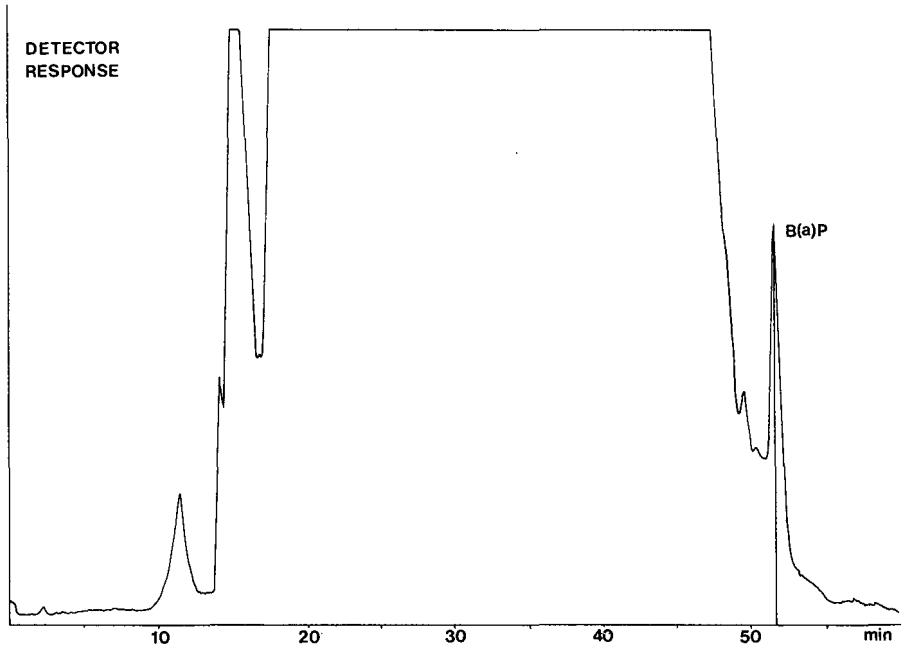

Fig. 4. Chromatogram of the benzo[*a*]pyrene containing heart-cut obtained from a sample of heavy diesel oil. The benzo[*a*]pyrene is labelled. The chromatographic conditions are outlined in the Experimental section.

would lengthen the analysis time and as the efficiency of these columns is relatively low, the heart-cut time would have to be increased significantly to maintain the high recovery. The long heart cut time, in addition to the lower acetonitrile concentrations, would mean that the sample would not be introduced as a small plug on the head of the second column and so the final resolution would be decreased.

Fig. 3 shows the final analytical chromatogram of an aviation fuel spiked with benzo[*a*]pyrene, so that the final injection contained 8 ng of the analyte. The analyte peak is baseline resolved from all interfering components suggesting that there has been a high degree of fractionation in the cyclodextrin column. This high degree of resolution allows very low levels of benzo[*a*]pyrene to be assayed.

Fig. 4 shows the final chromatogram of a heavy diesel oil. Although the benzo[*a*]pyrene has not been fully resolved, due to the far higher sample complexity, it is clearly visible and quantitation may be carried out precisely. The resolution of this sample may be improved by the incorporation of a further fractionation stage to reduce the fraction complexity without adversely affecting the recovery of benzo[*a*]-pyrene.

The method described in this paper can be used to give both quantitative and qualitative information about the amount of benzo[*a*]pyrene in various petroleum products. Significant advantages over off-line and other on-line techniques are achieved. In particular the system increases operator safety due to the reduced environment contamination and sample handling, and sample loss due to the reduced possible adsorption or volatization of the sample. The removal of any pre-analysis step, such as solid phase or solvent–solvent extraction significantly reduces the analysis time and analyst hours required for the determination. The sensivity is high due to the resolution of the sample and the almost complete transfer of the benzo[*a*]pyrene in the fraction to the analytical column. This highlights the advantages that multi-column techniques have over conventional methods. The selectivity towards the chosen analyte is high while the time spent resolving it from interferences is reduced. The limitation of this method lies in its cost and complexity, although this must be offset against the reduced analysis time and increased operator safety.

ACKNOWLEDGEMENTS

A. J. P. is in receipt of a Science and Engineering Research Council CASE award, co-sponsored by Esso Petroleum Company Ltd. (Esso Research Centre, Abingdon, U.K.). We are also indebted to Technicol for the supply of columns used in this study.

REFERENCES

1 D. Hoffman and C. E. Wynder, *Chemical Carcinogens, ACS Monograph Series No. 173*, American Chemical Society, Washington, DC, 1976.
2 R. D. Harvey (Editor), *Polycyclic Aromatic Hydrocarbons and Carcinogenesis, ACS Monograph Series No. 283*, American Chemical Society, Washington, DC, 1985.
3 M. L. Lee, M. V. Novotny and K. D. Bartle, *Analytical Chemistry of Polycyclic Aromatic Compounds*, Academic Press, New York, 1981.
4 D. J. Cookson, C. J. Rix, I. M. Show and B. E. Smith, *J. Chromatogr.*, 312 (1984) 237.
5 W. J. Sonnefeld, W. H. Zoller, W. E. May and S. A. Wise, *Anal. Chem.*, 54 (1982) 723.

6 W. E. May and S. A. Wise, *Anal. Chem.*, 56 (1984) 225.
7 *Cyclobond Handbook*, Advanced Separation Technologies, Whippany, NJ.
8 R. Woodberry, S. Ransom and C. Fu-Ming, *Anal. Chem.*, 60 (1988) 2621.
9 M. Olsson, L. C. Sander and S. A. Wise, *J. Chromatogr.*, 477 (1989) 277.
10 D. W. Armstrong, D. Wade, A. Alak, W. L. Hinze, T. E. Riehl and K. H. Bui, *Anal. Chem.*, 57 (1985) 234.
11 D. W. Armstrong, A. Alak, D. Wade, W. L. Hinze and T. E. Riehl, *J. Liq. Chromatogr.*, 8 (1985) 261.

Journal of Chromatography, 479 (1989) 125–133
Elsevier Science Publishers B.V., Amsterdam — Printed in The Netherlands

CHROM. 21 663

CHROMATOGRAPHIC DETERMINATION OF AMINES IN BIOLOGICAL FLUIDS WITH SPECIAL REFERENCE TO THE BIOLOGICAL MONITORING OF ISOCYANATES AND AMINES

I. DETERMINATION OF 1,6-HEXAMETHYLENEDIAMINE USING GLASS CAPILLARY GAS CHROMATOGRAPHY AND THERMIONIC SPECIFIC DETECTION

G. SKARPING*, M. DALENE, T. BRORSON, J. F. SANDSTRÖM, C. SANGÖ and A. TILJANDER
Department of Occupational and Environmental Medicine, University Hospital, S-221 85 Lund (Sweden)
(First received March 21st, 1989; revised manuscript received June 2nd, 1989)

SUMMARY

A capillary gas chromatographic method with thermionic specific detection was developed for the analysis of 1,6-hexamethylenediamine (HDA) (*C.A.* No. 124-09-4) in aqueous solution, human urine and plasma. The method is based on a derivatization procedure with ethyl chloroformate (*C.A.* No. 541-41-3) in a two-phase system, where HDA-diurethane is formed. The overall recovery was found to be 95 ± 5% for a concentration of 100 μg HDA/l of urine, 98 ± 5% for 1000 μg/l. In plasma the recovery was 106 ± 4% for 500 μg/l. The minimum detectable concentration in plasma and urine was found to be less than 10 μg/l. The use of heptafluorobutyric anhydride as a derivatization reagent is also discussed.

INTRODUCTION

Aliphatic diamines are industrially used as chelating agents and chemical reagents. 1,6-Hexamethylenediamine (HDA) is used for the manufacture of urethane coatings and of polyamides, *e.g.* Nylon-66, also in paints and as a curing agent for epoxy resins. HDA is moderately toxic[1–3], and has been associated with health hazards in the work environment[4,5].

Analogous endogenous diamines, *e.g.*, putrescine (1,4-diaminobutane) and cadaverine (1,5- diaminopentane), are known to have important roles in cell growth and differentiation. HDA has been identified in humans, as one in a series of metabolites of the cell-differentiating agent hexamethylenebisacetamide (HMBA)[6–9]. Rosenberg and Savolainen[10] have proposed that analysis of HDA in urine may be used as a test for occupational exposure to 1,6-hexamethylenediisocyanate (HDI).

The occurrence of diamines in working atmospheres, and the biochemical interest in di- and polyamines, has necessitated development of a series of analytical methods, including high-performance liquid chromatography (HPLC)[11–14], gas

0021-9673/89/$03.50

chromatography (GC)[15], ion-exchange and ion-pair chromatography[16,17] and thin-layer chromatography[18]. Monitoring of HDI in air using impinger flasks containing acidic aqueous solutions, where HDA is formed, was described by Dalene[15]. The amine was derivatized to the corresponding amide by reaction with a perfluoro fatty acid anhydride. Capillary GC with electron-capture (ECD) and thermionic specific detection (TSD) was used for quantitation.

A possibility for biological monitoring of exposure to HDI and HDA would be valuable, and the aim of this study was to develop an highly sensitive analytical method for the determination of HDA in biological fluids.

EXPERIMENTAL

Apparatus

A Varian 3500 gas chromatograph equipped with a Varian thermionic specific detector and a Varian 8035 automatic on-column injector was employed. The injector was cooled with liquid nitrogen. The injector starting temperature was 105°C for 5 s, and thereafter the temperature was increased with 150°C/min to a final temperature of 280°C, where it was kept for 7 min. Column parameters as in Fig. 2.

A Varian 3700 gas chromatograph equipped with a Varian thermionic specific detector and a Grob-type cold on-column injector with a water cooling system, designed and manufactured at our laboratories, was also used. Typical settings for the detector were: bead heating current, 3.10 A; bias voltage, − 3.9 V, detector temperature, 270°C; gas flow-rates; 3 ml/min of hydrogen, 175 ml/min of air and 20 ml/min of nitrogen as the make-up gas.

A Shimadzu GC–MS QP1000 EI/CI quadrupole mass spectrometer connected to a Shimadzu GC 9A gas chromatograph was used.

Chromatograms were recorded on Servogor Model 310 linear recorders, and Shimadzu C-R3A integrators were used for peak evaluation. An Heidolph VV 2001 Rota-vapor, rotating evaporator (Heidolph Elektro, Kelheim, F.R.G.) connected to an aspiration pump was used for evaporation, and a Sigma 3E-1 centrifuge (Sigma, Harz, F.R.G.) was employed for phase separation.

A Reacti-Vap™ Evaporator (Pierce) was used for evaporation of toluene sample solutions containing the carbamate derivative of HDA.

For enrichment and evaporation of solvent containing heptafluorobutyric anhydride (HFBA) derivatives, a vacuum desiccator connected to an aspirating pump was used. The apparatus was supplied with an electrically heated oven, designed and manufactured at our laboratory.

Columns

Fused-silica capillary columns with chemically bonded stationary phases, CP-Sil® 8 CB (Chrompack, Middelburg, The Netherlands), 12 m × 0.32 mm I.D., with a film thickness of 0.2 μm, and DB-5 (J & W Scientific, Folsom, CA, U.S.A.), 30 m × 0.24 mm I.D., with a film thickness of 0.5 μm were used.

Chemicals

Chemicals used were HDA, ethyl chloroformate, isobutyl chloroformate and toluene from Janssen (Beerse, Belgium). Trifluoroacetic anhydride (TFAA), penta-

fluoropropionic anhydride (PFPA) and heptafluorobutyric anhydride (HFBA) were from Pierce (Rockford, IL, U.S.A.), di-*n*-butylamine (DBA) and 1,4-butanediamine (BDA) from Fluka (Buchs, Switzerland), HCl, NaOH, NH_3 and K_2HPO_4 from Merck (Darmstadt, F.R.G.).

Standards

Synthesis of 1,6-hexamethylenediurethane and 1,4-butanediurethane. To 250 ml of a solution of toluene containing *ca.* 5 g of HDA or BDA were added 25 ml of 30% (w/w) ammonia and 5 g of sodium hydroxide dissolved in 250 ml of distilled water. Ethyl chloroformate (20 ml) was added dropwise with stirring, and the mixture was stirred for 10 min. The organic layer was separated and shaken four times with 200-ml portions of 0.1 *M* HCl, to remove unreacted amine and partially reacted amino-urethane. The toluene solution was then washed four times with 200-ml portions of water, and evaporated to dryness to remove the remaining ethyl chloroformate reagent. After recrystallization from ethyl acetate the derivatives were stored in an desiccator.

Standards and internal standards were identified by GC–mass spectrometry (MS), and the purity was tested using TSD and flame ionization detection (FID). The purity was also examined by elemental analysis, and was found to be better than 99%.

Synthesis of the isobutyl chloroformate derivative of DBA. To 250 ml of a toluene solution containing *ca.* 5 g of DBA, 25 ml of 30% (w/w) ammonia and 5 g of sodium hydroxide, dissolved in 250 ml of distilled water, were added. Isobutyl chloroformate was added dropwise to the solution with continuous stirring, and the mixture was stirred for 10 min. The organic layer was separated and shaken four times with 200-ml portions of 0.1 *M* HCl to remove unreacted amine. The toluene solution was then washed four times with 200-ml portions of water, and evaporated to dryness to remove the remaining ethyl chloroformate reagent. The residue was redissolved in ethyl acetate and eluted through a silica column (60 mm × 20 mm I.D.). The recrystallization from ethyl acetate was performed at −10°C.

Synthesis of 1,6-hexamethylenebisheptafluorobutyramide. After recrystallization of HDA from toluene, 0.2 g (1.6 mmol) of the amine and 1.6 g (4 mmol) of HFBA were dissolved in ethyl acetate, and the solution was heated to 150°C for 10 min. After cooling to room temperature, the excess of reagent and liberated acids were extracted with a 1 *M* phosphate buffer solution pH 7.0. The organic phase was eluted through a silica column (60 mm × 20 mm I.D.) with ethyl acetate, followed by evaporation of the ethyl acetate solution to dryness; *ca.* 500 mg (80%) of the amine were obtained.

Procedure

Preparation of standard solutions. Standard solutions of the derivatives of HDA were prepared by dissolving accurately weighed amounts of each derivative (*ca.* 60 mg/100 ml) in toluene. The solutions were then further diluted in toluene to appropriate concentrations. Standard solutions of HDA were prepared in acidic-aqueous solutions.

Sampling and storing of urine samples. Urine samples were acidified by the addition of 5 ml of aqueous 6 *M* HCl solution per *ca.* 100 ml of urine. The urine samples were stored in a refrigerator.

Work-up procedure

With chloroformates as the derivatization agents. A 2-ml urine or plasma sample was added to 3 ml of 6 *M* HCl. The mixture was heated at 100°C overnigh (hydrolysis). A 2-ml aliquot was transferred to a test-tube where 1 ml of 3% (w/w) aqueous NH_3, 3 ml of 5 *M* NaOH and 2 ml of toluene were added. The mixture was shaken and 100 μl of ethylchloroformate were added. The mixture was then shaken for 15 min at room temperature. A 1-ml aliquot of the toluene layer was evaporated to dryness by using a flow of nitrogen (30°C). A 1-ml volume of a toluene solution, containing an internal standard comprising the isobutyl chloroformate derivative of di-*n*-butylamine at the appropriate concentration, was added to the dry residue. The toluene layer was analysed by GC. The same procedure was used for aqueous samples where the hydrolysis step can be eliminated.

With anhydrides as the derivatization agents. A 2-ml urine sample was added to 3 ml of 6 *M* HCl. The mixture was heated at 100°C overnight. A 2-ml aliquot was transferred to a test-tube where 4 ml saturated NaOH and 3 ml toluene were added. The mixture was shaken for 5 min at room temperature. A 2-ml volume of the organic layer was transferred to a new 10-ml test-tube where 20 μl of HFBA were added. The solution was immediately shaken vigorously for 5 min on a Vortex mixer. The excess of HFBA and the acid formed were removed by shaking with 2 ml of 1 *M* phosphate buffer solution (pH 7.5). The toluene layer containing the amide formed was then transferred to a new test-tube, ready for injection on the chromatographic system. The same procedure was used for aqueous samples where the hydrolysis step can be eliminated.

Internal standard. The internal standards used were 1,4-butane diurethane, the isobutyl chloroformate derivative of di-*n*-butylamine (1 ng/μl) and the HFBA derivative of 1,4-butanediamine (1 ng/μl). A solution of toluene containing the internal standard was added to the dry residue from the work-up procedure before the GC analysis.

RESULTS AND DISCUSSION

Storage and treatment of samples

HDA-spiked urine samples were found to be stable after the acidification. No noticeable change in sample composition occurred even after storage in darkness at room temperature for several weeks.

The mixture was heated at 100°C overnight in order to hydrolyse the sample; a shorter time of hydrolysis was shown to result in lower recovery of HDA. However urinary elimination of compounds originating from exposure to HDI or HDA will rise a mixture of several metabolites and conjugates, of which free HDA probably consitutes a minor portion. The hydrolysis reaction obviously influences the possibility of separately determining these compounds, and consequently the method described only gives the sum of free HDA and hydrolysable HDA conjugates. Sample clean-up using a silica gel cartridge has been described as efficient[10]. However, our attempts to perform this and other similar procedures were unsuccessful due to severe losses (*ca.* 50%).

Work-up procedure

Chloroformates as reagents. Parameters for the derivatization of amines have

been studied in some detail[19]. In general, the derivatization reaction in a two-phase system, with an appropriate pH in the aqueous phase, will be faster than that in a single-phase system. The choice of pH depends on the basicity of the amine considered. For the reaction to occur at a reasonable rate at room temperature unprotonated amines must be present. For the two-phase derivatization of piperazine[19] (pK_a = 9.8) we found that with a phosphate buffer solution (pH 10) the reaction is quantitative in less than 5 min, with ammonia as a catalyst. However, this procedure gave unsatisfactory results for the very basic diamine HDA (pK_a = 11.9), whereas the reaction is quantitative only at pH > 12. The recovery for two-phase derivatization of HDA in urine (*ca.* 2 ng/μl) is quantitative, for ammonia concentrations higher than 1% (w/w) (Fig. 1). We found that the use of 3% ammonia is suitable, since the ammonia concentration in water solutions tend to decrease during storage. The amount of ethyl chloroformate added is not critical when using ammonia. The plot of the amount of ethyl chloroformate added *versus* recovery in Fig. 1 is virtually horizontal in the range 10–150 μl. It was also observed, for the system without ammonia, that the recovery decreased when the amount of ethyl chloroformate added was increased.

It should also be noted that the consumption of the reagent due to hydrolysis in the standard procedure is not critical if the reagent is added directly to the two phase system. This was established by adding the HDA-containing urine hydrolysate to the two-phase reaction mixture at different times. The same quantitative results were found for 0–1 min, whereafter the recovery decreased, and after 3 min only *ca.* 50% recovery was obtained. Injection of chloroformate reagents influences the detector sensitivity as described previously[19]. The evaporation step is essential to remove excess of reagent. The procedure is time consuming, when a Rota-vapor is used, as only a single sample can be evaporated. Evaporation by a flow of nitrogen simplifies routine analyses as nine samples can be treated simultaneously.

Anhydrides as reagents. The two-phase derivatization of aromatic diamines was recently studied[20]. However the two-phase derivatization procedure was originally

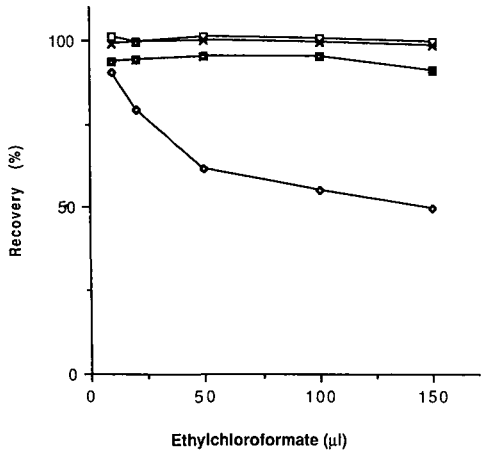

Fig. 1. The recovery of HDA-diurethane with variable amounts of the derivatization reagent (ethyl chloroformate) and different concentrations of ammonia: 0.0 (◇), 0.5 (■), 1.0 (□) and 5.0% (×).

developed for aqueous solutions, and has not yet successfully been used for urine samples containing aliphatic diamines. For urine samples the recoveries were low (less than 50%), and varied greatly, giving poor reproducibility. The derivatization procedure was therefore performed in toluene after extraction of aqueous urine hydrolysates.

The excess of reagent was efficiently removed from the organic phase by extraction with a 1 *M* phosphate buffer (pH 7.5) solution. For urine samples, using GC–TSD, the chromatograms of the derivatives showed a more complex picture compared to the corresponding chloroformate derivatives. Further work-up by liquid extraction, membrane extraction or by the use of extraction columns may be necessary.

Chromatography

The chromatographic behaviour of both the urethane and amide derivatives is excellent. The use of an apolar stationary phase with relatively low film thickness is

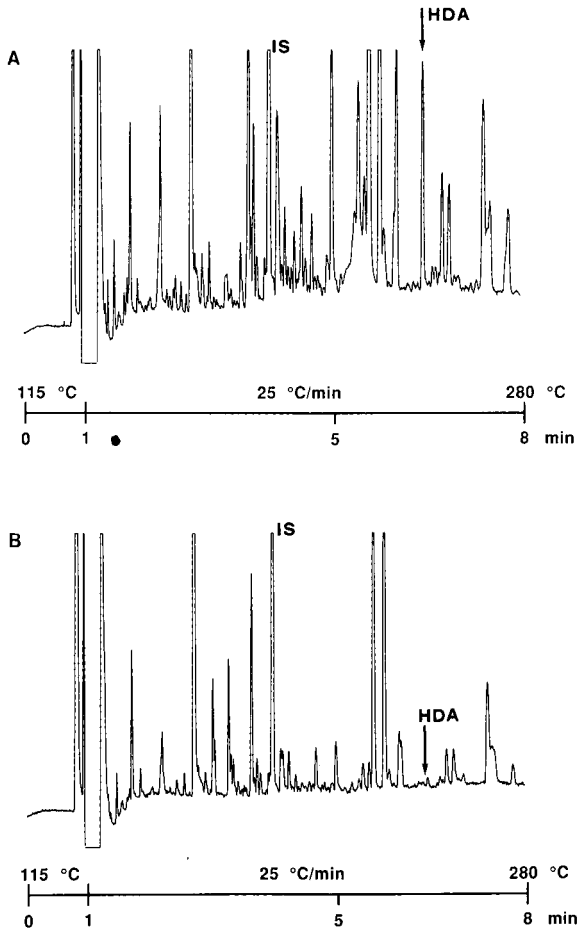

Fig. 2.

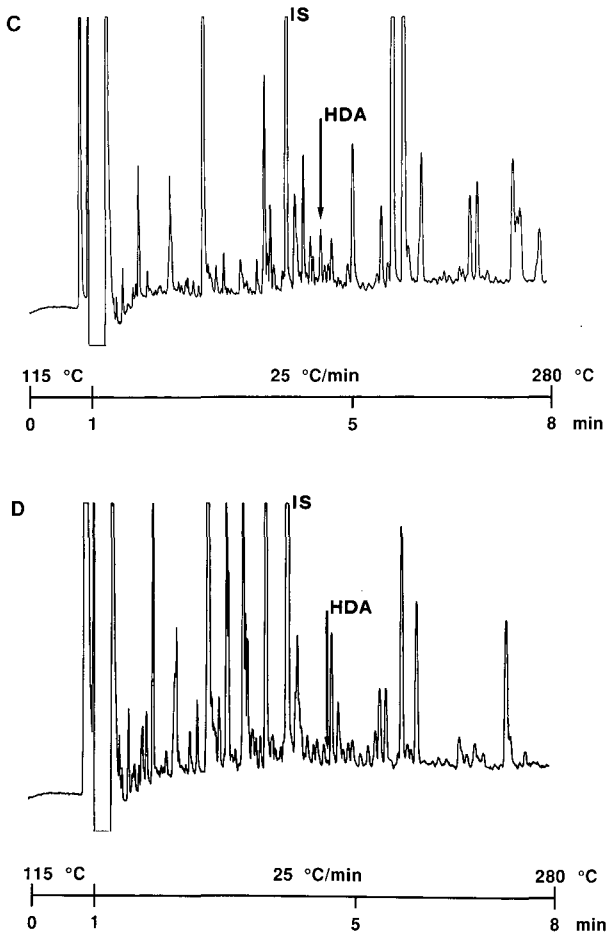

Fig. 2. Chromatograms of HDA at *ca.* 200 μg/l in hydrolysed urine treated with ethyl chloroformate (A) and HFBA (C) using TSD. Corresponding blank traces were for ethyl chloroformate (B) and for HFBA in urine (D). All chromatograms were performed using GC–TSD with on-column injection of 1 μl toluene solution. Internal standard (IS): the isobutyl chloroformate derivative of di-*n*-butylamine at 1 ng/μl. Capillary column: J&W fused silica coated with DB-5 bonded stationary phase (30 m × 0.24 mm I.D.), film thickness 0.5 μm. Temperature programming as shown. Carrier gas (helium) at 2.3 kg/cm^2. Thermionic specific detector: bead heating current, 3 A; bias voltage, −3.5 V; temperature 280°C. Flow-rates: hydrogen, 4; air,180; make-up (helium), 10 ml/min.

preferred, due to the fact the HDA-diurethane can decompose to HDI at elevated temperatures. Analysis of the HDA-diurethane by GC–MS showed that this compound actually decomposed into HDI. The HDI appeared as a tailing peak earlier in the chromatogram, and increased with increasing elution temperature. Due to the decomposition at elevated temperatures, higher film thicknesses should be avoided, and when using film thicknesses less than 0.8 μm no problems occurred. Chromatograms of urine samples, originating from an human oral administration of HDA, are

shown in Fig. 2, and for urine matrixes it is evident that the chloroformate procedure is a better choice than the anhydride procedure. No interfering peaks disturb the evaluation of the chromatogram.

Quantitative analysis

Recovery. The recovery was studied by spiking aqueous solutions, hydrolysed human urine and blood plasma, and performing the derivatization procedures as described above. Peak heights were compared to those of standards by using GC–TSD. With ethyl chloroformate as the reagent, the recovery for human urine was 95 ± 5% ($n=7$) for a concentration of 100 μg of HDA per litre and 98 ± 5% ($n=7$) for 1000 μg/l and for plasma 106 ± 4% ($n=6$) for 500 μg/l at a 95% degree of confidence.

Calibration graphs. Fig. 3 shows the calibration graph for HDA derivatives of ethyl chloroformate obtained by GC–TSD. Different amounts of HDA were added to urine and the work-up procedure was as described above. For each HDA concentration, two determinations with duplicate injections were made. No significant difference between plotted peak heights or peak area ratios, relative to the internal standard, was observed. The concentration range investigated, 10–350 μg/l urine, gave a correlation coefficient of 0.9998 for a plot of the area ratio for six concentrations. No noticeable differences were found between aqueous solutions and human urine.

Precision. When analysing substances present in complicated matrices such as urine and plasma, the addition of an internal standard to the sample before the analysis is strongly recommended. In this study, the internal standard chosen behaves similarly to the HDA derivatives in the chromatographic system. The overall precision, using the ethyl chloroformate work-up procedure and the di-*n*-butylamine derivative as the internal standard, was very good. The overall precision with the work-up procedure and GC analysis was about 6% ($n=6$) for 100 μg/l HDA-spiked urine, and 2% ($n=5$) for 1000 μg/l with duplicate samples and injections. The overall precision (R.S.D.) for urine samples was 5% (n = 8) at a concentration of 100 μg/l, and 3% at a concentration of 1000 μg/l.

Detection limit. Using GC–TSD the responses for the derivatives of HDA investigated were in the same range. In acidic aqueous air sampling solutions, where the chromatograms appear to be virtually free from interfering peaks, the detection limits were less than 10 pg injected amount, which corrsponds to a concentration of 10

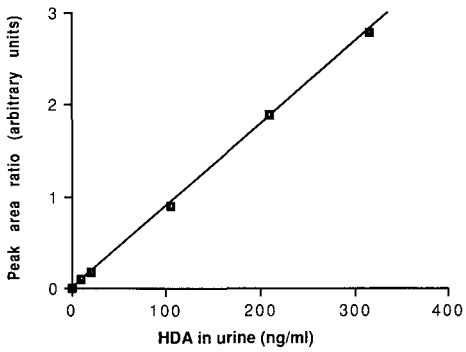

Fig. 3. Calibration graph for HDA in humane urine.

μg/l of sampling solution. The same detection limit was found for the ethyl chloroformate derivative in biological fluids. The detection limit can be further lowered by dissolving the dry residue in a smaller volume, and an enrichment factor of up to 50 is possible. The detection limit for the HFBA derivatization procedure, when used for biological samples such as urine, is considerable higher due to the interfering peaks (Fig. 2).

CONCLULIONS

The chromatographic behaviour of both the urethane and amide derivatives is excellent, and the choice of reagent is principally affected by the matrix and by the detection system used. For urine hydrolysates, the two-phase derivatization with ethyl chloroformate is preferable as the work-up procedure is performed in one step. The method presented offers enhanced possibilities to determine endogenous and exogenous aliphatic diamines at low concentrations (μg/l range) in biological fluids. The method is also applicable to the determination of HDI in air using the impinger technique and an acidic aqueous sampling solution.

ACKNOWLEDGEMENTS

The authors are indebted to Professor Staffan Skerfving, head of the Department of Occupational and Environmental Medicine (University of Lund), for valuable discussions and great interest in this work. We also gratefully acknowledge the skilful technical assistance of Anneli Påmark and the Swedish Work Environment Fund for financial support. We thank Dr. Jan Buijten, Chrompack, for supplying dedicated capillary columns and Dr. Mats Malmberg, Synthelec, Lund, for synthesis of derivatives.

REFERENCES

1 O. L. Dashiell and G. L. Kennedy, *J. Appl. Toxicol.*, 4 (1984) 320.
2 F. R. Johannsen, G. J. Levinskas, R. Ben-Dyke and G. K. Hogan, *Fund. Appl. Toxicol.*, 9 (1987) 504.
3 C. A. Manen, R. D. Hood and J. Farina, *Teratology*, 28 (1983) 237–242.
4 R. R. Beard and J. T. Noe, *Patty's Industrial Hygiene and Toxicology*, Wiley-Interscience, New York, 1981, p. 3135.
5 M. Sittig, *Handbook of Toxic and Hazardous Chemicals and Carcinogens*, Noyes Publications, Park Ridge, NJ, 1985.
6 E. Meilhoc, M-J. Moutin and H. B. Osborne, *Biochem. J.*, 238 (1986) 701.
7 P. S. Callery,M. J. Egorin, L. A. Geelhaar and M. S. B. Nayar, *Cancer Res.*, 46 (1986) 4900.
8 B. A. Conley, P. S. Callery, M. J. Egorin, B. Subramanyam, L. A. Geelhaar and S. Pan, *Proc. Annu. Meeting Am. Assoc. Cancer Res.*, 28 (1987) 311.
9 M. J. Egorin, E. G. Zuhowski, M. S. B. Nayar and P. S. Callery, *J. Chromatogr.*, 415 (1987) 148.
10 C. Rosenberg and H. Savolainen, *Analyst (London)*, 111 (1986) 1069.
11 N. D. Brown, M. P. Strickler and J. M. Whaun, *J. Chromatogr.*, 245 (1982) 101.
12 T. Saaden and T. Greibrokk, *J. Chromatogr.*, 247 (1982) 111.
13 H. M. L. J. Joosten and C. Olieman, *J. Chromatogr.*, 356 (1986) 311.
14 Y. Nishikawa, *J. Chromatogr.*, 392 (1987) 349.
15 M. Dalene, *Doctoral thesis*, Lund University, Lund, 1987.
16 C. W. Gehrke, K. C. Kuo, R. L. Ellis and T. P. Waalkes, *J. Chromatogr.*, 143 (1977) 345.
17 N. Sayem-el-Daher, R. E. Simard, L. L'Heureux and A. G. Roberge, *J. Chromatogr.*, 256 (1983) 313–321.
18 A. Shirahata, Y. Takeda, M. Kawase and K. Samejina, *J. Chromatogr.*, 262 (1983) 451.
19 G. Skarping, T. Bellander and L. Mathiasson, *J. Chromatogr.*, 370 (1986) 245.
20 L. Renman and G. Skarping, in preparation.

Journal of Chromatography, 479 (1989) 135–143
Elsevier Science Publishers B.V., Amsterdam — Printed in The Netherlands

CHROM. 21 664

CHROMATOGRAPHIC DETERMINATION OF AMINES IN BIOLOGICAL FLUIDS WITH SPECIAL REFERENCE TO THE BIOLOGICAL MONITORING OF ISOCYANATES AND AMINES

II. DETERMINATION OF 2,4- AND 2,6-TOLUENEDIAMINE USING GLASS CAPILLARY GAS CHROMATOGRAPHY AND SELECTED ION MONITORING

J. F. SANDSTRÖM, G. SKARPING* and M. DALENE
Department of Occupational and Environmental Medicine, University Hospital, S-221 85 Lund (Sweden)
(First received March 21st, 1989; revised manuscript received June 2nd, 1989)

SUMMARY

A capillary gas chromatographic method, using selected ion monitoring in the electron impact mode, was developed for the analysis of 2,4- and 2,6-toluenediamine (TDA), (*C.A.* Nos. 95-80-7 and 823-40-5) in aqueous solutions and human urine. The method is based on basic extraction of TDA from 2 ml of hydrolysed urine into toluene. The TDA was derivatized to an amide using a perfluorofatty anhydride. Three anhydrides were investigated, trifluoroacetic anhydride, TFAA (*C.A.* No. 407-25-0), pentafluoropropionic anhydride, PFPA (*C.A.* No. 356-42-3) and heptafluorobutyric anhydride, HFBA (*C.A.* No. 336-59-4). Trideuterated 2,4- and 2,6-TDA, ($C^2H_3C_6H_3(NH_2)_2$), were synthesized and used as internal standards. The molecular ions of TDA-amides ($m/z = 314$, 414 and 514) and the trideuterated TDA ($m/z = 317$, 417 and 517) were monitored. The correlation coefficient was 0.999 for 2,4-TDA and 0.998 for 2,6-TDA (0.3–8 μg/l) for the monitoring of molecular ions, and the correlation coefficient was 0.999 for 2,4-TDA and 0.998 for 2,6-TDA (0.3–8 μg/l) for the monitoring of $m/z = 295$ and 298 fragments of TDA-PFPA and trideuterated TDA-PFPA. The detection limit of TDA in human urine was *ca.* 0.1 μg/l. Hydrolysed urine from an exposed worker was found to contain 4 μg of TDA/l, with a workroom atmosphere of 1–10 μg/m^3 TDI. The overall recovery for PFPA derivatives was found to be 96 ± 4 for 2,4- and 106 ± 5% for 2,6-TDA from water and 100 ± 4 and 109 ± 6% from urine.

INTRODUCTION

Quantification of isocyanates and amines in trace levels in air has been of great interest for many years due to their possible environmental and occupational hazards. Toluene diisocyanate (TDI) is one of the main components in the manufacture of polyurethane foams and coatings. The related aromatic amine, toluenediamine

0021-9673/89/$03.50

(TDA), is used as an intermediate in polyurethane foam production, in elastomer production and in dyes. TDA has also been detected in urine hydrolysate after occupational exposure to TDI[1].

The analysis of aromatic amines in human body fluids is of great interest in order to develop analytical methods for the biological monitoring of exposure to these compounds[2–5].

Several analytical techniques have been used for the determination of aromatic amines in air and in biological fluids. The methods most frequently employed are liquid chromatography (LC) with ultraviolet (UV)[6–10] and electrochemical (ED)[10–14] detection, and gas chromatography (GC) with electron-capture[15–17] and thermionic specific detection (TSD)[16,17] or selected ion monitoring (SIM)[1].

Glass capillary GC and TSD of toluenediamines has been investigated at our laboratories. The adsorptive behaviours of the aromatic amines and the corresponding derivatives have been studied[17–20].

In this work we present a method for the determination of TDA in the low μg/l level in human urine using capillary GC and SIM in order to investigate the exposure to TDI during manufacture of polyurethanes. The choice of derivatization reagent and the internal standard is discussed in some detail.

EXPERIMENTAL

Apparatus

A Varian 3500 (Varian Associates, Walnut Creek, CA, U.S.A.) gas chromatograph equipped with a Varian thermionic specific detector and a Varian 8035 automatic on-column injector was employed. The injector starting temperature was 120°C for 5 s and thereafter the temperature was increased at 150°C/min to 250°C, where it was kept for 7 min. The injector was cooled with air or liquid nitrogen. The column was held isothermal at 115°C for 1 min and then increased at 15°C/min to 270°C, where it was held for 1 min. The carrier gas, helium at a flow-rate of 3 ml/min, was dried over molecular sieve 5A and deoxygenated using an "indicating Oxytrap" (Chrompack, Middelburg, The Netherlands).

A Shimadzu GC–MS QP1000 EI/CI (Shimadzu, Kyoto, Japan) quadrupole mass spectrometer connected to a Shimadzu GC-9A gas chromatograph, equipped with a Shimadzu autosampler (AOC-9), was used for identification and quantitative analysis. An Hamilton 701RN syringe, point style 5 needle, with a conical point and sidehole to minimize the septum coring was used. The autosampler was used in connection with a Shimadzu split/splitless injection system (SPL-G9). The capillary column outlet was mounted directly in the ion source. The starting temperature of the column oven was 95°C for 2 min. It was then raised at 20°C/min to 260°C, where it was kept for 2 min. The split exit valve was kept closed for 1 min after the injection. The temperatures of the ion source and the interface were 250°C. The capillar inlet pressure was 0.2 kg/cm^2 for capillary columns with an I.D. of 0.32 mm and 0.5 kg/cm^2 in the case of 0.24 mm I.D. The pressure of the ion source was *ca.* $1.5 \cdot 10^{-5}$ and $1.0 \cdot 10^{-5}$ Torr.

The instrument was used in the electron impact (EI) mode (20 and 70 eV) and set as follows: the molecular ions (M^+) of the three derivatives were monitored at $m/z = 314$ (toluenediamine trifluoroacetyl derivative, TDA-TFA), m/z 414 (toluenediamine pentafluoropropionyl derivative, TDA-PFP) and m/z 514 (toluenediamine

heptafluorobutyryl derivative, TDA-HFB). The molecular ions of trideuterated derivatives of TDA were monitored at $m/z = 317, 417$ and 517. The ion source filament was turned on after *ca.* 5 min and off after *ca.* 8 min. Ten measurements were made per second (rate 4). The tuning of the instrument (autotune) was performed using a standard sample inlet system and nonafluorotributylamine as a calibrant, all according to a standard procedure (70 eV). The resolution was optimized and no further centring was necessary.

For enrichment and evaporation of solvent, a vacuum desiccator connected to an aspirating pump was employed. The apparatus was equipped with an electrically heated oven, designed and manufactured at our laboratory.

To centrifuge the samples a Sigma 3E-1 (Harz, F.R.G.) centrifuge was used.

Columns

Four types of fused-silica capillary columns with chemically bonded stationary phases were used: Nordion® (Helsinki, Finland) NB-54 (25 m × 0.32 mm I.D.), with film thickness of 0.50 μm, Chrompack (Middelburg, The Netherlands) CP-Sil 8 CB (25 m × 0.32 mm I.D.) with film thickness of 1.2 μm, and CP-Sil 8 CB (25 m × 0.25 mm I.D.) with a film thickness of 0.12 μm and J & W Scientific (Folsom, CA, U.S.A.) DB-5 (30 m × 0.243 mm I.D.), with a film thickness of 0.25 μm.

Chemicals

Chemicals used were 2,4- and 2,6-TDA from Fluka (Buchs, Switzerland), heptafluorobutyric anhydride (HFBA), pentafluoropropionic anhydride (PFPA) and trifluoroacetic anhydride (TFAA) from Pierce (Rockford, IL, U.S.A.), toluene from Lab-Scan (Dublin, Ireland), nonafluorotributylamine, HCl, NaOH and K_2HPO_4 from Merck (Darmstadt, F.R.G.), trideuterated 2,4- and 2,6-TDA from Synthelec (Lund, Sweden) and ethanol from Kemetyl (Stockholm, Sweden).

Sampling

A 5-ml volume of 6 *M* HCl was added to *ca.* 100 ml of urine. The acidic urine samples were stored in a refrigerator. The samples were stable for at least 3 months without noticeable degradation.

Synthesis of perfluorofatty anhydride derivatives of TDA

A 2-g amount of TDA was dissolved in *ca.* 90 ml of toluene. The perfluorofatty anhydride (PFPA, TFAA or HFBA, *ca.* 12 g) was added gradually to the solution with stirring, and the mixture was allowed to stand with continuous stirring for 5 min. The molar ratio between the perfluorofatty anhydride and TDA was 2.2:1 (w/w). The reaction mixture was gradually heated to *ca.* 90°C and then extracted with 1 *M* phosphate buffer (pH 7.5) in order to remove excess of the reagent and acid formed. The organic phase was separated and evaporated to dryness using a rotating evaporator connected to an aspirating pump (temperature of the water-bath was kept at 30°C). The residue was recrystallized from ethanol–water (87:13, v/v), whereafter the TDA derivative was filtered off (Mesh G4), washed with cold distilled water and dried in a vacuum desiccator.

Preparation of standard solutions

Standard solutions of TDA in toluene were prepared by using the work-up procedure. The completeness of the reaction was checked by GC–TSD, and compared with solutions containing the synthesized standard. Standard solutions of TDA derivatives were prepared by dissolving the 2,4- and 2,6-TDA derivatives in toluene and further dilution to appropriate concentrations. Standard solutions of TDA and trideuterated TDA were prepared by dissolving the amines in 0.1 *M* HCl and then further dilution in aqueous solutions such as acidified human urine. Amine standards in acidic solutions (0.1 *M* HCl) or acidified human urine were stable for at least 3 weeks at room temperature.

Work-up procedure

To a 2-ml urine sample, 3 ml of 6 *M* HCl, containing the trideuterated TDA as internal standard (*ca.* 100 μg/l), were added. The acidified sample was then hydrolysed at 100°C overnight. A 2-ml aliquot of the acidified sample was transferred to a test-tube. A 4-ml volume of saturated NaOH and 3 ml of toluene were added. The mixture was then shaken for *ca.* 10 min and centrifuged (1500 *g*) for 5 min. A 2-ml volume of the organic layer was transferred to a new test tube and 20 μl of anhydride reagent were added. The mixture was immediately shaken vigorously for *ca.* 10 min. The excess of anhydride reagent and acid formed were removed by extraction with 2 ml of 1 *M* phosphate buffer solution (pH 7.5). A 1-ml volume of the toluene layer containing the amide formed was then transferred to a new test-tube. The samples were enriched by evaporation of the toluene solution in a vacuum desiccator at controlled temperature (30°C). The dry residue was finally diluted in 50 μl of toluene and then analysed.

The same procedure was used for aqueous samples but in this case the hydrolysis step was omitted.

RESULTS AND DISCUSSION

Standards

Standards of perfluorofatty anhydride derivatives of 2,4-TDA, 2,6-TDA, trideuterated 2,4- and 2,6-TDA were identified by GC–mass spectrometry (MS) and the purity was checked by GC–TSD and elemental analysis. The purity was found to be better than 99%. The isotopic purity was checked for all the fragments investigated. The ratios of the mass fragment $m/z = 417$ to that of $m/z = 414$ of the 2,4- and 2,6-TDA amide derivatives were $< 0.3\%$. The ratios of the mass fragment $m/z = 414$ to that of $m/z = 417$ of the trideuterated 2,4- and 2,6-TDA amide derivatives were $< 0.3\%$.

Internal standard

The determinations with GC–MS were performed using a trideuterated TDA as the internal standard. The three hydrogen atoms at the methyl group were exchanged to deuterium. There are several advantages of using deuterium labelled substances as internal standards. The chemical, physical and chromatographic properties of the trideuterated TDA are similar to those of TDA. The behaviour of trideuterated TDA is similar to that of TDA during storage and the work-up procedure. Trideuterated TDA is not naturally present in the sample and no interferences have been found for the mass fragments monitored. The similar fragmentation patterns of TDA and trideuterated TDA are favourable for easier calibration of the mass spectrometer.

Work-up procedure

GC–TSD was used to optimize the work-up conditions. The concentrations of the two aromatic amines studied were *ca.* 180 μg/l in urine. The isobutyl chloroformate derivative of di-*n*-butylamine was used as the internal standard. The internal standard diluted in toluene was added after the evaporation step. The procedure was studied by comparison of standard solutions of the derivatives in toluene and the dissolved residue after the enrichment step. The basic properties of the aromatic amine, TDA, determine the choice of extraction solution. The conditions of extraction of TDA in urine into toluene were optimized by variation of the pH and ionic strength. The use of 5 *M* NaOH saturated with NaCl gave a recovery of less than 70%. However the use of saturated NaOH yielded *ca.* 100% recovery. For aqueous test solutions a two-phase derivatization system can also be employed.

The enrichment step was studied. Evaporation of the solvent with a gentle flow of nitrogen gave losses of about 70–80%. No losses and excellent reproducibility were found in the evaporation step, when a vacuum desiccator connected to an aspirating pump equipped with an electrically heated oven was used.

Chromatography

TFAA, PFPA and HFBA derivatives of 2,4- and 2,6-TDA were studied. All compounds showed excellent chromatographic behaviour using GC–MS. However baseline separation of the isomers was not complete for the HFBA derivatives and the isomers of the TFAA derivatives showed somewhat broader peaks. However baseline separation of the 2,4- and 2,6-TDA PFPA derivatives was found for all capillary columns tested, no endogenous peaks from the urine extracts interfered in the analysis.

Detection

TSD. The limit of detection for the PFPA derivative of TDA with GC–TSD is *ca.* 10 μg/l. An aqueous solution of TDA can be further enriched, giving detection limits of less than 0.5 μg/l, and several μl of the solvent can be injected onto the column. The molar sensitivity for all the derivatives of TDA studied was virtually the same. However, when analysing urine samples considerable interferences were found, and *ca.* 50 μg/l can be quantitatively analysed without a further clean-up step.

Mass-selective detection. GC–MS and SIM was used for the determination of TDA-amides in the low μg/l range. A 1–4 μl volume of the sample solution (toluene) was injected into the chromatographic system. This amount may damage and contaminate the ion source and the high vacuum system. These problems were eliminated when the filament was switched off during the entrance of the solvent and switched on during the chromatography. Several hundreds of analyses were hence possible.

Several mass fragments were suitable for quantitative analysis. Mass spectra were obtained for the purpose of identification, and to choose the suitable fragment ions for quantitative analysis. Fig. 1 shows mass spectra of the derivatives of PFPA. The molecular ions (M^+) at $m/z = 414$ and 417 and fragment ions ($M^+ - C_2F_5$) at $m/z = 295$ and 298 are suitable for quantitation of TDA. The molecular ions were however chosen due to the sensitivity, the matrix and the relatively more significant information. An ionization voltage of 20 eV was chosen due to the better signal-to-noise ratio.

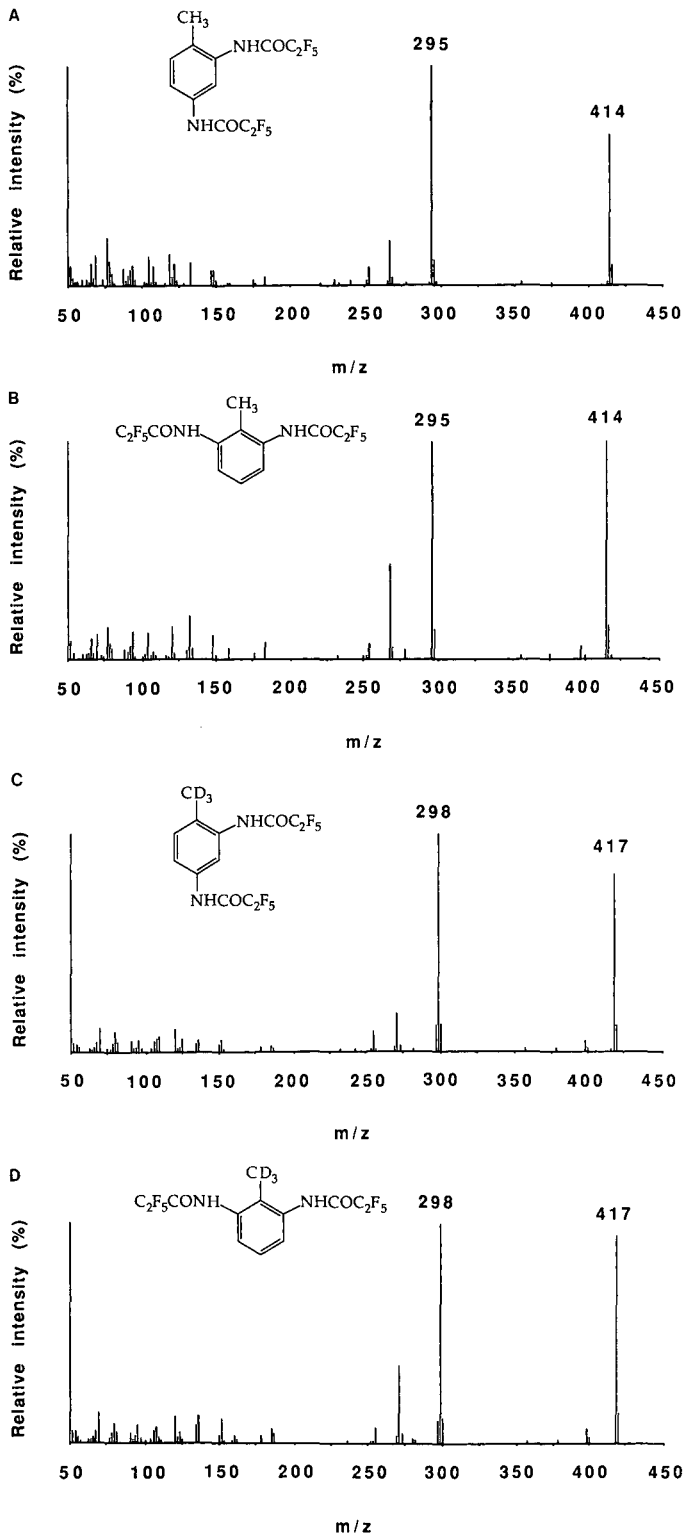

Fig. 1. Mass spectra obtained with EI at an ionization potential of 70 eV: (A) 2,4-TDA-PFPA derivative; (B) 2,6-TDA-PFPA derivative; (C) trideuterated 2,4-TDA-PFPA derivative; (D) trideuterated 2,6-TDA-PFPA derivative.

Quantitative analysis

Calibration graphs. Human urine was spiked with 2,4- and 2,6-TDA and the work-up procedure was performed. For each concentration two determinations with duplicate injections were made. The average values of the peak area ratio between TDA ($m/z=414$ and 295) and trideuterated TDA ($m/z=417$ and 298) were plotted. The calibration graphs were linear and passed through the origin. The calibration graph using SIM of the molecular ions for the concentration range 0.3–8 μg/l (peak area ratio 0–0.3) gave a correlation coefficient of 0.999 ($n=9$) for 2,4-TDA and 0.998 ($n=9$) for 2,6-TDA. The correlation coefficients using SIM of the ($M^+ - C_2F_5$) ions were 0.999 ($n=9$) for 2,4-TDA and 0.998 ($n=9$) for 2,6-TDA. No noticeable differences were found for peak height measurements when using HFBA as the derivatization reagent.

Recovery and precision. The overall recovery was studied for ten spiked urine samples containing *ca.* 145 μg/l of the two TDA isomers using GC–TSD. The urines were worked up according to the procedure, but without the presence of trideuterated TDA as the internal standard. Comparison was made by analysing the amide standards in toluene. The overall recoveries for 2,4- and 2,6-TDA was found to be 100 ± 4 and 109 ± 6% ($n=10$). The recoveries for TDA-spiked urine in the hydrolysis step studied by using GC–SIM 15 μg/l) were 100 ± 4% ($n=10$) for both 2,4- and 2,6-TDA. The values are given with a 95% confidence range.

An enrichment step using a vacuum desiccator connected to an aspirating pump was employed to increase the detection limit. Twentyfive samples were simultaneously evaporated within an hour. No carryover and no artefact were found during this procedure. More than a 40-fold enrichment of the sample was possible. The recovery in the enrichment procedure and 20-fold enrichment was found to be 100 ± 3 ($n=10$) for 2,4-TDA and 104±4% for 2,6-TDA ($n=10$). The overall recovery for aqueous solutions was similar. The values are given with a 95% confidence range.

The usefulness of a trideuterated internal standard is demonstrated by the high precision in the GC–SIM analysis at the low μg/l level. Ten different spiked urines at *ca.* 2 μg/l and ten different spiked urines at *ca.* 15 μg/l were analysed. The relative standard deviations for the ten samples for TFAA, PFPA and HFBA derivatives were determined. The samples were enriched ten times and the mean values for duplicate injections for both the peak area and peak height ratio were measured by monitoring the molecular ions and the ratio between the amine and internal standard varied between 2 and 5% (Table I). The values in the table are given with a 95% confidence range.

Detection limit

The detection limit, according to Miller and Miller[21], for TDA in human urine with GC–MS using the EI mode was *ca.* 0.1 μg/l for PFPA derivatives. The samples were treated according to the work-up procedure and with a 40-fold enrichment (the dry residue was dissolved in 25 μl of toluene).

Applications

The method is applicable to the monitoring of isocyanates and amines in air, collected in an impinger flask containing 10 ml of diluted hydrochloric acid. The potential of the method is illustrated by the high selectivity and sensitivity, less than

TABLE I

PRECISION IN THE GC-SIM ANALYSIS OF 2,4- AND 2,6-TDA IN HYDROLYSED HUMAN URINE AS THEIR PERFLUOROFATTY ANHYDRIDE DERIVATIVES

Injected volume: 1 μl. Internal standard (IS): trideuterated TDA. An autoinjector was used for splitless injections. Ten different urine samples spiked with 2,4- and 2,6-TDA with duplicate injections were determined. Values are relative standard deviations (%) in peak area and peak height, respectively. TFAA = trifluoroacetic anhydride derivative (M^+ at $m/z=314$); PFPA = pentafluoropropionic anhydride derivative (M^+ at $m/z = 414$) and HFBA = heptafluorobutyric anhydride derivative (M^+ at $m/z=514$).

Amine	*Conc. (μg/l)*	*TFAA*		*PFPA*		*HFBA*	
		DD[a]	*IS*[b]	*DD*	*IS*	*DD*	*IS*
2,4-TDA	14.4	7, 10	3, 3	19, 20	3, 4	17, 17	3, 3
	2.2	17, 19	4, 3	17, 17	2, 3	13, 14	4, 5
2,6-TDA	14.5	15, 19	4, 4	6, 6	2, 2	6, 6	2, 2
	2.2	5, 7	4, 5	12, 12	2, 3	9, 9	4, 4

[a] Direct determination without internal standard.
[b] The ratio between the amine and the internal standard.

1/500 of the present Swedish threshold limit value (TLV) (40 $\mu g/m^3$) with a sampling time of 15 min and with a flow-rate of 1 l/min.

Urine from a worker exposed to TDI at a flexibe foam factory was analysed, the workroom atmosphere containing 1–10 $\mu g/m^3$. The work-up procedure was performed and the sample was enriched 20 times and analysed with GC–SIM. The corresponding diamines of TDI, 2,4- and 2,6-TDA were found in the hydrolysed urine (*ca.* 4 μg/l). The chromatograms are shown in Fig. 2.

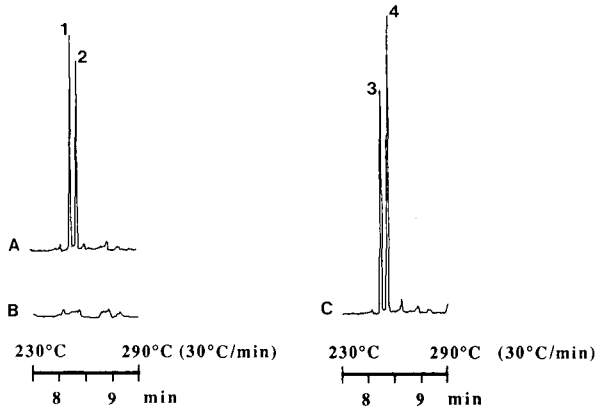

Fig. 2. SIM of hydrolysed urine samples using the EI mode (20 eV). (A) The molecular ion of the TDA-PFPA derivative ($m/z=414$) from a worker exposed to TDI, with an air concentration of 1–10 $\mu g/m^3$. The peaks correspond to a concentration of *ca.* 4 μg/l in hydrolysed urine of 2,4- and 2,6-TDA. (B) The molecular ion of the TDA-PFPA derivative ($m/z=414$) from a non-exposed subject. (C) The molecular ion of the trideuterated TDA-PFPA derivative ($m/z=417$) used as the internal standard. Peaks: 1 = PFPA derivative of 2,6-TDA; 2 = PFPA derivative of 2,4-TDA; 3 = PFPA derivative of trideuterated 2,6-TDA; 4 = PFPA derivative of trideuterated 2,4-TDA. Column: J&W fused silica coated with DB-5 bonded stationary phase (30 m × 0.243 mm I.D.), film thickness 0.25 μm. Inlet pressure of the carrier gas (helium): 0.5 kg/cm^2. Splitless injection (1 min) of 1 μl toluene. Temperature programming: isothermal at 95°C (2 min), increased at 10°C/min to 110°C, then at 30°C/min to a final temperature of 300°C.

CONCLUSIONS

A GC–SIM method is demonstrated for determination of TDA in hydrolysed human urine. Due to the high selectivity and sensitivity no special clean-up procedure is necessary. Several samples can be worked up simultaneously. The use of trideuterated 2,4- and 2,6-TDA results in accurate and precise determinations. The combination of high-resolution chromatography and selective detection is demonstrated to be appropriate for the analysis of TDA in biological matrices.

ACKNOWLEDGEMENTS

We are indebted to Professor Staffan Skerfving, head of the department of Occupational and Environmental Medicine, for his interest in this work. We also gratefully acknowledge the Swedish Work Environment Fund (AMFO-88-0161) for financial support.

REFERENCES

1 C. Rosenberg and H. Savolainen, *J. Chromatogr.*, 367 (1986) 385–392.
2 *Bioassay of 2,4-Diaminotoluene for Possible Carcinogenicity, Technical Report Series no. 162, CAS No. 95-80-7*, National Cancer Institue, Bethesda, MD, 1979.
3 *Bioassay of 2,6-Diaminotoluene Dihydrochloride for Possible Carcinogenicity, Technical Report Series no. 200, CAS No. 15481-70-6*, National Cancer Institue, Bethesda, MD, 1980.
4 B. B. Furlong, R. P. Weaver and J. A. Goldstein, *Carcinogenesis*, 8 (1987) 247–251.
5 P. H. Grantham, L. Mohan, T. Benjamin, P. P. Roller, J. R. Miller and E. K. Weisburger, *J. Environ Pathol. Toxicol.*, 3 (1980) 149–166.
6 C. Sangö, *J. Liq. Chromatogr.*, 2 (1979) 763.
7 S. Sardas, A. E. Karakaya and B. Sener, *Gazi Univ. Eczacilik Fak. Derg.*, 3 (1985) 89–94.
8 R. C. Snyder, W. C. Brumley, C. V. Breder and T. Fazio, *J. Assoc. Off. Anal. Chem.*, 65 (1982) 1388–1394.
9 E. H. Nieminen, L. H. Saarinen and J. T. Laaksalo, *J. Liq. Chromatogr.*, 6 (1983) 453–469.
10 M. Dalene, L. Mathiasson, G. Skarping, C. Sangö and J. F. Sandström, *J. Chromatogr.*, 435 (1988) 469–481.
11 C. J. Warwick, D. A. Bagon and C. J. Purnell, *Analyst (London)*, 106 (1981) 676–685.
12 D. A. Bagon and C. J. Purnell, *J. Chromatogr.*, 190 (1980) 175–182.
13 D. A. Bagon, C. J. Warwick and R. H. Brown, *Am. Ind. Hyg. Assoc. J.*, 45 (1984) 39–43.
14 M. S. Varney and M. R. Preston, *J. Chromatogr.*, 348 (1985) 265–274.
15 T. Hirayama, M. Ono, K. Uchiyama, M. Nohara and S. Fukui, *J. Assoc. Off. Anal. Chem.*, 68 (1985) 746–748.
16 C. Rosenberg and H. Savolainen, *J. Chromatogr.*, 323 (1985) 429–433.
17 G. Skarping, L. Renman and M. Dalene, *J. Chromatogr.*, 270 (1983) 207–218.
18 G. Skarping, C. Sangö and B. E. F. Smith, *J. Chromatogr.*, 208 (1981) 313–321.
19 G. Skarping, L. Renman, C. Sangö, L. Mathiasson and M. Dalene, *J. Chromatogr.*, 346 (1985) 191–204.
20 L. Renman and G. Skarping, in preparation.
21 J. C. Miller and J. N. Miller, *Statistics For Analytical Chemistry*, Ellis Horwood, Chichester, 1984.

Journal of Chromatography, 479 (1989) 145–152
Elsevier Science Publishers B.V., Amsterdam — Printed in The Netherlands

CHROM. 21 672

CHROMATOGRAPHIC DETERMINATION OF AMINES IN BIOLOGICAL FLUIDS WITH SPECIAL REFERENCE TO THE BIOLOGICAL MONITORING OF ISOCYANATES AND AMINES

III. DETERMINATION OF 4,4′-METHYLENEDIANILINE IN HYDROLYSED HUMAN URINE USING DERIVATIZATION AND CAPILLARY GAS CHROMATOGRAPHY WITH SELECTED ION MONITORING

A. TILJANDER, G. SKARPING* and M. DALENE
Department of Occupational and Environmental Medicine, University Hospital, S-221 85 Lund (Sweden)
(First received March 28th, 1989; revised manuscript received June 9th, 1989)

SUMMARY

A method is presented for the determination of 4,4′-methylenedianiline in hydrolysed human urine, based on a derivatization procedure with pentafluoropropionic anhydride and capillary gas chromatographic determination with selected ion monitoring. Dideuterated 4,4′-methylenedianiline was used as an internal standard. The ratio of the molecular ion of the 4,4′-methylenedianiline amide derivative (*m/z* 490) and the dideuterated 4,4′-methylenedianiline amide derivative (*m/z* 492) was used for quantitative analysis. The calibration graph was linear in the investigated range (5–30 μg/l in urine) with a correlation coefficient of 0.998. The precision was 3.4% for urine samples containing 26 μg/l and the detection limit was 2 μg/l. The overall recovery for urine samples containing 115 μg/l was 96 ± 5%. Urine samples from eight skin-exposed epoxy resin workers were examined and 4,4′-methylenedianiline was found in the concentration range 2–600 μg/l.

INTRODUCTION

4,4′-Methylenedianiline (MDA) is a commercially important diamine used as an intermediate in the preparation of epoxy resins, polyurethanes, rubber chemicals and polymers. By far the largest application for MDA is as an intermediate for isocyanates[1,2].

MDA has been reported to be hepatoxic in dogs[3], rats[4,5] and humans[6,7]. It has shown to be mutagenic in the Ames test in the presence of an S9 metabolic activation system[8]. MDA has also been reported to be carcinogenic in rats and mice[9]. MDA is absorbed readily through the skin[10], which causes problems when handling MDA. The determination of MDA in biological fluids from occupationally exposed persons[11,12] is therefore of major importance. The hydrolysis of authentic urine and the possible metabolites N-acetyl-MDA and N,N′-diacetyl-MDA has been describ-

0021-9673/89/$03.50

ed[11,13]. The capillary gas chromatographic (GC) trace determination of MDA has met with considerable difficulties owing to the easy oxidation and adsorbtion of MDA in the analytical system[14], which makes the use of a derivatization procedure necessary. Anhydrides have been reported as derivatization reagents for GC determinations of MDA[11,12,14–17]. Several techniques have been developed for the determination of MDA in matrices such as air sampling solutions[15,16,18], blood[17] and urine[11,12,19,20]. The detection methods used in GC methods are thermionic specific detection (TSD), electron-capture detection (ECD) and selected ion monitoring (SIM). For the determination of MDA in urine, detection limits in the range 5–10 μg/l[11,12,19] have been reported. 4,4'Methylenebis-2-chloroaniline[11] and 4,4'-ethylenedianiline (EDA)[12,17] have been used as internal standards for GC–SIM.

In this paper, a GC–SIM method is described for biological monitoring of MDA, at low μg/l levels, in human urine using dideuterated MDA ([$^2H_2$]MDA) as an internal standard.

EXPERIMENTAL

Equipment

The analyses were performed on a Shimadzu (Kyoto, Japan) QP1000 EI/CI quadrupole mass spectrometer. The mass spectrometer was connected to a Shimadzu GC-9A gas chromatograph equipped with an SPL-G9 split–splitless injection system and a Shimadzu AOC-9. The carrier gas was helium and the inlet pressure was 0.5 kg/cm^2. The injector temperature was 280°C. The split exit valve was closed for 1 min after injection. The oven temperature was isothermal at 100°C for 2 min, then increased at 30°C/min to 300°C, the final temperature being maintained for 2 min. The quadrupole mass-selective detector was operated in the electron-impact (EI) mode at 70 eV using SIM at *m/z* 490 and 492. The interface temperature was 250°C and the ion source temperature 300°C. The filament of the ion source was on between 7.5 and 10 min after the injection into the GC column. Five measurements were made per second. The mass spectrometer was calibrated with tris(nonafluorobutyl)amine according to the standard procedure.

The high-performance liquid chromatography (HPLC) system consisted of a Waters 600 multi solvent delivery system (Millipore-Waters, Milford, MA, U.S.A.), a Waters 712 WISP with variable injection volume, a Waters 490 programmable multi-wavelength detector and a Shimadzu C-R3A integrator.

A Varian (Walnut Creek, CA, U.S.A.) 3500 gas chromatograph equipped with a Varian thermionic specific detector and a Varian 8035 automatic on-column injector was employed. For separation of phases, a Model 3E-1 centrifuge (Sigma, Harz, F.R.G.) was used. For enrichment and evaporation, a vacuum desiccator connected to an aspirating pump was employed. The vacuum desiccator was equipped with an electrically heated oven, designed and manufactured in our laboratory.

Columns

Fused-silica capillary columns, with chemically bonded apolar stationary phases, were tested: Chrompack (Middelburg, The Netherlands) CP-Sil 8 CB (25 m × 0.32 mm I.D.) with film thicknesses of 1.2, 0.50 and 0.25 μm and CP-Sil 8 CB (25 m × 0.25 mm I.D.) with film thickness of 0.12 μm; Nordion (Helsinki, Finland) NB-54

(25 m × 0.32 mm I.D.) with film thicknesses of 1.0, 0.50 and 0.25 μm; and J & W Scientific (Folsom, CA, U.S.A.) DB-5 (30 m × 0.25 mm I.D.) with a film thickness of 0.25 μm.

The HPLC column was made of stainless steel (25 cm × 3 mm I.D.) and was packed with Nucleosil C_{18} particles (5 μm) (Marcherey-Nagel, Düren, F.R.G.).

Chemicals

MDA, EDA and 2,4-toluenediamine (2,4-TDA) were obtained from Aldrich (Beerse, Belgium). The [$^2H_2$]MDA [$C^2H_2(C_6H_4NH_2)_2$ hydrochloride] was synthesized at Synthelec (Lund, Sweden). Trifluoroacetic anhydride (TFAA), pentafluoropropionic anhydride (PFPA) and heptafluorobutyric anhydride (HFBA) were obtained from Pierce (Rockford, IL, U.S.A.), toluene and acetonitrile of HPLC grade from Lab-Scan (Dublin, Ireland), tris(nonafluorobutyl)amine, sodium hydroxide, hydrochloric acid, potassium dihydrogenphosphate and dipotassium hydrogenphosphate (anhydrous) from Merck (Darmstadt, F.R.G.) and ethanol from Kemetyl (Stockholm, Sweden).

Synthesis of MDA amide derivatives

A 17.5-g amount of PFPA was added to a solution containing 5.0 g of MDA and 90 ml of toluene. The mixture was slowly heated to 70°C, then cooled and evaporated to dryness on a rotating evaporator. The residue was recrystallized from ethanol–water (7:1) and the crystals were filtered and washed with the same mixture. The crystals obtained were dried in a vacuum desiccator. The HFBA derivative of MDA was synthesized in a similar manner.

Preparation of standard solutions

Stock solutions of MDA and [$^2H_2$]MDA were prepared in 0.1 *M* HCl at the 1 g/l level and diluted with 0.1 *M* HCl to the appropriate concentrations. A stock solution of MDA-PFPA derivative was prepared in ethanol at the 1 g/l level and was diluted with toluene to the desired concentrations. The solutions were stable for more than 10 weeks without any noticeable degradation when stored in a refrigerator.

Sampling

A 2-ml volume of 6 *M* HCl per 100 ml of urine was added to the urine samples. The acidified urine samples were stored in a refrigerator until analysis.

Work-up procedure

A 0.8-ml urine sample was placed in a 10-ml test-tube fitted with a PTFE cap and 1.2 ml of 6 *M* HCl and 0.1 ml of 0.5 mg/l [$^2H_2$]MDA solution were added. The test-tube was heated at 95–100°C for 2 h and then cooled to room temperature. Toluene (3 ml) and 4 ml of saturated aqueous NaOH solution were added and the mixture was shaken for 10 min and then centrifuged at 1500 *g* for 10 min. A 2-ml volume of the organic phase was separated and transferred to a new test-tube, 20 μl of PFPA were added and the solution was shaken for 5 min. Then, 2 ml of 1 *M* aqueous phosphate buffer (pH 7.5) were added and the mixture was shaken for 10 min. A 1-ml volume of the organic phase was transferred to a new test-tube and evaporated to dryness in a vacuum desiccator at 30°C. The dry residue was dissolved in 0.1 ml of toluene and 1 μl of this solution was injected into the GC–mass spectrometric (GC–MS) system.

RESULTS AND DISCUSSION

Standard

The identity of the MDA-PFPA derivative was confirmed by GC–MS and the purity was determined using both HPLC–UV detection ($\lambda = 245$ nm) and capillary GC–TSD. The purity was found to be better than 99%. The purity was further examined by elemental analysis and the experimental carbon, hydrogen and nitrogen percentages were found to differ by less than 0.2% from the calculated values.

Isotopic purity

The ratio of the mass fragment of *m/z* 492 to *m/z* 490 of the MDA-PFPA derivative was 3%, as expected from the naturally occurring isotopes in the MDA-PFPA derivative. The ratio of the mass fragment of *m/z* 490 to *m/z* 492 of the $[^2H_2]$MDA-PFPA derivative was 6% as a result of the remaining parent material.

Work-up procedure

Hydrolysis. Urine samples from workers exposed to MDA were hydrolysed under weakly acidic, strongly acidic and strongly basic conditions. The optimum conditions were 2 h at 95–100°C under strongly acidic conditions[13].

Extraction of MDA. The recovery was almost completely independent of whether 5 *M* NaOH or saturated NaOH was added to the hydrolysed urine sample. The foaming tendency was found to be less pronounced when saturated NaOH was used.

Derivatization. Three derivatization reagents, TFAA, PFPA and HFBA, were tested. The recoveries for the derivatization reactions were *ca.* 100%. Excess reagent and liberated acid were removed by extraction with 1 *M* phosphate buffer (pH 7.5) without any measurable losses of the MDA amide derivative.

Enrichment. The components of interest were enriched 10-fold. The removal of the remaining excess of reagent and the volatile impurities present in the sample increased the lifetime of the capillary column. The opportunities to enrich the sample further are obvious and the possibility of choosing an optimum solvent for the subsequent GC analysis is also feasible.

Chromatography

Capillary columns with an apolar stationary phase with a film thickness in the range 0.12–1.2 μm were tested. Of the three derivatives tested, the MDA-PFPA derivative showed the best column performance. The elution temperature was 300°C. No endogenous peaks from the urine extracts interfered in the analysis. The necessity to achieve an appropriate vacuum in the MS system defined the chromatographic system. A relative long capillary column, (20–30 m) of I.D. 0.25 mm was used to avoid a sub-atmospheric inlet pressure. The pressure in the ion source was *ca.* $2 \cdot 10^{-5}$ Torr. The column oven was maximally temperature programmed at 30°C/min owing to the better signal-to-noise ratio obtained. More than 1000 chromatographic analysis were made without any noticeable column degradation.

Internal standard

EDA, 2,4-TDA and $[^2H_2]$MDA were tested. EDA and 2,4-TDA gave unsatis-

factory precision. [$^2H_2$]MDA was found to be the best choice on the basis of the similar fragmentation pattern and chemical performance, and it is not expected to appear in a workplace environment.

Mass spectra

For the purpose of identifying and selecting suitable fragment ions for quantitative analysis, mass spectra of the PFPA derivatives of MDA and [$^2H_2$]MDA were obtained (Fig. 1). The fragmentation patterns for the two isotopes are very similar. Typical fragmentations were found[16,17] and the most abundant peaks were the molecular ions.

Detection

Thermionic specific detection. The molar sensitivity using GC–TSD is similar for the three derivatives of MDA investigated. The detection limit was *ca.* 40 fmole of MDA-PFPA derivative injected. Interfering peaks occur in the chromatograms from the urine samples, giving a practical detection limit of *ca.* 600 μg/l. The efficient use of a GC–TSD method for urine samples demands a more complete sample clean-up or a more selective derivatization procedure.

Selected-ion monitoring. The molecular ion was chosen owing to the sensitivity and the more significant information provided. The sensitivities of the PFPA and

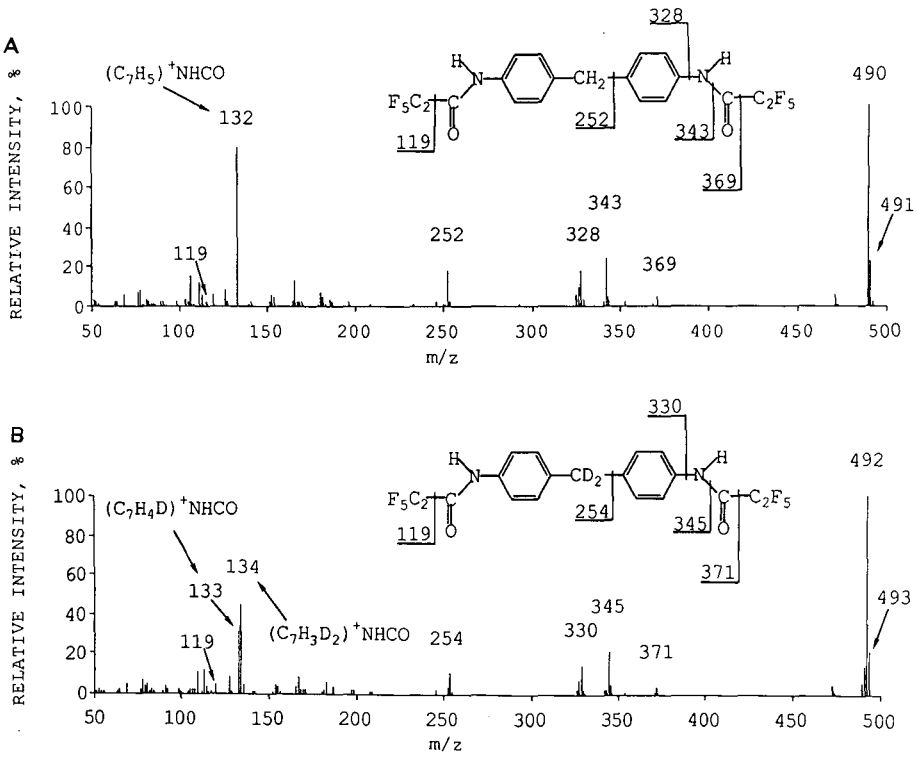

Fig. 1. Mass spectra obtained in the EI mode at an ionization potential of 70 eV: (A) MDA-PFPA derivative; (B) [$^2H_2$]MDA-PFPA derivative.

HFBA derivatives of MDA were about the same. However, the MDA-TFAA derivative was 10–20 times less sensitive. In this study, the detection limit was set by the instrument as no interfering peaks were found. Obviously for urine samples a lower detection limit can be obtained with further enrichment. However, the concentration of the internal standard influences the detection limit as $[^2H_2]$MDA unfortunately contains 6% of MDA.

Quantitative analysis

Recovery. The overall recovery was studied for seven urine samples containing 115 μg/l of MDA using an HPLC–UV system. The recovery was 96 ± 5% (95% confidence and $n = 7$).

Calibration graph. Seven different concentrations of MDA in urine were prepared, including a blank, according to the work-up procedure. For each concentration three determinations with duplicate injections were made by GC–MS. The calibration graph (Fig. 2) for the investigated concentration range of 5–30 μg/l of MDA in urine was linear and gave a correlation coefficient of 0.998 ($n = 7$; $y = 0.0158x + 0.0108$). Correction for the contribution of MDA from the $[^2H_2]$MDA internal standard was made by subtraction of a value of 0.06. Each point on the graph represented the corrected average value of the ratio of the peak area of the MDA-PFPA derivative to that of the $[^2H_2]$MDA-PFPA derivative.

Detection limit. The detection limit, defined as the urine sample concentration giving a signal equal to the blank signal plus three standard deviations[21], was 2 μg/l of MDA. No interfering peaks appeared when urine samples from ten persons were examined.

Accuracy and precision. Eight urine samples containing 26 μg/l of MDA were analysed. The relative standard deviation of the MDA peak area was 35%. The relative standard deviation of the peak area ratio of MDA to $[^2H_2]$MDA was 3.4%.

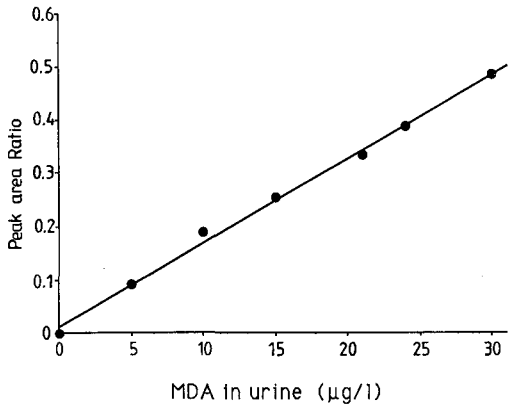

Fig. 2. Calibration graph for MDA in urine: ratio between the peak areas of the MDA-PFPA derivative and the $[^2H_2]$MDA-PFPA derivative from the worked-up urine *versus* the concentration of MDA in the original urine sample. Column, CP-Sil 8 CB (25 m × 0.25 mm I.D.) with a film thickness of 0.25 μm; inlet pressure of carrier gas (helium), 0.5 kg/cm^2; 1-μl splitless injection; temperature programme, isothermal at 100°C for 2 min, increased at 30°C/min to a final temperature of 300°C, then isothermal for 2 min.

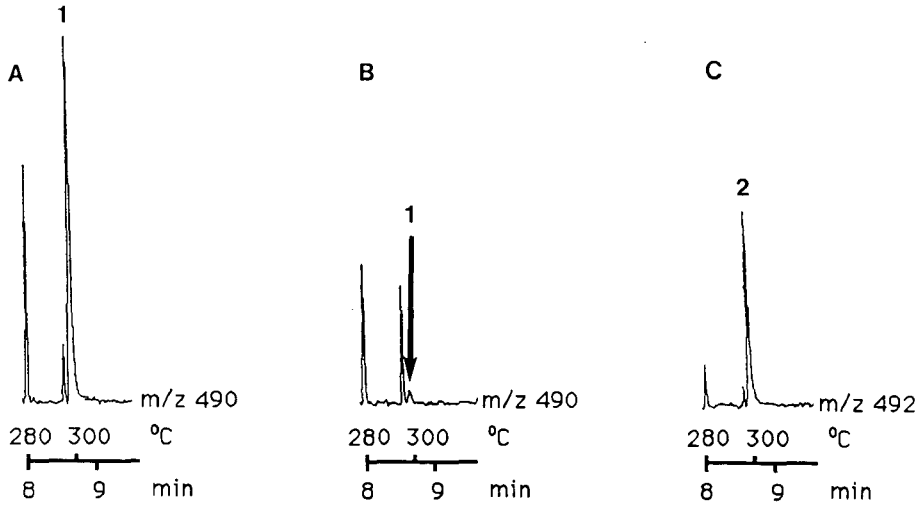

Fig. 3. Selected-ion chromatogram of urine samples using the EI mode. (A) Molecular ion of MDA-PFPA derivative from urine sample from an exposed worker. The peak corresponds to a concentration of 31 μg/l. (B) Molecular ion of MDA-PFPA derivative from urine sample from an unexposed worker. (C) Molecular ion of $[^2H_2]$MDA-PFPA derivative. Chromatographic conditions as in Fig. 2. Peak 1 = MDA-PFPA derivative; peak 2 = $[^2H_2]$MDA-PFPA derivative.

Application

An important application of the method is the biological monitoring of workers who are skin-exposed to MDA. Typical SIM of urine samples from occupationally exposed and non-exposed workers are shown in Fig. 3. MDA was found in the concentration range 2–600 μg/l in the hydrolysed urine samples from skin-exposed epoxy workers.

CONCLUSIONS

The method developed for assessing occupational exposure to MDA provides the selective and sensitive determination of MDA at low μg/l levels using GC–SIM. The use of $[^2H_2]$MDA as internal standard results in accurate and precise determinations.

ACKNOWLEDGEMENTS

We are indebted to Professor Staffan Skerfving, Head of the Department of Occupational and Environmental Medicine, for his interest in this work. Peter Berg and Anders Seldén (Department of Occupational Medicine, Örebro Medical Centre Hospital, Örebro, Sweden) and Robert Jackobsson (ASEA Brown Boveri, Västerås, Sweden) are thanked for supplying urine samples from MDA-exposed workers. We also gratefully acknowledge financial support from the Swedish Work Environment Fund (AMFO 88-0161).

REFERENCES

1 *Evaluation of the carcinogenic Risk of Chemicals to Humans, World Health Organization (IARC Monographs,* Vol. 39), International Agency for Research on Cancer, Lyon, 1986, p. 347.
2 M. Grayson (Editor), *Kirk-Othmer Encyclopedia of Chemical Technology,* Vol. 2, Wiley-Interscience, Toronto, 1978, p. 338.
3 W. B. Deichmann, W. E. MacDonald, M. Coplan, F. Woods and E. Blum, *Toxicology,* 11 (1978) 185.
4 S. Fukushima, M. Shibata, T. Hibino, T. Yoshimura, M. Hirose and N. Ito, *Toxicol. Appl. Pharmacol.*, 48 (1979) 145.
5 G. Pludro, K. Karlowski, M. Mankowska, H. Woggon and W-J. Uhde, *Acta Pol. Pharm.*, 26 (1969) 352.
6 D. B. McGill and J. D. Motto, *N. Engl. J. Med.*, 291 (1974) 278.
7 H. Kopelman, P. J. Scheuer and R. Williams, *Q. J. Med.*, 35 (1966) 553.
8 K. Tanaka, T. Ino, T. Sawahata, S. Marui, H. Igaki and H. Yashima, *Mutation Res.*, 143 (1985) 11.
9 E. K. Weisburger, A. S. K. Murthy, H. S. Lilja and J. C. Lamb, IV, *J. Natl. Cancer Inst.*, 72 (1984) 1457.
10 S. R. Cohen, *Arch. Dermatol.*, 121 (1985) 1022.
11 J. Cocker, W. Gristwood and H. K. Wilson, *Br. J. Ind. Med.*, 43 (1986) 620.
12 J. Cocker, L. C. Brown, H. K. Wilson and K. Rollins, *J. Anal. Toxicol.*, 12 (1988) 9.
13 A. Tiljander, G. Skarping and C. Sangö, in preparation.
14 G. Skarping, L. Renman and M. Dalene, *J. Chromatogr.*, 270 (1983) 207.
15 G. Skarping, C. Sangö and B. E. F. Smith, *J. Chromatogr.*, 208 (1981) 313.
16 G. Skarping, L. Renman and B. E. F. Smith, *J. Chromatogr.*, 267 (1983) 315.
17 M. Tortoreto, P. Catalani, M. Bianchi, C. Blonda, C. Pantarotto and S. Paglialunga, *J. Chromatogr.*, 262 (1983) 367.
18 R. M. Riggin, C. C. Howard, D. R. Scott and R. L. Hedgecoke, *J. Chromatogr. Sci.*, 21 (1983) 321.
19 C. Rosenberg and H. Savolainen, *J. Chromatogr.*, 358 (1986) 385.
20 P. Trippel-Schulte, J. Zeiske and A. Kettrup, *Chromatographia,* 22 (1986) 138.
21 J. C. Miller and J. N. Miller, *Statistics for Analytical Chemists*, Ellis Horwood, Chichester, 1984.

Journal of Chromatography, 479 (1989) 153–158
Elsevier Science Publishers B.V., Amsterdam — Printed in The Netherlands

CHROM. 21 660

HIGH-SENSITIVITY HIGH-PERFORMANCE LIQUID CHROMATOGRAPHIC ANALYSIS OF DIQUAT AND PARAQUAT WITH CONFIRMATION[a]

VERNE A. SIMON* and ANNE TAYLOR
Department of Health and Rehabilitative Services, State of Florida, 1217 Pearl Street, Jacksonville, FL 32202 (U.S.A.)
(First received June 20th, 1988; revised manuscript received May 5th, 1989)

SUMMARY

An isocratic high-performance liquid chromatographic (HPLC) assay for diquat and paraquat in well water is presented. This assay is a more rapid and sensitive version of our previously published method. A novel post-column reaction is used to confirm diquat and paraquat. Concentrations of 0.1–10 μg/kg of diquat and paraquat as the di-cations can be determined on 100-ml sample aliquots. Other HPLC methods are less sensitive and require larger volumes. Separation is achieved by solid-phase extraction on small (100 mg) bare silica columns. Chromatography is also carried out on bare silica. Both the mobile phase and the solid-phase extraction eluent are aqueous acidic solutions containing tetramethylammonium and ammonium ions.

INTRODUCTION

Paraquat and diquat are general herbicides for both terrestrial and aquatic plants. Both are double quaternary ammonium ions. Both paraquat and diquat are toxic to man, the former being implicated in many deaths[1]. Paraquat is structurally related to 1-methyl-4-phenyl-1,2,3,6-tetrahydropyridine (MPTP), a compound known to produce Parkinsonism in man[2], and paraquat has been shown to cause Parkinsonism in the leopard frog, *Rana pipiens* Schreber, when injected peritoneally[3].

Of published methods, those based on spectrophotometry[4–6] were neither sufficiently sensitive nor specific. Much of the chromatographic work on paraquat and/or diquat has concerned clinical samples with limits of detection at or above 100 μg/kg[7–9]. Liquid chromatography[10] and pyrolytic gas chromatography[11] have been employed to study natural waters, but detection limits were 50 or 10 μg/kg, respectively.

A high-performance liquid chromatographic (HPLC) method, not yet publish-

[a] Presented at the *12th International Symposium on Column Liquid Chromatography, Washington, DC, June 19–24, 1988*. The majority of the papers presented at this symposium have been published in *J. Chromatogr.*, Vols. 458 and 459 (1988) and 461 and 465, No. 1 (1989).

ed, has been developed for the United States Environmental Protection Agency (EPA) for diquat and paraquat[12]. This is a HPLC method employing diode-array detection and has minimum detection limits of 0.44 μg/kg for diquat and 0.80 μg/kg for paraquat using a 250-ml sample. The EPA method depends on UV-spectral scanning for qualitative confirmation.

An enzyme-linked immunosorbent assay (ELISA) has been reported[13] which has a detection limit of 1 or 0.1 μg/kg depending on the matrix. The ELISA method cannot be used for diquat and involves reagents not commercially available.

The present internally standardized isocratic HPLC method for diquat and paraquat is an improvement of our previously published work[14]. Samples are concentrated on smaller silica columns (100 mg) eluted with a smaller volume of an aqueous solution containing tetramethylammonium and ammonium ions at low pH, and chromatographed on silica with a similar but more dilute mobile phase. Two independent modes of detection are used: direct UV absorption at optimized wavelengths and UV absorption following post-column reaction with sodium hydrosulfite (sodium dithionite).

The present method achieves a ten-fold increase in sensitivity over our previous method. Thus both qualitative and quantitative confirmation is possible at a sensitivity which permits smaller sample size than any previous method.

EXPERIMENTAL

Materials

Downstream from the Model 501 analytical pump (Waters, Milford, MA, U.S.A.) was a Model LC600 autosampler (Perkin-Elmer, Norwalk, CT, U.S.A.). An Uptight guard column (Upchurch Scientific, Oak Harbor, WA, U.S.A.) was filled with Perisorb A, bare silica. The column consisted of two 33 mm × 4.6 mm I.D., 3-μm Perkin-Elmer bare silica cartridge columns in tandem. The column temperature was maintained by a Waters column oven and temperature control module.

Direct detection of analytes in the column effluent was provided by a diode-array detector, Model 235 (Perkin-Elmer). Following direct detection post-column reagent was pumped via a T-connection into the effluent stream using a Model E120 pump (Eldex Labs., San Carlos, CA, U.S.A.). Following post-column reaction (PCR) analyte derivatives were detected using a Model 783 variable-wavelength detector equipped with a tungsten lamp (ABI Analytical, Ramsey, NJ, U.S.A.).

Data were processed using an Omega-2 data station with an Epson EX-800 printer (Perkin-Elmer).

A twelve-station Visiprep vacuum manifold (Supelco, Bellefonte, PA, U.S.A.) was used to process solid-phase extraction (SPE) columns. SPE columns were 100 mg bare silica by Lida (Bensenville, IL, U.S.A.).

Tetramethylammonium hydroxide pentahydrate, ammonium sulfate, ammonium hydroxide, sulfuric acid, sodium hydroxide and sodium hydrosulfite, all reagent grade, were purchased from Fisher Scientific (Orlando, FL, U.S.A.). All membrane filters were purchased through Fisher Scientific.

Diquat dibromide (6,7-dihydrodipyrido[1,2-a:2′,1′-c]pyrazinediium dibromide) and paraquat dichloride (1,1′-dimethyl-4,4′-bipyridinium dichloride) were supplied by the EPA (Research Triangle Park, NC, U.S.A.). Diethylparaquat diiodide (1,1′-

diethyl-4,4′-bipyridinium diiodide) was supplied by Chevron (San Francisco, CA, U.S.A.).

Standard solutions. Diquat dibromide and paraquat dichloride were dried to constant weight at 110°C. The salts were cooled over Drierite at atmospheric pressure. The weighing form of diquat dibromide was taken to be the monohydrate, and paraquat dichloride was taken to be the tetrahydrate[15]. Stock solutions of each analyte, containing 100 ng/μl of the di-cations, were prepared in deionized water and stored at 4°C in plastic bottles.

Mobile phase. A solution of tetramethylammonium hydroxide pentahydrate (10.00 g) in 600 ml of water was adjusted to a pH between 2.5 and 5.0 by addition of 50% sulfuric acid. Ammonium sulfate (30.00 g) was added, and the volume was adjusted to 1 l with water. The solution was adjusted to a pH of 2.20 ± 0.02 with 50% sulfuric acid and filtered through a 0.45-μm Nylon filter (Fisher).

Post-column reagent. Sodium hydroxide (12.00 g) and sodium hydrosulfite (3.00 g) were dissolved in water, diluted to 1 l, and filtered through a 0.45-μm Metricel filter (Fisher Scientific). This solution must be prepared immediately before use.

Sodium hydrosulfite stored at atmospheric pressure over Drierite is usable for at least three months.

Solution A. Concentrated sulfuric acid (27.8 ml) was diluted to 1 l to produce a 1 *N* solution.

Solution B. Concentrated ammonium hydroxide (4 ml) was diluted with water to 200 ml.

Solution C (eluent). The eluent was prepared in the same way as the mobile phase except that 12.00 g rather than 10.00 g of tetramethylammonium hydroxide pentahydrate was used.

Methods

Reservoirs of 60-ml capacity were attached to 100-mg silica columns, using 1.5 cm × 6.4 mm O.D. Tygon tubing. To facilitate insertion into silica columns, the edge of the tubing was beveled, using scissors. The silica columns were inserted into a twelve-station vacuum manifold and pretreated by drawing through in series: solution A (2.5 ml), water (5 ml), solution B (2.5 ml) and water (5 ml).

Samples (20 or 100 ml) were fortified with diethylparaquat diiode (200 ng), which served as an internal standard. The samples were filtered at a dropwise rate through the silica columns. As soon as the columns became empty air flow was discontinued.

A 3-mm diameter, 0.45-μm Nylon filter was attached to the inlet of the silica column and a 3-ml polypropylene syringe was attached to the column outlet. The samples were gently eluted by forcing through with the syringe 500 μl of solution C in the reverse direction from sample loading. The eluate was collected in a tared polypropylene centrifuge tube, and sufficient solution C was added to adjust the weight to 0.50 ± 0.01 g. The tube was capped, vortex-mixed and stored at 4°C for later injection.

Extracts were transferred to 0.8-ml glass vials and placed in the autosampler programmed to inject 50 μl by overfilling a fixed loop. The mobile phase flow-rate was set at 0.8 ml/min, producing a pressure of 34.4 bar. The column consisted of two 33 mm × 4.6 mm I.D., 3-μm bare silica cartridge columns, which were heated to 70°C in a column oven.

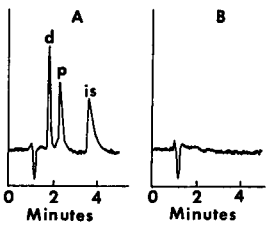

Fig. 1. (A) Analysis by direct detection of a 100-ml aliquot of well-water fortified with diquat (d), paraquat (p), and internal standard (I.S.). (B) The same well-water not fortified. The concentrations of diquat and paraquat (A) were 1 μg/kg and 10 ng of each, assuming 100% recovery, was injected.

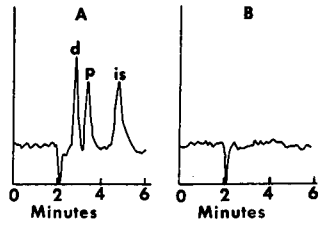

Fig. 2. (A) PCR analysis of a 100-ml aliquot of well-water fortified with diquat (d), paraquat (p), and internal standard (I.S.). (B) The same well-water not fortified. The concentrations of diquat and paraquat (A) were 1 μg/kg and 10 ng of each, assuming 100% recovery, was injected.

Monitoring wavelengths of 310 nm for diquat and 255 nm for paraquat were set on the diode-array detector for direct detection. Post-column detection was carried out simultaneously using a wavelength of 379 nm produced by a tungsten lamp. PCR detector was set at 0.001 a.u.f.s. with a time constant of 1 s. The flow-rate was 0.4 ml/min. The PRC mixing coil was a 2-m woven PTFE coil of 0.76 mm I.D. and was exposed to room air.

RESULTS AND DISCUSSION

The retention times by direct detection under the conditions described for diquat, paraquat, and the internal standard (diethylparaquat) were 1.9, 2.3 and 3.7 min, respectively. A typical chromatogram of well-water, spiked at 1 μg/kg with diquat and paraquat and carried through the procedure, is shown in Fig. 1 by direct detection and in Fig. 2 by detection following PCR. Retention times decrease with increasing tetramethylammonium ion concentration in the mobile phase.

In order to test the linearity of the method 100-ml samples of deionized water fortified with diquat and paraquat at 1.0, 3.0, 5.0 and 10 μg/kg were analyzed. Table I displays the slopes, intercepts, and correlation coefficients obtained by carrying out linear regression calculations of peak height with concentration for diquat and paraquat by direct and PCR detection. Table II shows the corresponding quantities for regression calculations using the ratio of the peak height of the analyte to that of the

TABLE I

CORRELATION OF PEAK HEIGHT WITH CONCENTRATION

In each case $n = 4$. Peak heights were in mV and concentrations were in μg/kg of the di-cations.

	Direct			*Post*		
	Slope	*Intercept*	*r*	*Slope*	*Intercept*	*r*
Diquat	45.1	−19.1	0.9997	48.3	−23.3	0.9997
Paraquat	45.6	−23.2	0.9998	40.4	−20.4	0.9998

TABLE II

CORRELATION OF ANALYTE TO INTERNAL STANDARD PEAK HEIGHT RATIO WITH CONCENTRATION

In each case $n = 4$. Concentrations were in μg/kg, as the di-cations.

	Direct			*Post*		
	Slope	*Intercept*	*r*	*Slope*	*Intercept*	*r*
Diquat	1.24	0.851	0.9947	1.19	0.783	0.9929
Paraquat	1.27	0.643	0.9954	0.998	0.619	0.9944

internal standard *versus* concentration. Clearly the use of peak-height ratios leads to smaller coefficients of correlation for both methods of detection. Analysts may wish to shorten analysis time by leaving out the internal standard.

In order to test the reproducibility of the method five 100-ml samples were analyzed at each of three concentrations, 0.1, 1 and 10 μg/kg. The coefficients of variation of peak height at each concentration are shown in Table III. The variability of peak height for direct detection is independent of concentration from 0.1 to 10 μg/kg for both diquat and paraquat. Using PCR peak height variability is comparable to that for direct detection at 10 μg/kg but increases for diquat as the concentration drops to 1 μg/kg and for paraquat as the concentration drops to 0.1 μg/kg.

The average recovery of diquat over the 0.1–10 μg/kg range was 117 ± 14% based on single point calibration using direct UV absorbance. By PCR the average diquat recovery was 119 ± 17%. Average paraquat recovery was 118 ± 12% by direct detection and 113 ± 19% by PCR detection.

It is important that samples be collected in plastic bottles as diquat and paraquat are adsorbed to glass[11]. Analytes are no longer adsorbed onto glass once dissolved in eluent (solution C).

Elution of SPE columns in the reverse direction is important in order to achieve high sensitivity. This technique has not led to serious interference with diquat or paraquat in more than 300 well-water samples.

Applying the present method to 20-ml sample volumes permits detection of diquat and paraquat at 1 μg/kg by both detection methods (data not shown). Our routine well-water monitoring is done on 20-ml sample aliquots.

TABLE III

VARIABILITY OF PEAK HEIGHT AT A GIVEN CONCENTRATION

Five extractions were made for each concentration. C.V. = Coefficient of variation.

Conc. (μg/kg)	*Direct detection: C.V. peak height (%)*		*Detection following PCR: C.V. peak height (%)*	
	Diquat	*Paraquat*	*Diquat*	*Paraquat*
0.1	3.7	6.5	15.2	19.8
1	7.5	6.1	11.9	4.6
10	4.1	6.1	4.1	5.9

A column temperature of 70°C was used to prevent excessive peak tailing. The silica columns tolerate the conditions of the assay well remaining usable for at least 400 injections.

Those interested in adapting the present method to more complex matrices should be aware that neither diquat nor paraquat are significantly eluted from silica by methanol, acetonitrile, or tetrahydrofuran. Such solvents may be useful in sample clean-up procedures.

Although a diode-array detector was used in the present method, it should be pointed out that the minimum requirement for all signals reported is a single time-programmable variable-wavelength detector. Thus confirmation is provided without the need for the UV-scanning capability used for confirmation by the proposed EPA method.

An improvement over our previously reported assay for diquat and paraquat has been presented, which allows lower detection limits (0.1 μg/kg *versus* 0.5 μg/kg) with smaller sample volumes (100 *versus* 250 ml). No other assay offers such high sensitivity for both diquat and paraquat. A volume of 20 ml suffices for detection at 1 ppb. The use of smaller sample volumes saves sample-preparation time, shipment costs, and storage space.

A unique PCR detection method, which compliments existing methods, allows confirmation of diquat and paraquat.

REFERENCES

1 H. M. Hassan and C. S. Moody, *Can. J. Physiol. Pharmacol.*, 60 (1982) 1367.
2 J. A. Javitch, R. J. D'Amato, S. M. Strittmatter and S. H. Snyder, *Proc. Natl. Acad. Sci. U.S.A.*, 82 (1985) 2177.
3 A. Barbeau, L. Dallaire, N. T. Buu, J. Poirier and E. Rucinska, *Life Sci.*, 37 (1985) 1529.
4 H. Maruyama and M. Ide, *J. Anal. Toxicol.*, 12 (1988) 33.
5 D. R. Jarvie and M. J. Stewart, *Clin. Chim. Acta*, 94 (1979) 241.
6 D. R. Jarvie, A. F. Fell and M. J. Stewart, *Clin. Chim. Acta*, 117 (1981) 153.
7 A. Pryde and F. J. Darby, *J. Chromatogr.*, 115 (1975) 107.
8 J. J. Miller, E. Sanders and D. Webb, *J. Anal. Toxicol.*, 3 (1979) 1.
9 R. Gill, S. C. Qua and A. C. Moffat, *J. Chromatogr.*, 255 (1983) 483.
10 I. Ahmad, *J. Assoc. Off. Anal. Chem.*, 66 (1983) 663.
11 A. J. Cannard and W. J. Criddle, *Analyst*, 100 (1975) 848.
12 W. J. Bashe, Technology Applications Inc., Cincinatti, OH 45268, personal communication.
13 J. VanEmon, B. Hammock and J. N. Seiber, *Anal. Chem.*, 58 (1986) 1866.
14 V. A. Simon, *LC · GC, Mag. Liq. Gas Chromatogr.*, 5 (1987) 899.
15 B. L. Worobey, *Pestic. Sci.*, 18 (1987) 245.

Journal of Chromatography, 479 (1989) 159–164
Elsevier Science Publishers B.V., Amsterdam — Printed in The Netherlands

CHROM. 21 670

Note

Optimization of size-exclusion separation of proteins on a Superose column

PAUL L. DUBIN* and JOSEPH M. PRINCIPI
Department of Chemistry, Indiana University–Purdue University at Indianapolis, 1125 East 38th Street, Indianapolis, IN 46205-2820 (U.S.A.)
(First received April 5th, 1989; revised manuscript received June 7th, 1989)

The chromatographic partition coefficient for size-exclusion chromatography (SEC) is obtained experimentally as

$$K_{SEC} = \frac{V_e - V_0}{V_t - V_0} \quad (1)$$

where V_e is the measured peak elution volume, V_0 is the column void volume or exclusion volume and V_t is the total column volume, *i.e.*, the sum of V_0 and the pore volume, V_p. Several treatments have appeared in which K_{SEC} is related to the dimensions of the stationary pores and the macromolecular solutes[1–3]. However, the migration of proteins on SEC columns is in fact typically influenced by electrostatic and hydrophobic factors, as well as by steric effects[4–6].

All aqueous SEC packings bear a discernible level of ionogenic groups which commonly produce a negative surface charge[8]; this stationary charge may interact with regions of similar or opposite charge on the proteins, leading to repulsion or retention. Such coulomb interactions are evidently most prominent in low ionic strength eluent, in the absence of screening by small ions. However, it is not at all clear that these interactions can be totally suppressed by the addition of salt, for two reasons. First, the reduction of protein solvation at high ionic strength may facilitate binding via enhanced hydrophobic interactions. Second, if the protein's ionic groups actually ion pair with those on the packing, as is indeed suggested by the common reference to "ion-exchange" mechanisms[9], then the interaction between the stationary phase and the protein may be so intimate that the ionic strength of the medium might not screen these interactions through the usual Debye–Hückel square root dependence. Put differently, the proximity of the stationary phase and the protein ionophores in the binding mode might preclude the intervention of the bulk electrolyte. Such considerations may be involved in the finding that protein retention volumes may display minima or maxima with increasing ionic strength for a number of SEC packings[4,10].

The role of the ionic strength (I) must primarily involve the effective distance of electrostatic forces, *i.e.*, the Debye length (see, *e.g.*, ref. 11), while the influence of pH

0021-9673/89/$03.50

on retention depends on the pK values of solute and packing ionogens. Repulsive forces should dominate at high pH, at which condition both packing and solute are negatively charged; the situation is more complex in neutral or acidic media, in which some regions of the protein bear a charge opposite in sign to that of the stationary phase. The net electrostatic force between the protein and the packing will then be quite sensitive to orientation and rotational freedom of the protein in the near proximity of the stationary phase.

The co-existence of several separation mechanisms is of course frequently exploited to maximize peak resolution[4]. In practise, this may involve the manipulation of solvent gradients with SEC packings that contain both hydrophobic and ionic substituents. Such mixed-mode chromatography however, vitiates the interpretation of retention volumes in terms of molecular dimensions. Furthermore, it is difficult to analyze the mangnitude of non-steric effects, unless conditions for "ideal" behavior can be identified as a point of reference. The determination of solvent conditions that correspond to "pure SEC" is therefore of practical and fundamental significance. In this report, we describe an empirical, but efficient procedure to identify such "ideal" conditions.

EXPERIMENTAL

Proteins obtained from Sigma (99+% purity) were thyroglobulin (bovine) (mol.wt. 669 000 daltons, pI = 4.6); apoferritin (horse spleen) (467 000 daltons, pI = *ca.* 5.0); catalase (bovine liver) (232 000 daltons, pI = 5.6), bovine serum albumin (66 000 daltons, pI = 4.8), ovalbumin (44 000 daltons, pI = 4.6), myoglobin (17 000 daltons, pI = 7.3) and cytochrome *c* (12 400 daltons, pI = 10.6). All proteins gave a single symmetrical chromatographic peak. Corresponding Stokes radii, obtained from a variety of references, were 85, 61, 52, 36, 28, 20 and 16 Å, respectively. Blue dextran was obtained from Pharmacia.

A prepacked Superose 6 column (30 cm × 1.00 cm I.D., Pharmacia) with a molecular weight range of 5000–500 000 (globular proteins) was eluted with sodium chloride–sodium phosphate buffer (9:1), at varying pH and ionic strengths, at 23 ± 1°C using a Milton Roy minipump. A Rheodyne procolumn filter (0.2 μm) was placed in-line to protect the column from particulate matter. The column exclusion volume and total permeable volume, as measured with blue dextran and deuterium oxide, were 14.58 and 22.42 ml, respectively. At a typical flow-rate of 0.35 ml min^{-1} the plate count, as measured by injection of 5% deuterium oxide, was 9000 m^{-1}. Samples, containing typically 3.5 mg ml^{-1} protein, were injected via a Rheodyne 7010 (200 μl) loop injector, after filtration through disposable nylon 0.45-μm syringe filter tips (National Scientific Co.). Detection was by refractive index (Waters Assoc., R401) or UV absorbance at 254 nm (Altex, Model 153).

RESULTS AND DISCUSSION

Geometric considerations suggest that, for solutes and pores with well defined symmetrical geometries

$$K_{SEC} = (1 - \alpha)^{\lambda} \qquad (2)$$

where $\alpha = R/r_p$ is the ratio of solute and pore sizes, and λ depends on pore geometry, *i.e.* $\lambda = 2$ for cylindrical pores and 3 for spherical pores[13]. Although direct methods fail to reveal a uniform pore geometry for any gel packing[14], data for neutral polysaccharides on porous glass packings are well fit by eqn. 2 using $\lambda = 2$ (ref. 15). Furthermore, these same results indicate that the effective cylindrical radius of the pores may be identified with the value from mercury porosimetry.

The evaluation of R is hardly straightforward: the macromolecular dimensional parameter that controls elution in SEC is the subject of debate. For solutes of near-spherical symmetry, retention may be predicted, with equal accuracy, by a number of variables, including the Stokes radius and the viscosity radius[16]. We have recently shown, however, that neither of these parameters uniformly determines K_{SEC} for asymmetric macromolecules of varying shapes[17]. For proteins, however, R may be identified with dimensions determined by hydrodynamic and other techniques. In this work, the Stokes radius, R_S, is employed.

If electrostatic and hydrophobic effects influence the retention of proteins, deviations from a geometric relation such as eqn. 2 are expected. For a series of globular proteins with different isoelectric points, such as those studied here, with pI ranging from 4.6 to 10.6, it is unlikely that these deviations could be uniform, because the charge states of the proteins studied vary widely at any chosen pH. Conversely, congruence of the data with eqn. 2 may be taken as indicating an absence of non-ideal interactions. The magnitude of the deviations from eqn. 2 may be quantitatively parameterized by the regression coefficient of plots of K_{SEC} *vs.* R_S; for this purpose it is not necessary to assume a specific form for $K_{SEC}(R_S)$, *i.e.*, a specific value for λ. Optimization of solvent pH and ionic strength may then be guided by maximization of the regression coefficient.

Since the dependence of K_{SEC} on I and pH is not known *a priori*, an empirical optimization procedure was used to identify the combination of I and pH corresponding to the largest value of the regression coefficient, presumably 1.00. A simplex method[18] was used to maximize the regression coefficient of $K_{SEC}(R_S)$ in the I, pH coordinate system, as shown in Fig. 1. Fig. 2 illustrates the dependence of K_{SEC} on R_S at conditions far from the optimum, while Fig. 3 shows the results obtained at the optimum conditions, $I = 0.38$, pH 5.5. As evident from the insert of Fig. 3, the data conform rather well to eqn. 2, with $\lambda = 2$. The result for thyroglobulin, not shown in the insert, deviates slightly from the curve, and we suggest that this largest protein might sample an average pore size different from that "seen" by the others.

Our results differ from those of Waldmann-Meyer[19] whose data for proteins on Agarose and Sephadex gels conformed to eqn. 3

$$K_{SEC} = k - R_S/R_x \cos\theta \tag{3}$$

corresponding to conical pore geometry. (Here R_x and θ are the geometric parameters of the pore.) This difference could arise in several ways, including an actual difference in pore geometry between the packings used in the two studies, or distortion of the data in ref. 19 through protein–packing interactions. In addition, discerning between eqns. 2 and 3 may require precision beyond that typically available.

We believe that Fig. 3 corresponds to pure size exclusion; therefore, under the conditions represented by the other vertices in Fig. 1, some protein–stationary phase

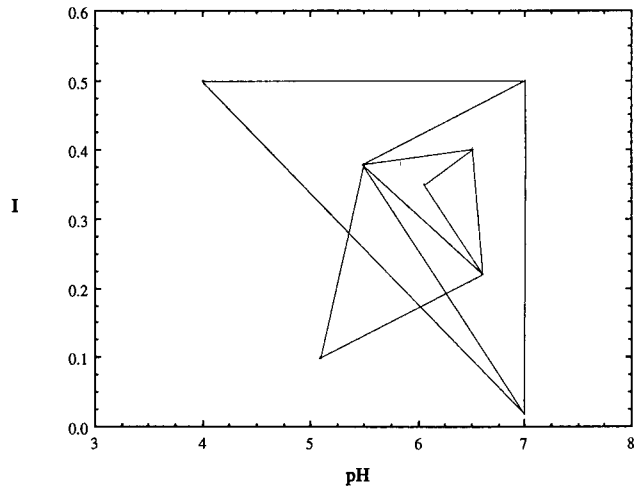

Fig. 1. Simplex optimization of the regression coefficient, r, of plots of K_{SEC} *vs.* R_S, for globular proteins in eluents of varying ionic strength, I, and pH, on Superose 6 column.

interactions take place. Such interactions are apparently difficult to suppress, even though the charge on Superose is presumably quite low in the pH range studied, and even though the hydrophobicity parameter[20] for this packing is low compared to other gels. It is also of interest to note that the optimal pH is below the isoelectric point of most of the proteins, so that the average protein net charge is opposite in sign to the charge on the packing. This effect, which would be expected to lead to enhanced retention through coulombic attraction, is obviously outweighed by the reduction of the packing charge at the lower pH. Kopaciewicz and Regnier[4] also noted the simultaneous effects of protein and packing charge for derivatized silica supports, and

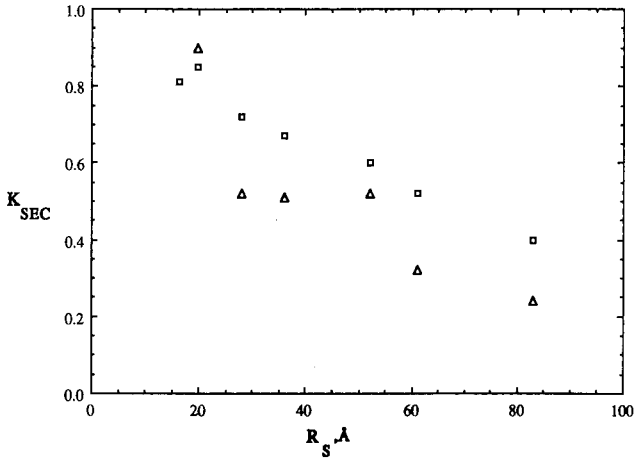

Fig. 2. K_{SEC} *vs.* R_S in mobile phase: (□) pH 6.04, I = 0.35 M; (△) pH 7.0, I = 0.01 M.

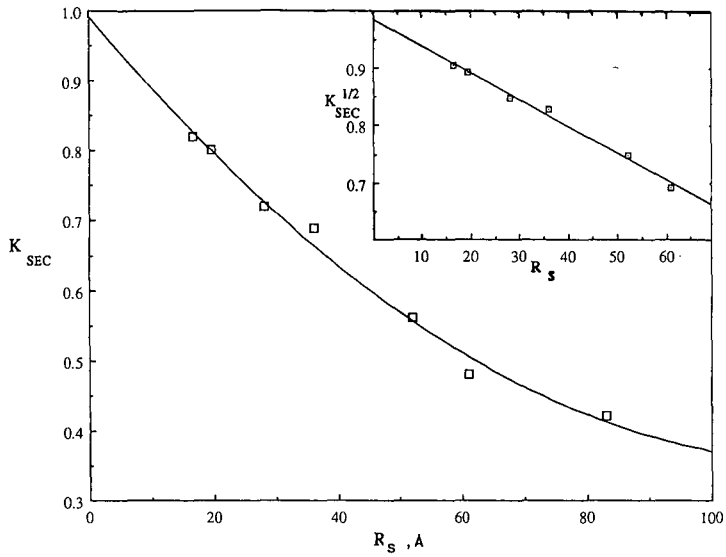

Fig. 3. K_{SEC} *vs.* R_S in optimized mobile phase, with pH 5.5, $I = 0.38$ *M*. Insert: data plotted according to eqn. 2 (see text for explanation).

Mori and Kato[21] similarly described the retention behavior of proteins on diol-bonded porous glass. Both of theses packings would be expected to have considerably larger surface charge densities than Superose.

Three semi-empirical treatments have dealt with electrostatic interactions in SEC[22–24], all of them focussing on repulsive effects that lead to early elution. These three approaches all relate the reduction in V_e to the dimensions of an electrical double layer, but the first two[22,23] assign the effect to the potential around the solute, while the third[24] emphasizes the double layer near the packing. While all three descriptions are cleary incomplete, the present results show the importance of the charge on the packing.

CONCLUSIONS

An empirical optimization procedure leads to mobile phase conditions under which a number of globular proteins with differing isoelectric points, show a dependence of K_{SEC} on Stokes radius in close agreement with that predicted from a simple geometric model. It is suggested that these conditions correspond to "ideal" SEC, and deviations therefrom to electrostatic interactions with the packing. Studies are currently underway to establish whether such "ideal" conditions exist for SEC stationary phases that are more hydrophobic or more highly charged than Superose 6.

ACKNOWLEDGEMENT

Partial support by a grant from S. C. Johnson & Son is gratefully acknowledged.

REFERENCES

1 E. F. Cassasa, *Macromolecules*, 9 (1976) 182–185, and references cited therein.
2 J. C. Giddings, E. Kucera, C. P. Russell and M. N. Meyers, *J. Phys. Chem.*, 72 (1968) 4397–4408.
3 M. E. Himmel and P. G. Squire, in P. L. Dubin (Editor), *Aqueous Size-Exclusion Chromatography*, Elsevier, Amsterdam, 1988, Ch. 1.
4 W. Kopaciewicz and F. E. Regnier, in M. T. W. Hearn, F. E. Regnier and C. T. Wehr (Editors), *High-Performance Liquid Chromatography of Proteins and Peptides*, Academic Press, Orlando, FL, 1983, pp. 151–159.
5 H. D. Crone, *J. Chromatogr.*, 92 (1974) 127–135.
6 G. Siepke, H. Müllner and U. Grau, *Angew. Chem., Int. Ed. Engl.*, 25 (1986) 535–552.
7 P. Roumeliotis, K. K. Unger, J. Kinkel, G. Brunner, R. Wieser and G. Tschank, in F. Lottspeich, A. Henschen and K. P. Hupe (Editors), *HPLC in Protein and Peptide Chemistry*, Walter de Gruyter, Berlin, 1981, pp. 72–82.
8 P. L. Dubin, in P. L. Dubin (Editor), *Aqueous Size-Exclusion Chromatography*, Elsevier, Amsterdam, 1988, Ch. 3.
9 H. G. Barth, *J. Chromatogr. Sci.*, 18 (1980) 409–429.
10 E. Pfannkoch, K. C. Lu, F. E. Regnier and H. G. Barth, *J. Chromatogr. Sci.*, 18 (1980) 430.
11 W. J. Moore, *Basic Physical Chemistry*, Prentice-Hall, Englewood Cliffs, NJ, 1983, p. 373.
12 T. Andersson, M. Carlsson, L. Hagel, P.-Å. Pernemalm and J.-C. Janson, *J. Chromatogr.*, 326 (1985) 33–44.
13 E. F. Cassasa, *J. Phys. Chem.*, 75 (1971) 3929–3939.
14 L. Hagel, in P. L. Dubin (Editor), *Aqueous Size-Exclusion Chromatography*, Elsevier, Amsterdam, 1988, Ch. 5.
15 H. Waldmann-Meyer, *J. Chromatogr.*, 350 (1985) 1–13.
16 M. Potschka, *J. Chromatogr.*, 441 (1988) 239–260.
17 P. L. Dubin and J. M. Principi, *Macromolecules*, 22 (1989) 1891–1896.
18 K. W. Burton and G. Nickless, *Chemometrics and Intelligent Laboratory Systems*, 1 (1987) 135–149.
19 H. Waldman-Meyer, *J. Chromatogr.*, 410 (1987) 233–248.
20 P. L. Dubin and J. M. Principi, *Anal. Chem.*, 61 (1989) 780–781.
21 S. Mori and M. Kato, *J. Liq. Chromatogr.*, 10 (1987) 3113–3126.
22 M. G. Styring, C. J. Davison, C. Price and C. Booth, *J. Chem. Soc., Faraday Trans. 1*, 80 (1984) 3051–3058.
23 M. Potschka, *Anal. Biochem.*, 162 (1987) 47–64.
24 P. L. Dubin, C. M. Speck and J. I. Kaplan, *Anal. Chem.*, 69 (1988) 895–900.

Journal of Chromatography, 479 (1989) 165–169
Elsevier Science Publishers B.V., Amsterdam — Printed in The Netherlands

CHROM. 21 704

Note

Gas chromatographic retention indices of tear gases on capillary columns

B. R. GANDHE*, R. C. MALHOTRA and P. K. GUTCH
Defence Research and Development Establishment, Tansen Road, Gwalior 474002 (India)
(First received March 6th, 1989; revised manuscript received June 14th, 1989)

Tear gas compounds (lacrimators) cause irritation of the eyes, nose, respiratory tract and skin with the consequent production of profuse tears and mucous. On prolonged exposure individuals may suffer acute pain in the chest, difficulty in breathing and vomiting[1]. Methods are required for their rapid and sensitive identification, and gas chromatography (GC) with a fused-silica capillary column is the method of choice due to its high resolution power and sensitivity.

The correlation of retention indices between an unknown and reference compound on two or more columns of different polarities is generally sufficient for identification purposes. The measurement of Kováts retention indices[2] is useful only when compounds with similar retention behaviour are to be studied, as the column temperature in these measurements is held constant. Recently, temperature-programmed retention indices using Van den Dool and Kratz equation[3] have been found to be useful for compounds of defence interest[4–7].

In this paper we report temperature-programmed retention indices for several tear gas compounds using Van den Dool's equation[3]. GC of these compounds as a class on a fused-silica capillary column and temperature-programmed retention indices for most of them have not previously been reported. Further, the measurement of retention indices on two columns with different polarities is shown to be applicable for the identification of tear gases in air.

EXPERIMENTAL

Standards

C_6–C_8 *n*-alkanes were purchased from BDH (Poole, U.K.) and C_9–C_{24} *n*-alkanes from Fluka (Buchs, Switzerland).

Tear gas compounds

Chloroacetone (A-Stoff) was obtained from Fluka and methyl ethyl ketone, benzyl chloride, benzyl bromide, ethyl cyanoacetate, benzoyl chloride and ethyl bromoacetate from BDH.

ω-Chloroacetophenone (CN) was prepared by chlorination of acetophenone[8]. *o*-Chlorobenzylidene malononitrile (CS) was prepared by condensation of *o*-chlorobenzaldehyde with malononitrile[9].

0021-9673/89/$03.50

The purity of all the compounds was checked by GC before further use and was found to be >99% in all instances. Further, CS and CN were characterized by IR and MS data (CS, $M^{+\cdot}$ = m/z 188; CN, M^{+} = m/z 154.) Their melting points were in good agreements with literature values.

Instrumentation

A Shimadzu Model GC-9APTF gas chromatograph equipped with a flame ionization detector and a Chromatopak C-R3A data processor was used. Two fused-silica capillary columns (30 m × 0.32 mm I.D.) with a 0.25-μm film of surface-bonded and cross-linked stationary phase were used: (a) DB-1701 (86% dimethyl-, 14% cyanopropylphenyl polysiloxane) and (b) DB-1 (100% dimethylpolysiloxane), supplied by J & W Scientific (Folsom, CA, U.S.A.). The carrier gas was nitrogen at 1.25 kg/cm^2 at the inlet. Hydrogen was supplied to the detector at 40 ml/min and air at 400 ml/min. The column oven temperature was held at 60°C for 2 min, increased at 8°C/min up to 200°C. The injector block was kept at 210°C and the detector block at 230°C. A splitless Grob-type injection system was used.

Measurement of retention indices

In order to measure the retention indices, generally solutions containing several tear gases in acetone together with *n*-alkane standards were injected on to the GC column. The sample size in each instance was about 0.1 μl. The amounts of individual tear gases and *n*-alkanes present were in the range 10–15 ng. The retention times were recorded with an accuracy of up to 0.001 min with the help of the Shimadzu C-R3A data processor.

In order to identify individual components in the mixture, an authentic sample of each tear gas was injected separately and its retention time was compared with that of the component in mixture.

Temperature-programmed retention indices for individual compounds were calculated as described in literature[3].

RESULTS AND DISCUSSION

Temperature-programmed retention indices for tear gas compounds on two capillary columns are given in Table I. The reliability of the retention indices depends on the accurate measurements of retention times and reproducible temperature programming and carrier gas flow-rates. The retention times were measured in up to 0.001-min increments. The reproduciblity of the temperature programming was satisfactory. The flow-rate of the carrier gas and other chromatographic conditions were maintained constant. The standard deviation of the retention index of any particular compound was less than 0.8 (n = 5).

Errors arising from deterioration of the stationary phase can be avoided by use of bonded phases. Application of a small sample size (0.1 μl) with nanogram level concentrations of the components helped in avoiding errors that generally arise from overloading of the column. The peaks were sharp and symmetrical even on polar phase. A typical chromatogram for some tear gas compounds obtained on the DB-1701 column is shown in Fig. 1.

As can be seen from the data in Table I, the retention indices on the polar

TABLE I

TEMPERATURE-PROGRAMMED RETENTION INDICES OF TEAR GAS COMPOUNDS ON DB-1 AND DB-1701 FUSED-SILICA CAPILLARY COLUMNS

Heating rate 8°C/min. Other GC conditions as described in the text.

Compound	*Retention index*[a]		
	DB-1	*DB-1701*	*ΔI*
Methyl ethyl ketone	721.6 ± 0.3	810.6 ± 0.2	89.0
Chloroacetone	850.6 ± 0.6	989.8 ± 0.4	139.2
Bromoacetone	876.5 ± 0.5	1027.6 ± 0.4	151.1
Ethyl bromoacetate	986.5 ± 0.5	1061.5 ± 0.6	75.0
Benzyl chloride	1002.2 ± 0.5	1122.5 ± 0.4	120.3
Ethyl cyanoacetate	1026.7 ± 0.4	1140.8 ± 0.4	114.1
Benzoyl chloride	1038.5 ± 0.6	1193.7 ± 0.7	155.2
ω-Chloroacetophenone (CN)	1229.8 ± 0.5	1471.7 ± 0.8	241.9
o-Chlorobenzylidene malononitrile (CS)	1487.6 ± 0.5	1810.4 ± 0.5	322.8

[a] Mean ± S.D. (n = 5).

stationary phase are higher than those on the non-polar phase. Further, the difference in the retention indices value on the polar and non-polar columns (ΔI) is higher for aromatic compounds such as CS and CN than for aliphatic compounds such as bromoacetone. The large variations in the ΔI values can be attributed to the different chemical natures and physical properties of the tear gases studied.

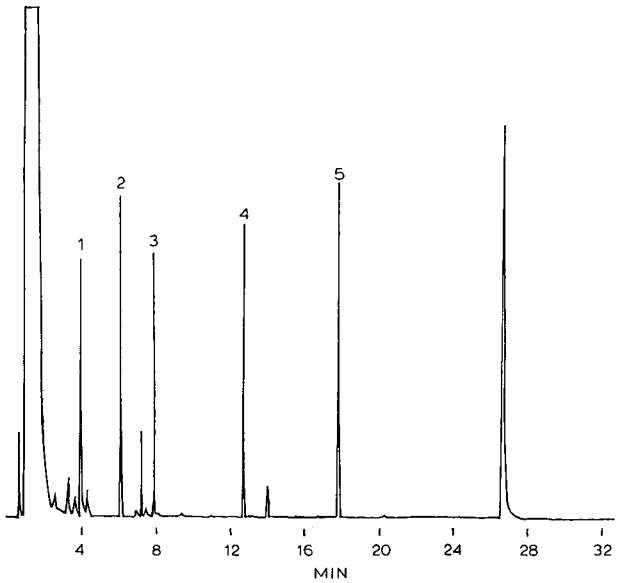

Fig. 1. Separation of tear gases on a DB-1701 fused-silica capillary column (30 m × 0.32 mm I.D., film thickness 25 μm). Chromatographic conditions are described in the text. Peaks: 1 = chloroacetophenone; 2 = benzyl chloride; 3 = benzoyl chloride; 4 = CN; 5 = CS.

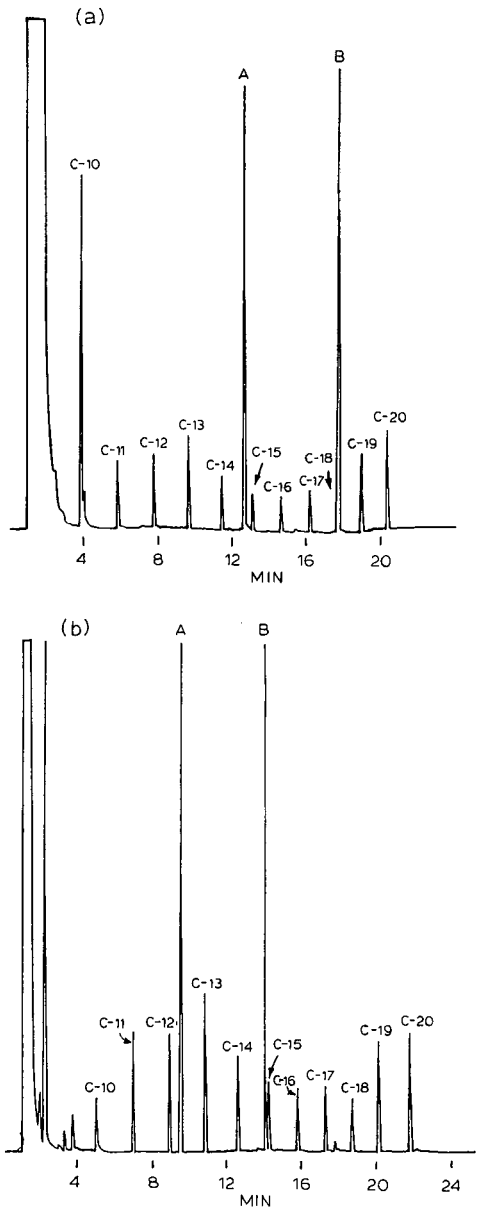

Fig. 2. Chromatograms obtained on (a) DB-1701 and (b) DB-1 columns for tear gas compounds recovered from a contaminated air sample. Peaks: A = CN; B = CS; C-10 to C-20 = *n*-alkanes.

The retention indices for CN and CS obtained here are in very good agreement with those reported by D'Agostino and Provost[4]. However, data for other compounds was not available in the literature.

TABLE II

RETENTION INDICES FOR CN AND CS RECOVERED FROM CONTAMINATED AIR IN COMPARISON WITH EXPECTED VALUES

GC conditions as described in the text.

Peak	*Retention index*[a]			
	DB-1		*DB-1701*	
	Observed	*Expected*[b]	*Observed*	*Expected*[b]
A (CN)	1226.5 ± 0.6	1229.8 ± 0.5	1470.8 ± 0.5	1471.7 ± 0.8
B[c] (CS)	1485.2 ± 0.7	1487.6 ± 0.5	1807.2 ± 0.6	1810.4 ± 0.5

[a] Mean ± S.D. (n = 5).
[b] See Table I.
[c] See Fig. 2.

Analysis of artificially contaminated air samples

To check the applicability of method for the identification of tear gas compounds in air, air in a closed container was artificially contaminated with vapours of CN and CS. It was then passed through a cold acetone trap (0°C) and the trap solution was subjected to GC analysis together with n-alkane standards. Typical chromatograms obtained on the two columns for CN and CS after recovery from air are shown in Fig. 2. Table II shows the observed and expected retention indices for these compounds, which are in good agreement.

ACKNOWLEDGEMENTS

The authors thank Brig. K. M. Rao, Director, DRDE, Gwalior, for providing facilities for this work and Dr. P. K. Ramachandran, Emeritus Scientist, for valuable suggestions. Thanks are also due to Mr. S. K. Shinde for technical assistance and Mr. Mitthan Lal for typing the manuscript.

REFERENCES

1 R. C. Malhotra and P. Kumar, *Def. Sci. J.*, 37 (1987) 281.
2 E. Kováts, *Helv. Chim. Acta*, 41 (1958) 1915.
3 H. Van den Dool and P. D. Kratz, *J. Chromatogr.*, 11 (1963) 463.
4 P. A. D'Agostino and L. R. Provost, *J. Chromatogr.*, 331 (1985) 47.
5 A. Manninen (Editor), *Systemátic Identification of Chemical Warfare Agents*, Ministry for Foreign Affairs of Finland, Helsinki, 1982, p. 37.
6 J. Cordonnier and A. Heyndrickx, in A. Heyndrickx (Editor) *Proceedings of the Second World Congress on New Compounds in Biological and Chemical Warfare, Ghent, August 24–27, 1986*, p. 500.
7 P. A. D'Agostino and L. R. Provost, *J. Chromatogr.*, 436 (1988) 399.
8 F. Siegfried, *Manual of Military Chemistry*, Vol. 1, NITS, U.S. Department of Commerce, Springfield, VA, 1982, p. 37.
9 B. B. Corson and R. W. Stoughton, *J. Am. Chem. Soc.*, 60 (1928) 2825.

Journal of Chromatography, 479 (1989) 170–175
Elsevier Science Publishers B.V., Amsterdam — Printed in The Netherlands

CHROM. 21 676

Note

Use of a stop-flow technique to study on-column decomposition in supercritical fluid chromatography

M. B. EVANS* and M. S. SMITH
Division of Chemical Sciences, Hatfield Polytechnic, College Lane, Hatfield, Hertfordshire (U.K.)
and
J. M. OXFORD
Biochemical Pharmacology Department, Glaxo Group Research, Park Road, Ware, Hertfordshire (U.K.)
(First received March 20th, 1989; revised manuscript received June 13th, 1989)

The on-column decomposition of analytes during chromatography can lead to reductions in peak area, shifts of baseline and in extreme cases complete loss of the analyte peak and appearance of new peaks. Whilst relatively common in gas chromatography (GC)[1–3], the phenomenon seldom occurs in liquid chromatography (LC) and a similar situation might be expected to apply to packed-column supercritical fluid chromatography (SFC).

During the course of a study of drug metabolites by SFC inconsistent quantitative results were observed for N-oxides[4]. Since for the same calibration solution peak areas appeared to vary with column residence time on-column decomposition was suspected. In order to test this proposition a systematic study has been performed using test solutes substances, that also are amenable to gas and liquid chromatography, for which the decomposition chemistry is well understood.

The results of this work, which clearly demonstrate that on-column decomposition can lead to errors in packed-column SFC now are presented.

EXPERIMENTAL

Apparatus

SFC was performed on 100 mm × 4.6 mm I.D. stainless-steel columns packed with 5-μm Spherisorb silica, 5-μm aminopropyl silica or 7-μm carbon black (Shandon, Runcorn, U.K.). Columns were heated in a Model TC 1900 oven (ICI Scientific Instruments, Dingley, Australia) at temperatures up to 91°C. The mobile phase consisting of mixtures of carbon dioxide (British Oxygen Gases, London, U.K.) and methanol was pumped through the system by Model 302 and 303 piston pumps (Gilson, Middleton, WI, U.S.A.) controlled by means of an Apple II GS microcomputer. The pump head was cooled to −15°C by means of a RTE-4 refrigerated bath circulator (Jencons, Leighton Buzzard, U.K.) to facilitate the filling of the pump with liquid mobile phase. Samples were introduced by means of a Rheodyne Model 7125 injector fitted with a 20-μl sample loop. The column effluent was monitored by a Model 757 variable wavelength UV detector (Kratos Analytical, Ramsey, NJ,

0021-9673/89/$03.50

U.S.A.) set at 254 nm. A Tescom back-pressure regulator (Tescom Instruments, Elk River, MI, U.S.A.) was used to maintain supercritical conditions.

The high-performance LC (HPLC) system consisted of Model PU 4015 piston pump (Philips Analytical, Cambridge, U.K.), a Rheodyne Model 7125 injector fitted with a 10-μl injector loop and a Model PU 4025 UV detector (Philips Analytical) operated at 254 nm. Chromatography was performed on 250 mm × 4.6 mm I.D. stainless-steel columns packed with 10-μm Partisil ODS-1 or 5-μm Spherisorb silica (Phase Separations, Queensferry, U.K.). The columns were thermostated by means of a Model TC 1900 oven (ICI Scientific Instruments).

The GC experiments were carried out on a Model 204 gas chromatograph (Philips Analytical) equipped for packed and capillary column operation with on-column injection and flame ionization detection. Chromatography was performed on 2 m × 4 mm I.D. glass columns packed with 10% (w/w) OV-1 or PEG 20M on 80–100 mesh Chromosorb P and a 10 m × 0.32 mm I.D. fused-silica capillary coated with PEG 20M, film thickness 0.5 μm (Thames Chromatography, Maidenhead, U.K.). Nitrogen or helium was used as carrier gas with a Model 151/3G toggle valve (Hoke International, Harrow, U.K.) in the gas line to enable stop-flow operation.

Materials

HPLC-grade methanol and acetonitrile were obtained from BDH (Poole, U.K.) whilst 2-phenylpropan-2-ol, 1-phenylpropan-2-ol, 2-phenylpropan-1-ol and propiophenone were obtained from Aldrich (Gillingham, U.K.).

RESULTS AND DISCUSSION

There is increasing evidence to suggest that SFC is appropriate for the assay of thermally liable compounds[5–7]. Normally such compounds are polar in nature and require the use of mobile phase with high percentages of polar modifiers, such as methanol, which in turn necessitate operation at elevated temperatures to maintain supercritical conditions. For instance, Cheuh and Prausnitz[8] have shown that for a carbon dioxide–methanol (80:20, v/v) mixture column temperatures in excess of 75°C are necessary. At such temperatures on-column degradation of thermally liable compounds is a possibility, especially with silica-based stationary phases, where acid-catalysed elimination reactions can occur. In order to test this thesis a series of phenylalkanols with primary, secondary and tertiary hydroxyl groups have been examined by stop-flow SFC and for comparison by GC and LC.

Rapid on-column reactions generally are associated with the appearance of additional peaks due to the fragmentation of molecules. On the other hand relatively slow on-column reactions lead to apparently normal chromatograms but with reduced peak areas which lead to unsuspected quantitative errors. Two techniques may be used to detect on-column reactions which are not manifested by the appearance of additional peaks or baseline disturbance. The first involves the measurement of peak areas for a labile test substance relative to those of a stable internal standard for a range of column temperatures. Here reductions of retention and associated peak areas at the higher temperatures can lead to uncertainties, also comparisons are complicated by differences in solute residence times. These limitations can be overcome by the second method, stop-flow chromatography, which involves interuption of the elution process

by stopping the mobile phase flow when the solutes are midway down the column. The analyte and internal standard thus trapped on the column continue to undergo dynamic partition and or adsorption equilibria and any associated chemical reactions. Subsequent elution of the solutes by resumption of the mobile phase flow yields a chromatogram from which peak area measurements may be made to indicate the extent of analyte decomposition. The latter approach was preferred in the present work.

As test compounds were chosen a range of phenyl propanols with increasing ease of dehydration due to the presence of primary (I), secondary (II) or tertiary (III) hydroxyl groups.

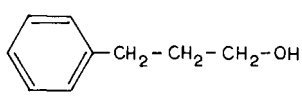

I

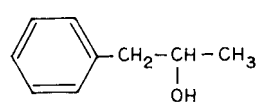

II

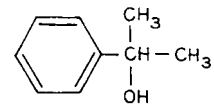

III

In the presence of acidic catalysts the alcohols undergo an E1 reaction[9] following initial protonation to yield conjugated propenylbenzenes via a carbocation:

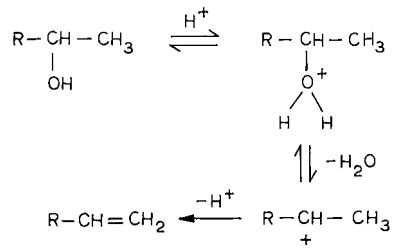

Silica-based stationary phases, which are commonly used in chromatography, have acidic surfaces owing to the presence of silanol groups which could act as a source of protons[10] for the initial step of the decomposition reaction.

In a preliminary experiment all three alcohols were studied by stop-flow SFC using a silica column at 91°C with an input pressure of 141 bar. For each measurement the mobile phase flow was stopped once the sample was judged to be half-way down the column. Peak areas of test alcohol and propiophenone (internal standard) were measured on the resumption of flow. Taking a normal chromatogram as a reference point the peak area ratios were used to calculate the relative reaction rates shown in Fig. 1. As expected the tertiary alcohol displayed the greater rate of dehydration. Furthermore the results suggest that significant quantitative errors could arise except where high mobile phase flow-rates are employed. On-column decomposition of the primary and secondary alcohols in contrast was insignificant.

Bonded phases with reduced silanol contents would be expected to be less catalytic and this is borne out in practice as illustrated by data obtained using an

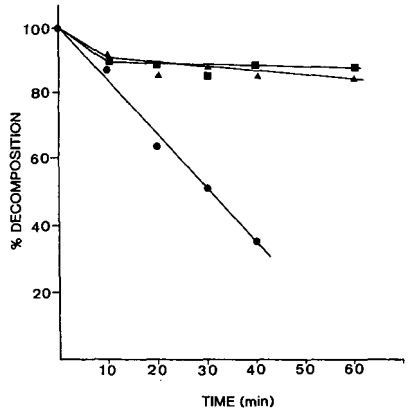

Fig. 1. On-column decomposition of phenylpropanols during stop-flow SFC on a 5-μm Spherisorb silica column at 91°C with carbon dioxide–methanol (99:1, v/v) mobile phase and UV detection at 245 nm. Compounds: ■ = I; ▲ = II; ● = III.

aminopropyl column, see Fig. 2. Even better results were obtained using a graphitized carbon black column where no discernible decomposition occurred. However, retentions on this phase were significantly greater than on the silica-based phases, owing to its greater affinity towards aromatic compounds.

No significant on-column decompositon of 2-phenylpropan-2-ol was found to occur during reversed-phase LC under normal conditions. However, in the presence of acidic eluents and elevated column temperatures moderately rapid decomposition

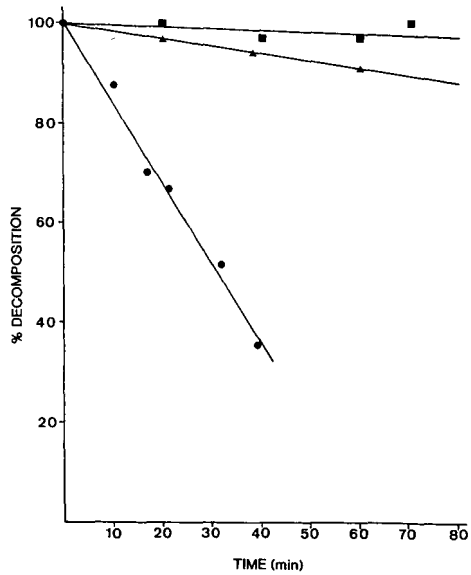

Fig. 2. Effect of stationary phase upon the on-column decomposition of 2-phenylpropan-2-ol during stop-flow SFC at 91°C. Stationary phases: ■ = graphitized carbon black; ▲ = aminopropyl silica; ● = silica gel.

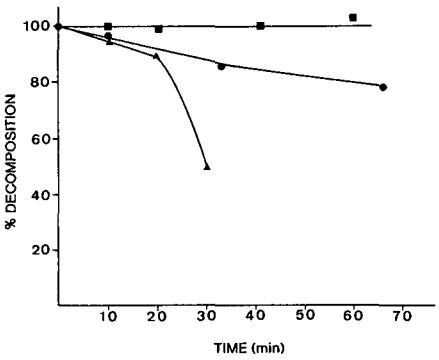

Fig. 3. On-column decomposition of 2-phenylpropan-2-ol during stop-flow normal- and reversed-phase liquid chromatography. ▲ = 5-μm Spherisorb silica at room temperature with *n*-heptane–isopropanol (97.5:2.5, v/v) as eluent; ● = 10-μm Partisil ODS at 81°C with acetonitrile–0.1 *M* phosphoric acid (55:45, v/v) as eluent; ■ = 10-μm Partisil ODS at room temperature with acetonitrile–water (55:45, v/v) as eluent. Propiophenone used as internal standard.

occurred under stop-flow conditions, as shown in Fig. 3. Under normal-phase conditions with silica gel as stationary phase and *n*-heptane–isopropanol as eluent rapid analyte decomposition occurred even at room temperature. It is interesting to note that 2.5% of isopropanol in the mobile phase was apparently insufficient to prevent protonation of the analyte molecules leading to their decomposition.

Consistent with previous observations[11] on-column reactions were found to occur during stop-flow GC on both OV-1 and PEG 20M packed columns. On the other hand, no decomposition was apparent with the PEG 20M fused-silica capillary column as might have been expected. However, the results in the latter case were less conclusive owing to the extensive zone dispersion which occurred whilst the carrier gas flow was suspended. An observation that is consistent with the differences between analyte gas phase diffusion in open-tubular and packed chromatographic columns[12].

The results of this work demonstrate that caution should be exercised when analysing labile substances, particularly those prone to acid catalysed elimination reactions, on silica-based columns, not only in GC but also LC and SFC.

ACKNOWLEDGEMENTS

Financial assistance from NAB and Glaxo Group Research (to M.S.S.) is acknowledged along with technical assistance from Miss Jane Fordham.

REFERENCES

1 M. B. Evans, *Chromatographia*, 3 (1970) 337.
2 M. B. Evans and B. Williamson, *Chem. Ind. (London)*, (1970) 1171.
3 M. B. Evans and B. Williamson, *Chromatographia*, 5 (1972) 264.
4 M. B. Evans, J. M. Oxford and M. S. Smith, in preparation.
5 P. Schoemaker and F. Verhoeven, *Trends Anal. Chem.*, 6 (1987) 10.
6 T. Takeuchi, Y. Hashimoto and D. Ishii, *J. Chromatogr.*, 402 (1987) 328.

7 Ph. Morin, M. Caude and R. Rosset, *J. Chromatogr.*, 407 (1987) 87.
8 P. L. Cheuh and J. M. Prausnitz, *AIChE J.*, 13 (1967) 1099.
9 F. Carey and R. Sunbury, *Advanced Organic Chemistry*, Plenum, London, 2nd ed., 1984.
10 M. L. Hair and W. Hertt, *J. Phys. Chem.*, 74 (1970) 91.
11 M. B. Evans, *Ph.D. Thesis*, London University, 1967.
12 R. M. Smith, *Gas and Liquid Chromatography in Analytical Chemistry*, Wiley, Chichester, 1988.

Journal of Chromatography, 479 (1989) 176–180
Elsevier Science Publishers B.V., Amsterdam — Printed in The Netherlands

CHROM. 21 666

Note

Gas chromatographic separation of diastereomeric dicarbamate derivatives of γ- and δ-lactones

K.-H. ENGEL*

Technische Universität Berlin, Institut für Biotechnologie, Fachgebiet Chemisch-technische Analyse, Seestrasse 13, D-1000 Berlin 65 (F.R.G.)

R. A. FLATH

Western Regional Research Center, USDA-ARS, 800 Buchanan Street, Albany, CA 94710 (U.S.A.)

and

W. ALBRECHT and R. TRESSL

Technische Universität Berlin, Institut für Biotechnologie, Fachgebiet Chemisch-technische Analyse, Seestrasse 13, D-1000 Berlin 65 (F.R.G.).

(First received April 12th, 1989; revised manuscript received June 7th, 1989)

Lactones are an important group of chiral compounds playing significant roles in several foods[1]. In spite of their powerful contributions to overall flavour impressions, the amounts of lactones in natural systems are mostly very low, and sensitive analytical techniques are required to determine their naturally occurring enantiomeric compositions. Recently a major breakthrough has been achieved by direct capillary gas chromatographic (GC) separation of enantiomers of γ-lactones using modified cyclodextrin as a chiral stationary phase[2]. However, the conversion into diastereomeric derivatives followed by separations on non-chiral (commonly available) stationary phases is still a useful and easily applicable alternative for laboratories with standard GC equipment.

The GC separation of diastereomeric ketals obtained by direct reaction with optically pure 2,3-butanediol has been described for δ-lactones[3,4]. In general the formation of diastereomeric derivatives of lactones requires an opening of the ring to obtain intermediates with reactive functional groups. Enantiomers of 4- and 5-hydroxyalkanoic acid esters, derived from γ- and δ-lactones, were separated after conversion into (*R*)-1-phenylethylcarbamates[5]. Opening of the lactone ring to give 4-hydroxyalkanoic acid isopropylesters and subsequent derivatization with (*S*)-O-acetyllactyl chloride[6] was applied to determine the configurations of γ-deca- and γ-dodecalactone in peach[7] and strawberry[8]. The corresponding diastereomeric esters of (*S*)-tetrahydro-5-oxo-2-furancarboxylic acid have been used to investigate chiral δ-lactones[9]. Reactive functional groups can also be obtained by reduction of γ- and δ-lactones to 1,4-and 1,5-diols, respectively. Separations of the corresponding diesters of (*S*)-O-acyllactic acids have been reported[10].

This paper presents the capillary GC separation of diastereomeric dicarbamates obtained by derivatization of 1,4- and 1,5-diols with (*R*)-(+)-1-phenylethyl isocyanate.

0021-9673/89/$03.50

EXPERIMENTAL

Chemicals

(*R*)-(+)-1-Phenylethyl isocyanate (PEIC) and 4-dimethylaminopyridine (DMAP) were obtained from Fluka (Neu-Ulm, F.R.G.). Racemic γ- and δ-lactones were gifts from Haarman & Reimer (Holzminden, F.R.G.) and Firmenich (Geneva, Switzerland). All solvents were redistilled before use.

Derivatization

Reduction of γ- and δ-lactones to 1,4- and 1,5-diols. Lithium aluminium hydride was added to a solution of lactones (in a typical experiment 0.5 μl of an equimolar mixture of C_5–C_{11} γ-lactones) in 0.2 ml dry diethyl ether. After shaking at room temperature for 15 min and addition of 1 *M* HCl (1 ml) the mixture was extracted with chloroform (2 × 20 ml). The chloroform extracts were washed (1 ml $NaHCO_3$, 1 ml water) and dried with sodium sulphate. The solvent was evaporated and the residue redissolved in 200 μl diethyl ether.

Conversion into diastereomeric dicarbamates. After transferring the solution to a screw-capped reaction vial the diethyl ether was removed by using a stream of nitrogen. The residue was dissolved in 25 μl toluene containing 1% DMAP. A 2 μl volume of (*R*)-(+)-PEIC was added and the mixture was kept at 60°C for 24 h. After addition of 250 μl dichloromethane the solution was subjected to GC analysis.

Capillary GC

Capillary GC separations were carried out on a 30 m × 0.32 mm I.D. DB 210 column (film tickness 0.25 μm; J&W Scientific) installed in a Carlo Erba Fractovap Series 2150 gas chromatograph, equipped with a split (1:25) and flame ionization detection (FID). Injector temperature: 230°C. Detector temperature: 275°C. Carrier gas (hydrogen), 0.85 bar; flow-rate, u (225°C) = 55 cm/s. Temperature programme from 220 to 260°C at 1°C/min.

Capillary GC–mass spectrometry (MS)

A Finnigan MAT 4500 series quadrupole gas chromatograph–mass spectrometer coupled with an Incos data system was used. The fused-silica column (described above) was inserted directly into the ion source. Ionization voltage: 70 eV. Ion source temperature: 180°C. Speed: 1 scan/s. Mass range (m/z): 33–500.

RESULTS AND DISCUSSION

Diastereomeric dicarbamates were obtained from chiral γ- and δ-lactones by reduction with lithium aluminium hydride and subsequent derivatization of the 1,4- and 1,5-diols formed, with (*R*)-(+)-1-phenylethyl isocyanate (Fig. 1). The GC separation of diastereoisomers obtained by this procedure from an homologous series of racemic lactones is shown in Fig. 2.

Complete conversion into dicarbamates at moderate temperature was achieved by using DMAP as a catalyst[11]. DMAP has also been employed to obtain carbamate diastereoisomers from the sterically hindered tertiary alcohol linalool[12]. The presence of water and/or traces of acid has to be avoided; they cause the reaction to yield only

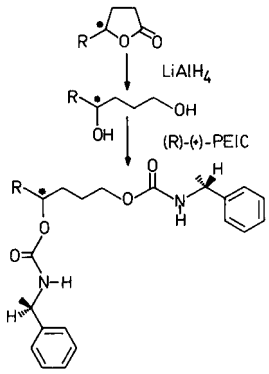

Fig. 1. Conversion of γ-lactones into diastereomeric dicarbamates (R = from $-CH_3$ to $-C_7H_{15}$).

a mixture of mono- and dicarbamates. Quantitative derivatization, however, is necessary to prevent possible discrimination of enantiomers.

The identities of the derivatives were confirmed by GC–MS. Mass spectra of the dicarbamates were mainly characterized by fragmentations of the 1-phenylethylcarbamoyloxy moieties of the molecules. The spectra obtained from an homologous

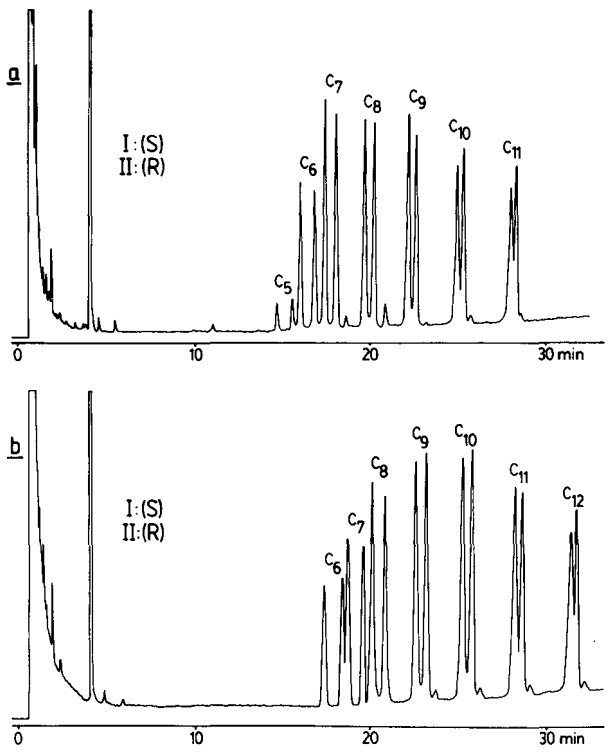

Fig. 2. Gas chromatographic separation of di[(*R*)-1-phenylethyl]carbamates derived from racemic γ-lactones (a) and δ-lactones (b); for conditions see Experimental.

series of lactones were very similar. The ten most intense fragments (*m/z*, relative intensity, %) of the dicarbamate derived from (*S*)-1,4-octanediol are representative: 105 (100), 120 (60), 132 (47), 164 (21), 106 (32), 166 (30), 150 (29), 69 (25), 77 (18), 147 (16). The spectrum also showed minor but diagnostic fragment ions at M − 15, M − 105, M − 164 and M − 165. Apart from slight differences in the intensities, the mass spectrum of the diastereomeric dicarbamate was identical.

The order of elution was determined by derivatizing optically enriched reference compounds obtained by reduction of oxo precursors using baker's yeast[13,14] and by resolution of racemic lactones by means of chromatography on cellulose triacetate[15]. Within the homologous series of C_5–C_{11} γ- and C_6–C_{12} δ-lactones the dicarbamates derived from (*S*)-lactones are eluted before the derivatives of the corresponding (*R*)-enantiomers.

The derivatives of the higher homologues exhibit only low volatilities. Elution and (partial) resolution of these diastereoisomers without exceeding the upper temperature limit of the column was achieved by using hydrogen as a carrier gas. The separation factors, α, of the diasteromeric pairs separated are listed in Table I. The separation strongly depends on the structures of the lactones. The α values decrease with increasing length of the alkyl side chains of the lactones.

Special attention has to be paid to the fact that the retention times of dicarbamates derived from γ-lactones partly match those of δ-lactones. Starting from chain length C_8, the first dicarbamate eluted derived from δ-lactones is co-eluted with the second of the diastereomeric derivatives obtained from the corresponding γ-lactones. Therefore, in natural systems where both γ- and δ-lactones of the same chain length are present a preseparation, *e.g.*, by means of preparative GC, prior to the derivatization procedure is necessary.

The method described has been applied to determine the naturally occurring enantiomeric compositions of γ- and δ-lactones in mango fruits[16]. Due to the above-mentioned disadvantages (low volatilities and low separation factors of the higher homologues), accurate chirality determinations can be carried out only for lactones up to chain length C_8. Improved derivatization techniques have been worked out and will be published elsewhere[17].

TABLE I

SEPARATION FACTORS (α) OF DIASTEREOMERIC DICARBAMATE PAIRS DERIVED FROM γ- AND δ-LACTONES

Column: DB 210, see Experimental. Column temperature: 240°C (isothermal).

γ-Lactone	α	*δ-Lactone*	α
Valerolactone	1.078	Hexalactone	1.080
Hexalactone	1.069	Heptalactone	1.075
Heptalactone	1.051	Octalactone	1.056
Octalactone	1.039	Nonalactone	1.042
Nonalactone	1.032	Decalactone	1.033
Decalactone	1.023	Undecalactone	1.025
Undecalactone	1.018	Dodecalactone	1.019

ACKNOWLEDGEMENT

Financial support by a grant from the Deutsche Forschungsgemeinschaft, Bonn, F.R.G., is gratefully acknowledged by K.H.E.

REFERENCES

1 H. Maarse and C. A. Vissher (Editors), *Volatile Compounds in Food—Qualitative Data, Supplement 4*, TNO-CIVO, Zeist, The Netherlands 1987.
2 W. A. König, S. Lutz, C. Colberg, N. Schmidt, G. Wenz, E. v.d. Bey, A. Mosandl, C. Günther and A. Kustermann, *J. High Resolut. Chromatogr. Chromatogr. Commun.*, 11 (1988) 621.
3 G. Saucy, R. Borer, D. P. Trullinger, J. B. Jones and K. P. Lock, *J. Org. Chem.*, 42 (1977) 3206.
4 R. Tressl and K.-H. Engel, in P. Schreier (Editor), *Analysis of Volatiles*, Walter de Gruyter, Berlin, New York, 1984, p. 323.
5 R. Tressl, K.-H. Engel, W. Albrecht and H. Bille-Abdullah, *ACS Symp. Ser.*, 289 (1985) 43.
6 A. Mosandl, M. Gessner, C. Günther, W. Deger and G. Singer, *J. High Resolut. Chromatogr. Chromatogr. Commun.*, 10 (1987) 67.
7 M. Feuerbach, O. Fröhlich and P. Schreier, *J. Agric. Food Chem.*, 36 (1988) 1236.
8 G. Krammer, O. Fröhlich and P. Schreier, in P. Schreier (Editor), *Bioflavour '87*, Walter de Gruyter, Berlin, New York, 1988, p. 89.
9 M. Gessner, W. Deger and A. Mosandl, *Z. Lebensm.-Unters.-Forsch.*, 186 (1988) 417.
10 W. Deger, M. Gessner, C. Günther, G. Singer and A. Mosandl, *J. Agric. Food Chem.*, 36 (1988) 1260.
11 G. Höfle, W. Steglich and H. Vorbrüggen, *Angew. Chem.*, 90 (1978) 602.
12 A. A. Rudmann and J. R. Aldrich, *J. Chromatogr.*, 407 (1987) 324.
13 M. Utaka, H. Watabu and A. Takeda, *J. Org. Chem.*, 52 (1987) 4363.
14 M. Gessner, C. Günther and A. Mosandl, *Z. Naturforsch. Teil C*, 42 (1987) 1159.
15 E. Francotte and D. Lohmann, *Helv. Chim. Acta*, 70 (1987) 1569.
16 R. Tressl, K.-H. Engel and W. Albrecht, in S. Nagy, J. A. Attaway and M. E. Rhodes (Editors), *Adulteration of Fruit Juice Beverages*, Marcel Dekker, New York, Basle, 1988, p. 67.
17 K.-H. Engel, W. Albrecht and J. Heidlas, *J. Agric. Food Chem.*, submitted for publication.

Journal of Chromatography, 479 (1989) 181–188
Elsevier Science Publishers B.V., Amsterdam — Printed in The Netherlands

CHROM. 21 746

Note

Liquid chromatographic analysis of bromination reactions of metal trifluoroacetylacetonates

T. J. CARDWELL* and T. H. LORMAN
Analytical Chemistry Laboratories, Chemistry Department, La Trobe University, Bundoora, Victoria 3083 (Australia)
(First received March 29th, 1989; revised manuscript received July 4th, 1989)

Many of the electrophilic substitution reactions investigated by Singh and Sahai[1] and Joshi and Pathak[2] and some of those studied by Collman *et al.*[3,4] have included trivalent metal β-diketonates with unsymmetrical ligands. These octahedral metal complexes display geometrical isomerism yet it is surprising that there is only one brief reference to this type of isomerism in these early investigations: isomers were claimed for the substituted products of the formylacetone chromium(III) chelate[4] but no supporting evidence was given[5].

In two previous papers from these laboratories, it was demonstrated that gas chromatography (GC) was effective in separating the mono-, bi- and tri-substituted products in the bromination of the trifluoroacetylacetonates of chromium and rhodium[6,7]. In the separation of the rhodium compounds, the chromatogram clearly showed the presence of geometrical isomers in the bi- and tri-brominated derivatives[7] whereas the corresponding chromatogram for the chromium compounds showed that isomers seemed to be present only in the mono-substituted derivative[6].

The geometrical isomers of cobalt(III) and chromium(III) chelates of trifluoroacetylacetone, benzoylacetylacetone and 2,2-dimethylhexane-3,5-dione have been separated by high-performance liquid chromatography (HPLC) in the adsorption mode[8] and this technique has also been recommended for the analysis of electrophilic substitution reactions involving labile or thermally unstable metal β-diketonates[9]. In this paper, the effects of the presence of geometrical isomers in electrophilic substitution reactions is investigated and HPLC is applied to the separation of isomeric forms of the products in the bromination of some trivalent metal trifluoroacetylacetonates.

EXPERIMENTAL

The trifluoroacetylacetonates of chromium(III), rhodium(III) and cobalt(III) were prepared by the method of Fay and Piper[10] and samples were purified by column chromatography on acid-washed alumina using chloroform as eluent. As this eluent yields mixtures of isomers, the identities of the chelates were established by the presence of molecular ions in their mass spectra. Highly pure samples of the meridional isomers were isolated (i) after several recrystallisations from benzene–hexane

0021-9673/89/$03.50

(50:50) followed by column chromatography on acid-washed alumina using hexane–benzene (20:80) as eluent[10] or (ii) using preparative liquid chromatography with dichloromethane–hexane (20:80) as the mobile phase. The purity of the meridional isomer was confirmed by HPLC and its identity (for rhodium and cobalt chelates) was established by NMR.

Bromination of the metal chelates was performed in chloroform at room temperature using a 4:1 mole ratio of bromine to metal complex. The reaction mixture was analysed as follows: the solvent was rapidly removed in a stream of nitrogen, the residue was washed successively with aqueous sodium bicarbonate, aqueous sodium bisulphite and water, air-dried and then it was dissolved in hexane or the HPLC mobile phase to a concentration of 0.5–1.0%. The reaction time under these conditions is indicated in each of the figure legends.

HPLC was carried out by injecting 20 μl of sample solution into either an Altex 420 chromatograph fitted with an Hitachi 100-10 variable-wavelength detector or a Laboratory Data Control system consisting of a Constametric IIG pump and an LDC UV monitor set at 254 nm. Two analytical columns were used; a Phase Separations 5-μm Spherisorb silica column (250 × 4.6 mm I.D.) and a 7-μm Zorbax column (150 × 4.6 mm I.D.), slurry-packed using isopropanol as slurry solvent at a pressure of 4500 p.s.i. Preparative liquid chromatography of solutions containing 100–500 mg complex in hexane was performed on a Waters Prep LC-system 500 using a PrepPak-500 silica radical compression cartridge and a refractive index detector. Electron impact mass spectra of the chelates were recorded on a JEOL JMS D-100 mass spectrometer by direct insertion probe introduction of solid samples at 70 eV. NMR spectra were obtained on a JEOL JNM-FX200 Fourier transform NMR spectrometer and samples were made up in deuterochloroform with tetramethylsilane as internal standard.

RESULTS AND DISCUSSION

Bromination of Cr(tfa)$_3$.

Using dichloromethane–hexane (20:80), resolution of the geometrical isomers of chromium trifluoroacetylacetonate, $Cr(tfa)_3$, was readily achieved by normal-phase adsorption HPLC in good agreement with the previous results of Uden *et al.*[8]. It was confirmed that the meridional (*mer*) isomer was eluted ahead of the facial (*fac*) isomer by injecting samples enriched in one isomer according to the method of Fay and Piper[10]. In the bromination of a mixture of isomers of $Cr(tfa)_3$, one would expect each of the brominated products to display geometrical isomerism but the HPLC analysis in Fig. 1C indicates that there are more components in the reaction mixture than could be explained simply by geometrical isomerism. The last two peaks, identified on the basis of their retention volumes (V_R) of 9.9 and 16.0 cm^3, are the geometrical isomers of the unreacted chromium chelate, $Cr(tfa)_3$. In a previous paper, the authors used mass spectral evidence to identify the major peaks in the gas chromatogram of the above reaction mixture to be the mono-, bi- and tri-brominated derivatives of $Cr(tfa)_3$, eluted in the order[6] $Cr(tfa)_3 < Cr(tfa)_2(Brtfa) < Cr(tfa)(Brtfa)_2 < Cr(Brtfa)_3$, where Brtfa represents the brominated trifluoroacetylacetonate anion. In an attempt to identify the components giving rise to the peaks in Fig. 1C, samples of the individual GC peaks were collected in small quantities for analysis by HPLC.

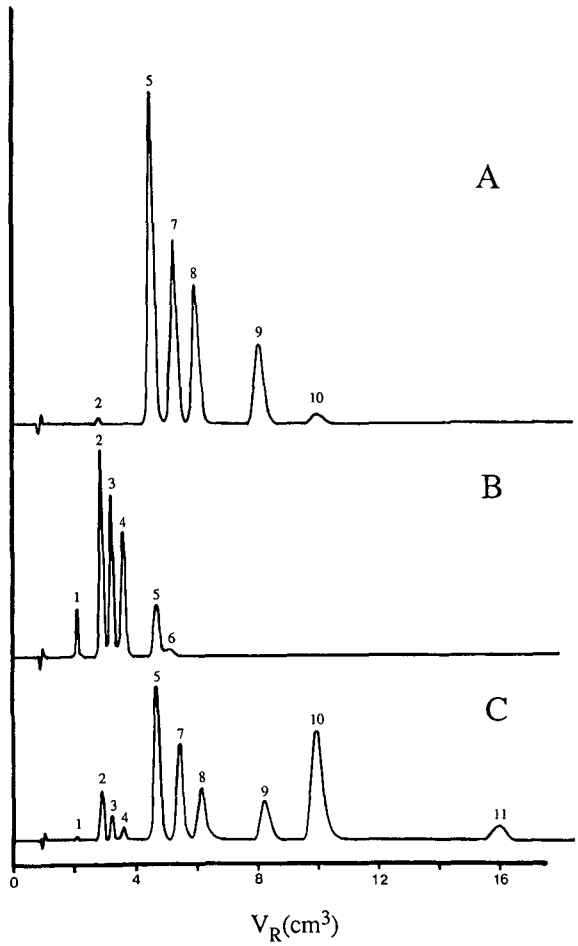

Fig. 1. Liquid chromatograms of samples of (A) the mono- and (B) the bi-brominated chromium trifluoroacetylacetonate, as collected by GC, and (C) of the reaction mixture of brominated $Cr(tfa)_3$ sampled after 45 min. Column: 5-μm Spherisorb silica, 250 × 4.6 mm I.D.; mobile phase: dichloromethane–hexane (20:80) at 1 cm^3 min^{-1}. Peaks: 1 = *mer*-$Cr(Brtfa)_3$; 2,3,4 = *mer*-$Cr(Brtfa)_2(tfa)$; 6 = *fac*-$Cr(Brtfa)_2(tfa)$; 5,7,8 = *mer*-$Cr(Brtfa)(tfa)_2$; 9 = *fac*-$Cr(Brtfa)(tfa)_2$; 10 = *mer*-$Cr(tfa)_3$; 11 = *fac*-$Cr(tfa)_3$.

The last eluting GC peak corresponds to the first LC peak (V_R = 2.1 cm^3 in Fig. 1) and hence its identity is the tri-brominated chromium chelate. The liquid chromatograms for the samples of mono- and bi-brominated chelates are shown in Figs. 1A and 1B. The last peak in Fig. 1A (V_R = 9.9 cm^3) is clearly due to traces of the *mer* isomer of $Cr(tfa)_3$ in the collected sample of the mono-brominated species. The latter appears to give rise to four major peaks with retention volumes ranging from 4.4 to 8.6 cm^3 under these conditions yet only two components were observed in the gas chromatogram of this sample. Mass spectral data for collected fractions of each of the four HPLC peaks are practically identical and the spectra show parent ions at m/z = 591 and 589 in an intensity ratio of 1:1, indicating that the four components corre-

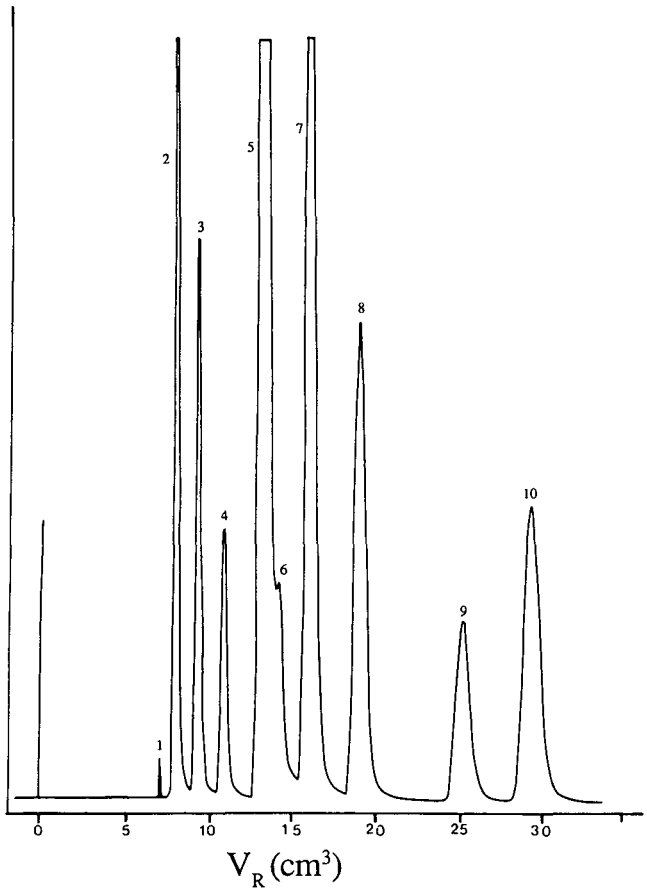

Fig. 2. Liquid chromatogram of the bromination reaction mixture of $Co(tfa)_3$ sampled after 90 min. Column: 7-μm Zorbax silica, 150 × 4.6 mm I.D.; mobile phase: dichloromethane–hexane (8:92) at 1 cm^3 min^{-1}. Peaks: 1 = *mer*-$Co(Brtfa)_3$; 2,3,4 = *mer*-$Co(Brtfa)_2(tfa)$; 6 = *fac*-$Co(Brtfa)_2(tfa)$; 5,7,8 = *mer*-$Co(Brtfa)(tfa)_2$; 9 = *fac*-$Co(Brtfa)(tfa)_2$; 10 = *mer*-$Cr(tfa)_3$.

spond to the mono-brominated species[6]. For the bi-brominated chelate sample (Fig. 1B), the peaks at V_R = 2.1 and 4.5 cm^3 arise from the tri- and mono-brominated species, respectively, which are present as impurities; hence, there appears to be four components in the bi-brominated sample also although the fourth component (V_R = 5.0 cm^3) is often difficult to detect in the chromatogram of the reaction mixture because of overlap with early eluting peaks attributed to the mono-brominated complex.

The peak area ratios of the four components for the bi-brominated chelate are relatively constant for all reactions, regardless of the reaction time or the initial isomeric ratio of $Cr(tfa)_3$; this is not unexpected as the bi-brominated species appear late in a reaction and by that stage, isomerisation would have occurred already so that an equilibrium isomeric mixture would be observed. On the otherhand, bromination reactions of $Cr(tfa)_3$ enriched with the *fac* isomer produce greater proportions of the

fourth component (V_R = 8.1 cm^3) for the mono-brominated species and if left in solution, this component decreases while the other three species increase in total peak area implying that isomerisation may be taking place on standing. This is not unusual as it has been found that the *fac* isomers of trifluoroacetylacetonates of trivalent metals isomerise to the more stable *mer* isomers in solution[10]. As the *mer* isomer is eluted before the *fac* isomer, these observations also suggest that the *mer* isomer of the partially brominated metal trifluoroacetylacetonates accounts for three peaks and the *fac* isomer one peak in the HPLC chromatogram. Only one peak is detected for the tri-brominated species by HPLC and this is in agreement with the observations in GC[6].

Bromination of Co(tfa)$_3$ and Rh(tfa)$_3$.

Analyses of reaction mixtures from the bromination of cobalt and rhodium trifluoroacetylacetonates, shown in Figs. 2 and 3, yield remarkably similar results to those observed for the chromium system. Samples of the individual rhodium complexes collected in GC again show that four well resolved peaks are observed in HPLC for the mono- and bi-brominated derivatives (Fig. 3). Confirmation of the identity of each peak in the liquid chromatography of the rhodium complexes was made by mass spectral analysis of a fraction of the peak collected from the exit line of the LC detector. All four peaks with retention volumes in the range 19–33 cm^3 in Fig. 3 had similar spectra; the fragmentation patterns (Table I) and the 1:1 intensity ratio

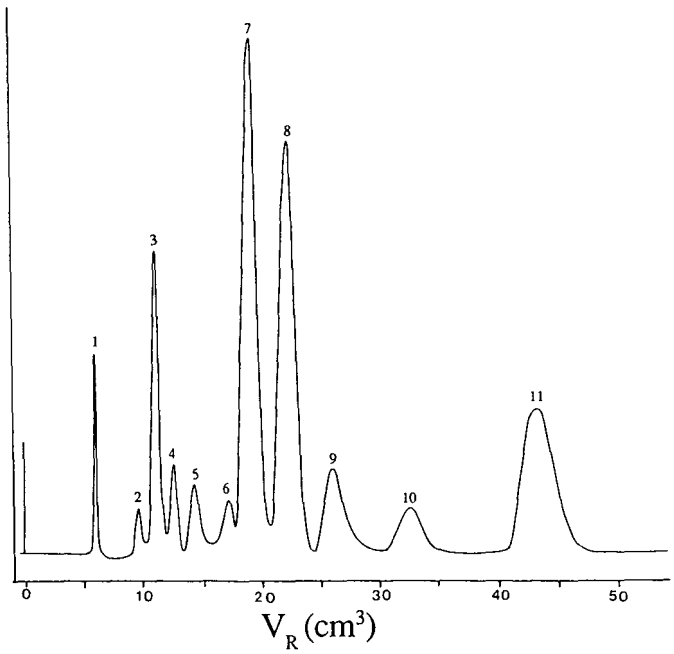

Fig. 3. Liquid chromatogram of the bromination reaction mixture of Rh(tfa)$_3$ sampled after 2 h. Columns as in Fig. 2; mobile phase: dichloromethane–hexane (6:94) at 1 cm^3 min^{-1}. Peaks: 1 = *mer*-Rh(Brtfa)$_3$; 2 = *fac*-Rh(Brtfa)$_3$; 3,4,5 = *mer*-Rh(Brtfa)$_2$(tfa); 6 = *fac*-Rh(Brtfa)$_2$(tfa); 7,8,9 = *mer*-Rh(Brtfa)(tfa)$_2$; 10 = *fac*-Rh(Brtfa)(tfa)$_2$; 11 = *mer*-Rh(tfa)$_3$.

TABLE I

RELATIVE INTENSITIES OF FRAGMENT IONS IN THE MASS SPECTRA OF $Rh(tfa)_3$ AND ITS BROMINATED DERIVATIVES

Ion	*Rh(tfa)$_3$*	*Rh(Brtfa)(tfa)$_2$*	*Rh(Brtfa)$_2$(tfa)*	*Rh(Brtfa)$_3$*
M^+	50	38	43	40
$[M-(tfa)]^+$	100	12	26	–
$[M-(Brtfa)]^+$	–	100	100	100
$[M-(Brtfa)-CF_2]^+$	–	15	6	1
$[M-(Brtfa)-CF_3]^+$	–	28	23	13
$[M-(Brtfa)-2CF_3]^+$	–	17	14	7
$[M-(Brtfa)-(tfa)]^+$	–	23	9	–
$[M-2(tfa)]^+$	9	–	–	–
$[M-2(Brtfa)]^+$	–	–	43	80
$[M-2(tfa)-CF_3]^+$	4	–	–	–
$[M-2(Brtfa)-CF_3]^+$	–	–	13	7

of the parent ions at m/e = 642 and 640 indicate that all components in this group of LC peaks are mono-brominated species. The four peaks with V_R = 11.0–17.2 cm^3 are bi-brominated species which give parent ions at m/e = 722, 720 and 718 in a ratio of 1:2:1. The tri-brominated rhodium complex displays two isomers in GC and HPLC, the first eluting in each case being the *mer* isomer as shown later. The *fac* and *mer* isomers of the tri-brominated complexes gave similar spectra with parent ions at m/e = 802, 800, 798 and 796 in an intensity ratio of 1:3:3:1. Table I lists the data for the major fragments in the mass spectra of brominated derivatives of $Rh(tfa)_3$

As the HPLC results provide very strong evidence that there are three components for the *mer* isomer of each of the partially brominated chelates, it was of interest to carry out bromination reactions on the *mer* isomer only. Pure samples of the *mer* isomers of $M(tfa)_3$ were isolated by fractional recrystallisation[10] or preparative LC and bromination reactions were performed as described above for mixtures of isomers. HPLC analysis of the rhodium reaction mixture yielded a similar chromatogram to that in Fig. 3 and the peak due to the *fac* isomer of the initial rhodium reactant was absent. In all three metal systems, four peaks and not three were observed for the partially brominated chelates.

NMR spectroscopy

In order to characterize all of the components giving rise to the various liquid chromatographic peaks by NMR spectroscopy, attempts were made to isolate sufficient quantities of each of the species. Although fractional recrystallization was found to be suitable in the isolation of the chromium compounds[6], separation of the brominated rhodium chelates requires preparative LC using dichloromethane–hexane (10:90) and it was only possible to isolate *mer*-$Rh(tfa)_3$ and $Rh(Brtfa)_2(tfa)$. Two samples of the bi-brominated derivative were isolated; analytical HPLC showed that one of these samples contained only the first eluting component (V_R = 11.0 cm^3, Fig. 3) whereas the other sample contained the first three of the four components attributed to the bi-brominated complex.

^1H NMR spectroscopy has been found to be extremely useful in the character-

ization of the configurations of isomers of trivalent metal trifluoroacetylacetonates. The *fac* isomer of $Rh(tfa)_3$ was reported to give single resonances for the methyl and methine protons at 2.36 and 5.99 ppm, respectively, whereas the *mer* isomer gave three methyl resonances at 2.35–2.40 ppm and three methine resonances at 5.98–6.03 ppm[10,11]. The sample corresponding to the peak with V_R = 6.1 cm^3 in Fig. 3 has three methyl group resonances at 2.72–2.75 ppm and no methine proton resonance; this is consistent with non-equivalent methyl groups in a *mer* configuration and bromination of all three chelate rings, as in $Rh(Brtfa)_3$. A mixture of the isomers of the tri-brominated complex shows four methyl groups resonances at 2.72–2.76 ppm.

The spectra of the two isolated samples of the bi-brominated rhodium chelate were identical and had three methyl resonances at 2.30–2.32 ppm indicative of a *mer* configuration and in each case, a single methine resonance was observed at 5.96 ppm arising from one unbrominated ligand. As there is no evidence of another methyl resonance peak in the ^1H NMR spectrum of the sample which displays three HPLC peaks, this indicates that the *mer* isomer of this compound consists of three components and hence the *fac* isomer gives one HPLC peak. This supports the earlier suggestions of solution isomerisation for the mono-brominated species observed in the HPLC monitoring of the bromination of $Cr(tfa)_3$ initially enriched in the *fac* isomer.

^{13}C NMR spectra were also run on the above rhodium samples collected by preparative LC. As these data confirm the assignment of *mer* configurations already derived from the ^1H NMR spectral data but provide no additional structural information, they are not presented in this paper. ^1H and ^{13}C NMR spectra were both unsuccessful in differentiating the individual components of the *mer* isomers of the partially brominated chelates.

On the basis of the NMR and mass spectral data for the brominated rhodium chelates and the close similarities of the elution profiles of bromination reaction mixtures of all three trifluoroacetylacetonates, it is concluded that the *mer* isomers of the partially brominated trifluoroacetylacetonates of chromium(III), rhodium(III)

TABLE II

CHROMATOGRAPHIC RETENTION DATA FOR METAL TRIFLUOROACETYLACETONATES AND THEIR BROMINATED DERIVATIVES

Column: 7-μm Zorbax silica, 150 × 4.6 mm I.D.; mobile phase: dichloromethane–hexane (10:90); column dead volume: 1.9 cm^3. *mer* (1/2/3) = Three components of the *mer* partially brominated derivatives.

Metal complex	*Isomer*	*Capacity factors for individual components*		
		M = Cr	*M = Rh*	*M = Co*
$M(Brtfa)_3$	*mer*	1.95	1.2	2.3
	fac	–	1.9	–
$M(Brtfa)_2(tfa)$	*mer* (1/2/3)	2.65/2.95/3.25	2.05/2.3/2.6	2.6/3.05/3.5
	fac	4.3	3.15	4.6
$M(Brtfa)(tfa)_2$	*mer*(1/2/3)	4.1/4.6/5.2	3.6/4.05/4.7	4.3/5.1/6.0
	fac	7.25	6.05	7.8
$M(tfa)_3$	*mer*	7.8	7.95	8.9
	fac	12.95	12.7	14.1

and cobalt(III) consist of three components which are readily separated by normal-phase HPLC. The chromatographic capacity factors for the parent metal chelates and their brominated derivatives have been determined under identical chromatographic conditions and the data are listed in Table II.

REFERENCES

1 P. R. Singh and R. Sahai, *Indian J. Chem.*, 8 (1970) 178.
2 K. C. Joshi and V. N. Pathak, *J. Chem. Soc., Perkin Trans. I,* (1973) 57.
3 J. P. Collman, R. A. Moss, H. Maltz and C. Heindel, *J. Am. Chem. Soc.*, 83 (1961) 531.
4 J. P. Collman, *Angew. Chem., Int. Ed. Eng.*, 4 (1965) 132.
5 J. P. Collman and E. T. Kittleman, *J. Am. Chem. Soc.*, 83 (1961) 3529.
6 T. J. Cardwell and T. H. Lorman, *Inorg. Chim. Acta,* 53 (1981) L103.
7 T. J. Cardwell and T. H. Lorman, *Inorg. Chim. Acta,* 120 (1986) L5.
8 P. C. Uden, I. E. Bigley and F. H. Walters, *Anal. Chim. Acta,* 100 (1978) 555.
9 T. J. Cardwell and T. H. Lorman, *Inorg. Chim. Acta,* 85 (1984) 1.
10 R. Fay and T. Piper, *J. Am. Chem. Soc.*, 85 (1962) 500.
11 R. C. Mehrotra, R. Bohra and D. P. Gaur, *Metal β-Diketonates and Allied Derivatives,* Academic Press, London, 1978.

Journal of Chromatography, 479 (1989) 189–193
Elsevier Science Publishers B.V., Amsterdam — Printed in The Netherlands

CHROM. 21 741

Note

High-performance liquid chromatographic analysis of *Solanum* steroidal alkaloids

S. F. OSMAN*

Eastern Regional Research Center, Agricultural Research Service, U.S. Department of Agriculture, 600 East Mermaid Lane, Philadelphia, PA 19118 (U.S.A.)

and

S. L. SINDEN

Beltsville Agricultural Research Center, Agricultural Research Service, U.S. Department of Agriculture, Beltsville, MD 20705 (U.S.A.)

(First received April 24th, 1989; revised manuscript received July 4th, 1989)

Solanum species contain as major secondary metabolites, steroidal alkaloids usually as glycosides (generally referred to as glycoalkaloids). Earlier interest centered on the use of these compounds as starting material for synthetic production of steroidal hormones[1]; however, more recent interest has been on the role of these compounds in pest resistance and culinary quality of edible Solanaceous crops such as potato[2]. In the development of new hybrid strains it is desireable to know the alkaloid compositions of the wild species parents and their hybrids so that new alkaloids are not inadvertently introduced into our food crops. There are many methods that have been described for glycoalkaloid analysis using high-performance liquid chromatography (HPLC)[3–5] thin-layer chromatography (TLC)[6] or gas chromatography (GC)[7]; however, all of these techniques have significant limitations which are mainly due to the hydrophobic (aglycone)–hydrophilic (carbohydrate) dicotomous nature of the glycoalkaloid structure. HPLC has been particularly useful in the analysis of potato glycoalkaloid mixtures. However, separations by HPLC depend, for the most part, on the structure of the carbohydrate portion of the molecule. At this time only glycoalkaloids that have gross differences in aglycone structure can be separated by HPLC when they contain glycosidic units of similar polarity.

We have recently been examining the glycoalkaloid composition of some disease and pest resistant somatic hybrids obtained by protoplast fusion. The glycoalkaloids in these hybrids have similar structures which we were unable to separate by available methods. For analysis of these hybrids, we have concentrated on analyzing the aglycones (*i.e.*, steroidal alkaloids) rather than attempting to separate the glycoalkaloids in the mixture.

For the analysis of somatic hybrids between *S. brevidens* and *S. tuberosum*, the separation of saturated from Δ^5 (5,6 unsaturated) alkaloids presented an especially difficult chromatographic challenge. Methods described for the analysis of the steroidal alkaloids by GC[8], HPLC[9,10] and TLC[11] were of limited use because of poor resolution and/or low sensitivity of detection. In this paper we describe a method for

the separation and quantitation of *Solanum* steroidal alkaloids by reversed-phase HPLC which is particularly useful for the separation of saturated from unsaturated alkaloids.

EXPERIMENTAL

Materials

Solanidine, demissidine, tomatidine and solasodine were purchased from Sigma (St. Louis MO, U.S.A.), leptinidine (23-hydroxysolanidine), acetylleptinidine, 23-hydroxy- and 23-acetyldemissidine and 5-tomatidenol were isolated from plant tissue as the glycosides and partially purified by ammonia precipitation. The glycosides were hydrolyzed in 1 *M* methanolic HCl. The individual aglycones were isolated by preparative TLC on silica gel using appropriate solvent systems[11]. The purified aglycones were characterized by either gas chromatography– or direct probe–mass spectrometry.

Alkaloid mixtures from *Solanum* hybrids were prepared by hydrolysis of the glycoalkaloid mixture with 1 *M* methanolic HCl.

All solvents were high-purity grade from Burdick & Jackson, (St. Louis, MO, U.S.A.).

Chromatographic procedure

HPLC analyses were carried out on a Hewlett-Packard 1090 instrument fitted with a Supelcosil LC-18-DB (5 μm) column (25 cm × 4.6 mm I.D.) (Supelco, Bellefonte, PA, U.S.A.) and a Model 1037A refractive index (RI) detector (Hewlett-Packard). The mobile phase was acetonitrile –methanol–ethanolamine (60:40:0.001) and the flow-rate was 0.5 ml min^{-}

RESULTS AND DISCUSSION

The HPLC chromatogram for the steroidal alkaloids shown in Fig. 1 is given in Fig. 2. These nine steroidal alkaloids are the major aglycones of the *Solanum*

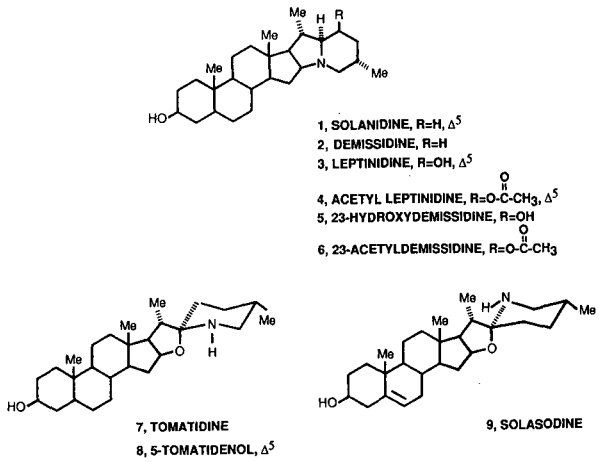

Fig. 1. Structures of *Solanum* steroidal alkaloids. Me = Methyl.

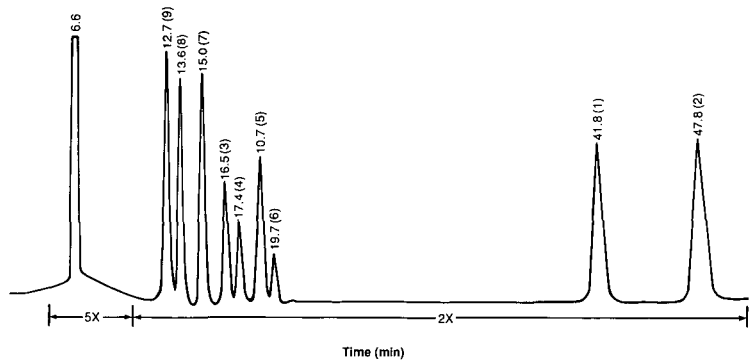

Fig. 2. Reversed-phase HPLC of *Solanum* steroidal alkaloids. For conditions, see Experimental.

glycoalkaloids[12] as well as glycoalkaloids that have only been found in experimental hybrids[13]. Other alkaloid aglycones have been reported[12], however, these rare aglycones were not available to us.

Although partial separation of demissidine and its Δ^5 analogue, solanidine has been achieved by capillary GC[8], other such analogues cannot be separated under the same conditions. The alkaloids, as is the case observed with steroids in general, decompose at the high temperatures required in the GC analysis which adversely effects sensitivity, quantitation (we have been able to detect lower concentrations of solanidine which elutes at 240°C than tomatidine which elutes at 270°C) and resolution.

One objection to the use of HPLC for analysis of the steroidal alkaloids has been the poor sensitivity of available detection devices. Generally, these compounds exhibit no appreciable absorption above 200 nm which limits the use of UV detection. Tomatidine and 5-tomatidenol have been separated by normal-phase HPLC with UV detection; however, 210 μg of tomatidine was injected and base line separation was not achieved[9]. Until recently, detectors were not sufficiently sensitive to use for the level of detection required in analysis of alkaloid extracts, however, RI detectors are now available that can detect these compounds at concentration levels well below that required in most, if not all, analyses. Using tomatidine as a representative alkaloid, we have determined that one can detect quantities as low as 200 ng which is approximately a thousand fold increase in sensitivity over that reported for UV detection without the problem of UV variable response for different chromophores.

The HPLC analysis of the steroidal alkaloid fraction of a *Solanum* hybrid[14] (supplied to us by Dr. J. P. Helgeson, Agricultural Research Service, U.S. Department of Agriculture, University Wisconsin, U.S.A.) which contains Δ^5 and saturated analogues is shown in Fig. 3a. For comparison purposes, the GC for this same mixture is shown in Fig. 3b. HPLC analysis of this mixture revealed two components (22 and 24.5 min) which were not readily apparent by other chromatographic procedures. It was established by mass spectrometry on collected samples of these peaks that the compounds are hydroxysolanidanes, the former being unsaturated and the latter the saturated compound. However, on the basis of retention (see Fig. 2) and mass spectral data, these compounds are not 23-hydroxysolanidine or 23-hydroxydemissidine. The superior separation of the saturate/Δ^5 pairs compared to GC is evident.

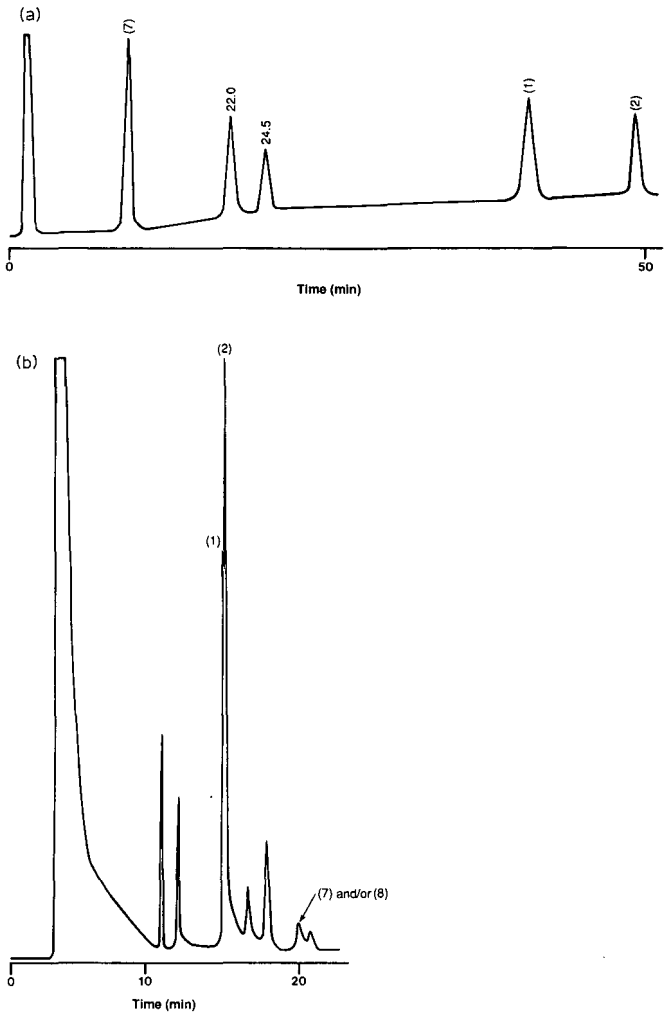

Fig. 3. Analysis of alkaloid fraction of *S. brevidens* × *S. tuberosum* hybrid. (a) HPLC chromatogram; (b) GC chromatogram. For conditions, see ref. 8.

The chromatogram of the tuber alkaloids of the commercial potato variety, Kahtadin, is shown in Fig. 4. Although there are some minor unidentified compounds in this alkaloid extract, one alkaloid, solanidine represents at least 90% of the sample.

Of all the reported methods for separating *Solanum* steroid alkaloids, in our estimation, this HPLC method provides the best separation of saturated and Δ^5 analogues (*e.g.*, solanidine and demissidine). Chromatographic conditions can be varied depending on the composition of the alkaloid mixture. On the basis of preliminary results we have for the separation of partially characterized dihydroxy steroidal alkaloids using a solvent mixture of acetonitrile–methanol (85:15) at a flow-rate of 0.5 ml min^{-1} provides better resolution of the solvent peaks from the

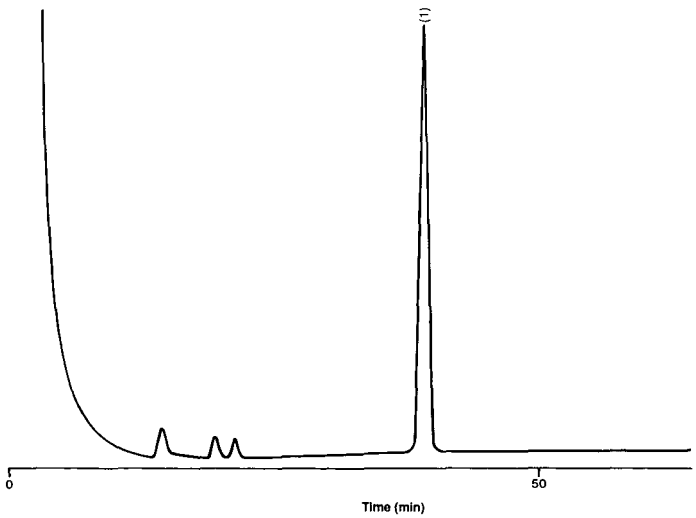

Fig. 4. HPLC chromatogram of the alkaloid fraction from the cultivated potato variety, Kathadin.

compounds of interest. If the alkaloid mixture contains compounds that are in the order of polarity or less polar than solasodine the 60:40 solvent mixture at a flow-rate of 1 ml min^{-1} results in shorter analysis time without significant loss of resolution. It is necessary in all solvent systems to include ethanolamine even when using the DB-modified column in order to obtain good elution profiles for these alkaloids.

ACKNOWLEDGEMENT

The authors wish to thank Ms. Joanne O'Conner for her technical assistance.

REFERENCES

1 K. Schreiber, in R. H. F. Manske (Editor), *The Alkaloids*, Vol. X, Academic Press, New York, 1968, pp. 1–192.
2 S. F. Osman, *Food Chem.*, 11 (1983) 235.
3 R. J. Bushway, *J. Chromatogr.*, 247 (1982) 18.
4 R. J. Bushway, J. L. Bureau and J. King, *J. Agric. Food Chem.*, 34 (1986) 277.
5 A. S. Carman, S. S. Kuan, G. M. Ware, O. J. Francis, Jr. and G. P. Kirschenheuter, *J. Agric. Food Chem.*, 34 (1986) 272.
6 P. M. Boll, *Acta Chem. Scand.*, 16 (1962) 181.
7 S. F. Herb, T. J. Fitzpatrick and S. F. Osman, *J. Agric. Food Chem.*, 23 (1975) 520.
8 W. J. M. van Gelder, *J. Chromatogr.*, 331 (1985) 285.
9 I. K. Hunter, M. Y. Walden and E. Heftmann, *J. Chromatogr.*, 198 (1980) 363.
10 I. K. Hunter, M. Y. Walden, J. R. Wagner and E. Heftmann, *J. Chromatogr.*, 118 (1976) 259.
11 P. Gregory, S. L. Sinden, S. F. Osman, W. M. Tingey and D. A. Chessin, *J. Agric. Food Chem.*, 29 (1981) 121.
12 H. Ripperger and K. Schreiber, in R. G. A. Rodrigo (Editor), *The Alkaloids*, Vol. XIX, Academic Press, New York, 1981, pp. 81–192.
13 S. L. Sinden, K. L. Deahl and L. L. Sanford, *Am. Potato, J.*, 63 (1986) 455.
14 S. Austin and J. P. Helgeson, in D. von Wettstein and N. Chua (Editors), *Plant Molecular Biology*, Plenum, New York, 1987, pp. 209–222.

Journal of Chromatography, 479 (1989) 194–199
Elsevier Science Publishers B.V., Amsterdam — Printed in The Netherlands

CHROM. 21 674

Note

Determination of hydrogen sulphide by porous-layer open-tubular column gas chromatography–mass spectrometry

SVEN JACOBSSON* and OLLE FALK
Kabi Pharma, Research and Development Department, Box 1828, S-171 26 Solna (Sweden)
(First received February 15th, 1989; revised manuscript received June 8th, 1989)

Numerous papers[1–24] have been published on the determination of volatile sulphur compounds such as hydrogen sulphide in various matrices as mouth air, petroleum gases, atmosphere samples and aqueous samples. Generally, volatile sulphur compounds are determined by gas chromatography. Gas chromatographic analyses of, for example, hydrogen sulphide have mainly been carried out using packed columns. The separation of hydrogen sulphide is often performed on packing materials such as Porapak Q, N or QS[1–8]. However, several other packing materials and stationary phases have come into use, *e.g.*, Carbopack[2,9,10], Triton X-305[11,12], Chromosorb P and 102[13,14], Chromosil 330[15], Tenax GC[16], polyphenyl ether[12,17] and various methylsilicone phases[18–20]. The determination of hydrogen sulphide on capillary columns has been performed with non-polar or medium-polarity silicone phases[21–24]. For capillary columns to retain hydrogen sulphide sufficiently to provide separation from air components the columns have to be operated at sub-ambient temperatures. Commonly used detection techniques are flame photometric and thermal conductivity detection, although mass spectrometry has also been used in combination with capillary columns.

Recently, porous-layer open-tubular (PLOT) columns with PoraPLOT Q deposited on the column wall have become commercially available. In this paper we demonstrate the usefulness of such a column interfaced to a mass spectrometer for the headspace analysis of hydrogen sulphide in liquid and solid samples.

EXPERIMENTAL

Gas standards of 10 ppm (standard grade A) and 992 ± 50 ppm hydrogen sulphide were obtained from AGA (Lidingö, Sweden). Sampling and injections were carried out with gas-tight syringes.

A PLOT column 10 m × 0.32 mm I.D. with PoraPLOT Q deposited on the column wall (Chrompak, Middelburg, The Netherlands) was either kept at 40°C or temperature programmed, the linear flow velocity of the carrier gas (helium) being 40 cm/s at 40°C.

The gas chromatograph–mass spectrometer was a Shimadzu (Kyoto, Japan) QP-1000 in the selected ion monitoring (SIM) mode. The ion of m/z 34, corresponding to the molecular ion of H_2S, was monitored. The electron-impact energy was 70 eV and the ion source temperature was 250°C.

0021-9673/89/$03.50

To prevent particles from the column to entering and contaminating the ion source, the PLOT column was connected to the ion source via deactivated fused silica. A piece of deactivated quartz-wool was placed in the low-volume connector between the PLOT column and the fused silica.

For high hydrogen sulphide concentrations (amount of H_2S sampled > 2 ng), ordinary split injection could be used; however, for lower concentrations cryogenic focusing of the headspace sample was necessary. In this work the cryogenic focusing system (Fig. 1) was used throughout. A detailed description of a similar system has been published elsewhere[25]. Briefly, the hydrogen sulphide present in the headspace sample was injected into the dynamic headspace chamber and transferred to a cold trap by a flow of helium (20 ml/min). The cold trap was made of a deactivated fused silica (35 cm × 0.25 mm I.D.). This fused-silica tube was placed inside a U-shaped glass tube (1.6 mm O.D. × 0.7 mm I.D.), which was suspended in a Dewar flask containing liquid nitrogen. Around the glass tube a Kanthal A wire was coiled to achieve rapid heating on reinjection. With use of the cryogenic focusing technique relative large headspace volumes (1–10 ml) could be injected on to the capillary column without the need for splitting.

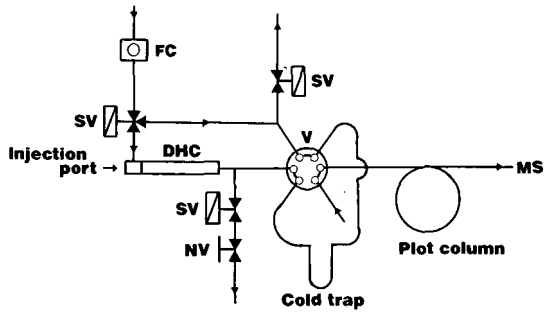

Fig. 1. Schematic diagram of the cold trap–reinjection interface. DHC = Dynamic headspace chamber used as an injector; FC = flow controller; MS = mass spectrometer; NV = needle valve; SV = solenoid valve; V = Valco six-port valve.

Liquid samples were analysed by use of the static headspace method. For quantitative determination, the standard additions technique was used. The sample was equilibrated in a glass vial (9 ml) with a aluminium-coated silicone septum. A known volume of the hydrogen sulphide gas standard was added to the liquid phase of the sample by means of a gas-tight syringe. The headspace of the equilibrated sample was examined by PLOT column gas chromatography–mass spectrometry. As the gaseous hydrogen sulphide was added to the liquid phase, the headspace concentration of hydrogen sulphide incrased with time and reached equilibrium within 60 min (Fig. 2). To simulate standard sample conditions, a liquid phase (N-acetyl-cysteine in water, 25 mg/ml) that had been heat treated at 120°C for 20 minutes prior to the equilibrium study was used.

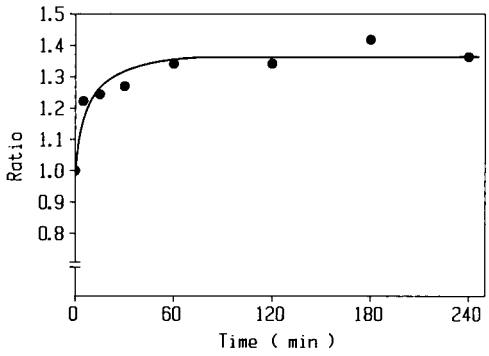

Fig. 2. Headspace concentration of hydrogen sulphide after addition of hydrogen sulphide gas (0.7 μg H_2S) to the aqueous phase (0.5 ml), containing N-acetylcysteine (25 mg/ml). The concentration is given as the ratio of the amount obtained after addition to that obtained prior to addition.

RESULTS AND DISCUSSION

The concept and preparation of PLOT columns are not new and date back to the early days of capillary gas chromatography[26,27]. Theoretically, PLOT columns should take advantage of the selectivity of the adsorbent–solid material deposited as a thin layer on the wall and on the large plate numbers that are generated by capillary columns. However, only recently have PLOT columns become commercially available from various suppliers.

The packing material is deposited on the wall as a layer with a film thickness of 10 μm. This solid layer may be assumed to redistribute on drastic pressure changes, and therefore care must be taken with installation and running the column. Further, in order to prevent particles from the column entering to the ion source, the precautions given under Experimental were employed. Under these conditions, the use of the PLOT column was found to be highly compatible with mass spectrometry. The PLOT column was connected to the mass spectrometer for more than 2 months without any serious contamination of the ion source, *i.e.*, the calibration set parametes for the ion source and the quadropole did not change over that period.

With the cryogenic focusing technique, linear calibration graphs for gas standards of hydrogen sulphide were obtained in the range 0.07–53 ng (Fig. 3). The best determination of hydrogen sulphide was obtained by use of peak height, as peak-area integration became restricted in the lower picogram range owing to less well defined hydrogen sulphide peaks (Fig. 4). Moreover, as can be seen in Fig. 4, the water present in the injection system also had a negative effect on the hydrogen sulphide peak. However, for higher amounts of hydrogen sulphide, the trace level of water present in the injection system did not constitute any problem with respect to peak shape (see Fig. 4C). Hydrogen sulphide is baseline separated from water under equimolar conditions, but a large excess of water distorts the SIM signal of hydrogen sulphide (m/z 34). The response of water at m/z 34 is attributed mainly to cluster formation. This cluster formation was not studied in any depth, but is probably related to the ion source temperature and pressure, *i.e.*, the amount of water injected. As an illustration, the headspace injection of 8 μg of water through the capillary column gave

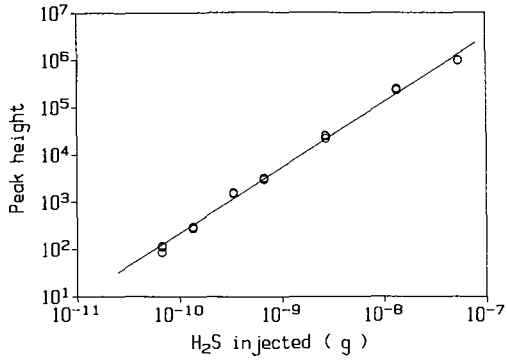

Fig. 3. Calibration graph for gas standards of hydrogen sulphide (r = 0.9994).

a response of the order of 0.01% at m/z 34 relative to that of m/z 18. The precision (relative standard deviation) of the cryogenic focusing method for gaseous standards of hydrogen sulphide was 1.13% at the 53-ng level ($n=5$) and 7.30% at the 0.67-ng level ($n=5$).

As hydrogen sulphide has a low boiling point (−60.7°C) the use of headspace analysis has been explored for the analysis of solid and liquid samples. The applicability of headspace analysis for the determination of hydrogen sulphide in various aqueous samples was studied. As the presence of water may have a negative effect on the SIM signal relating to hydrogen sulphide, the effect of water on the hydrogen sulphide peak was studied by co-injection of various amounts of water. Too large amounts of water (> 10 μg) can cause a decrease in the hydrogen sulphide peak. This restricts the headspace volume that could be sampled and analysed directly over an aqueous sample, *e.g.*, the largest headspace volume to be sampled over an aqueous

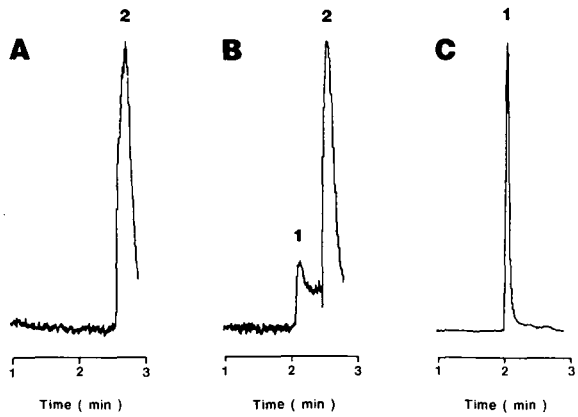

Fig. 4. (A) Blank chromatogram. (B) SIM chromatogram of 70 pg of hydrogen sulphide (peak 1). The peak at a retention time of 2.7 min (peak 2) was caused by water present in the carrier gas of the cryogenic focusing system (and is probably due to cluster formation of water). (C) SIM chromatogram of 3 ng of hydrogen sulphide.

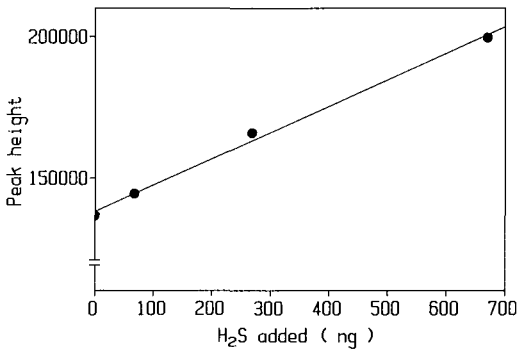

Fig. 5. Standard addition calibration graph. Addition of gaseous hydrogen sulphide to an aqueous sample (1.0 ml) at 25°C.

solution at 25°C and analysed as such is *ca.* 400 μl. Further, this also calls for identical procedures in calibration and analysis of the aqueous sample in order to generate reliable quantitative results. The standard additions method fulfils this criterion. By use of the standard additions method, hydrogen sulphide could be quantitatively determined (Fig. 5).

The precision (relative standard deviation) of the headspace analysis method was 4.4% at a hydrogen sulphide concentration of 1.4 μg/ml in an aqueous sample. The sample was repeatedly analysed five times. With the proposed method, concentrations of hydrogen sulphide in aqueous solutions in the low ng/ml range can be determined with a limit of detection of *ca.* 1 ng/ml (Fig. 6). If greater sensitivity is needed, however, an approach would be to use stripping analysis in combination with the cryogenic focusing device. A prerequisiste of such a method, however, is that water has to be removed prior to the trap, *e.g.*, by calcium chloride[14], in order to prevent plugging of the cold trap.

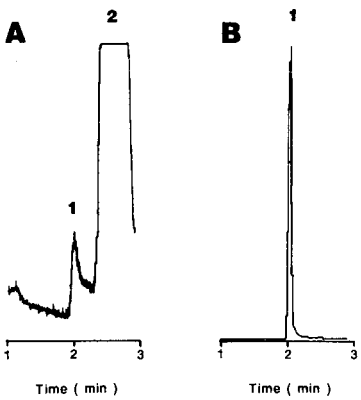

Fig. 6. (A) SIM chromatogram of 1.4 ng/ml of hydrogen sulphide (peak 1) in an aqueous sample (peak 2 = water). (B) SIM chromatogram of 1.6 μg/ml of hydrogen sulphide in an aqueous sample. The equilibrium temperature was 25°C and the headspace volume sampled was 100 μl.

A distinct advantage with the PLOT column is that the sub-ambient column temperatures that are generally needed for capillary column separations of many gaseous and highly volatile compounds can be circumvented. The combination of a PLOT column separation and mass spectrometric detection also provides a highly selective determination of hydrogen sulphide, with a sensitivity comparable to or better than that of flame photometric detection.

REFERENCES

1 C. N. Jones, *Anal. Chem.*, 39 (1967) 1858.
2 L. Giry, M. Chaigneau and L.-P. Ricard, *Analusis*, 6 (1978) 203.
3 N. Kishima, *Anal. Chem.*, 58 (1986) 1255.
4 F. Andrawes, G. Holzer, E. Roedder, E. K. Gibson, Jr., and J. Oro, *J. Chromatogr.*, 302 (1984) 181.
5 T. L. C. de Souza, *J. Chromatogr. Sci.*, 22 (1984) 470.
6 L. Huber and H. Obbens, *J. Chromatogr.*, 349 (1985) 465.
7 P. P. Deprez, P. D. Franzmann and H. R. Burton, *J. Chromatogr.*, 362 (1986) 9.
8 G. A. Cutter and T. J. Oatts, *Anal. Chem.*, 59 (1987) 717.
9 F. Mangani, F. Bruner and N. Penna, *Anal. Chem.*, 55 (1983) 2193.
10 P. G. Slater and L. Harling-Bowen, *Analyst (London)*, 111 (1986) 1059.
11 A. H. H. Tameesh, A. O. Bender and T. M. Sarkissian, *J. Chromatogr.*, 321 (1985) 59.
12 J. Macák, J. Kubát, V. Dobal and J. Mizera, *J. Chromatogr.*, 286 (1984) 69.
13 W. K. Al-Thamir, *J. High Resolut. Chromatogr. Chromatogr. Commun.*, 8 (1985) 143.
14 A. Tangerman, *J. Chromatogr.*, 366 (1986) 205.
15 C. Leck and L. E. Bågander, *Anal. Chem.*, 60 (1988) 1680.
16 K. J. Rygle, G. P. Feulmer and R. F. Scheideman, *J. Chromatogr. Sci.*, 22 (1984) 514.
17 A. R. Blachette and A. D. Cooper, *Anal. Chem.*, 48 (1976) 729.
18 H. J. Rath and J. Wimmer, *Chromatographia*, 13 (1980) 513.
19 A. Tangerman,M. T. Meuwese-Arends and J. H. M. van Tongeren, *Clin. Chim. Acta*, 130 (1983) 103.
20 K. C. Campbell, M. L. Mirza, S. J. Thomson and G. Webb, *Analyst (London)*, 110 (1985) 1039.
21 S. O. Farwell, S. J. Gluck, W. L. Bamesberger, T. M. Schutte and D. F. Adams, *Anal. Chem.*, 51 (1979) 609.
22 J. Kangas, *J. Chromatogr.*, 346 (1985) 405.
23 M. Termonia, M. Guns and F. Gillard, *Int. J. Environ. Anal. Chem.*, 20 (1985) 69.
24 J. W. de Leeuw, E. W. B. de Leer J. S. Sinninghe Damsté and P. J. W. Schuyl, *Anal. Chem.*, 58 (1986) 1852.
25 A. Hagman and S. Jacobsson, *J. Chromatogr.*, 395 (1987) 271.
26 I. Halász and Cs. Horváth, *Nature (London)*, 197 (1963) 71.
27 M. J. E. Golay, *Anal. Chem.*, 40 (1968) 382.

Journal of Chromatography, 479 (1989) 200–205
Elsevier Science Publishers B.V., Amsterdam — Printed in The Netherlands

CHROM. 21 689

Note

Supercritical fluid extraction of *s*-triazine herbicides from sediment[a]

V. JANDA*
Prague Institute of Chemical Technology, Department of Water Technology and Environmental Engineering, Suchbatarova 5, CS-166 28 Prague 6 (Czechoslovakia)
and
G. STEENBEKE and P. SANDRA
University of Ghent, Laboratory of Organic Chemistry, Krijgslaan 281(S4), B-9000 Ghent (Belgium)
(First received March 3rd, 1989; revised manuscript received June 12th, 1989)

Supercritical fluid extraction (SFE) is a very useful technique for the isolation of organic compounds from a solid matrix. It has been used for the analysis of flavours and fragrances from natural products[1], toxic organics from resins[2], polycyclic compounds and polychlorinated biphenyls from environmental solids[3] and other compounds (ref. 4 and references cited therein).

Carbon dioxide is mostly used as a supercritical fluid because of its low critical temperature (32°C) and pressure (73 bar), which allows SFE to be performed at relatively low temperatures, avoiding thermal decomposition of analytes. Carbon dioxide is a non-explosive and relatively inert gas at normal temperature and pressure, which simplifies subsequent concentration of the compounds isolated by SFE. It is also possible to couple SFE with capillary gas chromatography (GC)[3,4]. Complete transfer of analytes from SFE directly into a capillary column is achieved by this on-line modification and lower detection limits may be reached.

The aim of this work was to measure the recovery of *s*-triazine herbicides from river sediment by SFE. The compounds used are listed in Table I.

TABLE I

s-TRIAZINE HERBICIDES STUDIED

Common name	*Systematic name*
Simazine	2-Chloro-4,6-bisethylamino-*s*-triazine
Atrazine	2-Chloro-4-ethylamino-6-isopropylamino-*s*-triazine
Propazine	2-Chloro-4,6-bisisopropylamino-*s*-triazine
Terbutylazine	2-Chloro-4-ethylamino-6-*tert.*-butylamino-*s*-triazine
Cyanazine	2-Chloro-4-ethylamino-6-(1-cyano)isopropylamino-*s*-triazine

[a] Presented at the *10th International Symposium on Capillary Chromatography, Riva del Garda, May 22–25, 1989.*

0021-9673/89/$03.50

EXPERIMENTAL

Supercritical fluid extraction

All the SFEs were performed using a Varian 8500 syringe pump. The extractions were performed at a pressure of carbon dioxide of 230 bar and a temperature 48°C. The density of carbon dioxide under these conditions is about 0.80 g/ml[5]. The apparatus is shown schematically in Fig. 1. The cartridge for extraction of the sediment was constructed according to Fig. 2. The pressure of the supercritical carbon dioxide in the cartridge was maintained by means of a capillary fused-silica restrictor (30 cm × 25 μm I.D.). The time of SFE was 30 min and during this period approximately 18 ml of liquid carbon dioxide were pumped into the SFE system. The cartridge had an inner volume 0.57 ml and 500 mg of the sediment were extracted. The outlet of the restrictor was immersed in methanol in the test-tube to trap the isolated compounds. Although the test-tube was placed in the oven, losses of methanol during SFE were acceptable because it was cooled by carbon dioxide expansion from the restrictor (during SFE ice was precipitated on the outer wall of the test-tube from moisture in the oven). The volume of methanol in the test-tube was 1 ml at the beginning of the SFE and decreased to approximately 0.5 ml by stripping with gaseous carbon dioxide within the 30-min period. Venting of methanol vapour from the test-tube did not affect the recovery of *s*-triazines as they are relatively non-volatile and evaporation of a solvent is a common step, *e.g.*, for concentration of extracts from water[6]. The decrease in the methanol volume was corrected for by addition of an internal standard before chromatographic analysis.

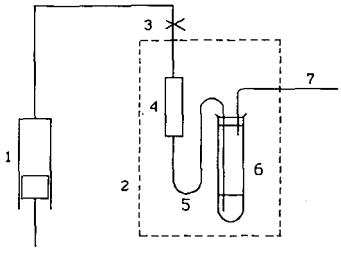

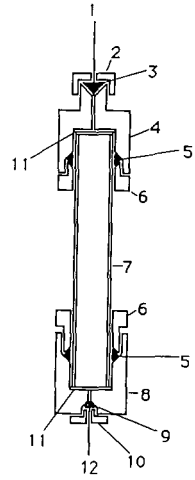

Fig. 1. Apparatus for SFE (not to scale). 1 = Pump for liquid carbon dioxide; 2 = oven; 3 = shut-off valve; 4 = cartridge with sample of sediment (for details see Fig. 2); 5 = restrictor; 6 = test-tube with methanol; 7 = fused-silica capillary (0.32 mm I.D.) for venting gaseous carbon dioxide.

Fig. 2. Extraction cartridge. 1 = Stainless-steel capillary; 2 = tubing union; 3 = metal ferrule; 4 = female nut; 5 = metal fitting; 6 = male nut; 7 = stainless-steel tubing; 8 = female nut; 9 = Vespel ferrule; 10 = male nut; 11 = stainless-steel frit; 12 = restrictor.

Capillary gas chromatography

For the GC analyses a Varian 3700 gas chromatograph equipped with a flame ionization detector and a laboratory-made cold on-column injector was used. The column was a fused-silica capillary (30 m × 0.3 mm I.D.) coated with Superox 20M. The temperature was programmed from 70 to 220°C at 20°C/min and then held at 220°C for 8 min. Hydrogen was used as the carrier gas (inlet pressure 0.95 bar). Volumes up to 2 μl were injected. No deterioration in peak shape was observed. Eicosane was used as an internal standard. Even very complex mixtures of *s*-triazines can be separated on poly(ethylene glycol)-based stationary phases[7].

High-performance liquid chromatography

For the separation of *s*-triazines, silica gel[8], amino- or cyano-bonded stationary phases[9,10] with a non-polar mobile phase or a reversed phase with methanol–water as the mobile phase[11,12] have been applied. Ultraviolet detection is very suitable as *s*-triazines exhibit strong absorbance at 220–240 nm[11]. An HP 1090 liquid chromatograph equipped with diode-array detector and a 25 cm × 0.46 cm I.D. column packed with reversed phase was used. The greatest absorbance was observed in the 220–225 nm region for all the compounds tested. For the measurements a wavelength of 225 nm was used. The flow-rate of the mobile phase [methanol–water (65:35, v/v)] was 1 ml/min. Volumes of 10–25 μl of the extract were injected. Thyophylline was used as an internal standard for high-performance liquid chromatographic (HPLC) experiments.

Recovery of s-*triazines from sediment*

The sediment was dried through lyophilization. A weighed amount (0.5 g) was spiked by a methanolic solution of *s*-triazines and the solvent was allowed to evaporate from the slurry overnight. The spiked sediment was then subjected to SFE. The extract after SFE was analysed by capillary GC or HPLC after addition of an internal standard. For the analyses of the lowest concentrations of *s*-triazines, methanol was evaporated by means of a mild stream of nitrogen to a final volume of 200 μl.

Simultaneously, a reference mixture representing 100% recovery was prepared by addition of the same amount of *s*-triazines and internal standard to methanol. Recoveries were calculated from the responses of a given compound corrected on the response of the internal standard obtained from analysis of the methanolic solution after SFE and of the "100% recovery" solution, respectively.

RESULTS AND DISCUSSION

Recoveries of SFE of *s*-triazines from the sediment by pure supercritical carbon dioxide are given in column B in Table II. It can be seen that recoveries are high, with the exception of simazine. The poor recovery of the latter might be explained by its low solubility in low-polarity solvents, including benzene. As the polarity of carbon dioxide is roughly similar to that of benzene, this explains why the recovery of simazine is low.

In the next experiment (column C in Table II), 20 μl of methanol were added directly into the SFE cartridge (into the inlet side of supercritical carbon dioxide) just before SFE. This simple modification of the supercritical carbon dioxide polarity

TABLE II

RECOVERY OF *s*-TRIAZINES BY SFE WITHOUT (B) AND WITH (C) METHANOL ADDITION

Compound	*Concentration in sediment (ppm)*	*Recovery (%)*	
		B	*C*
Propazine	60.8	96.4	96.4
Terbutylazine	40.2	82.4	91.8
Atrazine	60.2	86.2	91.0
Simazine	28.0	42.5	92.0
Cyanazine	81.2	92.4	90.2

increased the recovery of simazine considerably (see also Fig. 3). During all further experiments methanol was added to the cartridge before SFE.

For the analyses of the extracts given in Table II, flame ionization detection (FID) was used. Although the sensitivity of GC was sufficient for the analysis of lower concentration of triazines, the FID selectivity does not permit this, as interfering

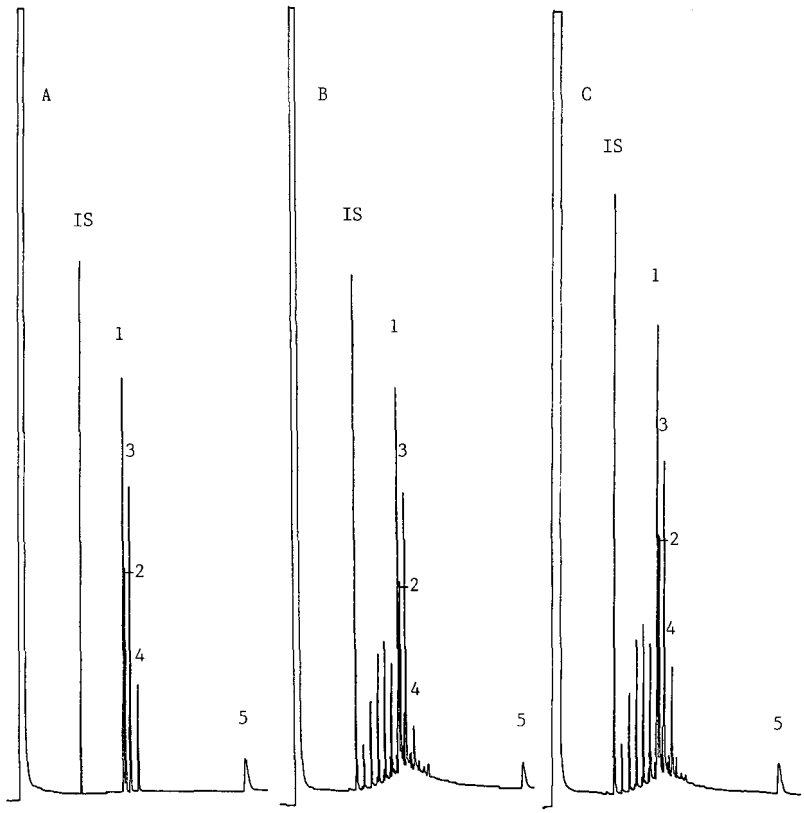

Fig. 3. GC analyses. (A) "100% recovery" solution; (B) SFE with pure carbon dioxide; (C) SFE with methanol addition. Peaks: IS = internal standard (retention time 4.10 min); 1 = propazine (6.62 min); 2 = terbutylazine (6.68 min); 3 = atrazine (6.96 min); 4 = simazine (7.44 min); 5 = cyanazine (13.67 min). Volume injected: 1.5 μl.

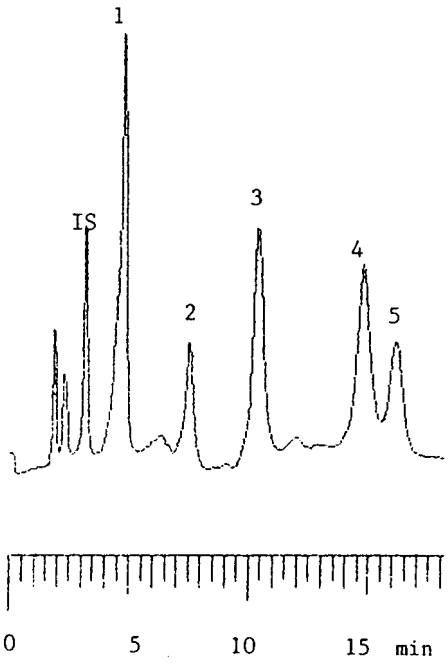

Fig. 4. HPLC analysis of *s*-triazines in sediment after SFE. Peaks: IS = internal standard; 1 = cyanazine; 2 = simazine; 3 = atrazine; 4 = propazine; 5 = terbutylazine. Volume injected: 10 μl.

compounds were co-extracted from the sediment by SFE. Interfering peaks overlap with *n*-alkanes (heneicosane and higher) which were originally present in the sediment. However, no particular attempt was made to identify these compounds unambiguously in this work. GC-selective ion monitoring can be applied to detect lower concentrations. In this work, however, the lower concentrations were measured by HPLC with diode-array detection (Fig. 4). Recoveries are summarized in Table III. Fig. 4 refers to concentrations given in the first column in Table III. HPLC showed a high selectivity even for the lowest concentrations tested, with the exception of propazine and terbutylazine, where interferences also occurred.

TABLE III

RECOVERY OF *s*-TRIAZINES FROM SEDIMENT (HPLC ANALYSES)

Compound	*Concentration (ppb)*	*Recovery (%)*	*Concentration (ppb)*	*Recovery (%)*	*Concentration (ppb)*	*Recovery (%)*
Cyanazine	4060	102.5	406.0	95.8	81.2	97.1
Simazine	1400	103.4	140.0	98.3	28.0	93.2
Atrazine	3010	95.8	301.0	102.0	60.2	91.8
Propazine	3040	103.5	304.0	94.1	60.8	ND[a]
Terbutylazine	2010	97.1	201.0	94.2	40.2	ND[a]

[a] Not detectable owing to interferences.

REFERENCES

1 S. B. Hawthorne, M. S. Kreiger and D. J. Miller, *Anal. Chem.*, 60 (1988) 472.
2 J. H. Raymer and E. D. Pellizzari, *Anal. Chem.*, 59 (1987) 1043.
3 S. B. Hawthorne and D. J. Miller, *J. Chromatogr.*, 403 (1987) 63.
4 I. L. Davies, M. W. Raynor, J. P. Kithinji, K. D. Bartle, P. T. Williams and G. E. Andrews, *Anal. Chem.*, 60 (1988) 683A.
5 R. W. Bally and C. A. Cramers, in D. Ishii, K. Jinno and P. Sandra (Editors), *Proc. 7th Int. Symp. on Capillary Chromatography*, University of Nagoya Press, Nagoya, 1986, p. 560.
6 V. Janda, in P. Sandra and W. Bertsch (Editors), *Proc. 6th Int. Symp. on Capillary Chromatography*, Hüthig, Heidelberg, 1985, p. 296.
7 E. Matisová, J. Krupčík, O. Liška and N. Szentiványi, *J. Chromatogr.*, 169 (1979) 261.
8 P. Dufek and V. Pacáková, *J. Chromatogr.*, 187 (1980) 341.
9 P. Dufek, V. Pacáková and E. Terařová, *J. Chromatogr.*, 191 (1980) 115.
10 E. Smolková and V. Pacáková, *Chromatographia*, 11 (1978) 698.
11 H. Jork and B. Roth, *J. Chromatogr.*, 144 (1977) 39.
12 M. Popl, Z. Vozňáková, V. Tatar and J. Strnadová, *J. Chromatogr. Sci.*, 21 (1983) 39.

Journal of Chromatography, 479 (1989) 206–211
Elsevier Science Publishers B.V., Amsterdam — Printed in The Netherlands

CHROM. 21 680

Note

High-performance liquid chromatography of metribuzin and non-polar metabolites extracted from leaf tissues

HELEN A. NORMAN*, CHARLES F. MISCHKE and JUDITH B. St. JOHN
Weed Science Laboratory, U.S. Department of Agriculture, Agricultural Research Service, Building 001, Room 29, BARC-West, Beltsville, MD 20705 (U.S.A.)
(First received August 1st, 1988; revised manuscript received June 6th, 1989)

Metribuzin [4-amino-6-(1,1-dimethylethyl)-3-(methylthio)-1,2,4- triazin-5(4H)-one] (Fig. 1) is an asymmetric triazinone herbicide which effectively controls certain grass and broadleaf weeds infesting soy bean, tomato and other crops. The rate of metabolism of metribuzin to less phytotoxic compounds is thought to determine the relative tolerance of different crop cultivars to metribuzin[1–4]. Frear *et al.*[5] have identified two polar metabolites, the β-D-(N-glucoside) conjugate and the malonyl β-D-(N-glucoside) conjugate, as the initial and major degradation products in tomato.

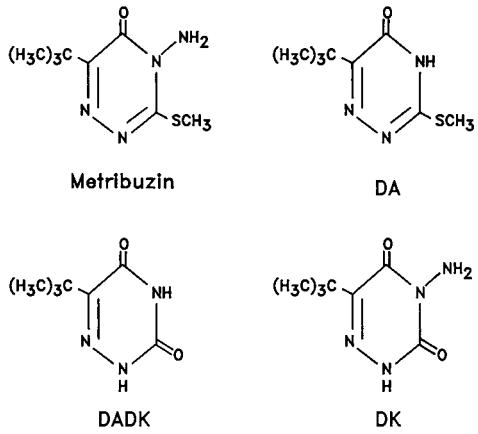

Fig. 1. Structure of metribuzin and non-polar metabolites.

In contrast, the major pathway of metabolism of metribuzin in soy bean involved an initial oxidation of the methylthio group to yield a reactive sulfoxide intermediate[6]. This sulfoxide could then undergo peptide conjugation with homoglutathione or possibly degrade to non-polar metabolites, specifically the diketo (DK) and the deaminated diketo (DADK) forms of metribuzin. Small amounts of the deaminated (DA) form of metribuzin, DK and DADK (Fig. 1) were reported as plant metabolites in sugar-cane[7], potato[8] and several weed species[9,10]. These non-polar

0021-9673/89/$03.50

products were also formed as degradation products in the soil[11] and by photochemical reaction on surfaces and in solution[12,13].

Metribuzin and DA, DADK and DK metabolites have previously been resolved and quantified by thin-layer chromatography (TLC) and gas–liquid chromatography (GLC) procedures[1,3,4,14–16].Some GLC analyses utilizing electron-capture detectors[14,16] required extensive sample cleanup on liquid chromatography columns, and also that metribuzin be separated from non-polar metabolites and analyzed independently[16]. The use of flame photometric detection in GLC can eliminate interferences present in non-purified extracts[17]. Jarczyk[18,19] has described detailed GLC determinations of metribuzin and metabolite residues using a nitrogen-specific alkali flame ionization detector.

Parker *et al.*[20] developed an alternative technique based on an isocratic HPLC system for the resolution of metribuzin, DK, DADK and DA on a C_{18} column with detection by absorbance at 254 or 280 nm. Quantitation limits by direct peak integration ideally were 1–2 ng for standard mixtures of metribuzin and each of the non-polar metabolites. These limits of detection were not achievable in extracts from biological material because of interferences from naturally occurring components that could not be separated satisfactorily from the compounds of interest.

In this report, we describe an HPLC mobile phase providing increased resolution of metribuzin, DK, DADK and DA on a C_{18} column. We have also developed a new procedure for the rapid removal of interfering compounds extracted from leaf tissues together with the herbicide and non-polar metabolites. This routinely allowed quantitative detection limits as low as 0.2 ng. Radioactivity in ^{14}C-labelled non-polar metabolites and the parent compound can be determined simultaneously by coupling UV detection with an in-line radioactivity monitor.

EXPERIMENTAL

Standards and solvents

Standards of metribuzin and the metabolites DA, DADK and DK were provided by Mobay (Kansas City, MO, U.S.A.). Stated purities for these compounds were 97.3, 99.9, 92.9 and 99.1%, respectively. [5(ring)-^{14}C]Metribuzin (20.8 Bq/mmol) (96.3% purity) was also supplied by Mobay. All organic solvents used were HPLC-grade (Fisher Scientific, Fairlawn, NJ, U.S.A.). Water used in HPLC analyses was purified through NANOpure II and ORGANICpure units (Barnstead, Sybron Corp., Boston, MA, U.S.A.). All HPLC solvents utilized were filtered through 0.5-μm Millipore filters (Millipore, Bedford, MA, U.S.A.).

Plant material and ^{14}C-incubation

Sweet potato (*Ipomoea batatas*) and soy bean (*Glycine max*) plants were grown in greenhouse conditions in a potting soil consisting of a 2:1 (v/v) mixture of composted potting soil and sand. Leaf tissue was harvested from the apical portion of the growing stem and used in the extraction and ^{14}C-incubation experiments.

Sweet potato stems with attached leaves were excised and transferred to 125-ml erlenmeyer flasks containing 100 ml of tap water for the ^{14}C-incubation experiments. Roots had developed on the cuttings after incubation for 3 days in an 18 h photoperiod (200 μEinsteins m^{-2} s^{-1}) at 26°C wih a 17°C dark period. The isolated cuttings were

then incubated for 48 h in flasks containing 100 ml of $5 \cdot 10^{-6}$ *M* metribuzin containing 0.5 μCi [^{14}C]metribuzin (20.8 Bq/mmol). At the end of the incubation period, cuttings were rinsed with running water and placed in 100 ml of $5 \cdot 10^{-6}$ *M* metribuzin for an additional 72 h.

Sample preparation

Leaf tissue (2.5 g fresh weight) was homogenized with 20 ml of methanol–water (8:2, v/v) using a Polytron. Spiked samples were prepared by adding 2.5 μg each of metribuzin, DA, DADK and DK, dissolved in methanol to the homogenates. An equivalent amount of methanol was added to blank samples. Homogenates were vaccum filtered, and then plant residue on the filter was rinsed with 20 ml of methanol–water (8:2, v/v) followed by 10 ml of methanol. Combined filtrates were evaporated *in vacuo*. The sample was dispersed in 25 ml of chloroform and partitioned with 20 ml of 0.1 *M* potassium chloride. The chloroform layer was recovered and the aqueous phase re-partitioned twice with chloroform. Combined chloroform fractions were dried *in vacuo* at 35°C and the residue re-dissolved in 200–500 μl of diethyl ether. This re-dissolved residue was then applied to a C_{18} Sep-Pak cartridge (Waters Assoc., Milford, MA, U.S.A.). Diethyl ether was evaporated by passing nitrogen gas through the Sep-Pak. Metribuzin and non-polar metabolites were then eluted with 20 ml of acetonitrile–water (50:50, v/v). The eluate was dried *in vacuo* and the residue next solubilized in chloroform and applied to a silica Sep-Pak cartridge (Waters Assoc.). Metribuzin and non-polar metabolites were eluted from the Sep-Pak cartridge with 20 ml of chloroform. The final extracts were dried and then re-dissolved in the mobile phase prior to HPLC analysis.

HPLC analyses

HPLC analyses were conducted utilizing an ACS Model 351 solvent delivery system (Applied Chromatography Systems, Luton, U.K.), a Rheodyne Model 7125 syringe-loading sample injector with a 50-μl loop and a 25 cm × 4.6 mm I.D. Beckman Ultrasphere (5 μm) reversed-phase C_{18} column. The mobile phase was 0.05 *M* acetic acid–acetonitrile–methanol (67:28:5, v/v/v) delivered at a flow-rate of 0.9 ml min^{-1}. Samples for injection (50 μl) were taken from final extracts dissolved in this mobile phase. Compounds were detected at 280 nm with a Linear UV1S 203 variable wavelength detector, and elution profiles were recorded and integrated by a HP 3390A integrator (Hewlett-Packard, Avondale, PA, U.S.A.). After injection of 20 samples, the column was cleaned with tetrahydrofuran at a flow-rate of 1 ml/min for 2 h to remove strongly retained contaminants. Radioactivity was determined after the peaks were first detected at 280 nm and then eluted through a Flo-One Beta (Model IC) HPLC radioactive flow detector (Radiomatic Instruments and Chemical Co., Tampa, FL, U.S.A.) with Flo-Scint III (Radiomatic Instruments and Chemical Co.) as scintillator mixed with the HPLC eluate by means of the Flo-One component pump operating at 4.5 ml/min. Under these conditions, the counting efficiency for ^{14}C was approximately 80%.

TLC separation of metribuzin and metabolites

Silica gel HF plates (Analabs, Norwalk, CT, U.S.A.) were used for TLC of [^{14}C]metribuzin, DA, DADK and DK. Tissue extracts for TLC were first purified

through C_{18} and silica Sep-Paks, then re-dissolved in ethanol and applied to plates, developed in benzene–chloroform–*p*-dioxane (4:3:3, v/v/v)[1]. Metribuzin, DA, DADK and DK standards were used for co-chromatography and detection by UV light. The resolved compounds were scraped from the TLC plate and extracted from the silica with 50% ethanol and counted for radioactivity using a Beckman LS 1801 liquid scintillation counter.

RESULTS AND DISCUSSION

Standards of metribuzin and the non-polar metabolites, DK, DADK and DA, were optimally resolved by reversed-phase HPLC separation utilizing 0.05 *M* acetic acid–acetonitrile–methanol (67:28:5, v/v/v) as the mobile phase (Fig. 2). Reproducible quantitation by peak integration at 280 nm was recorded between 0.2 ng and 100 μg of the standards. Parker *et al.*[20] used reversed-phase separation with a mobile phase consisting of methanol–0.05 *M* acetic acid (62:38, v/v), delivered at 1 ml/min, to separate these same compounds with detection limits of 1–2 ng at 280 nm.

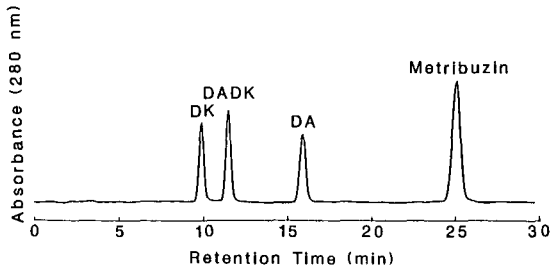

Fig. 2. Reversed-phase HPLC separation of metribuzin and non-polar metabolite standards. Column: Beckman Ultrasphere (5 μm, 250 mm × 4.6 mm). Mobile phase: 0.05 *M* acetic acid–acetonitrile–methanol (67:28:5, v/v/v), 0.9 ml/min; detection by UV absorbance (280 nm).

Chromatograms of samples from sweet potato leaf extracts which were spiked with a mixture of metribuzin and non-polar metabolite standards (2.5 μg per 2.5 g tissue) before or after filtration through C_{18} and silica Sep-Paks are compared in Fig. 3A and B, respectively. The peaks defined correspond to approximately 25 ng each of metribuzin, DK, DADK and DA. Without Sep-Pak purification (Fig. 3A), unidentified components eluted immediately before or concurrently with the compounds of interest and background signals were elevated. Successive elution of the extracts through C_{18} and silica Sep-Pak with the solvents described, removed most of the interfering contaminants (Fig. 3B). The unidentified peaks remaining in samples filtered through Sep-Paks were also found in blank tissue extracts. They were sufficiently resolved from metribuzin, DK, DADK and DA to allow reproducible quantitation of metribuzin and the metabolites to a limit of 0.2 ng. An equivalent chromatogram of samples from soy bean leaf extracts purified by Sep-Pak filtration is shown in Fig. 4. The recoveries of metribuzin and each of the non-polar metabolites added to the tissue extracts of both sweet potato and soy bean were 92–94%.

The excellent HPLC resolution allowed the direct determination of [^{14}C]metri-

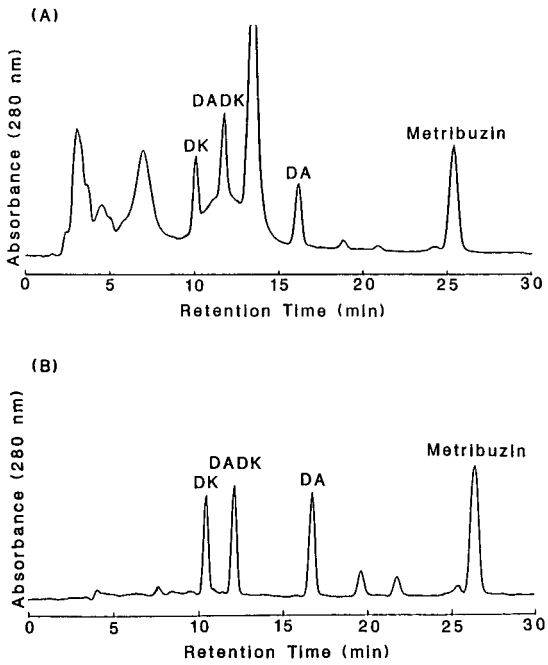

Fig. 3. Chromatograms of sweet potato leaf extracts spiked with metribuzin and non-polar metabolites and then injected (A) before or (B) after filteration through Sep-Paks. HPLC conditons. see Fig. 2.

buzin, DK, DADK and DA by liquid scintillation counting after they first eluted through the UV detector and then eluted through an in-line radioactivity detector. Flow-rates of HPLC mobile phase and scintillation fluid of 0.9 and 4.5 ml/min, respectively, were optimal for peak resolution and counting efficiency. Fig. 5 records a radiogram of [^{14}C]metribuzin and ^{14}C-metabolites resolved by the HPLC system. The sample mixture was extracted from sweet potato leaf tissue. The overall recovery of radioactivity from the HPLC column in a 30-min run time was 93–95%. The distribution of counts between the different compounds resolved was in close

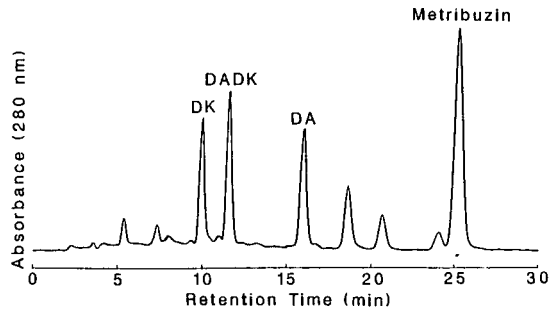

Fig. 4. Chromatograms of soy bean leaf extracts spiked with metribuzin and non-polar metabolites. HPLC conditions, see Fig. 2.

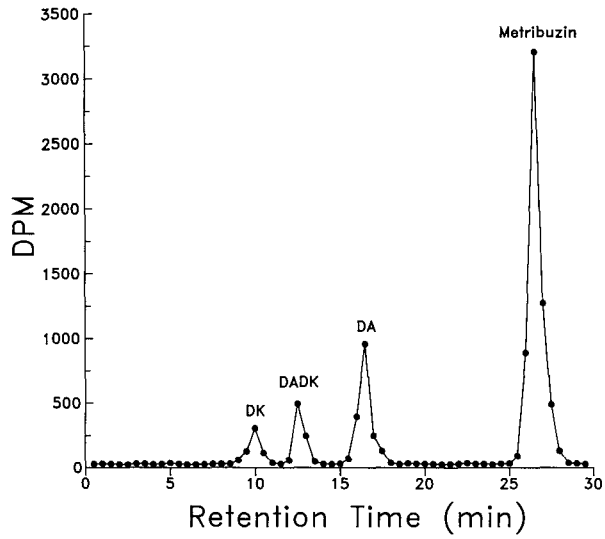

Fig. 5. Radiogram of ^{14}C-metribuzin and ^{14}C-metabolites extracted from sweet potato leaf tissue and resolved by HPLC. Conditions, see Fig. 2. Flow-rates: mobile phase, 0.9 ml/min, scintillation fluid, 4.5 ml/min.

agreement with values determined in aliquots of the same sample mixture separated by TLC. Utilization of HPLC for resolution avoids possible losses during collection of zones from TLC plates and allows simultaneous quantitation.

REFERENCES

1 B. L. Mangeot, F. W. Slife and C. E. Rieck, *Weed Sci.*, 27 (1979) 267.
2 G. R. Stephenson, J. E. McLeod and S. C. Phatak, *Weed Sci.*, 24 (1976) 161.
3 S. W. Gawronski, L. C. Haderlie, R. H. Callihan and H. Gawronski, *Weed Res.*, 26 (1986) 307.
4 S. W. Gawronski, L. C. Haderlie and J. C. Stark, *Weed Res.*, 27 (1987) 49.
5 D. S. Frear, E. R. Mansager, H. W. Swanson and F. S. Tanaka, *Pestic. Biochem. Physiol.*, 19 (1983) 270.
6 D. S. Frear, H. W. Swanson and E. R. Mansager, *Pestic. Biochem. Physiol.*, 23 (1985) 56.
7 M. W. Hilton, N. S. Nomura, W. L. Yauger and S. S. Kameda, *J. Agric. Food Chem.*, 22 (1974) 578.
8 R. H. Callihan, G. F. Stallknecht, R. B. Dwelle and M. Blicharczyk, *Am. Potato J.*, 53 (1976) 253.
9 T. G. Hargroder and R. L. Rogers, *Weed Sci.*, 22 (1974) 238.
10 M. A. Mann and W. J. McLeod, *Can. J. Plant Sci.*, 58 (1978) 485.
11 M. S. Sharom and G. R. Stephenson, *Weed Sci.*, 24 (1976) 153.
12 P. Bartl, H. Parlar and K. Korte, *Z. Naturforsch.*, 316 (1976) 1122.
13 B. E. Pape and M. J. Zabik, *J. Agric. Food Chem.*, 20 (1972) 72.
14 G. R. B. Webster, S. R. MacDonald and L. P. Sarna, *J. Agric. Food Chem.*, 23 (1975) 74.
15 G. R. B. Webster and G. J. Reimer, *Pestic. Sci.*, 7 (1976) 292.
16 J. S. Thornton and C. W. Stanley, *J. Agric. Food Chem.*, 25 (1977) 380.
17 F. G. von Stryk, *J. Chromatogr.*, 56 (1971) 345.
18 H. J. Jarczyk, *Pflanzenschutz-Nachr. Bayer (Ger. Ed.)*, 31 (1978) 84.
19 H. J. Jarczyk, *Pflanzenschutz-Nachr. Bayer (Ger. Ed.)*, 36 (1983) 63.
20 C. E. Parker, G. H. Degen, E. O. Abusteit and F. T. Corbin, *J. Liq. Chromatogr.*, 6 (1983) 725.

Journal of Chromatography, 479 (1989) 212–215
Elsevier Science Publishers B.V., Amsterdam — Printed in The Netherlands

CHROM. 21 677

Note

Separation of cationic technetium-99m amine complexes on porous graphitic carbon

M. F. EMERY
Division of Radioisotopes, MRC Clinical Research Centre, Watford Road, Harrow, Middlesex HA1 3UJ (U.K.)
and
C. K. LIM*
Division of Clinical Cell Biology, MRC Clinical Research Centre, Watford Road, Harrow, Middlesex HA1 3UJ (U.K.)
(First received April 17th, 1989; revised manuscript received June 12th, 1989)

Technetium-99m has almost ideal physical properties (half-life, $t_{\frac{1}{2}} = 6.1$ h, γ energy 140 keV) for diagnostic imaging studies in nuclear medicine using single photon emission computer tomography (SPECT). It is readily available as sodium pertechnetate (TcO_4^-) from commercial generators. Analysis of technetium complexes evaluated as potential radiopharmaceuticals has mainly relied on paper chromatography[1–3] and instant thin-layer chromatography[2–4], although high-performance liquid chromatography (HPLC) is increasingly being employed[5–7].

Cationic technetium complexes of linear and macrocyclic amines have been synthesised as possible imaging agents[8–14], but so far only one HPLC method has been reported for their analysis[15]. This was because of the difficulties in eluting these compounds from silica-based reversed-phase columns[15] and a styrene–divinylbenzene bonded phase (Hamilton PRP-1) was suggested as an alternative. However, although some degree of separation has been achieved with this system using PRP-1, further improvement in resolution is required particularly between pertechnetate (TcO_4^-) and the complexes. This paper describes the complete separation of TcO_4^- and the monocationic amine complexes dioxo(ethylenediamine)-, dioxo(1,5,8,12-tetraazadodecane)- and *trans*-dioxo(1,4,8,11-tetraazacyclotetradecane)-technetium on a porous graphitic carbon (PGC) column with acetonitrile in 1% trifluoroacetic acid as eluent. The system is suitable for monitoring the radiochemical purity of these potential radiopharmaceuticals and for metabolism studies.

EXPERIMENTAL

Materials and reagents

Ethylenediamine (en_2) and stannous tartrate were from Sigma (Poole, U.K.). 1,5,8,12-Tetraazadodecane (ta) was from Aldrich (Gillingham, U.K.). 1,4,8,11-Tetraazacyclotetradecane or cyclam (cyc) was from Lancaster Synthesis (Morecambe, U.K.).

0021-9673/89/$03.50

Sodium pertechnetate (TcO_4^-) was eluted from an Ultratechnekow FM generator (Mallinckrodt Diagnostia, The Netherlands). The eluate was diluted with isotonic saline to give a working solution of 0.2–1 mCi/ml (7.4–37 MBq/ml).

Trifluoroacetic acid (TFA) and hydrochloric acid were AnalaR grade from BDH. Acetonitrile was HPLC grade from Rathburn (Walkerburn, U.K.).

Preparation of technetium amine complexes

Stannous tartrate was used as the reductant. A saturated solution was made by adding the solid to nitrogen purged 0.01 *M* HCl. The solution was filtered through a Millex GS 0.22-μm filter (Millipore, Harrow, U.K.) into a nitrogen-filled vial and constantly purged with nitrogen. The ligand solutions (20–50 m*M*) were made up in water. All reagents were freshly made before used.

The reaction was carried out in a capped vial by mixing 1 ml of ligand solution, 1 ml of sodium pertechnetate working solution and 1 ml of filtered stannous tartrate solution. The mixture was shaken and allowed to stand at room temperature for 15–30 min before injection into the liquid chromatograph. The complexes were stable for at least 2 h.

High-performance liquid chromatography

A Varian Associates (Walnut Creek, CA, U.S.A.) Model 5000 liquid chromatograph was used. The radiomatic detector was home made and consisted of a PTFE tubing wound around the outside of a 1.3-cm diameter plastic tube placed in a thallium-activated sodium iodide crystal well with the photomultiplier tube linked to a scintillation adoptor 288 and ratemeter 248 both from ESI Nuclear (Redhill, U.K.). The detector coil flow volume was 160 μl.

The separation was carried out on a 10 cm × 4 mm PGC (7-μm spherical particles) column (Hypercarb; Shandon Southern Scientific, Runncorn, U.K.). For the separation of mixtures, step-wise elution was used. The column was eluted with acetonitrile–1% TFA (2:98, v/v) for 14 min and then changed to acetonitrile–1% TFA (10:90, v/v) for the elution of the last peak (total time 20 min). For individual technetium amine complexes, isocratic elution with an appropriate mixture of acetonitrile and 1% TFA was sufficient.

RESULTS AND DISCUSSION

PGC is a new packing material for reversed-phase chromatography[16,17]. It is chemically stable to extreme pH and is free of silanol groups which are common to silica-base reversed-phase materials. PGC is much more hydrophobic and retentive than conventional C_8 or C_{18} reversed-phase packings and is therefore ideal for separating compounds which are difficult to retain on silica-based columns. In addition, PGC can interact electronically with solutes having lone pair electrons[18,19] because of the presence of the band of delocalised π-electrons. The above properties suggested the possibility of retaining and separating technetium amine complexes on PGC where silica-base materials have already failed[15].

The separation of a mixture containing $[TcO_2en_2]^+$, $[TcO_2ta]^+$, $[TcO_2cyc]$ and TcO_4^- is shown in Fig. 1. The elution order of the cationic species, $[TcO_2en_2]^+ < [TcO_2ta]^+ < [TcO_2cyc]^+$, is that expected for reversed-phase chromatography since the hydrophobicity of the compounds increased in that order.

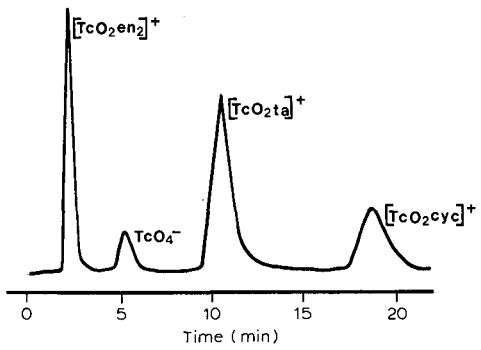

Fig. 1. Separation of technetium-99m amine complexes and pertechnetate on porous graphitic carbon. Mobile phase: acetonitrile–1% TFA (2:98, v/v) for 14 min, then 10:90 (v/v) for 6 min; flow-rate, 1 ml/min. Detection: radiometric.

TFA was chosen as the aqueous component of the mobile phase for two reasons. Firstly, it forms ion pairs with the cationic technetium amine complexes but, unlike long-chain ion-pairing agents, does not confer strong hydrophobicity on the solutes which may lead to excessive retention on the highly hydrophobic PGC. Secondly, TFA is an excellent competing agent for electronic interaction chromatography (EIC) on PGC, thus allowing the retention times of the anionic TcO_4^- to be precisely controlled by simply adjusting the concentrations of TFA in the mobile phase[19]. Retention of inorganic oxo-anions, including TcO_4^-, on PGC has been shown to be exclusively electronic interaction[19]. The PGC column is stable under the strongly acidic condition used and no deterioration of column performance was observed after prolonged usage with 1% TFA as eluent.

The ability of PGC to simultaneously separating cations and anions based on a combination of hydrophobic and electronic interactions is unique. It is anticipated that many novel applications will be developed by exploiting these chromatographic properties. The method described here is well suited for checking the purity of technetium amine complexes and for studying the metabolism of these potential radiopharmaceuticals. It is also well suited for the semi-preparative isolation of individual technetium amine complex with 0.9% NaCl instead of TFA as the major mobile phase component. After removal of acetonitrile by evaporation the preparation in saline can be used directly.

REFERENCES

1 A. M. Zimmer, W. Majewski and S. M. Spies, *Eur. J. Nucl. Med.*, 7 (1982) 88.
2 D. Webber, A. M. Zimmer and S. M. Spies, *J. Nucl. Med. Technol.*, 11 (1983) 15.
3 P. J. Robbins, *Am. J. Hosp. Pharm.*, 40 (1983) 629.
4 R. J. Kowalsky and J. R. Creekmore, *J. Nucl. Med. Technol.*, 10 (1982) 15.
5 A. D. Nunn, *J. Chromatogr.*, 255 (1983) 91.
6 G. M. Wilson and T. C. Pinkerton, *Anal. Chem.*, 57 (1985) 246.
7 G. J. de Groot, H. A. Das and C. L. de Ligny, *Int. J. Appl. Radiot. Isot.*, 36 (1985) 349.
8 J. Simon, S. Zuckman, D. E. Troutner, W. A. Volkert and R. A. Holmes, *Radiochem. Radioanal. Lett.*, 47 (1981) 111.
9 J. R. Thornback and A. E. Theobald, *Int. J. Appl. Radiot. Isot.*, 32 (1981) 833.

10 S. Seifert, R. Muenze and B. Johannsen, *Radiochem. Radioanal. Lett.*, 54 (1982) 153.
11 P. Blauenstein, G. Pfeiffer, P. A. Schubiger, G. Anderegg, K. Zollinger, K. May, Z. Proso, E. Ianovici and P. Lerch, *Int. J. Appl. Radiat Isot.*, 36 (1985) 315.
12 W. A. Volkert, D. E. Troutner and R. A. Holmes, *Int. J. Appl. Radiat. Isot.*, 33 (1982) 891.
13 D. E. Troutner, J. Simon, A. R. Ketring, W. Vokert and R. A. Holmes, *J. Nucl. Med.*, 21 (1980) 443.
14 M. E. Kastner, M. J. Lindsay and M. J. Clarke, *Inorg. Chem.*, 21 (1982) 2037.
15 T. J. Hoffman, W. A. Volkert, D. E. Troutner and R. A. Holmes, *Int. J. Appl. Radiat. Isot.*, 35 (1984) 223.
16 M. T. Gilbert, J. H. Knox and B. Kaur, *Chromatographia*, 16 (1982) 138.
17 J. H. Knox, B. Kaur and G. R. Millward, *J. Chromatogr.*, 352 (1986) 3.
18 B. J. Bassler, E. Garfunkel, R. A. Hartwick and R. Kaliszan, *J. Chromatogr.*, 461 (1989) 139.
19 C. K. Lim, *Biomed. Chromatogr.*, 3 (1989) 92.

Journal of Chromatography, 479 (1989) 216–219
Elsevier Science Publishers B.V., Amsterdam — Printed in The Netherlands

CHROM. 21 744

Letter to the Editor

Reduced variation in retention times of biogenic amines by temperature control in liquid chromatography with electrochemical detection

Sir,

It is known that in high-performance liquid chromatography (HPLC) with electrochemical detection (ED) large fluctuations in column temperature can affect retention times, peak heights and other separation characteristics. However, in air-conditioned or centrally heated laboratories temperature fluctuations are small during a 24-h period. The effects of these relatively small temperature fluctuations on separation characteristics have not been adequately investigated. The objectives of this study were (1) to investigate the magnitudes of changes in retention times of biogenic amines when separations are performed in an air-conditioned laboratory and (2) to determine if these changes can be reduced to acceptable levels by stabilizing the temperatures of column and mobile phase with a simple system of heating jackets and temperature controllers.

EXPERIMENTAL

Separations of dopamine (DA), norepinephrine (NE), 3,4-dihydroxybenzylamine (DHBA), and serotonin (5-HT) were performed using an LC-4A amperometric detector, a Phase II, 5 μm, ODS, reversed-phase C_{18} column, and a glassy carbon working electrode (Bioanalytical Systems, West Lafayette, IN, U.S.A.). The mobile phase (pH 3.0) included monochloroacetic acid (14.15 g/l), sodium hydroxide (4.675 g/l), EDTA (250 mg/l), octanesulfonic acid (300 mg/l), 1.4% tetrahydrofuran, and 2% acetonitrile. The flow-rate of the mobile phase was 1.7 ml/min, the sensitivity of the detector was 1 nA full scale, and the potential of the working electrode was 0.8 V with reference to a Ag/AgCl reference electrode.

The room, column and mobile phase temperatures were monitored with the help of temperature probes (Yellow Springs Instrument, Yellow Spring, OH, U.S.A.). In the first part of the study, separations were performed without controlling the temperature. In the second part, the temperatures of the column and mobile phase reservoir were maintained at 29.4–30.1°C and 43.2–44.0°C, respectively, with the help of custom-fitting heating jackets (Glas-Col, Terre Haute, IN, U.S.A.). The temperatures of the heating jackets on the column and mobile phase reservoir were controlled by Model 720 Lab Temperature Controllers (Dowty Electronics, Brandon, VT, U.S.A.).

RESULTS AND DISCUSSION

During a 24-h period, the temperature in the air-conditioned laboratory fluctuated between 24.8 and 27.5°C (Fig. 1A). This fluctuation caused the column

0021-9673/89/$03.50

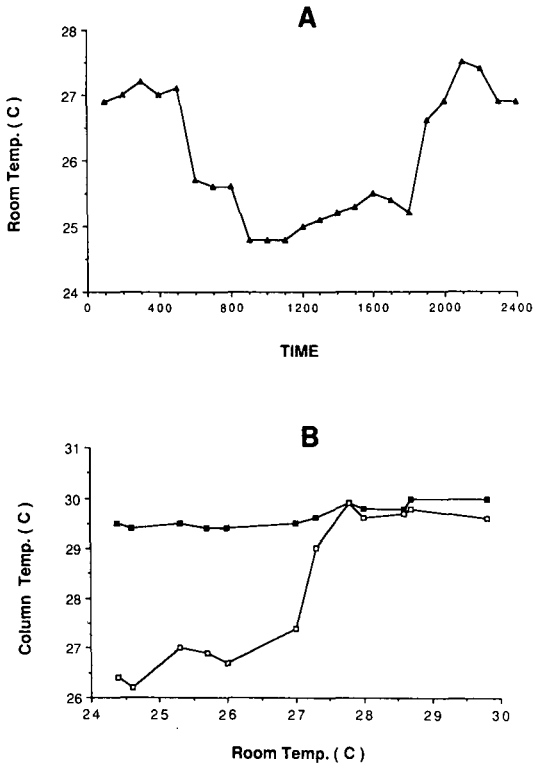

Fig. 1. (A) Fluctuations in room temperature in an air-conditioned laboratory during a 24-h period. (B) Fluctuations in the temperature of analytical column in an air-conditioned laboratory. Open squares = temperature of the column was not stabilized; closed squares = temperature of the column was stabilized at 29.4–30.1°C with the help of a heating jacket and a temperature controller.

temperature to vary between 26.2 and 29.9°C (Fig. 1B). The use of heating mantles on the column and mobile phase reservoir stabilized the column temperature between 29.4 and 30.1°C, although the room temperature continued to fluctutate as before.

When temperatures of the mobile phase and column were not controlled, the differences between the shortest and the longest retention times were 6.9%, 10.4%, 14.5% and 15.8% for NE, DHBA, DA and 5-HT, respectively (Table IA). By contrast, when temperatures of the column and mobile phase reservoir were stabilized the variability in retention times decreased to 0%, 4.1%, 3.8% and 5.1% for NE, DHBA, DA and 5-HT, respectively (Table IB).

These results indicate that variations in the retention times of biogenic amines can be reduced by stabilizing the temperatures of the column and mobile phase with a simple system of heating jackets and temperature controllers. When the column temperature was maintained within a range of 0.7°C, the longest retention times for DA, DHBA and 5-HT were only 5% or less longer than the shortest retention times, and the variation in the retention time of NE was undetectable. This represents a substantial narrowing of the variability in retention times and leads to increased confidence in the identity of the compounds being separated.

TABLE I

RETENTION TIMES OF BIOGENIC AMINES AND DHBA

A: Retention times were determined in an air-conditioned laboratory without stabilizing the temperatures of analytical column and mobile phase; the room and column temperatures fluctuated between 24.8 and 27.5°C and between 26.2 and 29.9°C, respectively. B: Retention times were determined in the same laboratory but the column and mobile phase temperatures were stabilized by a simple system of heating jackets; the room temperature fluctuated as before, but fluctuations in the column temperature were reduced to 0.7°C (between 29.4 and 30.1°C).

Trial	*Retention time (min)*							
	A				*B*			
	NE	*DHBA*	*DA*	*5-HT*	*NE*	*DHBA*	*DA*	*5-HT*
1	3.1	5.3	8.7	26.4	3.0	5.0	8.1	24.6
2	3.1	5.1	8.3	25.2	3.0	5.0	8.0	24.2
3	3.1	5.2	8.2	25.0	3.0	5.0	8.0	23.8
4	3.1	5.0	8.1	24.5	3.0	5.0	8.0	23.6
5	3.1	5.1	8.2	24.6	3.0	5.0	8.0	24.0
6	3.1	5.2	8.2	25.2	3.0	5.1	8.0	24.4
7	3.1	5.1	8.1	24.8	3.0	5.0	8.0	23.8
8	3.0	5.0	7.8	23.3	3.0	5.0	7.9	23.8
9	2.9	4.8	7.7	22.8	3.0	4.9	7.8	23.8
10	2.9	4.8	7.6	22.8	3.0	5.0	8.0	23.4
11	3.0	4.8	7.6	23.2	3.0	5.0	8.0	23.4
12	3.1	5.0	8.0	25.2	3.0	5.0	8.0	23.7
Range	0.2	0.5	1.1	3.6	0.0	0.2	0.3	1.2

The results indicate that temperature fluctuations during a 24-h period are rather substantial even in air-conditioned laboratories and lead to almost parallel changes in column temperatures and, consequently, to variations in retention times and annoying doubts and errors in identification of compounds. The temperature-controlling system used in this study minimizes these hazards by maintaining variability in the column temperature within a range of 0.7°C. Even this small variability can be eliminated by using a more sensitive temperature controller. On the whole, the temperature controlling system used in this study is simpler and less expensive than ovens, glass column jackets and cumbersome circulating water baths.

Another advantage of the system is that it permits preheating of the mobile phase just before its entry into the column. This is considered essential for achieving maximum efficiency in HPLC–ED, since it prevents formation of a temperature gradient in the column and the consequent peak-splitting phenomenon[1,2].

It has been shown that high column temperatures reduce retention times by as much as 40% and increase resolution by producing sharper and higher peaks[3]. The temperature controlling system used in this study has the capacity to maintain column temperature at higher levels of 50 or 60°C. The resultant increase in resolution and decrease in run times would be especially useful when a large number of samples is being analyzed[3]. Excessive increases in column temperature, however, are not advisable when the compounds being separated are thermally labile and when low boiling solvents are used in the mobile phase.

ACKNOWLEDGEMENT

The work was approved as Kansas Agricultural Experiment Station contribution No. 1 88-511-J.

Neuroendocrine Research Laboratory,
Department of Anatomy and Physiology,
VMS 228, Kansas State University,
Manhattan, KS 66506 (U.S.A.)

D. L. PALAZZOLO
S. K. QUADRI*

1 R. E. Shoup, *Curr. Sep.*, 2 (1980) 1.
2 R. J. Perchalski and B. J. Wilder, *Anal. Chem.*, 51 (1979) 774.
3 F. Hefti, *Curr. Sep.*, 2 (1980) 13.

(First received April 24th, 1989; revised manuscript received July 3rd, 1989)

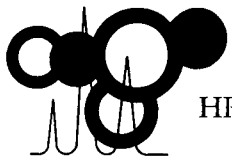

Ninth International Symposium on HPLC of Proteins, Peptides and Polynucleotides

PRELIMINARY PROGRAM

The Ninth International Symposium on HPLC of Proteins, Peptides and Polynucleotides will be held at the Wyndham Franklin Plaza Hotel in Philadelphia, Pennsylvania USA from November 5-8, 1989.

Sunday, Nov. 5th, 1989

12:00 P.M. Registration

6:00 P.M. Welcome Reception

Monday, Nov. 6th, 1989

8:00 A.M. Registration

9:00 A.M. Welcome

9:10 A.M. I. COLUMN TECHNOLOGY & SUPPORT MATERIALS
Retention behavior on porous and non-porous, polymeric packings. Discussions of Hydrophobic Interaction and Perfusion Chromatography. A columns comparison of packings will also be presented.
Speakers: B. Sebille, N. Afeyan, G. Rozing, A. Alpert and K. Unger

11:10 A.M. II. CHROMATOGRAPHIC BEHAVIOR
Physicochemical and Microenvironmental contributions to Protein Separation will be discussed. Additionally, structure-retention relationships and protein electrostatics in both chromatography and electrophoresis will be presented.
Speakers: Cs. Horvath, M. Hearn, R. Chicz and L. Haggerty

2:00 P.M. III. ANALYTICAL & MICROPREPARATIVE APPLICATIONS I
Techniques and examples of protein purification and isolation on the micro-scale will be presented.
Speakers: R. Hodges, L. Duffy, Ting-Po I, J. Dandeu and A. Jungbauer

4:00 P.M. Poster Sessions I, II, III

6:00 P.M. Reception at Art Museum

Tuesday, Nov. 7th, 1989

8:30 A.M. IV. PREPARATIVE/PROCESS CHROMATOGRAPHY
Theoretical and Practical Aspects of Large scale chromatography and membrane separations.
Speakers: L. Snyder, S. Yamamoto, E. Lightfoot, E. Kroeff, V. Garg and D. Wampler

11:40 A.M. V. ANALYTICAL & MICROPREPARATIVE APPLICATIONS II
A variety of topics will be discussed including protein properties, in process assays and alternative mobile phases.
Speakers: T. van Sommeren, P. DePhillips, B. Welinder and R. Condell

2:30 P.M. Poster Sessions IV, V, VI

3:30 P.M. VI. STRUCTURAL STUDIES
Protein isolation, characterization & sequencing.
Speakers: J. L'Italien, D. Crimmins, M. Schlittler, C. Zezza and T. Schlabach

6:00 P.M. Discussion Session & Social Events
—Column Technology and Retention Mechanisms
—Electrokinetic Techniques
—Preparative Chromatography
—Separation Strategy

Wednesday, Nov. 8th, 1989

8:00 A.M. Discussion Session

9:00 A.M. VII. SPECIAL TOPICS
Capillary Electrophoresis, Light Scattering and HPLC-MS will be discussed by:
B. Karger, E. Hild, H. Stuting and I. Jardine

11:00 A.M. VIII. QUALITY CONTROL OF PROTEINS
Protein Quantitation and Tryptic Mapping Studies for Q.C.
Speakers: D. LeFeber, M. Dumas, P. Chong, S. Renlund and O. Fox

2:00 P.M. Poster Sessions VII, VIII, IX

3:30 P.M. IX. POLYNUCLEOTIDES AND CARBOHYDRATES
Purifications of Polynucleotides will be presented by:
J. Kirkland, D. Riesner, E. Katz and D. Cecchini

5:00 P.M. Closing Remarks

ANNOUNCEMENT

6th International Symposium on Separation Science and Biotechnology

Bahia Mar Hotel & Yachting Center, Fort Lauderdale, Florida
January 16-18, 1990
Lois Ann Beaver, Chairman

AMONG THE FEATURED PARTICIPANTS ARE

- **Mark D. Dibner**, Director, Biotechnology Information Division, North Carolina Biotechnology Center, Research Triangle Park, NC
- **Catherine Fenselau**, Professor & Chairman, Dept. Chemistry, University of Maryland, Baltimore County, MD
- **Georges Guiochon**, Professor, Department of Chemistry, University of Tennessee and Oak Ridge National Laboratory, TN
- **Ronald R. Hahn**, Vice President, Alan Patricof Associates, New York, NY
- **William S. Hancock**, Senior Scientist, Medicinal & Analytical Chemistry Department, Genentech, South San Francisco, CA
- **Csaba Horvath**, Professor, Department of Chemical Engineering, Yale University, New Haven, CT
- **E. N. Lightfoot, Jr.**, Professor, Department of Chemical Engineering, University of Wisconsin, Madison, WI
- **Jay Olpin**, Technical Director, Research & Production, Cell Systems, Middletown, MD
- **Fred E. Regnier**, Professor, Department of Biochemistry, Purdue University, West Lafayette, IN
- **Richard O. Roblin III**, Vice President for Biomedical Products, Biotronic Systems Corporation, Rockville, MD

POSTER SESSION

You are invited to submit an abstract to the Symposium Manager for consideration for inclusion in the program. Abstracts should be limited to one, single-spaced typed page, stating title, authors (indicate presenter), addresses, text & references. Include a complete address & telephone number.

ABSTRACTS AND ALL CORRESPONDENCE SHOULD BE ADDRESSED TO

Mrs. Janet Cunningham • Symposium Manager • Barr Enterprises
P. O. Box 279, Walkersville, Maryland 21793 USA
Phone (301) 898-3772 • FAX (301) 898-5596

PUBLICATION SCHEDULE FOR 1989

Journal of Chromatography and Journal of Chromatography, Biomedical Applications

MONTH	J	F	M	A	M	J	J	A	S	
Journal of Chromatography	461 462 463/1	463/2 464/1	464/2 465/1 465/2	466 467/1 467/2	468 469 470/1 470/2	471 472/1 472/2 473/1	473/2 474/1 474/2 475	476 477/1 477/2	478/1 478/2 479/1	The publication schedule for further issues will be published later
Bibliography Section		486/1		486/2		486/3		486/4		
Biomedical Applications	487/1	487/2	488/1 488/2	489/1 489/2	490/1 490/2	491/1	491/2	492 493/1	493/2 494	495

INFORMATION FOR AUTHORS

(Detailed *Instructions to Authors* were published in Vol. 478, pp. 453–456. A free reprint can be obtained by application to the publisher, Elsevier Science Publishers B.V., P.O. Box 330, 1000 AH Amsterdam, The Netherlands.)

Types of Contributions. The following types of papers are published in the *Journal of Chromatography* and the section on *Biomedical Applications:* Regular research papers (Full-length papers), Notes, Review articles and Letters to the Editor. Notes are usually descriptions of short investigations and reflect the same quality of research as Full-length papers, but should preferably not exceed six printed pages. Letters to the Editor can comment on (parts of) previously published articles, or they can report minor technical improvements of previously published procedures; they should preferably not exceed two printed pages. For review articles, see inside front cover under Submission of Papers.

Submission. Every paper must be accompanied by a letter from the senior author, stating that he is submitting the paper for publication in the *Journal of Chromatography*. Please do not send a letter signed by the director of the institute or the professor unless he is one of the authors.

Manuscripts. Manuscripts should be typed in double spacing on consecutively numbered pages of uniform size. The manuscript should be preceded by a sheet of manuscript paper carrying the title of the paper and the name and full postal address of the person to whom the proofs are to be sent. Authors of papers in French or German are requested to supply an English translation of the title of the paper. As a rule, papers should be divided into sections, headed by a caption (*e.g.*, Summary, Introduction, Experimental, Results, Discussion, etc.). All illustrations, photographs, tables, etc., should be on separate sheets.

Introduction. Every paper must have a concise introduction mentioning what has been done before on the topic described, and stating clearly what is new in the paper now submitted.

Summary. Full-length papers and Review articles should have a summary of 50–100 words which clearly and briefly indicates what is new, different and significant. In the case of French or German articles an additional summary in English, headed by an English translation of the title, should also be provided. (Notes and Letters to the Editor are published without a summary.)

Illustrations. The figures should be submitted in a form suitable for reproduction, drawn in Indian ink on drawing or tracing paper. Each illustration should have a legend, all the *legends* being typed (with double spacing) together on a *separate sheet.* If structures are given in the text, the original drawings should be supplied. Coloured illustrations are reproduced at the author's expense, the cost being determined by the number of pages and by the number of colours needed. The written permission of the author and publisher must be obtained for the use of any figure already published. Its source must be indicated in the legend.

References. References should be numbered in the order in which they are cited in the text, and listed in numerical sequence on a separate sheet at the end of the article. Please check a recent issue for the layout of the reference list. Abbreviations for the titles of journals should follow the system used by *Chemical Abstracts.* Articles not yet published should be given as "in press" (journal should be specified), "submitted for publication" (journal should be specified), "in preparation" or "personal communication".

Dispatch. Before sending the manuscript to the Editor please check that the envelope contains three copies of the paper complete with references, legends and figures. One of the sets of figures must be the originals suitable for direct reproduction. Please also ensure that permission to publish has been obtained from your institute.

Proofs. One set of proofs will be sent to the author to be carefully checked for printer's errors. Corrections must be restricted to instances in which the proof is at variance with the manuscript. "Extra corrections" will be inserted at the author's expense.

Reprints. Fifty reprints of Full-length papers, Notes and Letters to the Editor will be supplied free of charge. Additional reprints can be ordered by the authors. An order form containing price quotations will be sent to the authors together with the proofs of their article.

Advertisements. Advertisement rates are available from the publisher on request. The Editors of the journal accept no responsibility for the contents of the advertisements.